OCS Study
MMS 2001-043

Sublethal Effects of Toxicants on Organisms: A Modeling Approach with Dynamic Energy Budgets

Final Technical Summary

Final Study Report

U.S. Department of the Interior
Minerals Management Service
Pacific OCS Region

Sublethal Effects of Toxicants on Organisms: A Modeling Approach with Dynamic Energy Budgets

Final Technical Summary

Final Technical Report

Authors

Roger Nisbet
Erik B. Muller
Principal Investigators

Prepared under MMS Cooperative
Agreement Nos. 14-35-0001-30761 and 14-35-0001-30758
by
Southern California Educational Intiative and
Coastal Marine Institute
Marine Science Institute
University of California
Santa Barbara, CA 93106

U.S. Department of the Interior
Minerals Management Service
Pacific OCS Region

Camarillo
March 2001

Disclaimer

This report has been reviewed by the Pacific Outer Continental Shelf Region, Minerals Management Service, U.S. Department of the Interior and approved for publication. The opinions, findings, conclusions, or recommendations in this report are those of the author, and do not necessarily reflect the views and policies of the Minerals Management Service. Mention of trade names or commercial products does not constitute an endorsement or recommendation for use. This report has not been edited for conformity with Minerals Management Service editorial standards.

Availability of Report

Extra copies of the report may be obtained from:
U.S. Dept. of the Interior
Minerals Management Service
Pacific OCS Region
770 Paseo Camarillo
Camarillo, CA 93010
phone: 805-389-7621

A PDF file of this report is available at:
http://www.coastalresearchcenter.ucsb.edu/CMI/

Suggested Citation

The suggested citation for this report is:

Roger Nisbet and Erik Muller. Sublethal effects of toxicants on organisms: a modeling approach with dynamic energy budgets. MMS OCS Study 2001-043. Coastal Research Center, Marine Science Institute, University of California, Santa Barbara, California. MMS Cooperative Agreement Number 14-35-0001-30761 and 14-35-0001-30758. 164 pages.

Table of Contents

FINAL TECHNICAL SUMMARY

STUDY TITLES:

Study I. Effects of Metal Toxicants on the Energy Budgets of Marine Organisms: A Modeling Approach

Study II. Assessing Toxic Effects on Population Dynamics Using Individual-Based Energy Budget Models

REPORT TITLE: Sublethal effects of toxicants on organisms: a modeling approach with dynamic energy budgets

CONTRACT NUMBER: Study I: 14-35-0001-30761; **Study II:** 14-35-0001-30758

SPONSORING OCS REGION: Pacific

APPLICABLE PLANNING AREA: Southern California

FISCAL YEAR(S) OF PROJECT FUNDING: Study I: FY95, FY96, FY97-FY98 no cost extension; **Study II:** FY 98, FY 99, FY 2000 no cost extension

COMPLETION DATE OF THE REPORT: March 2001

COST(S): Study I: FY 95 - $72,556, FY 96 - $75,030; **Study II:** FY 26,876, FY 22,824

CUMULATIVE PROJECT COST: Study I: $147,586; **Study II:** $49,700

PROJECT MANAGER: Russell J. Schmitt

AFFILIATION: University of California, Santa Barbara

PRINCIPAL INVESTIGATORS: [1]Roger Nisbet, [2]Erik Muller

ADDRESS: [1]Department of Ecology, Evolution and Marine Biology, University of California, Santa Barbara, CA 93106, [2]Marine Science Institute, University of California, Santa Barbara, CA 93106

KEYWORDS: toxicity model; growth model; dynamic energy budgets; food quality; starvation; herbivore stoichiometry; produced water; synthesizing unit; Droop model; Monod model; mutliple limitations;

BACKGROUND: This project and its follow-up were motivated by observations of Osenberg *et al.* (1992, Spatial scale of ecological effects associated with an open coast discharge of produced water. Pages 387-402. *in* J. P. Ray and F. R. Engelhardts, editors. Produced water: technological/environmental issues and solutions. Plenum Press, New York.) that the marine mussel *Mytilus californianus* grows and reproduces less in the vicinity of oil production platforms in the Santa Barbara Channel. Although they could not find increased environmental levels of contaminants common in produced water, they established that the mussels had accumulated barium in their shell to a level related to their distance to the nearest platform. Barium is a component of produced water, and the accumulation of this compound in mussels is a measure for the exposure of mussels to this and other compounds in produced water. Similar observations were made with other marine invertebrates. Their results show that impacts on biological variables were detectable over much greater distances than

physical variables. This implies that organisms integrate small changes in physiological properties over moderate time intervals and thereby produce significant effect. The results are important for two reasons. First, biological effects are necessary to detect very low levels of contamination. Second, population dynamics can be very sensitive to small changes in the physiological performance of individuals. This second point is particularly significant as direct ecological impacts at the level of populations and communities are commonly unmeasurable, especially for organisms with some dispersing life stage.

OBJECTIVES: To develop models that describe the sublethal effect of toxicants on the vital rates of marine organisms.

DESCRIPTION: Models for subletal effects of toxicants requires two components: a model describing the growth and reproduction of marine organisms *in the absence* of toxicants; and a model describing sublethal toxic effects for implementation in growth models. Both modeling components should be mechanistically justifiable, experimentally testable, and maximally general. The last point is especially important in light of the enormous number of possible combinations of species of organism and toxicant; moreover, it is rare to find a single pollutant in the environment, as usually a cocktail of toxicants is present. It is thus highly desirable to have one or a few models that fit many organism toxicant combinations. For the first modeling component, we developed and analyzed several dynamic energy budget (DEB) models. A DEB model describes the rates at which organisms assimilate and utilize energy from food for maintenance, growth, reproduction and development. These rates depend on the state of the organism (age, size, sex, nutritional status, etc.) and the state of its environment (food density, temperature, etc.). In DEB models, toxic effects show up as changes in parameter values. Although toxicants can have many different biochemical effects, it is feasible to summarize different modes of toxicant action through a few toxicity functions that describe alterations in the rates of feeding, respiration, growth and reproduction due to toxicant action, since the DEB modeling framework is sparse in parameters.

SIGNIFICANT CONCLUSIONS: The most important finding from this study is that it is possible to describe many sublethal effects with a few simple toxicity functions. In these functions, toxic compounds affect the parameters determining the acquisition of energy and maintenance of viable physiological functions. Those parameters are affected simultaneously and the effect functions share the scaling (toxicity) parameter; thus, there is no need to distinguish effects on separate physiological parameters. Marine organisms included in the study are *Mytilus californianus, M. edulis* and *Crassostrea gigas*, toxicants included toluene, pentachlorophenol, tributyltin, mercury, copper, cadmium, various polyaromatic hydrocarbons, and produced water, and response variables included feeding rates, respiration rates, growth and reproduction.

A second important conclusion is that care should be taken to interpolate observations about toxic effects on the level of individuals to predictions on populations and communities. Several compensatory mechanisms are in effect with the result that effects on the population level may appear at multiple trophic levels.

STUDY RESULTS: The study advanced along two lines: the development of DEB models and the development of toxicity models. There are two classes of DEB model: net assimilation and net-production models, the first class being at a more advanced state of development at the start of the project. To bring the net-production class of models on par with the net-assimilation models, we developed a net-production model that describes the growth of all life stages of an organism (Lika and Nisbet, 2000). Furthermore, we explored the generality and testability of the most advanced net-assimilation model, the kappa-rule model, and its potential for use in ecotoxicology (Nisbet *et al.*, 2000). Because food limitation and starvation phenomena are likely to aggrevate toxicological effects, we studied the dynamics of the kappa-rule model in a variable food environment (Muller and Nisbet, 2000). The model predicts that marine mussels have enhanced growth and reduced survival in strongly variable resource environments, and that mussels favoring growth over reproduction are more susceptible to stress (e.g., introduction of toxic compounds, food stress) than their conspecifics with a relatively high reproductive output. We also found that the quality of food (with regard to nutrient content) can have a profound effect on populations of herbivores and detritivores (Muller *et al.*, in review).

Although DEB models are sparse in parameters, the number of ways of including sublethal effects is still undesirably large, especially since information about which parameter may be affected by a certain toxicant is generally lacking. In an early contribution (Muller and Nisbet, 1997), we explored the possibility of simplifying and generalizing toxic effects on parameters that determine the rates of energy allocation in an organism. In a subsequent manuscript (Muller and Nisbet, in preparation), we tested this generalization with a wide variety of combinations of organism and toxicant and show that it offers a good description of how toxicants change the rates of feeding, respiration and growth. Marine organisms included in the study are *Mytilus californianus, M. edulis* and *Crassostrea gigas*, toxicants included toluene, pentachlorophenol, tributyltin, mercury, copper, cadmium, various polyaromatic hydrocarbons, and produced water. We also found that the generalization gives a good description of changes in reproduction rates. These findings have implications for population dynamics, and we found that although the introduction of a toxicant always leads to an initial decline of production, the long term effect may be positive or negative, depending on compensatory mechanisms (Nisbet *et al.*, 1997). To further investigate the potential effects of compensatory mechanisms, we performed a sensitivity analysis of the effects of contaminants on equilibrium densities in simple food chains (Nisbet et al., *in prep*). This work recognized that contaminants can affect rate processes at *all* trophic levels as well as influencing input and recycling of nutrients.

STUDY PRODUCTS:

Muller, E.B. and Nisbet, R.M. (1997) Modeling the Effect of Toxicants on the Parameters of Dynamic Energy Budget Models, *In* Environmental Toxicology and Risk Assessment: Modeling and Risk Assessment (Sixth Volume), p 71-81, F.James Dwyer, Thomas R. Doane and Mark L. Hinman Eds., American Society for Testing and Materials.

Nisbet, R.M., Muller, E.B., Brooks, A.J. and Hosseini, P. (1997) Models relating individual and population response to contaminants. Environmental Modeling and Assessment 2, 7-12.

Nisbet, R. M., Muller, E. B., Lika, K. and Kooijman, S. A. L. M. (2000) From molecules to ecosystems through dynamics energy budget models. Journal of Animal Ecology, 69:913-926.

Muller, E.B., Nisbet, R.M. (2000) Survival and Production in Variable Resource Environments. Bulletin of Mathematical Biology, 62:1163-1189.

Lika, K, and Nisbet, R.M. (2000) A Dynamic Energy Budget Model Based on Partitioning of Net Production. Journal of Mathematical Biology, 41:361-386.

Muller, E.B. and Nisbet, R.M. Sublethal effects of toxicants: a dynamic energy budget modeling approach compared to experimental results. In Preparation (manuscript included in full report).

Muller, E.B., Nisbet, R.M., Kooijman, S.A.L.M., Elser, J.J. and McCauley, E. Stoichiometric Food Quality and Herbivore Dynamics. Under review with Ecology Letters.

FINAL STUDY REPORT

INTRODUCTION

This project and its follow-up were motivated by observations of Osenberg *et al.* (1992) that the marine mussel *Mytilus californianus* grows and reproduces less in the vicinity of oil production platforms. Although they could not find increased environmental levels of contaminants common in produced water, they established that the mussels had accumulated barium in their shell to a level related to their distance to the nearest platform. Barium is a component of produced water, and the accumulation of this compound in mussels is a measure for the exposure of mussels to this and other compounds in produced water. Thus, very low levels of pollutants in the environment may induce significant sublethal toxic effects. Our broad aim was to develop models that describe the sublethal effect of toxicants on the vital rates of marine organisms.

We approached our problem along two distinct lines:

- development of models that describe the growth and reproduction of marine organisms *in absence* of toxicants;
- development of modules describing toxic effects that could be implemented in those growth models.

Below we elaborate on the results of the two lines of investigation. In both lines we used three guiding principles:

- the models should be mechanistically justifiable
- the models should be experimentally testable;
- the models should be maximally general.

The first principle is required to maximize the predictive power of a model and to make its limitations explicit. The second point is obvious. The last point is very important in light of the enormous number of possible combinations of species of organism and toxicant. Moreover, it is rare to find a single pollutant in the environment; usually a cocktail of toxicants is present. It is thus highly desirable to have one or a few models that fit many organism toxicant combinations. The three guiding principles, however, may conflict one another. The first and second principle tend to make models more exclusive, while the last principle leads, by default, to inclusive models. The art of modeling is then to find the best compromise.

GROWTH MODELS

Organisms acquire energy from their environment and use it for growth and propagation. These and other expenditures are commonly modeled in terms of budgets. The simplest models assume a few fluxes that do not change over time, and use a mass or energy balance equation to analyze experimental results. A well-known example of this type of model in ecotoxicology is the “Scope For Growth” methodology. Although these models are useful in the analysis of toxicological data, they cannot be used to predict the effects of toxicants in a dynamic environment. More complex models use dynamic equations to describe the change of a potentially large number of many different budgets and fluxes. Models of both types abound

in biology, and most are too specific as they decribe the particulars of a few genera only. Our interest is in simple dynamic models with a limited number of budgets, which we call dynamic energy budget (DEB) models. A DEB model describes the rates at which organisms assimilate and utilize energy from food for maintenance, growth, reproduction and development. These rates depend on the state of the organism (age, size, sex, nutritional status, etc.) and the state of its environment (food density, temperature, etc.).

At the start of the project only one DEB model existed that met our guiding principle of maximum generality (see above), the kappa rule model, developed by Kooijman (1986) and subsequently generalized (Kooijman 2000). There are two classes of DEB model: net assimilation and net-production models. The kappa rule model is an example of the family of net assimilation models. To bring the net-production class of models on par with the net-assimilation models, we developed a net-production model that describes the growth of all life stages of an organism (Lika and Nisbet, 2000; see below for copies of published papers, manuscripts and conference abstracts). Furthermore, we explored the generality and testability of the kappa-rule model and its potential for use in ecotoxicology (Nisbet *et al.*, 2000). Although the kappa rule model has been used to describe the growth of many species, including many marine organisms, its implications for organisms in dynamic food environments remained largely obscure. Because food limitation and starvation phenomena are likely to aggrevate toxicological effects, we studied the dynamics of this model in a variable food environment (Muller and Nisbet, 2000). The model predicted enhanced growth and reduced survival in strongly variable environments. Food limitation can be experienced as a limitation of food *quantity*, which is the standard assumption in growth models, and as a limitation of food *quality*, especially for herbivores, such as mussels feeding on algae or diatoms. We explored the stoichiometric requirements of food for growth (Muller *et al.*, in review).

TOXICITY MODELS

At the start of this project, toxicity models in a DEB modeling context dealt mainly with the accumulation of pollutants in organisms, *i.e.*, without physiological toxic effects, or with the lethal effects of toxicants. We aimed at developing toxic effect functions describing *sublethal* effects of toxicants. Toxicants can have many different biochemical effects, and it thus may seem difficult or impossible to fit many different toxic compounds in one modeling framework. However, DEB models provide such a framework, since those models are relatively sparse in parameters. In DEB models, toxic effects show up as changes in parameter values, and since those parameters are few in number, it is feasible to summarize different modes of action on the biochemical level through a few toxicity functions that describe alterations in the rates of feeding, respiration, growth and reproduction due to toxicant action.

Although DEB models are sparse in parameters, the number of ways of including sublethal effects is still undesirably large, especially since information about which parameter may be affected by a certain toxicant is generally lacking. In an early contribution (Muller and Nisbet, 1997), we explored the possibility of simplifying and generalizing toxic effects on parameters that determine the rates of energy allocation in an organism. In a subsequent manuscript (Muller and Nisbet, in preparation), we test this generalization with a wide variety of

combinations of organism and toxicant and show that it offers a good description of how toxicants changes the rates of feeding, respiration and growth. We also found that the generalization gives a good description of changes in reproduction rates. These findings have implications for population dynamics, and we found that although the introduction of a toxicant always leads to an initial decline of production, the long term effect may be positive or negative, depending on compensatory mechanisms (Nisbet *et al.*, 1997). To further investigate the potential effects of compensatory mechanisms, we performed a sensitivity analysis of the effects of contaminants on equilibrium densities in simple food chains (Nisbet et al., *in prep*). This work recognized that contaminants can affect rate processes at *all* trophic levels as well as influencing input and recycling of nutrients. Model predictions are qualitatively consistent with data published by Carman et al. (2000), who found both high mortality of crustacean grazers, and elevated ammonium flux in diesel-contaminated benthic communities.

REFERENCES

Carman, K.R., Bianchi TS, and Kloep F (2000). Influence of grazing and nitrogen on benthic algal blooms in diesel fuel-contaminated saltmarsh sediments. Environ. Sci. Technol. 34: 107-111.

Lika, K., Nisbet, R. M. (2000). "A dynamic energy budget model based on partitioning of net production". *Journal of Mathematical Biology*, **41**: 361-386.

Muller, E. B., Nisbet, R. M. (2000). "Survival and production in variable environments". *Bull. of Math. Biol.*, **62**: 1163-1189.

Nisbet, R.M., Muller, E.B., Brooks, A.J., Hosseini, P. (1997). " Models relating individual and population response to contaminants". *Environmental Modeling and Assessment*, **2**: 7-12.

Nisbet, R.M., Muller, E.B., Lika, K., Kooijman, S.A.L.M. (2000). "From molecules to ecosystems through dynamic energy budget models". *J. Anim. Ecol.*,**69**: 913-926.

Osenberg, C. W., Schmitt, R. J., Holbrook, S. J. and Canestro, D. 1992. Spatial scale of ecological effects associated with an open coast discharge of produced water. Pages 387-402. *in* J. P. Ray and F. R. Engelhardts, editors. Produced water: technological/environmental issues and solutions. Plenum Press, New York.

MODELING THE EFFECT OF TOXICANTS ON THE PARAMETERS OF DYNAMIC ENERGY BUDGET MODELS

Erik B. Muller and Roger M. Nisbet

REFERENCE: Muller, E.B. and Nisbet, R.M., "**Modeling the effect of toxicants on the parameters of dynamic energy budget models**," 6th Symposium On Environmental Toxicology And Risk Assessment: Modeling And Risk Assessment, ASTM STP 622, J. Dwyer, T. Doane and M. Hinman Eds., American Society for Testing and Materials, Philadelphia, 1996.

ABSTRACT: Toxicants negatively affect the rates of growth and reproduction of organisms. Dynamic energy budget models offer a convenient mathematical framework to describe growth and reproduction by individuals. Since these models take into account the lipid content of an animal, the accumulation of toxicants is easily incorporated. This paper deals with the subsequent effect of toxicants on growth and reproduction. We argue that the concept of non-competitive inhibition is appropriate to describe the increased maintenance demands and reduced assimilation due to toxicant action. In this way, energy investment in growth and reproduction are indirectly reduced.

KEYWORDS: toxicity model, energy budget, DEB, non-competitive inhibition, reproduction, toxicant.

Several research groups are currently engaged in developing mathematical models relating the effects of toxic compounds on individuals and populations of aquatic organisms [1, 2, 3]. The importance of this research is that many management decisions require insight into potential long-term effects of toxicants on populations, but much experimental information relates to measured, short-term effects on individuals. The research has two main parts: (i) modeling the effects on individual growth, reproduction and mortality of toxicant-induced changes in the rates of acquisition and utilization of energy by individual organisms, and (ii) determining the implications for population dynamics of these changes.

Toxicants affect organisms by changing some component(s) of the energy budget, as has been demonstrated by Scope For Growth studies [4, 5]. Dynamic energy budget (DEB) models describe the rules by which individual organisms assimilate and utilize energy from food [6, and references therein]. They incorporate feeding and assimilation rates dependent on the state of the individual and the environment, together with rules for energy allocation to maintenance, growth and reproduction (including priorities for energy allocation when food is scarce). Thus they provide a convenient mathematical framework within which to model the mechanisms whereby vital biological rates (growth, reproduction, respiration) are influenced by exposure to contaminants.

A recent theoretical study [7] has shown that the demography of a population of food-limited organisms at equilibrium is very sensitive to details of the assumptions on their energy allocation priorities. The sensitivity arises because energy allocation priorities determine whether the primary effect of environmental stress is to change fecundity, juvenile

development time, juvenile mortality or adult mortality. That work was motivated by work on individual-based models of *Daphnia* populations [8, 9, 10], but the conclusions have wide applicability. In particular, there is potential for population dynamics to be affected, not only by the priorities for energy allocation, but also by the ways in which energy flows are influenced by toxicants. Thus we need to understand how to incorporate the effects of toxicants into DEB models.

For any particular situation, we require three models:

- a DEB model
- a bioaccumulation model that describes the exchange of toxicants with the environment and their fate within an organism on the basis of physical properties (e.g. lipophilicity and affinity for ligands)
- a model that describes the effects of toxicants on the parameters of the dynamic energy budget model.

The first two models are easily combined, as has been shown previously [6, 11]. This is because the state variables of the first model (stored energy density and a measure of size) relate to the lipid and aqueous fractions, which are called compartments in a bioaccumulation model. We are developing the third model with three requirements: it should be mechanistically underpinned, it should be applicable to a wide range of toxicants and it should be mathematically tractable. This paper is a preliminary report of progress towards this model. From experimental literature at different levels of biological organization, we argue that the concept of non-competitive inhibition is useful to represent the sub-lethal action of many toxicants, and show how the parameters of a DEB model will be affected. We illustrate our approach with some calculations on the effects of "produced water" (discharge from marine petroleum production) on the growth of mussels.

DYNAMIC ENERGY BUDGET MODELS

There are two types of dynamic energy budget models, designated kappa rule model and net production model. It is beyond the scope of this paper to present them in detail; in-depth expositions can be found elsewhere [2, 6]. Instead, some basic notions are given here for the case when an adult grows under no-starvation conditions. Figure 1 outlines the energy flows in the models.

Three types of biomass are distinguished: energy reserves, structural or core biomass and gonads. The state variables are stored energy density, e, and structural biovolume, V. Food is taken up and converted into energy at a rate that is a function of the food density in the environment and of the size of an animal. Energy is spent on maintenance (at a rate proportional to core biomass), growth (proportional to size increase) and reproduction. The principal differences lie in the rules for energy allocation. In the net production model, maintenance demands are first debited from assimilated energy; what is left is partitioned between growth and energy reserves, depending how much energy is stored in the reserves. When the energy density exceeds a threshold value e_{tr}, energy is allocated from the reserves to reproduction at a rate σ proportional to the excess stored energy density. In the kappa rule model, assimilated energy is first added to the energy reserves. A fixed fraction κ of the energy flowing out of the reserves is spent on maintenance and growth, whereby maintenance demands take priority. The remainder is then used for reproduction.

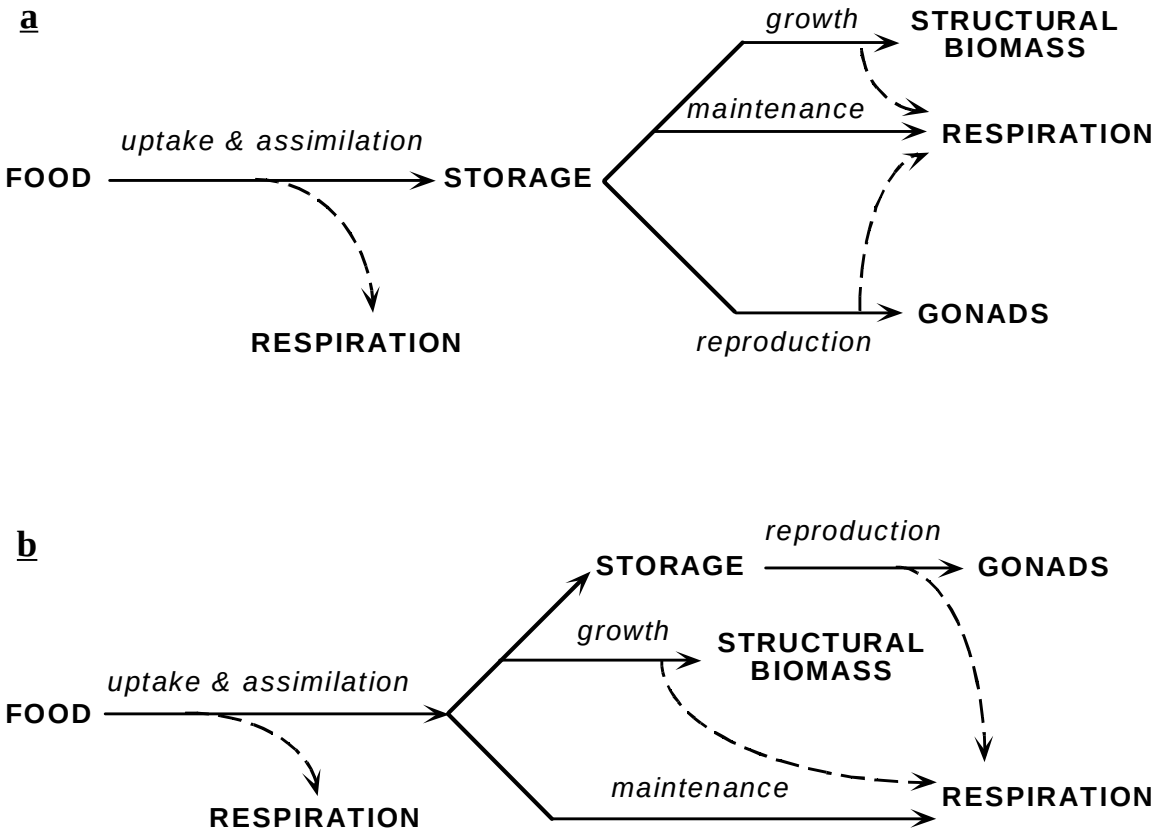

FIG. 1 Overview of energy flows (italics) and sources or sinks (bold) in an adult at non-starvation conditions as they are considered by the two dynamic energy budget models: (a) kappa rule model; (b) net production model. The dashed lines designate the overhead costs involved in assimilation, growth and reproduction.

TABLE Dynamics in a growing and reproducing adult.

KAPPA RULE MODEL	**NET PRODUCTION MODEL**
scaled stored energy density:	
$\frac{de}{dt} = \upsilon V^{-1/3}(f-e)$	$\frac{de}{dt} = \left(1-e^3\left(1+\frac{e}{\gamma}\right)\right)\left\{\frac{\upsilon f}{V^{1/3}} - m\gamma\right\} - \sigma(e-e_{tr})$
growth:	
$\frac{dV}{dt} = \frac{e\upsilon V^{2/3} - mgV}{e+g}$	$\frac{dV}{dt} = e^3\left(\frac{\upsilon f}{\gamma} V^{2/3} - mV\right)$
scaled energy to reproduction:	
$\frac{de_{rm}}{dt} = \frac{(1-\kappa)}{V_m}\left\{ge\frac{(\upsilon V^{2/3} - mV)}{(g+e)} - mgV_p\right\}$	$\frac{de_{rm}}{dt} = \frac{\sigma V}{V_m}(e-e_{tr})$

The resulting dynamics of growth, scaled reproduction (e_{rm}) and stored energy density are summarized in the Table. They are given to show how the dynamics are affected when toxicants are present (see below). The symbols not yet introduced, m, g, γ, $\dot{v}$ and V_m, are compound parameters reflecting maintenance costs, growth costs in the kappa rule model, growth costs in the net production model, the maximal assimilation rate and the maximal volume an organism will reach at unlimited food conditions, respectively. Finally, f is the scaled food density and V_p is the volume of an individual reaching adulthood.

MODELING THE EFFECTS OF TOXICANTS

To model the effects of toxicants on growth and reproduction, a mechanistic concept is needed that can be used for many toxicants. This section focuses on what toxicants have in common from an energetic point of view, and how their action might be modeled in a dynamic energy budget framework. Toxicants that are primarily mutagens and other irreversible damaging agents are not dealt with here. It should be noted, though, that they affect mortality and the production of viable offspring and may therefore play an important role on the population level.

Many toxicants of ecotoxicological interest tend to interact with macromolecules. Cadmium, mercury and other heavy metals, either in ionic form or bound to an organic compound, bind to proteins [12]. This is because they have a high affinity for ligands, such as sulphydryl groups in amino acids, and may consequently disrupt the sulfur bridges in proteins. As a result, heavy metals change the tertiary conformation of enzymes, compete with the proper cofactor during synthesis of metallo-enzymes, and thereby inhibit many enzymatic reactions.

Another important group of toxicants is the class of lipophilic compounds, which includes aromatic and aliphatic compounds but also the organo-metals mentioned before. They have a high affinity for the apolar fractions in an organism and, therefore, readily dissolve in biomembranes, where they are believed to practice their main toxic activities [13]. This is in line with what has been known from quantitative structure activity relationship (QSAR) studies, which is that an effect of a toxicant is inversely related to its octanol-water partitioning coefficient [4]. Since this coefficient is proportional to the partitioning coefficient between cell membrane and buffer [14, 15], the octanol-water partitioning coefficient is often successfully applied in toxicity studies [3, 4, 11].

Lipophilic compounds are toxic because they affect the membrane structure and the enzymes embedded therein [13]. Membranes containing these toxicants show an increased permeability to ions [15], so their function as a barrier is affected. This leads to the dissipation of energy and a reduction in metabolic rates [16, 17]. This is enhanced when the toxicant is a weak acid or base, so that it can cross the membrane in its undissociated, lipophilic form and then dissociates. In this way, protons are carried over the membrane. The interaction of enzymes with the membrane is affected by lipophilic toxicants causing enzymatic reactions to be hampered. The mechanism is poorly understood, but resembles the inhibitory effects of heavy metals.

So, many pollutants are toxic as a result of chemical affinities. This not only defines their partitioning behavior among body compartments, but also their effects on metabolism. In

the context of this paper, this means that the rates of energy fluxes and conversion efficiencies are reduced in the presence of toxicants. Consequently, we need assumptions to describe the effects of toxicants on the rate of energy fluxes and conversion efficiencies.

For the effect on energy fluxes, we propose to use the concept of the non-competitive inhibitor, which is a classic in enzyme kinetics [18]. This concept is based on Michaelis-Menten kinetics but additionally assumes an inhibitor that reversibly binds to an enzyme, which completely inhibits the formation of a product. The binding of substrate and inhibitor are independent processes. If the chemical pseudo-equilibria are approached rapidly, the rate of the enzymatic reaction Vi is given by

$$V_i = V_0\left(1+\frac{I}{K_i}\right)^{-1}$$

where V0 is the rate in absence of inhibitors, I the inhibitor concentration and Ki the saturation constant. When more, independently acting inhibitors are present, the net rate is obtained by adding the respective fractions of concentrations and saturation constants to the denominator.

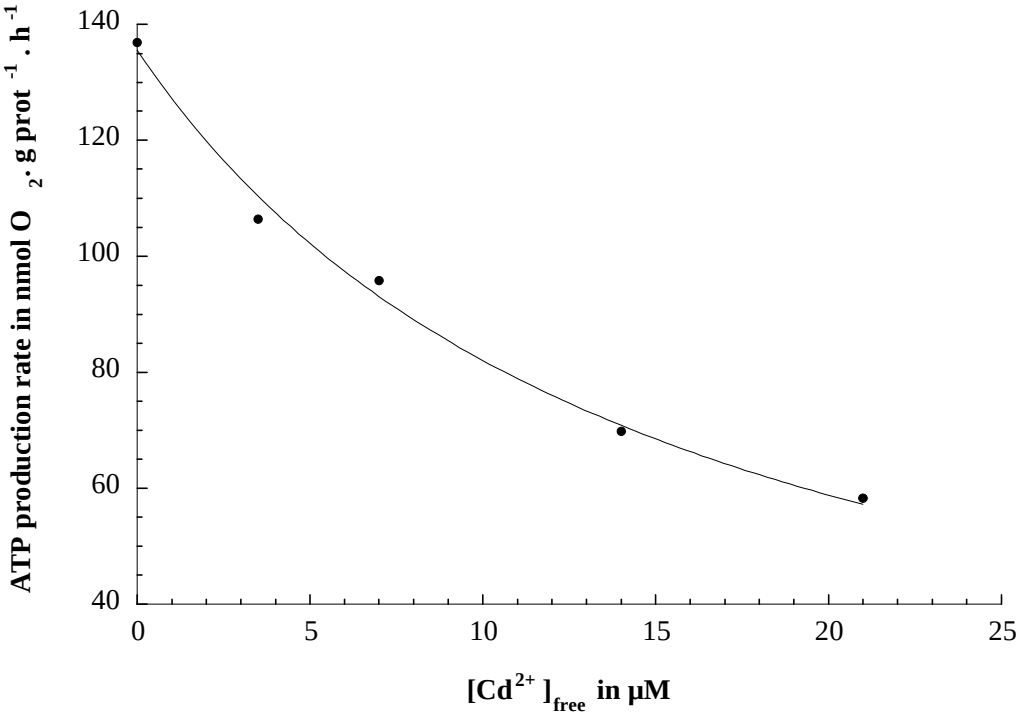

FIG. 2 The rate of ATP production by mitochondria is inhibited by cadmium. The rate is appropriately described by non-competitive inhibition kinetics with K_i = 15.3 (±1.1) µM (see equation above). Data from Kesseler and Brand [19].

This relationship operates on the molecular level. Dynamic energy budget models, however, are focused on individual organisms. Two arguments support our proposal to use the concept of the non-competitive inhibitor in dynamic energy budget modeling. First, non-competitive inhibition kinetics can be satisfactorily applied to systems that are more complex than single enzyme mixtures. Figure 2 illustrates that the inhibition of mitochondria by cadmium is appropriately described in a non-competitive way. Similarly, the respiration rate of cell suspensions with *Nitrobacter winogradskyi* is non-competitively inhibited by nitrous acid [20]. The second argument is that dynamic energy budget models treat the conductance of energy in a way that is conceptually similar to Michaelis-Menten kinetics. The link to non-competitive inhibition kinetics is thus a natural one.

We also need to consider the effects of toxicants on energy conversion efficiencies. The efficiency of oxidative phosphorylation in potato tuber mitochondria is almost unchanged at low cadmium concentrations (see Figure 3), while the rate of ATP production drops immediately (see Figure 2). At higher cadmium concentrations, the efficiency is reduced, although not as drastically as the reduction in the ATP formation rate. This suggests that at relatively low toxicant concentrations the primary toxic effect is on rates. Because this effect is quite large, the toxicant concentration at which an animal cannot survive is relatively low (see below). Thus it is consistent with these data to assume that the toxic effect on conversion efficiencies is negligible at physiologically relevant toxicant concentrations, though of course other toxicants may have a more pronounced effect on conversion efficiencies.

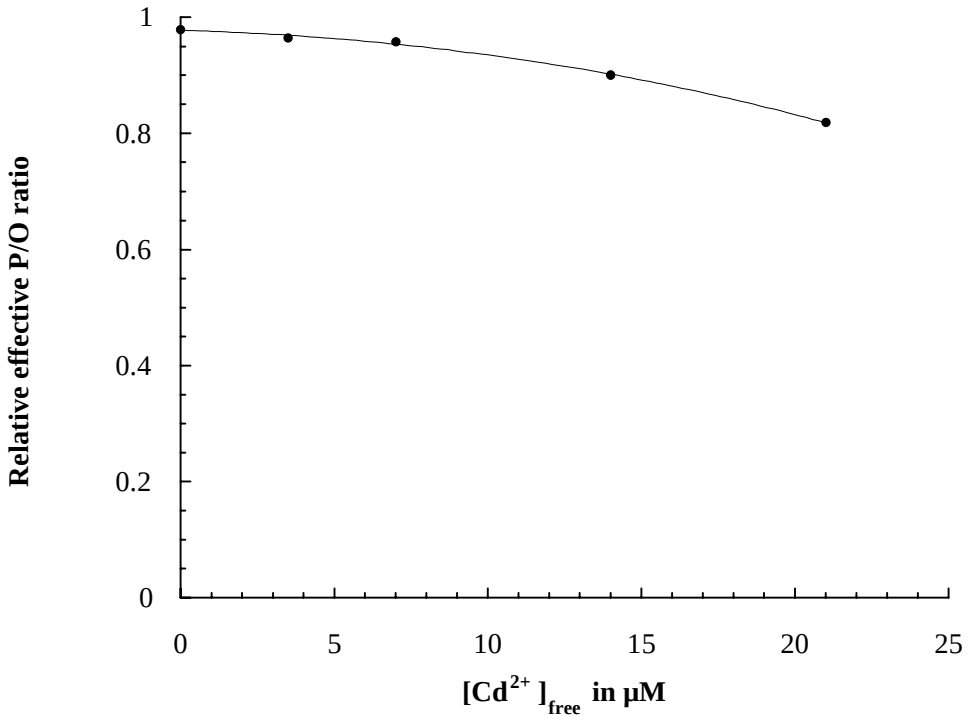

FIG. 3 Cadmium reduces the efficiency of oxidative phosphorylation, which is expressed as the fraction of ATP formation and oxygen consumption relative to the theoretical maximum stoichiometry. Data from Kesseler and Brand [19].

Having concluded that toxic effects are most likely to affect the rate parameters of the DEB models, we note that there are two parameters of that kind in both models: the energy conductance rate υ, which includes the assimilation rate, and the maintenance rate, m. The energy flux to growth is derived on the basis of balance equations and thus does not contain an independent rate parameter. This is also the case for energy used for reproduction in the kappa model formulation. The net production model, however, contains an independent reproduction rate parameter, σ. For the sake of simplicity, we assume that toxicants act equally adversely on all energy fluxes, thereby considering that the biochemistry involved has presumably a lot in common. When data show otherwise, there is, of course, no objection to differentiate between toxic effects on the rate parameters. Then, υ and σ are here simply multiplied by the same function of the toxicant concentration as were enzymatic rates before. The implementation of toxicants in the maintenance rate is more subtle. Maintenance demands are defined as the amount of energy required to keep an animal in a viable state for a period of time. This means that an animal cannot cut down on maintenance. To get sufficient energy to processes involved in maintenance, the maintenance rate should be multiplied by the inverse of the toxic effects function. The expressions for the rate parameters then become:

$$\upsilon_c = \frac{\upsilon_0}{1+c}$$
$$m_c = m_0(1+c)$$
$$\sigma_c = \frac{\sigma_0}{1+c}$$

where c is the toxicant concentration scaled to the saturation constant. Just as for non-competitive inhibitors, adding more toxicants is a matter of adding their scaled concentrations to the denominator. In an environment that is polluted with various toxicants, the final response will be dominated by the few compounds that are readily taken up and are present at the highest concentrations and are the most toxic.

APPLYING THE TOXIC EFFECT FUNCTIONS

To utilize the functions describing the effect of toxicants on rate parameters, we need to define the toxicant concentration c. Toxicants that are dissolved in adipose tissue are unlikely to exert direct effects. On the other hand, those dissolved in the lipid bilayer of membranes have a large impact. The simplest solution is to consider the target sites of toxicants as a part of structural biomass and assume that the water content of energy reserves and reproductive matter is negligible. The idea is that energy reserves and reproductive matter consist mainly of lipids and other insoluble storage materials [6]. The consequence is that energy reserves and reproductive matter are biochemically relatively inactive and thus hardly subject to toxic action. There are quite a few subtleties, though, involved in the mapping of biochemical composition to model variables [6], but these are beyond the scope of this paper. Then in accordance with others [1], the toxicant concentration in the aqueous fraction is the concentration in the toxic effect functions. This argument also covers lipophilic toxicants,

since the concentration in biomembranes is proportional to the aqueous concentration when equilibria are rapidly settled.

The toxicant concentration in the aqueous fraction can be described with a bioaccumulation model [11]. The key notions are that toxicant exchange with the environment is via the aqueous fraction, and that toxicants partition over body compartments, which depends on their affinity for the biochemical composition of the compartments. Since the compartment sizes are determined by the dynamic energy budget model, our effect functions fit in naturally under the restriction that the toxicant is not metabolized.

Some compounds have no effect when present at low concentrations. The maximum concentration at which no effect is observed is the no effect concentration. Some compounds are essential for growth but become toxic at higher concentrations. Among them are copper, zinc and nickel that are cofactors in metallo-enzymes. The concentration of such compounds in ionic form is controlled by metallothioneins that have a high affinity for such ions. Such proteins have also a high affinity for heavy metals without a known physiological function, such as cadmium and mercury. As a result, an organism may contain small concentrations of a heavy metal and yet show no physiological response. Whatever mechanism is behind the no effect concentration, it can be accounted for by correcting the concentration expected on the basis of partitioning behavior. The no effect concentration is then an additional parameter, which can be estimated to assess the risks of a toxicant [1].

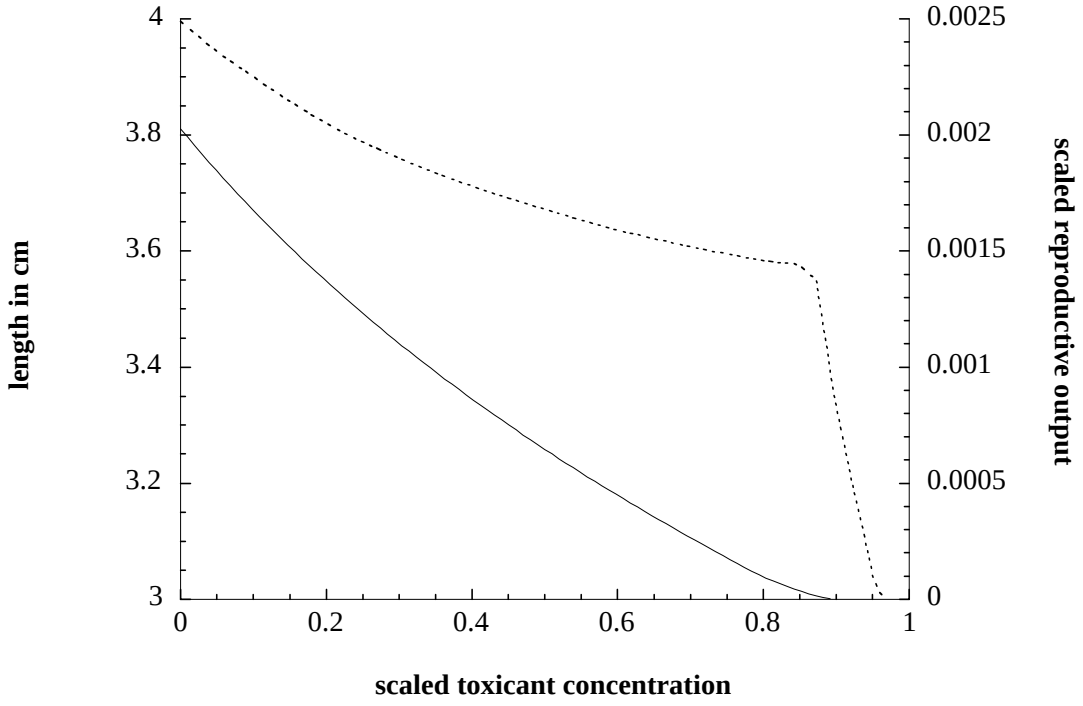

FIG. 4 The final length and cumulative reproductive output of a mussel is indirectly reduced by toxic effects on the assimilation and maintenance rate. The results were calculated with simulations by assuming an initial 3 cm mussel in a constant environment during 120 days.

To illustrate the impacts of toxicants, we predicted the growth and reproduction of the bay mussel *Mytilus edulis* with numerical methods. The purpose is to study how healthy, 3 cm long mussels that are outplanted near oil production platforms would be affected by toxicants in produced water [21]. For this we used the kappa rule model, which has been parameterized for bay mussels [22]. The environmental conditions and aqueous toxicant concentrations were supposed to be constant. As a result, the toxicant concentrations are scaled versions of each other and can be treated as a single variable. Furthermore, 10 % of the energy flowing out of the reserves is assumed to be used for reproduction and the scaled food density selected was 80% of its maximum value. Then, the predicted length and reproductive output after 120 days is shown in Figure 4. It is obvious that growth and reproduction are strongly affected by toxicants, although indirectly via a decreased assimilation rate and increased maintenance requirements. A 3 cm long mussel cannot grow at scaled toxicant concentrations above 0.9. Then, the reproductive output drastically declines. This is because mussels are starving and need to cut down on reproduction in order to meet maintenance. At a scaled toxicant concentration slightly below 1, reproduction stops as well. From that concentration onwards, where the maintenance rate is doubled and the energy conductance rate halved, a 3 cm long mussel will die because of starvation.

DISCUSSION

We started this paper by noting that a model of the effects of toxicants on growth and reproduction of organisms has 3 components: a DEB model, a bioaccumulation model, and a model of the effects of toxicants on the parameters of the DEB model. Previous work has addressed problems relating to the formulation of DEB models appropriate for application to toxicology [1, 2], and the formulation of bioaccumulation models [6, 11]. There is a much smaller literature on the third component, and the work reported here represents some preliminary ideas on that problem.

Our main conclusion is that the action of many toxicants are properly characterized by non-competitive inhibition. For this, we have analyzed data from experiments on the effects of toxicants at the level of single enzymes, organelles and organisms. The mechanism provides an underpinning for functional forms assumed by Kooijman and co-workers in recent research [1]. For example, they assumed that the first order Maclaurin expansion of an unknown toxicity function gives a satisfactory approximation under physiological relevant conditions. In other words, effects are linear in the toxicant concentration. This gives similar results to ours for the effect on maintenance rate, but for other rates gives a linear decrease which can only be valid at small concentrations; otherwise energy fluxes would become negative at high toxicant concentrations, which means that energy reserves are leaking into the environment. Here, ingestion and assimilation are irreversible processes even at relatively high toxicant concentrations, as they should be.

An increase in realism yields a model that can be applied to situations in which organisms are seriously affected by toxicants. Kooijman and co-workers have principally centered on no effect levels and included effects on conversion efficiencies. They analyzed data on growth and reproduction by assuming that toxic effects are exerted through one rate process or conversion efficiency at a time. For the estimation of the no effect concentration,

they have shown that it hardly matters which process is supposed to be affected. This is because the no effect concentration is to depend on when a mechanism starts to take effect rather than the mechanism itself. Hence, this approach has yielded a powerful tool to analyze standard toxicity tests. Our approach should be applicable to study the effects of toxicants on the growth and reproduction of individuals.

The next logical step is to test the model with experimental data on growth and reproduction. For this we will use data from mussels outplanted near an oil production platform [21]. Finally, we recall that this work was motivated by questions in population and ecosystem dynamics. It is possible to incorporate an assumption of non-competitive inhibition by a toxicant into a very simple biomass-based model of a plant-herbivore system. The result is a model that is capable of exhibiting a wide range of types of population dynamics (Nisbet and Hosseini, unpublished research). Of particular interest is the existence of a set of parameter values for which the fate of the system depends on initial conditions. This will also be a subject of future research.

Acknowledgments We thank Andy Brooks, Bas Kooijman, Erik Noonburg, Craig Osenberg, Russ Schmitt and Will Wilson for discussions and advice. This research was supported by the Office of Naval Research (Grant No N00014-93-1-0952), and by the Minerals Management Service, U.S. Department of the Interior, under MMS Agreement No. 14-35-0001-30761. The views and conclusions contained in this document are those of the authors and should not be interperted as necessarily representing the official policies, either express or implied, of the U.S. Government.

REFERENCES

[1] Kooijman, S.A.L.M. and Bedaux, J.J.M., "Analysis of toxicity test on *Daphnia* survival and reproduction", Water Research in press.

[2] Nisbet, R.M., Ross, A.H. and Brooks, A.J., "Emperically-based dynamic energy budget models: theory and an application to ecotoxicology", Nonlinear World 3:85-106, 1996.

[3] Lassiter, R.R. and Hallam, T.G., "Survival of the fattest: implications for accute effects of lipophilic chemicals on aquatic populations", Environmental Toxicology and Chemistry 9:585-595, 1990.

[4] Donkin, P., Widdows, J., Evans, S.V., Worral, C.M. and Carr, M., "Quantitative structure-activity relationships for the effect of hydrophobic organic chemicals on rate of feeding by mussels (*Mytilus edulis*), Aquatic Toxicology 15:277-294, 1989.

[5] Widdows, J., Donkin, P., Brinsley, M.D., Evans, S.V., Salkeld, P.N., Franklin, A., Law, R.J. and Waldock, M.J., "Scope for growth and contaminant levels in North Sea mussels *Mytilus edulis*", Marine Ecology Progress Series 127:131-148.

[6] Kooijman, S.A.L.M., "Dynamic energy budgets in biological systems", Cambridge University Press, UK, 1993.

[7] Gurney, W.S.C., Middleton, D.A.J., Nisbet, R.M., McCauley, E., Murdoch, W.W. and De Roos, A.M., "Individual energetics and the equilibrium demography of structured populations", Theoretical Population Biology in press.

[8] Gurney, W.S.C., McCauley, E., Nisbet, R.M. and Murcdoch, W.W., "The physiological ecology of *Daphnia*: formulation and tests of a dynamic model of growth and reproduction", Ecology 71:716-732, 1990.

[9] Nisbet, R.M., Gurney, W.S.C., Murdoch, W.W. and McCauley, E., "Structured population models: a toool for linking effects at individual and population level", Biological Journal of The Linnean Society 37:79-99, 1989.

[10] McCauley, E., Nisbet, R.M., De Roos, A.M., Murdoch, W.W. and Gurney, W.S.C., "Structured population models of herbiverous zooplankton", Ecology in press.

[11] Kooijman, S.A.L.M. and Van Haren, R.J.F., "Animal energy budgets affect the kinetics of xenobiotics", Chemosphere 21:681-694, 1990.

[12] Byczkowski, J.Z., "Effects of metal compounds on mitochondrial function: a review", The Science of the Total Environment 37:133-162, 1984.

[13] Sikkema, J., De Bont, J.A.M. and Poolman, B., "Mechanisms of membrane toxicity of hydrocarbons", Microbiological Reviews 59:201-222, 1995.

[14] Machleidt, H., Roth, S. and Seeman, P., "The hydrophobic expansion of erythrocyte membranes by the phenol anesthetics", Biochimica et Biophysica Acta 255:178-189, 1972.

[15] Seeman, P., "The membrane actions of anesthetics and tranquilizers", Pharmacological Reviews 24:583-655, 1972.

[16] Leão, C. and Van Uden, N., "Effects of ethanol and other alcohols an passive proton influx in the yeast *Saccharomyces cerevisiae*", Biochimica et Biophysica Acta 774:43-48, 1984.

[17] Cartwright, C.P., Juroszek, J.-R., Beavan, M.J., Ruby, F.M.S., De Morais, S.M.F. and Rose, A.H., "Ethanol dissipates the proton-motive force across the plasma membrane of *Saccharomyces cerevisiae*", Journal of General Microbiology 132:369-377, 1986.

[18] Segel, I.H., "Enzyme kinetics: behavior and analysis of rapid equilibrium and steady-state enzyme systems", John Wiley & Sons, New York, 1993.

[19] Kesseler, A. and Brand, M.D., "Localisation of the sites of action of cadmium on oxidative phosphorylation in potato tuber mitochondria using top-down elasticity analysis", European Journal of Biochemistry 225:897-906, 1994.

[20] Boon, B. and Laudelot, H., "Kinetics of nitrite oxidation by *Nitrobacter winogradskyi*", Biochemical Journal 85:440-447, 1962.

[21] Osenberg, C.W., Schmitt, R.J., Holbrook, S.J. and Canestro, D., "Spatial scale of ecological effects associated with an open coast discharge of produced water", In: Produced Water (eds. Ray, J.R., and Engelhard, F.R.), Environmental Science Research 46:387-402, 1992.

[22] Van Haren, R.J.F. and Kooijman, S.A.L.M., "Application of a dynamic energy budget model to *Mytilus edulis* (L.)", Netherlands Journal of Sea Research 31:119-133.

Environmental Modeling and Assessment 2 (1997) 7–12

Models relating individual and population response to contaminants

R.M. Nisbet, E.B. Muller, A.J. Brooks and P. Hosseini

Department of Ecology, Evolution and Marine Biology, University of California, Santa Barbara, CA 93106, USA

Even when present at sub-lethal levels, toxic compounds have an effect on the dynamics of a population, expressed through altered growth and reproduction rates. We explore some of the potential effects of toxicants on populations, using a simple model that considers a generic toxicant and populations of two species, a primary producer, and a consumer living under food-limited conditions. The toxicant is assumed to affect the consumers only, and it may enter them either directly from the environment or via their food, the latter opening the possibility of biomagnification. The initial response of the consumer to introduction of a toxicant is invariably a decline in its fecundity and density. However, in the longer term, the equilibrium densities of both producer and consumer may increase or decrease, depending on parameter values and ambient toxicant levels. The surprising case of an increased equilibrium in response to the toxicant occurs if, in the absence of toxicant, the consumers held the producers at a very low level, analogous to 'overfishing' in fishery studies. If the toxicant enters the consumer via food, multiple, non-trivial equilibria are possible. The complex, but interpretable, dynamics exhibited by these simple models will be used to guide studies with more realistic models, for whose development this study forms a prelude.

1. Introduction

Concepts related to *energy flow* are used in studies at all levels of biological and ecological organization. Energetic processes are important in determining the consequences of environmental stress, notably in responses to sub-lethal concentrations of contaminants, which commonly influence assimilation and respiration rates. For example, energetic processes in mussels are affected by metals, organometals and organics, and have been characterized in terms of *scope for growth*, defined as the difference between assimilation and respiration rates. A comprehensive study of this type (Widdows et al. [15]) showed a strong correlation between scope for growth and body burdens of many toxicants in mussels from various North Sea locations. Contaminants also directly or indirectly affect growth and reproduction (e.g., Kooijman and Bedaux [6] and references therein), and may have effects on the population dynamics of simple systems, e.g., a study by Borgmann et al. [1] of changes in the dynamics of *Daphnia* in mesocosms with added cadmium.

Many environmental concerns involve multi-generation population and/or community effects, but most experimental data are obtained from short-term experiments on individuals. *Structured population models*, in which a population is assumed to consist of a very large number of individuals sharing a common environment (e.g., Metz and Diekmann [7]; Tuljapurkar and Caswell [14]), have the potential to relate the large body of physiological information on individual responses to environmental stress with the less accessible issues of population dynamics and demography. The key to the use of structured population models is a testable model of growth, reproduction and mortality of individual organisms (e.g., Murdoch et al. [11]), and we have argued elsewhere (Nisbet et al. [13]) that *dynamic energy budget* (DEB) models (Kooijman [5]) are ideal for this purpose. DEB models describe the assimilation of food by individual organisms and its allocation to growth and reproduction. Nisbet et al. [13] reviewed two families of DEB model which differ only in the assumed priorities for distributing energy, and made preliminary studies of the effects of toxicants on individual performance by making use of empirical data on toxicant-induced changes in assimilation and respiration rates.

In general, a model of individual response to toxicant exposure will have three components: (i) a DEB model predicting growth and reproduction; (ii) a bioaccumulation model describing the exchange of toxicant between organism and environment and its partitioning within the organism; and (iii) a model of toxicant action. Toxicants act on processes at the molecular and suborganismal level, but it is assumed that the effects of these processes may be described through changes in the instantaneous values of the parameters in a DEB model (Kooijman and Bedaux [6]; Muller and Nisbet [8]). From a study of published data on the effects of free cadmium on rates and efficiencies of ATP production, Muller and Nisbet [8] proposed that rate parameters were affected more strongly than conversion efficiencies and that the effect of toxicants was well described by non-competitive inhibition kinetics.

This paper addresses a few of the implications for population dynamics of the individual responses to toxicants suggested by Muller and Nisbet. Each individual grows and reproduces in accordance with a very simple DEB model. We focus on situations where a 'consumer' population is regulated through food availability and show that in such cases, the long-term effects of toxicants may be that both consumers and food settle to new equilibrium densities. We show that the long-term changes in demographic quantities such as fecundity (which are commonly measured in toxicity tests) for individuals in food limited populations may be very different from short-term responses measured at

constant food density. We also investigate how the fate of a population depends on the state of the population and its environment at the time when exposure to the toxicant starts.

2. A simple dynamic energy budget model

2.1. Biomass dynamics

The simplest DEB-based model of a food limited population leads to dynamics which are described by equations very similar to the well-known Lotka–Volterra equations. We consider two species, 'primary producers' or 'food' with density $F(t)$ and 'consumers' with density $C(t)$. We assume that in the absence of consumers, the producers would grow logistically with parameters r and K, and make the following assumptions concerning the consumers:

- Consumers search randomly for food at a rate proportional to their biomass.
- All food encountered is eaten and converted into consumer biomass with a constant efficiency e.
- Consumers have a constant per capita death rate m.
- All consumers have a constant respiration rate b per unit biomass.

The producer biomass density changes through time in accordance with the differential equation

$$\frac{\mathrm{d}F}{\mathrm{d}t} = rF(1 - F/K) - aFC, \tag{1}$$

where a denotes the volume or area searched per unit time per unit of consumer biomass. The consumer dynamics can be derived by considering the biomass balance: new biomass is produced by conversion of food, and biomass is lost through death and respiration. Thus

$$\frac{\mathrm{d}C}{\mathrm{d}t} = eaFC - (m + b)C. \tag{2}$$

Provided K is large enough for the producer to support a consumer population, the model predicts stable equilibria given by

$$F^* = \frac{m + b}{ea}, \qquad C^* = \frac{r}{a}\left[1 - \frac{m + b}{eaK}\right]. \tag{3}$$

2.2. Equilibrium demography

The equation for consumer biomass could be derived without a rule describing how assimilate is partitioned between growth and reproduction. This is because the assimilation efficiency is assumed to be constant, regardless of the allocation of assimilate. In order to model *demographic* properties, such as fecundity and age structure, we need additional assumptions. Suppose all individuals have biomass w_b at birth, and mature (i.e., start reproduction) when they attain a critical biomass w_m. Juveniles assign 100% of net production (assimilation minus maintenance) to biomass. If net production is positive, adults assign a fraction $\mu(w)$ of net production to biomass and the remainder to reproduction. If net production is negative, adults cease reproduction. With these assumptions, the biomass, w, of an *individual* changes according to the differential equation

$$\frac{\mathrm{d}w}{\mathrm{d}t} = g(w, t) \equiv \xi\big[eaF(t) - b\big]w, \tag{4}$$

where

$$\xi = \mu(w) \quad \text{if } eaF(t) - b > 0 \text{ and } w > w_m, \tag{5}$$

and $\xi = 0$ otherwise.

The dynamics of a population are described by two partial differential equations (PDEs). An age distribution, $f(\tau, t)$, is defined by specifying that $f(\tau, t)\,\mathrm{d}\tau$ is the number of consumers with ages in an infinitesimal age interval $\tau \to \tau + \mathrm{d}\tau$ at time t. As all consumers are assumed to experience the same common food environment $F(t)$, individuals born at the same time grow at the same rate. Then $w(\tau, t)$ is defined as the weight of an individual aged τ at time t. The population dynamics are then obtained from the solutions of two simultaneous PDEs:

$$\frac{\partial f}{\partial t} + \frac{\partial f}{\partial \tau} + mf = 0, \tag{6}$$

$$\frac{\partial w}{\partial t} + \frac{\partial w}{\partial \tau} = -g(w, t), \tag{7}$$

which have to be solved with the renewal conditions

$$f(0, t) = w_b^{-1} \int_0^\infty (1 - \xi)\big[eaF(t) - b\big]w(\tau, t)f(\tau, t)\,\mathrm{d}\tau, \tag{8}$$

$$w(0, t) = w_b. \tag{9}$$

At a constant food density $\overline{F}$, the fecundity (i.e., number of offspring produced per unit time) of an adult of weight w is

$$\beta = \frac{w}{w_b}(1 - \xi)\big[ea\overline{F} - b\big] \tag{10}$$

and the time required for a juvenile to grow from birth to maturity is

$$T_J = \big(ea\overline{F} - b\big)^{-1} \ln\left[\frac{w_m}{w_b}\right]. \tag{11}$$

By contrast, if the consumer population is food limited and at equilibrium, the producer density cannot have an arbitrary value, but must take the value that makes consumer birth and death rates equal. The time T_J taken to grow through the juvenile stage can be derived by replacing $\overline{F}$ in equation (11) with F^* from equation (3) to obtain

$$T_J = \frac{1}{m} \ln\left[\frac{w_m}{w_b}\right]. \tag{12}$$

General theory for the equilibrium demography of food limited populations was developed by Gurney et al. [3]. The

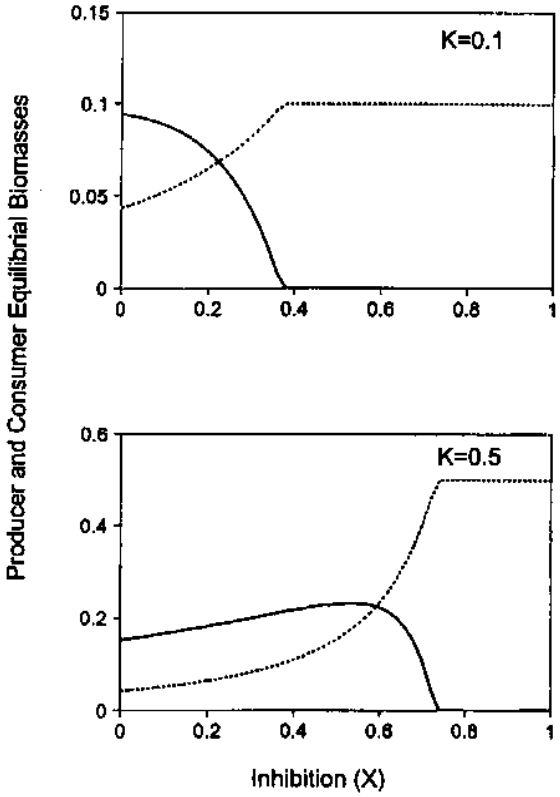

Figure 1. Predicted producer and consumer equilibrium biomasses for the basic model as a function of the scaled inhibitory effect of a toxicant for two values of producer carrying capacity; $K = 0.1$ and $K = 0.5$. Other parameter values were as follows: $a = 6.0$, $e = 0.5$, $d = 0.03$, $b = 0.1$, $r = 1.0$ and $\mu = 0.9$. Broken line – predicted producer equilibrial biomass. Solid line – predicted consumer equilibrial biomass.

formulae in that paper are greatly simplified by the assumption of a constant per capita death rate, the equilibrium values of the through stage survival for juveniles, S_J, and the mean fecundity, $\overline{\beta}$, being related to each other and to T_J by the equations

$$\overline{\beta} S_J = m, \qquad S_J = \exp(-mT_J). \tag{13}$$

2.3. Effects of a toxicant

We now consider the effects of a generic toxicant which influences rate processes in a manner similar to that proposed by Muller and Nisbet [8]. We assume that the toxicant enters the consumer directly from the environment and quickly attains a pseudo-equilibrium state in which the toxicant level in the animal is directly proportional to the ambient concentration. Then, as the ambient toxicant concentration increases, the assimilation rate reduces hyperbolically and the respiration rate increases linearly. The net assimilation efficiency, e is unchanged, but a and b change as follows:

$$a \to \frac{a}{1 + c/c_0}, \qquad b \to b(1 + c/c_0), \tag{14}$$

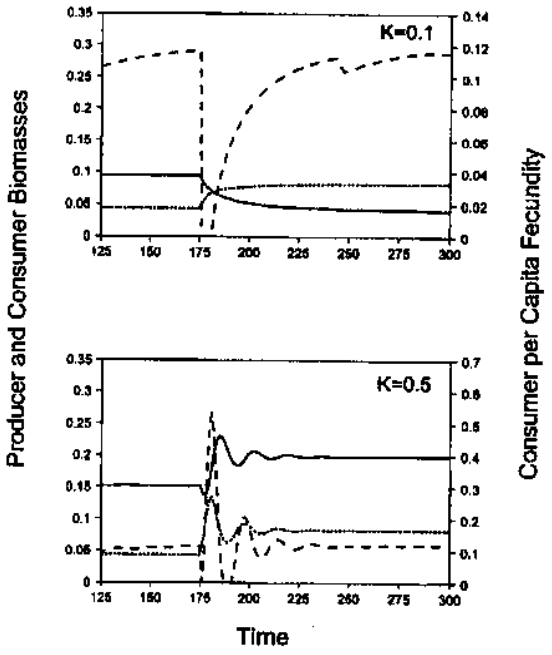

Figure 2. Producer and consumer biomasses, and consumer per capita fecundity for the basic model against time before and after the introduction of a toxicant at time $t = 175$. Results are shown for two different levels of producer carrying capacity; $K = 0.1$ and $K = 0.5$. The scaled inhibitory effect (X) of the toxicant was set equal to 0.3 in both cases. Parameter values as in figure 1 with in addition: $W_b = 1.0$, $W_m = 4.0$. Solid line – predicted producer biomass. Dotted line – predicted consumer biomass. Broken line – predicted consumer per capita fecundity.

where c_0, the half-saturation constant, is the concentration at which assimilation is halved and respiration is doubled. The toxicant reduces the weight specific assimilation rate a by an inhibition factor $X = c/(c + c_0)$, and increases the maintenance requirements.

Since the presence of a toxicant reduces a and increases b, it follows from equation (3), that toxicants increase the equilibrium producer density. However, the effect on the equilibrium consumer density depends on parameter values, and figure 1 exemplifies situations where consumer density may increase or decrease depending on the value of K. The eye-catching result is that the equilibrium consumer density may increase as a result of toxicant action. This arises because the combination of a reduced weight-specific feeding rate and a higher maintenance rate implies that a higher equilibrium food density is necessary to sustain a consumer population. And although the enhanced respiration mitigates the final result, a higher food density may support a higher consumer density (see equation (3)). This counter-intuitive result is analogous to what is predicted by existing fishery models: if the consumer is 'overfishing' at equilibrium, then a reduced fishing rate will ultimately yield a higher standing crop.

Figure 2 illustrates the effects of adding toxicant to a population initially at equilibrium in an uncontaminated environment. The biomass densities move to new values con-

sistent with the graphs in figure 1, but of more interest is the change in demographic quantities. The *initial* effect of the toxicant is to reduce (for example) the mean fecundity as predicted by equation (10), but equations (12) and (13) show that the *equilibrium* values of the consumer's demographic attributes are independent of a and b, the model parameters potentially affected by toxicants. Thus the effects of toxicant-induced changes in these parameters must ultimately be balanced by the effects of the increase in producer density. Figure 2 confirms this.

3. More complex dynamics

In the previous section, we assumed that the toxicant concentration within the consumer was always proportional to the level in the environment. However, many animals absorb contaminants by eating contaminated food, so that the internal concentration of toxicant at any time depends on the organism's feeding history. We now investigate a particularly simple model of this situation, using an unstructured formalism similar to that used in many models of elemental flow in microbiological systems (e.g., Kooijman [5], and references therein).

We use the term toxicant *density* to represent the amount of toxicant per unit of system volume. If absorbed by an organism, we say the toxicant is bound in that organism; otherwise we say it is in the 'environment'. The ambient toxicant density in the environment, $S_E(t)$, is just a regular concentration, but the toxicant densities in food and consumer, $S_F(t)$ and $S_C(t)$ respectively, are less intuitive quantities, being the total amount of toxicant bound in the food or consumer, scaled to the system volume. Such density measures are convenient, because they are not diluted by growth of the producer or consumer.

If toxicant enters the system at a volume-specific rate Γ, and is absorbed by the 'producer' organisms at a rate $\alpha F S_E$, then

$$\frac{dS_E}{dt} = \Gamma - \alpha F S_E + \text{'recycling'}, \qquad (15)$$

where the constant α can be interpreted in a manner analogous to the parameter a in equation (1), and represents the volume cleared of toxicant per unit time per unit biomass mass of producers. The term 'recycling' represents any toxicant that is released from organisms back to the environment, and is discussed later.

Absorption of toxicant causes the concentration of toxicant bound in the producers to increase at a rate $\alpha F S_E$. Toxicant is transferred to the consumer pool when contaminated food is eaten. Thus the concentration of toxicant bound in the producers obeys the equation:

$$\frac{dS_F}{dt} = \alpha F S_E - a C S_F. \qquad (16)$$

Modeling the amount of toxicant bound in the consumer introduces a few further subtleties. First, since a consumer only successfully absorbs a fraction e of ingested food, we require an assumption about the toxicant associated with the remaining unassimilated food. This requires a model of egestion and of subsequent processing of egested material in the environment. For maximum simplicity, we here assume that all toxicant in egested food is instantaneously recycled to the environment. Second, respiration does not affect the density (as defined above) of toxicant bound in the consumer. Third, we assume that toxicant bound in dead consumers disappears from the system. Then changes in S_C are described by the differential equation

$$\frac{dS_C}{dt} = eaCS_P - mC. \qquad (17)$$

The 'recycling' term in equation (15) is $(1-e)aCS_P$, and equation (15) becomes

$$\frac{dS_E}{dt} = \Gamma - \alpha F S_E + (1-e)aCS_P. \qquad (18)$$

The dynamics of the system are now described by five equations: (1), (2), (16), (17), and (18).

Our measure of bound toxicant density, though convenient for writing down balance equations, has little biological significance. A more meaningful measure is *toxicant quota*, q_F (or q_C), defined as the amount of bound toxicant per unit of producer (or consumer) biomass. With this definition,

$$S_F = F q_F \quad \text{and} \quad S_C = C q_C. \qquad (19)$$

We now assume that the consumer parameters, a and b, vary with toxicant quota in a manner similar to that implied by non-competitive inhibition. Thus in place of equation (14), we substitute

$$a \to \frac{a}{1 + q_C/q_0}, \qquad b \to b(1 + q_C/q_0). \qquad (20)$$

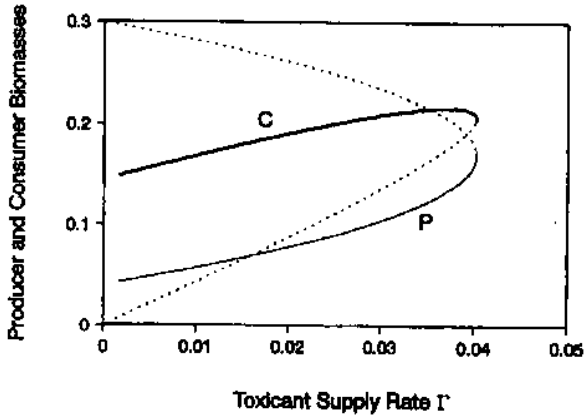

Figure 3. Predicted producer and consumer equilibrium biomasses as a function of the toxicant supply rate, Γ, for the model with toxicant absorbed via the food. Parameters are: $a = 6.0$, $e = 0.5$, $d = 0.03$, $b = 0.1$, $q_0 = 1$, $r = 1.0$ and $K = 0.3$. Thin line – predicted producer equilibrium biomass. Thick line – predicted consumer equilibrium biomass. Broken lines denote unstable equilibria. There is always an alternate, locally stable equilibrium with $P^* = 0.3$ and $C^* = 0.0$.

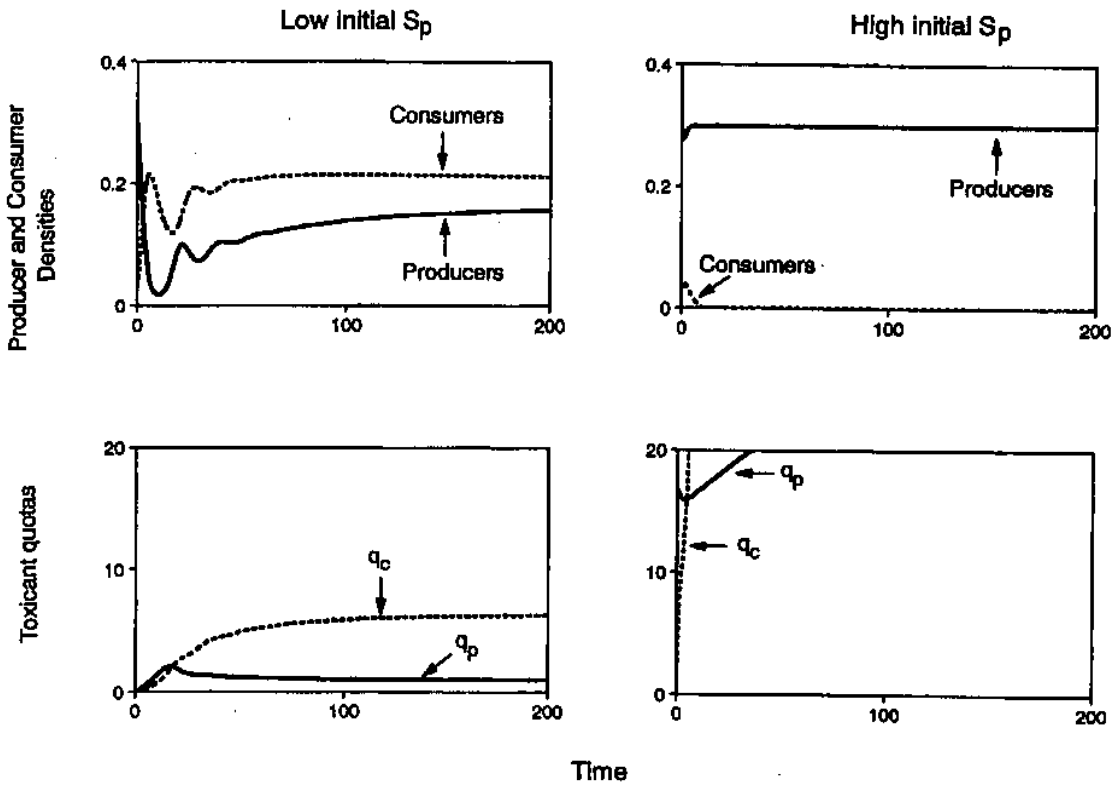

Figure 4. An example of the dependence of final system state on initial conditions for the situation depicted in figure 3. Two sets of numerical solutions are shown, with parameters as in figure 3, but different initial values of S_P, the concentration of toxicant bound in the producers.

Figure 3 shows the variation in producer and consumer equilibrium densities with changes in Γ, the toxicant supply rate. Comparison with figure 1 reveals many similarities, for example the existence of a critical toxicant supply rate above which the consumers are driven extinct. However, there is one noteworthy difference between the two figures: the existence in figure 3 over all values of Γ of multiple equilibria with the fate of the system depends on initial conditions. The continuous lines in that figure represent locally stable equilibria, the alternate stable equilibria having the producers at carrying capacity and the consumers extinct. Note that for these parameters, as the toxicant supply rate increases, the values of the stable equilibrium values of both producers and consumers also increase. However, the range of initial conditions that lead to extinction also increases. Figure 4 gives an example of trajectories approaching the different equilibria.

4. Discussion

The dynamics of ecological systems are complex, and realistic mathematical models are commonly analytically intractable. For this reason, it is useful to study caricatures of real systems in order to obtain intuition and insight into possible mechanisms. Progress then involves studying *both* simple *and* more complex models of the same system. This approach has proved successful in a number of population dynamic studies, where variants of a few models that exploit very simple assumptions (e.g., Lotka–Volterra, Nicholson–Bailey) are used to guide the formulation, analysis and testing of more realistic models (Murdoch and Nisbet [10] and references therein).

Using simple models, this paper explores the impacts of toxicants on population dynamics. We started by arguing that models of the population level consequences of toxicants should be based on dynamic energy budget models of individuals. Population dynamics are then derived using a well developed formalism for structured population models. In general, the resulting models are mathematically intractable and involve several partial differential equations that must be solved simultaneously. Numerical analysis of such equations is being used in some ecotoxicological studies (e.g., Hallam et al. [4]). Here we made a series of simplifying assumptions which lead to Lotka–Volterra-like, ordinary differential equations for biomass dynamics. Similarly, we simplified the description of toxicant action, and ignored subtleties associated with bioaccumulation. In the future, we will move towards more complex models in order to broaden our understanding of toxic impacts on populations.

Two 'take-home' messages emerged from this study. The first concerns how, following introduction to a closed, food-limited system, toxicants affect the short-term and long-term (multi-generation) behavior of populations. The short-term effect of a toxicant is similar to a step-down in food density: lower fecundity and slower juvenile development. However, these short term demographic changes lead to fluctuations in consumer density, which in turn cause fluctuations in producer density, and so on. The end result is the establishment of a new (higher) equilibrium producer density at which the fecundity and juvenile development time have the same values as in the uncontaminated environment. This precise result is a consequence of the very specific assumptions of our model, but the compensatory mechanisms just discussed will occur in any model of a closed system unless there are no density dependent rates in the consumers (Murdoch [9], Murdoch et al. [12]). We do *not* in general expect demographic quantities to return to their original values, but we *do* expect significant compensation.

The second conclusion from our study concerns the multiple equilibria found in the model where the toxicant entered the consumer via the producers. It is common to find complex dynamics in even the simplest population models, and it becomes important to evaluate the biological plausibility of the *mechanisms* behind the complexity. The multiple equilibria in our model arose because we included no mechanism to limit bioaccumulation in the producer population. Whether this assumption is reasonable or not depends on the system under study. The message is that population dynamics will be influenced strongly by the recycling of toxicant within the entire system, and that a realistic, DEB-based model of population dynamics will in general require coupling to a model of recycling within the system.

Acknowledgements

We thank Tom Hallam, Bas Kooijman, Dina Lika, Erik Noonburg, Andre de Roos, Russ Schmitt, Will Wilson for discussions and advice. This research was supported by the Office of Naval Research (Grant No. N00014-93-1-0952), and by the Minerals Management Service, U.S. Department of the Interior, under MMS Agreement No. 14-35-0001-30761. The views and conclusions contained in this document are those of the authors and should not be interpreted as necessarily representing the official policies, either express or implied, of the U.S. Government.

References

[1] U. Borgmann, E.S. Millard and C.C. Charlton, Effect of cadmium on a stable, large volume, laboratory ecosystem containing *Daphnia* and phytoplankton, Can. J. Fish. Aquat. Sci. 46 (1989) 399–405.

[2] P. Donkin et al., Quantitative structure-activity relationships for the effect of hydrophobic organic chemicals on rate of feeding by mussels (*Mytilus edulis*), Aquat. Toxicol. 15 (1989) 277–294.

[3] W.S.C. Gurney et al., Individual energetics and the equilibrium demography of structured populations, Theoret. Pop. Biol. 49 (1996) 344–368.

[4] T.G. Hallam and E.T. Funasaki, Ecotoxicological retrospective assessment: determination of causality from a model environment employing summary statistics, Env. Toxicol. Risk Ass., Modeling and Risk Assessment 6 (1996) (submitted).

[5] S.A.L.M. Kooijman, *Dynamic Energy Budgets in Biological Systems* (Cambridge University Press, New York, 1993).

[6] S.A.L.M. Kooijman and J.J.M. Bedaux, Analysis of toxicity test on *Daphnia* survival and reproduction, Water Res. 30 (1996) 1711–1723.

[7] J.A.J. Metz and O. Diekmann, *The Dynamics of Physiologically Structured Populations* (Springer, Berlin, 1986).

[8] E.B. Muller and R.M. Nisbet, Modeling the effect of toxicants on the parameters of dynamic energy budget models, Sym. Env. Tox. and Risk Ass., Modeling and Risk Assessment, ASTM STP 622 6 (1996) (submitted).

[9] W.W. Murdoch, Population regulation in theory and practice, Ecology 75 (1994) 271–287.

[10] W.W. Murdoch and R.M. Nisbet, Frontiers of population ecology, in: *Frontiers of Population Ecology*, eds. R.B. Floyd, A.W. Sheppard and P.J. De Barro (CSIRO Press, Melbourne, 1996) pp. 31–43.

[11] W.W. Murdoch et al., Individual-based models: combining testability and generality, in: *Individual-Based Models and Approaches in Ecology*, eds. D.L. DeAngelis and L.J. Gross (Routledge, Chapman and Hall, New York, 1992) pp. 18–35.

[12] W.W. Murdoch et al., Plankton abundance and dynamics across nutrient levels: tests of hypotheses, Ecology (1996) (submitted).

[13] R.M. Nisbet, A.H. Ross and A.J. Brooks, Empirically-based dynamic energy budget models: theory and an application to ecotoxicology, Nonlin. World 3 (1996) 85–106.

[14] S. Tuljapurkar and H. Caswell, *Structured Population Models in Marine, Freshwater, and Terrestrial Systems* (Chapman and Hall, New York, 1996).

[15] J. Widdows et al., Scope for growth and contaminant levels in North Sea mussels *Mytilus edulis*, Mar. Ecol. Progr. Ser. 127 (1995) 131–148.

Journal of Animal Ecology 2000, **69**, 913–926

From molecules to ecosystems through dynamic energy budget models

R. M. NISBET*, E. B. MULLER*, K. LIKA† and S. A. L. M. KOOIJMAN‡

**Department of Ecology, Evolution and Marine Biology, University of California, Santa Barbara, CA 93106-9610, USA; †Department of Biology, University of Crete, PO Box 2208, GR-71409 Iraklion-Crete, Greece; and ‡Department of Theoretical Biology, Vrije Universiteit, de Boelelaan 1087, 1081 HV Amsterdam, The Netherlands*

Summary

1. Dynamic energy budget (DEB) models describe how individuals acquire and utilize energy, and can serve as a link between different levels of biological organization.

2. We describe the formulation and testing of DEB models, and show how the dynamics of individual organisms link to molecular processes, to population dynamics, and (more tenuously) to ecosystem dynamics.

3. DEB models offer mechanistic explanations of body-size scaling relationships.

4. DEB models constitute powerful tools for applications in toxicology and biotechnology.

5. Challenging questions arise when linking DEB models with evolutionary theory.

Key-words: bioenergetics, dynamic energy budgets, ecosystems, ecotoxicology, population dynamics.

Journal of Animal Ecology (2000) **69**, 913–926

Introduction

One aim of theory in biology is to relate processes at different organizational levels (molecules, cells, organisms, populations, ecosystems). For example, the cell cycle may be described in terms of a sequence of molecular events, and population dynamics may be based on the dynamics of individual organisms interacting with their environment. The questions of interest are different at each level, but two basic principles invariably operate: biological systems obey the laws of thermodynamics and biological entities are the result of evolutionary processes. Thermodynamic laws constrain fluxes of energy and elemental mass, which are most conveniently identified at the level of individual organisms, while evolution makes stringent demands on the reproductive performance and viability of individuals. Thus, a general model describing the acquisition of energy by an individual organism, and its utilization for growth, reproduction and survival, has the potential to link to processes at other levels.

Correspondence: R.M. Nisbet, Department of Ecology, Evolution and Marine Biology, University of California, Santa Barbara, CA 93106-9610, USA. E-mail: nisbet@lifesci.ucsb.edu

A successful model based on such dynamic energy budgets (DEB) must be consistent with molecular, cellular and other suborganismal processes, and should provide the energetic basis for the dynamics of populations and ecosystems. Moreover, to make evolutionary sense, the model should recognize shared physiological and biochemical properties across a wide range of species, and must therefore aim at maximal generality.

Here, we discuss progress towards theory based on a DEB model. We review recent results regarding links between levels of biological organization, and we highlight open questions. We discuss how DEB models relate growth, reproduction and respiration of individual organisms to feeding, in a way that admits tests against experimental data. We show that DEB models yield insight on subcellular processes, and that they make testable predictions about the dynamics of populations. We conjecture that they will contribute to our understanding of ecosystems. Because of their generality, DEB models yield a theory of body-size scaling relationships, and are powerful tools for a diverse range of applications. The apparent successes of DEB models in describing a broad range of phenomena pose challenges for the theory of evolution of energy allocation strategies.

Principles of dynamic energy budget modelling

CONCEPTS AND MODEL FORMULATION

DEB models use differential equations to describe the rates at which individual organisms assimilate and utilize energy from food for maintenance, growth, reproduction and development. These rates depend on the state of the organism (age, size, sex, nutritional status, etc.) and the state of its environment (food density, temperature, etc.). Solutions of the model equations represent the life history of individual organisms in a potentially variable environment.

One important use of DEB models is to relate observed patterns of growth, development, reproduction and mortality in a particular organism to empirical information on feeding rates and maintenance requirements, the goal of such studies being to get a close match between data and model descriptions for a particular species (e.g. Gurney *et al.* 1990; McCauley *et al.* 1990; Ross & Nisbet 1990; Mangel 1996). A second use, which is the subject of this essay, takes a single, parameter-sparse, mechanistic model, and describes a broad spectrum of biological phenomena and life forms. Species differ only in their parameter values. A well-known example of this approach is the von Bertalanffy theory of growth (von Bertalanffy 1957), which fits the growth of many organisms very well with only two parameters. Von Bertalanffy based his work on a model by Pütter which assumes that the rate of growth of body mass is the difference between the rates of food uptake and utilization. If the former is proportional to surface area, the latter is proportional to body mass, and the shape of the organism does not change through life, then a measure L of the length of an organism of age, a, is given by $L = L_\infty - (L_\infty - L_b)[1 - \exp(-\gamma a)]$, where L_b and L_∞ represent, respectively, the length at birth and the ultimate length, and the parameter γ, commonly called the von Bertalanffy growth rate, characterizes the rate of approach to the final size.

Many empirically based population and evolutionary studies of energy budgets use 'net production' or 'scope for growth' models (e.g. Paloheimo *et al.* 1982; Ross & Nisbet 1990; Widdows & Donkin 1991; Nisbet *et al.* 1996; Andersen 1997; Lika & Nisbet, in press), which make assumptions about allocating the energy from food that remains after maintenance needs have been met. However, almost all work on such models focuses on a single life stage, and we are aware of no work with these models that links levels of biological organization. In this essay, we concentrate on the model for which the most comprehensive body of theory exists, namely the κ-rule model developed by Kooijman (1986, 1993, 2000). Our aim is *not* to evaluate this particular model in comparison with others. It is to *use* the model as a vehicle for demonstrating the power of DEB models in relating phenomena at different levels of organizations.

The physiological and physico-chemical rationale for the κ-rule model assumptions have been extensively discussed elsewhere (Kooijman 1993, 2000). Figure 1 shows the primary energy fluxes, and Tables 1 and 2 list the assumptions and some equations. Input of energy to an organism involves transfer of material across surfaces (gut wall, membranes of cells and organelles, etc.), before it is spent on volume-dependent processes, such as growth and maintenance (assumptions 1 and 3). As a result, many physiological rates can be expressed as a weighted sum of an area and volume measure; see for example the equations for reproduction and respiration in Table 2 and Fig. 2. An organism aims at a stable internal environment (homeostasis:

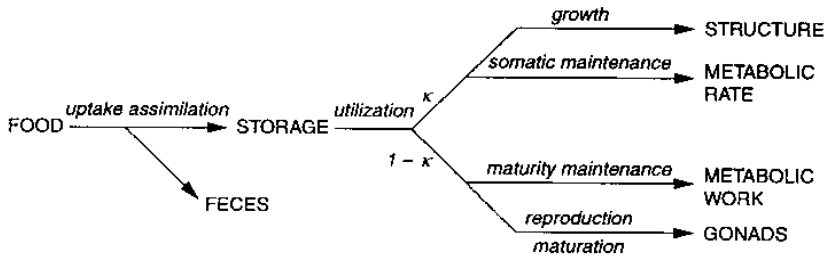

Fig. 1. An example of a DEB model (the κ-rule model of Kooijman 1993). An organism ingests food at a rate dependent on its size and the food density. Energy is extracted from food and added to the reserves. The rate at which energy becomes available to the organism depends on its size and stored energy density. Somatic maintenance has absolute priority for energy. By default, a fixed proportion κ of the available energy is allocated to somatic maintenance and growth combined, and the remaining $1-\kappa$ to either maturation (for embryos and juveniles) or to reproduction and maturity maintenance (for adults). Growth ceases when this fixed fraction κ just meets somatic maintenance demands. Then, the organism may still reproduce, provided that energy made available exceeds the requirements for somatic and maturity maintenance. (See Table 1 for assumptions and Table 2 for equations.)

Journal of Animal Ecology, **69**, 913–926

Table 1. Assumptions of the κ-rule DEB model. A mechanistic basis for these assumptions is presented in Kooijman 2000)

1. Food uptake is proportional to surface area and depends hyperbolically on food density.
2. The dynamics of energy density in reserves is a first order process, with a rate that is inversely proportional to the volumetric length.
3. A fixed fraction of the energy flowing out of the reserves is used for somatic maintenance plus growth (i.e. increase in structural biomass), the rest for maturity maintenance plus maturation or reproduction. This allocation rule is called the κ-rule.
4. The chemical compositions of structure and reserves are constant. Since the amount of reserves can change relative to the amount of structural biomass, the chemical composition of an individual may change. The following are constant:
   (i) the conversion efficiency of food into energy;
   (ii) the cost to maintain a unit of structural biovolume;
   (iii) the cost to maintain the acquired level of maturity.
5. Hazard rate (rate of ageing) is proportional to the accumulated 'damage'. In addition:
   (i) damage production is proportional to the changed DNA;
   (ii) DNA change is proportional to respiration.
6. If the investment into maturation exceeds a given threshold value, the organism changes its stage, i.e. it switches from the embryonic stage to the juvenile stage by initiating the feeding process, or from the juvenile stage to the adult stage by ceasing maturation and initiating the production of gametes (eggs, sperm). Asexually reproducing microorganisms behave as juveniles.
7. The initial conditions are:
   (i) initial structural biomass is negligibly small;
   (ii) reserve density at hatching equals that of mother at egg laying;
   (iii) initial damage is negligibly small.

Table 2. Equations of the κ-rule model for a growing organism. Dynamics of an organism experiencing food stress and of non-feeding life stages are detailed in Kooijman (1993)Q1

State variables	L: length (α cubic root of structural biovolume) $[E]$: stored energy density (i.e. stored energy per cubed length)
Environment	X: food density
Assimilation	$\{\dot{A}_m\} L^2 f; f = \frac{X}{K + X}$
Dynamics	$\frac{dL}{dt} = \frac{\dot{v}}{3} \frac{[E]/[E_m] - L_h/L_m - L/L_m}{g + [E]/[E_m]}$ $\frac{d[E]}{dt} = \frac{\{\dot{A}_m\}}{L}\left(f - \frac{[E]}{[E_m]}\right)$
Hazard rate	$h(t) = \dot{p}_a L^{-3} \int_0^t (L^3(\tau_1) - L_h^3 + \dot{m} \int_0^{\tau_1} L^3(\tau_2) d\tau_2) d\tau_1$
Reproductive rate	$\beta(t) \propto \frac{[E]/[E_m]}{g + [E]/[E_m]} (L_e L^2 + L^3) - L_p^3$
Primary parameters	
K	saturation coefficient
$\{\dot{A}_m\}$	maximum assimilation rate per surface area
$[E_m]$	maximum storage energy
$[\dot{M}]$	maintenance energy per unit size per unit time
$[G]$	energy costs for a unit increase in size
L_p	length at puberty
L_h	heating length (endotherms only)
κ	fraction of utilized energy spent on maintenance and growth
$\dot{p}_a$	ageing acceleration
μ	population growth rate
Compound parameters	
$\dot{v}$	energy conductance: $\frac{\dot{A}_m}{[E_m]}$
$\dot{m}$	maintenance rate coefficient: $\frac{\dot{M}}{[G]}$
g	investment ratio: $\frac{[G]}{\kappa[E_m]}$
L_m	maximum length: $\frac{\kappa\{\dot{A}_m\}}{[\dot{M}]} = \frac{\dot{v}}{\dot{m}g}$
L_e	reserve length: $\frac{\dot{v}}{\dot{m}} = gL_m$

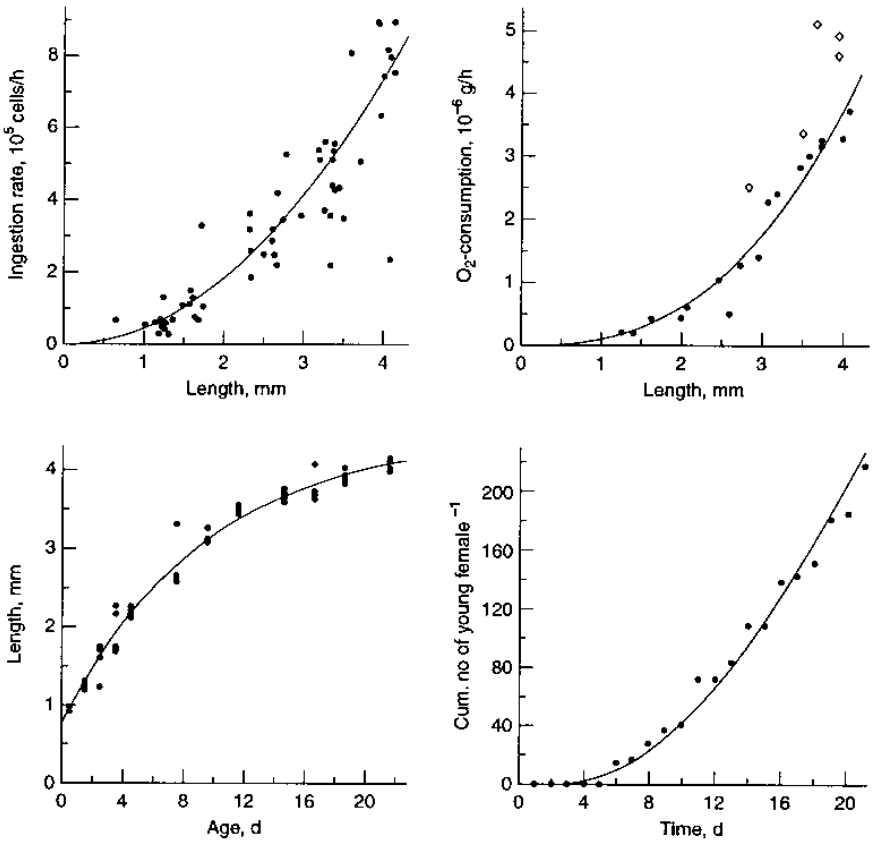

Fig. 2. The κ-rule model makes good predictions about feeding, respiration, growth and reproduction of *Daphnia magna* in a constant environment. The curves represent model fits to experimental results. The expressions above the graphs were derived from the rules in Table 1 and equations in Table 2. The estimated parameters are: von Bertalanffy growth rate γ (0·115 day^{-1}), ultimate length L_∞ (4·36 mm), reserve-length L_e (1·8 mm), length at puberty L_p (1·8 mm), maintenance rate coefficient [m (1·18 day^{-1}). Note that the reserve-length occurs in several expressions.

assumptions 2 and 4), and somatic and reproductive tissues compete for available energy (assumption 3).

Mathematically, the dynamics of a heterotrophic system are determined by two ordinary differential equations describing changes in size and density of reserves. Once these equations have been solved, many other quantities can be calculated. These include such obvious targets as reproductive output (see Table 2), but also ones that are less conspicuously part of the modelling framework, such as the development time of eggs, body composition in terms of macromolecules, and mass fluxes, e.g. respiration, disposal of nitrogen waste products and evaporation of water (Kooijman 1995). These latter calculations do not require new state variables, but do require information on the stoichiometry of the transformations being considered.

The basic model has one substrate ('food') and one type of reserve. It can be generalized in a systematic way to describe multiple substrates and many types of reserves (Kooijman 2000). The one-substrate, one-reserve model described above then emerges as a limiting case in two situations: if only one substrate is limiting, or if the relative abundance of substrate types is constant and turnover times of the various reserves have the same value. The multi-substrate generalizations are needed to describe the dynamics of autotrophic systems, since plants and algae experiencing a nutrient limitation maintain, in addition to energy reserves, stocks of nutrients. A description of their dynamics thus involves assumptions about these additional pools of nutrients (Zonneveld 1996; Zonneveld 1998a; Zonneveld 1998b; Kooijman 2000).

MODEL TESTING

DEB models make testable predictions about the performance of organisms in any given environment, and thereby help identify mechanisms respon-

Journal of Animal Ecology, **69**, 913–926

sible for observed patterns in experimental data. For example, the κ-rule model predicts that growth under constant environmental conditions is of the von Bertalanffy type, and that an adult may continue to reproduce long after growth has ceased. These qualitative features are observed in studies of many organisms, and constitute strong *prima facie* evidence that the model is capturing some essential, and very general, features of the dynamics of these individuals.

Direct testing of the core assumptions on energy allocation and homeostasis is remarkably difficult. Ideally, we require data on a large number of combinations of output variables and environment; this is seldom available. Access to data from dynamically varying environments is particularly important, since many model predictions regarding individual performance in an unchanging environment are insensitive to some of the assumptions. For example, experiments in which organisms grown in one food environment are transferred to higher or lower food are powerful (Kooijman 1986; Gurney *et al.* 1990; McCauley *et al.* 1990). A more fundamental difficulty is that the key state variables relate in subtle ways to experimental data. Size in a DEB model is really a measure of energy allocated to structural biomass, and energy stored in reserves is an experimentally elusive entity. Links between these state variables and real size and storage require new assumptions. Body mass in a DEB model combines the structural part and the energy reserves, and does not yield a direct measurement of either, although for micro-organisms, changes in body mass composition with population growth rate can be used to identify the contribution of structural biomass and reserves to each chemical compound (Muller 1994; Hanegraaf 1997; P.P.F. Hanegraaf *et al.*, unpublished). Similarly, assumptions about energy flows are not directly testable, as many flows (e.g. the 'utilization' flow in Fig. 1) are not measurable.

Many model tests are thus indirect. Parameters are estimated independently from data on (very) different physiological processes and checked for consistency. For example, the maintenance rate coefficient, a compound parameter defined as the ratio of the volume-specific maintenance and growth costs, has been estimated not only from data on weight loss during starvation, but also from data on respiration ontogeny during the embryonic period. Even data on the survival probability as a function of age give access to the maintenance rate parameter for individuals in laboratory conditions where the physiologically based 'hazard rate' in Table 2 can be assumed to be a major component of mortality (see Kooijman (1993) p. 109 for examples of such calculations for the pond snail *Lymnaea stagnalis*). As another example, data on respiration vs. size and on reproduction vs. age both yield estimates of the reserve-length, a parameter compounded from four primary parameters (see Table 2). Figure 2 illustrates that the same value for the reserve-length is appropriate in describing respiration and reproduction in the waterflea *Daphnia magna*. The figure also shows that growth and feeding are well described by the κ-rule model, using parameters consistent with the previous fits.

In the search for mechanisms, deviations from model predictions are at least as instructive as data that support it. For example, experiments on time to starvation in the pond snail *Lymnaea stagnalis* have shown that the length of day influences the allocation of energy to reproduction (Zonneveld 1992). This result has led to a modified version of the model, demonstrating that particular model elements may vary in some situations without destroying the basic integrity of the model structure (chapter 4 in Kooijman 1993). As another example, although the *Daphnia* data in Fig. 2 are consistent with the κ-rule model, many other published experiments on growth of individual *Daphnia* show a long-term upward trend in length that is not predicted by the model (Fig. 1 of McCauley *et al.* 1990; Noonburg *et al.* 1998). Prolonged growth may be the result of changing the priorities of energy allocation with age or may reflect slow adaptations that involve changes in other model parameters.

The fact that a large body of data is well described by the κ-rule model supports the view that although organisms are complex and differ greatly from each other, their basic features can be described using a common modelling framework. A challenge for rival models is to achieve similar width of coverage. A more demanding challenge is to design experiments capable of discriminating among rival DEB models, as well as to delineate the circumstances where predictions are insensitive to the choice of DEB model-for example Ross & Nisbet (1990) showed that a modified form of the κ-rule model and a net production model give equally good fits to data of growth of the marine mussel *Mytilus edulis*. This last issue affects strategy for DEB applications; for example, should a worker analysing the results of toxicity tests (see later section) be concerned about the choice of DEB model used in that work?

Linking levels of biological organization

The dynamics of individuals depend on cellular processes which, in turn, depend on molecular processes. Similarly, the cumulative performance of a large number of individuals determines the dynamics of a population and, ultimately, the dynamics of ecosystems. This section gives examples of how DEB models link the various levels of biological organization in such a way that the dynamics at different levels of organization are self-consistent.

Journal of Animal Ecology, **69**, 913–926

MOLECULAR PROCESSES

Dynamics at the individual level constrain processes at the molecular level. For example, a bacterium may increase the synthesis rates of macromolecules only if it has previously taken up sufficient nutrients and energy. Since uptake rates depend on size, so must synthesis rates. However, the relationship between rates of uptake and synthesis is indirect because of the role played by intermediate pools of intracellular metabolites. The link can be understood using the κ-rule model, through assumptions about the composition of structure and reserves (see Table 1). For example, fast-growing cells of *Escherichia coli* require rapid protein synthesis, and contain about 10 times as many ribosomes as cells in a poor environment (Bremer & Dennis 1987). The intracellular concentration of RNA, which is for the most part ribosomal RNA, thus increases drastically when food conditions improve. In the κ-rule model, a higher food level leads to an increase in the density of the energy reserves. Consequently a major part of ribosomal RNA may be interpreted as 'reserves', playing a key role in balancing the acquisition and utilization of energy in the cell. With this interpretation, the κ-rule model predicts relationships between the cell division rate, the turn-over rate of ribosomes, and the mean elongation rate, i.e. the rate at which ribosomes proceed along a strand of messenger RNA (Kooijman *et al.* 1991). These predictions correspond well with experimental results, see Fig. 3.

DEB models also provide an explanation for specialization in bacteria. Individuals that discard unnecessary genomic information are predicted to have a selective advantage over individuals from the parent strain (Stouthamer & Kooijman 1993). The argument uses two additional assumptions (cf. Donachie & Robinson 1987): a cell must achieve a certain critical size for DNA replication to start, and the duplication of DNA proceeds at a fixed rate. Then, cells with a smaller genome will divide at a smaller size, causing the mean cell size in a population to decrease. In non-filamentous organisms, the mean surface area to volume ratio then increases, which leads to a higher individual growth rate, a shorter division interval and, consequently, a higher population growth rate. In circumstances where natural selection acts to maximize population growth rate, cells with a large genome then have a selective disadvantage, even though the direct costs involved in maintaining and duplicating unnecessary DNA are negligibly low. A similar argument may be used to explain why some micro-organisms store the information on (large parts of) some metabolic routes on megaplasmids. The time to duplicate the genomic information decreases with the number of origins of replication, causing the mean cell size to decrease and the population growth rate to increase.

POPULATION DYNAMICS

Solution of DEB model equations provides life-history information, i.e. a schedule for reproductive output and one component of mortality, for organisms experiencing any given environment. This provides an opening to population dynamics.

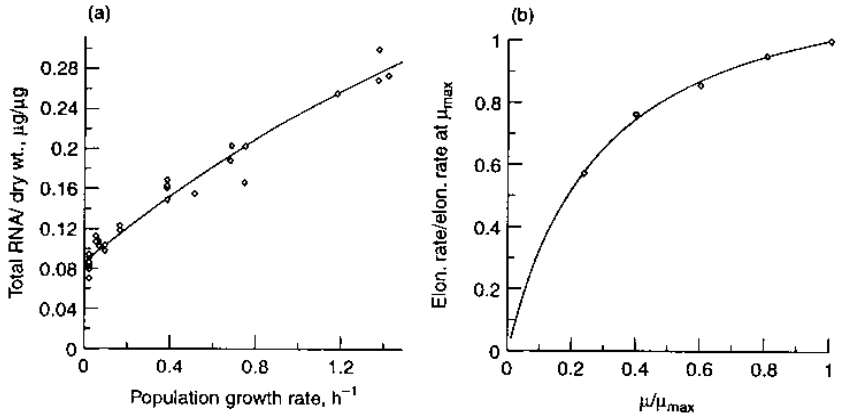

Fig. 3. The κ-rule model defines how the mass of structure and reserves change as a function of food conditions. This determines how principal biochemical components are partitioned between structure and reserves, and therefore how the concentrations of these components change as a function of the population growth rate, μ. In (a) this model expectation is fitted with measured RNA concentrations in *Escherichia coli* using three free parameters (data from Koch 1970). This partitioning also implies how the activity of principal biochemical components relates to the growth rate. In (b) the model fit of the mean elongation rate of ribosomes in *Escherichia coli* is shown using two free parameters (data from Bremer & Dennis 1987). See pp. 250–252 of Kooijman (1993) for details.

Journal of Animal Ecology, **69**, 913–926

In a constant environment a population will ultimately grow exponentially; and it is possible to calculate the rate of exponential growth in any given environment from generalizations of the Lotka equation. Such calculations motivated one of the earliest applications of DEB theory to ecotoxicology (Kooijman & Metz 1984). A population at equilibrium neither grows nor declines, implying that the average lifetime reproductive output, R_0, per individual in the population is one. If $S(t)$ denotes the proportional of a cohort that survive to age t, then

$$R_0 = \int_0^\infty \beta(t)S(t)dt \qquad \text{eqn 1}$$

Table 2 shows that the reproductive rate $\beta(t)$ can be obtained from the DEB model solutions which, in turn, depend on the food density in the environment (represented by the scaled functional response). Survival in most populations is determined in part by the hazard rate which is also obtained from the DEB model, but also by other factors (e.g. predation, parasitism) that are unrelated to energetics. Equation 1 can be solved to determine the food density at which the population will be in equilibrium. We can then calculate any demographic properties of a population at equilibrium (Gurney *et al.* 1996; de Roos *et al.* 1997), including time to reproductive maturity, mean fecundity of adults, and the ratio of adults to juveniles.

To move beyond representations of stationary, or exponentially growing, populations requires structured population models. These models relate the complete dynamics of a population to the dynamics of individual organisms and, in general, involve partial differential equations or integral equations (de Roos 1997). The equations simplify to a set of ordinary differential equations when all energy fluxes depend in a similar way on size (Kooijman 1993; Nisbet *et al.* 1997). This simplification is valid for filamentous organisms, approximately valid for micro-organisms and may be a reasonable approximation for many other organisms (Nisbet *et al.* 1997).

With the κ-rule model, further simplifications lead to equations that may still essentially capture the behaviour of a system and, in quite a few cases, are analogous to well-known model formulations. If fluctuations in energy reserves are ignored, the ordinary differential equations are equivalent to the Lotka–Volterra-like, biomass-based, dynamic equations widely used in modelling aquatic populations. Such biomass equations have been shown to yield predictions in good agreement with laboratory studies of zooplankton populations (Nisbet *et al.* 1997). They have also been successfully used to model competition among zooplankters in fluctuating environments (McCauley *et al.* 1996; Nisbet *et al.* 1997), and to study the stability of natural plankton assemblages (Murdoch *et al.* 1998). Similar biomass-based equations are widely used in microbiology; for example, the model of Marr and Pirt (Marr *et al.* 1962; Pirt 1965). This model without reserve dynamics simplifies further to the formulation of Monod (1942) when maintenance requirements are ignored. If, conversely, reserve dynamics are considered but maintenance requirements are omitted, the Marr–Pirt model is consistent with the formulation of Droop (1973). The DEB model is not only a close relative of this highly successful model; it also provides a mechanistic explanation of it.

The power of the DEB approach becomes really apparent in situations where it is not legitimate to neglect fluctuations in reserve density. Energy reserves act as a buffer between an organism's demand and a potentially variable environment and may therefore strongly affect the pattern of population fluctuations (Kooi & Kooijman 1994a; Kooi & Kooijman 1994b; Kooi & Kooijman 1997; Kooi *et al.* 1999). Figure 4 demonstrates the importance of reserves for a food chain with substrate, bacteria and slime moulds. The quality of the fit by the κ-rule model is striking when compared with previous attempts that did not consider reserve dynamics (Tsuchiya *et al.* 1972; Bazin *et al.* 1974; Bazin & Saunders 1979). Figure 4 illustrates this comparison for one of the traditional models, the Monod model. This failure of traditional models indeed led to the controversial speculation that feeding rates are determined by the level of resource per consumer rather than by resource level itself, an idea that ecologists revisit intermittently as in the recent explosion of interest in 'ratio dependence' (Arditi & Ginzburg 1989; Arditi *et al.* 1991). As Fig. 4 shows, however, the feeding rate may reasonably be assumed to depend directly on the resource level, provided the importance of energy reserves in a variable environment is recognized.

ECOSYSTEM DYNAMICS

There is a long tradition of measurement and modelling of energy flows in ecosystems. DEB theory may contribute to this effort. In ecosystem modelling, the state variables relate to energy and elemental matter within functional groups of populations, such as primary producers and herbivores. As with population models, simplification to a system of ordinary differential equations is possible when feeding and maintenance rates scale in identical manner with body size (Kooijman & Nisbet 2000). In ecosystems, such scaling may arise for two very different reasons. First, if a single species dominates the functional group, the simplifications described in the section on population dynamics may be applicable. The second possibility is that a functional group contains a number of species with the overall spec-

Journal of Animal Ecology, **69**, 913–926

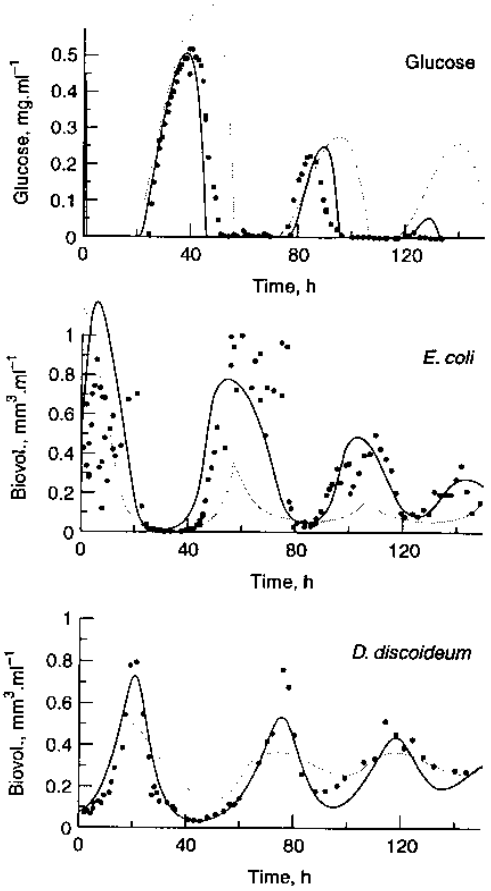

Fig. 4. Fits of the κ-rule model (solid line) and Monod model (dotted line) to data from a food chain in a continuous culture. The food chain consists of glucose X_0, the bacterium *Escherichia coli* X_1 and the slime mold *Dictyostelium discoideum* X_2. The variables e_1 and e_2 represent scaled measures of reserve density in the bacteria and slime mould, respectively. The dilution rate $p = 0{\cdot}064\,h^{-1}$ and glucose concentration in the feed $X_r = 1$ mg ml^{-1}.
The κ-rule parameter values and equations are as follows.

$X_0(0)$:	0·582 mg ml^{-1}		
$X_1(0)$:	0·466 mm^3	$X_2(0)$:	0·069 ml^{-1}
$e_1(0)$:	1 –	$e_2(0)$:	1 –
K_1 :	0·443 μg/ml	K_2:	0·180 mm^3/ml
g_1 :	0·861 –	g_2:	4·430 –
$\dot{m}_1$:	0·008 h^{-1}	$\dot{m}_2$:	0·158 h^{-1}
$\dot{v}_1$:	0·689 h^{-1}	v_2:	2·046 h^{-1}
$[\dot{I}_m]_1$:	0·651 mg/mm^{-3} h	$[\dot{I}_m]$:	20·262 h^{-1}

trum of sizes much larger than the size range spanned by any one species. The feeding and assimilation rates of an individual are proportional to surface area (see Table 1), but the theory of body-size relationships discussed in the next section predicts that the constants of proportionality depend linearly on the maximum body length an organism can attain. Thus, the feeding rate of a functional group of organisms scales as a volume. If maintenance rate is still assumed to be proportional to volume, then a functional group both feeds and expends energy on maintenance at rates proportional to the total volume it occupies.

The full potential of DEB models for ecosystem modelling is unknown, since the only examples known to the authors do not explicitly recognize reserves. Yet, there are models of flow of energy and elements that make a convincing case that ecosystems do truly have dynamics. The state of the art is well illustrated by models of carbon and nitrogen dynamics in three fjord ecosystems (Scottish sea lochs) (Ross *et al.* 1993a; Ross *et al.* 1993b; Ross

Journal of Animal Ecology, **69**, 913–926

et al. 1994; Gurney & Nisbet 1998). The model subdivides the loch into compartments, with water flow between compartments. The fjord exchanges water with the open ocean. The food chain has three components: primary producers, herbivores (predominantly copepods), and carnivores (predominantly jellyfish). Figure 5 compares observed concentrations of phytoplankton and of dissolved inorganic nitrogen with predictions from a model of this sort. Model parameters are estimated either from independent data, or by fitting using only data from one loch. The trajectories for the other lochs are then well predicted on the assumption that the biological interactions are unchanged, and that only differences between the three systems lie in the values taken by hydrodynamic parameters.

Life histories and body-size relationships

DEB model assumptions also have implications for *inter*specific comparisons of physiological rates. In DEB theory *intra*specific differences in physiological rates derive solely from different values of state variables. By contrast, individuals of different species also have different parameter values: an adult mouse and juvenile rat of the same size grow and reproduce at entirely different rates, despite their similarity in size. Kooijman (1988, 1993; chapter 6) showed that the assumptions in Table 1 imply that parameter values will tend to co-vary among species, since the maximum body length, L_m, is a simple function of model parameters.

Parameters can be classified as being either 'intensive' or 'extensive'. An intensive parameter characterizes molecular processes, which depend on densities. Because densities do not scale with size, interspecific changes in the values of an intensive parameter do not vary among species in a systematic way. Extensive parameters, by contrast, relate to physical design, and can be shown to scale with maximum body length. Since most physiological quantities, including L_m itself, are functions of intensive and extensive parameters, it is possible to represent these quantities as functions of L_m, and thereby derive body size scaling relations.

Using this line of reasoning, the von Bertalanffy growth rate at high food levels turns out to be approximately inversely proportional to maximum length. Figure 6a tests this prediction with data from a wide variety of organisms, whose maximum sizes

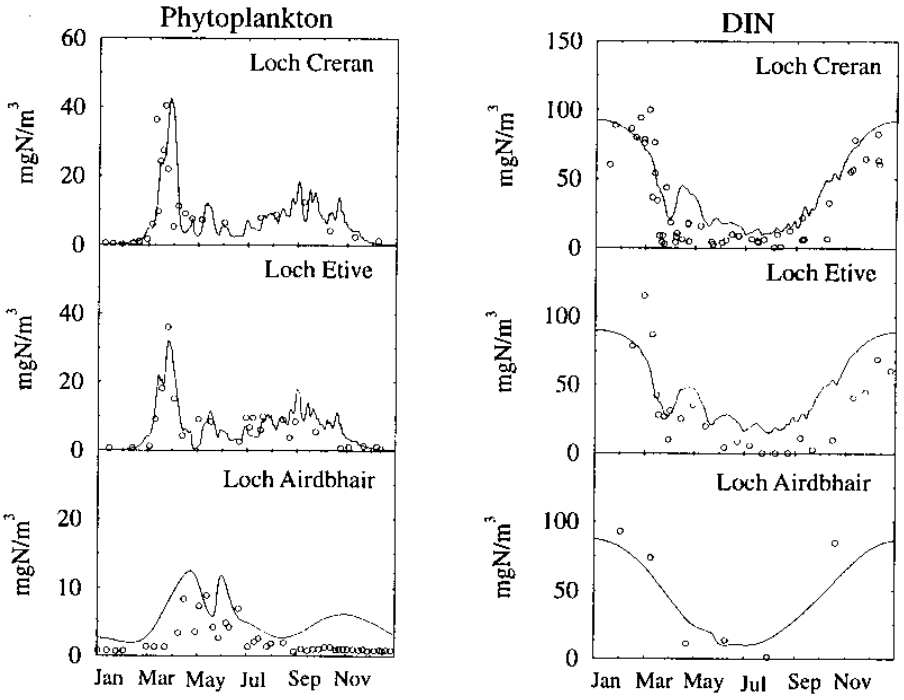

Journal of Animal Ecology, **69**, 913–926

Fig. 5. Comparison of the annual cycle in phytoplankton and in disolved inorganic nitrogen (DIN) predicted by the sea-loch model in Gurney & Nisbet (1998) with the observed annual cycles in the three Scottish sea-lochs. The 'biological' parameters take the same values in each system; the hydrodynamic parameters differ. Reproduced with permission of W.S.C. Gurney.

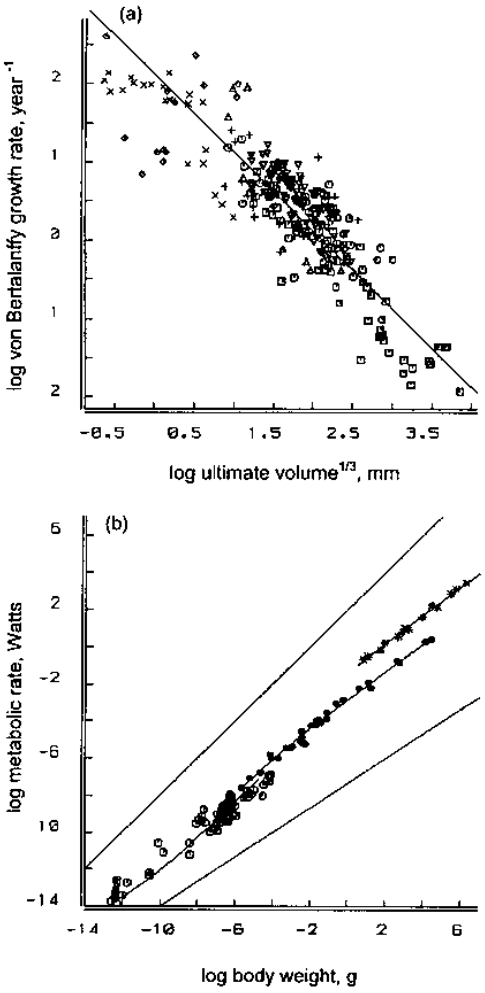

Fig. 6. The DEB model predicts interspecific body size scaling relationships. (a) The scaling of the von Bertalanffy growth rate as a function of the ultimate size of birds (▽), mammals (□), reptiles and amphibians (△), fish (○), crustaceans (×), molluscs (+), other species (◇) and model expectation (line). Data have been normalized to a body temperature of 25°C using the Arrhenius' relationship (see Kooijman 2000, p. 282 for further details). (b) The metabolic rate as a function of body weight of unicellulars (○, at 20°C), ectotherms (●, at 20°C) and endotherms (✳, at 39°C). The metabolic rate is proportional to the respiration rate. The slope of the upper and lower line represent allometric scalings with body weight to the power 2/3 and 1, respectively. Other curves represent model fits to the data (see Kooijman 2000, p. 272).

cover a range of more than four orders of magnitude. The environmental conditions at which many of these data were collected are unknown and may explain part of the scatter in the data. Also, variability in the life-history parameter κ, a constituent of the von Bertalanffy growth rate, may have caused some scatter. However, the trend is consistent with the κ-rule model.

The interspecific variation of the weight-specific respiration rate can be derived along similar lines. In ectothermic species, it is predicted to decrease as body weight increases, because reserves (which are assumed not have maintenance requirements) then represent an increasing proportion of the organism's weight. Total respiration rate turns out to be a linear combination of terms proportional to the maximum surface area and the maximum volume of a species. This apparently contrasts with the many empirical studies that describe the relationship allometrically as maximum body volume raised to some power. However, graphs of both relationships are almost identical if the exponent in the allometric relationship has a value in the range 0·66–1·0, the maximum span consistent with DEB theory. This range contains the popularly quoted value of 0·75 as well as most empirical estimates for groups of organisms (Calder 1984; West *et al.* 1997). Figure 6b demonstrates the ability of DEB theory to describe the scaling of respiration rate with body size in unicellulars, ectotherms and endotherms.

Coincidentally, the κ-rule model predicts that respiration rate scales with size in a broadly similar way intraspecifically, although, as explained above, the mechanisms involved are different from those generating the interspecific relationships. Individuals of the same species differ in values of the state variables, not in parameter values. Because small individuals invest relatively more energy in growth than large ones, the respiration rate is a linear combination of the actual surface area and volume of an organism. This relationship is again often close to the empirical result that respiration rates are proportional to volume to the power 0·75.

Not every parameter is predicted to vary systematically from species to species. Life-history parameters representing, for example, strategic choices about energy allocation (e.g. the parameter κ) and the critical size for changing a life stage (L_p), are likely to be adaptive. The theory only predicts interspecific variations in parameters representing physiological and biochemical processes.

As noted earlier, deviations from the predictions of mechanistic models can be most instructive. When a particular species deviates from expected interspecific patterns, we can look for the responsible parameters, and obtain a better understanding of why this species differs from others. For example, tube noses incubate their eggs for a long time in comparison with other similarly sized birds. Also, this species has relatively large eggs and large hatchlings. However, when the incubation time is corrected for egg size, those differences disappear (see p. 232 in Kooijman 1993). Understanding their long incubation time thus involves their relatively large egg size. Further analysis reveals that if a species increases egg size, it will have a shorter chick stage, with this reduction exceeding the increase in

Journal of Animal Ecology, **69**, 913–926

incubation time. As a result, the breeding season becomes shorter, which makes ecological sense for open ocean birds.

In summary, DEB models can be used to derive interspecific scaling relationships between physiological attributes and body size. The derivation does not invoke any optimization arguments. Here the DEB approach contrasts with other theories of metabolic scaling, such as the recent model of West *et al.* (1997) that assumes minimization of the energy required to transport metabolites in an isomorphic, space-filling, fractally branching tube system. Childress & Somero (1990) take an intermediate position regarding the role of evolution, in which they contrast the tight scaling of aerobic metabolic power in fish, with high, size-dependent variability in anaerobic power (a significant component to total output in skeletal muscle) and argue that natural selection played a major role only in determining the strength of the anaerobic contribution. An important challenge for theorists and experimentalists is to identify ways of testing these theories.

Applications

Mechanistic models can be of great value in applied science, and offer many benefits over pure empiricism. Consider, for instance, the responses of laboratory animals in routine toxicity tests. The longer the experiment lasts and the smaller the organisms are, the more drastic the observed response will be. The observed effects thus depend on experimental design, a fact that obviously complicates the formulation of toxicological standards. We illustrate below that the dependence of results on time and size can be understood with DEB models; several formulations were, in fact, developed to address this kind of problem (Hallam *et al.* 1989; Kooijman & Bedaux 1996a). We also briefly describe how DEB theory is used in biotechnological problems.

Toxic compounds may affect growth, reproductive output and survival. In a DEB model, a description of toxic effects is based on mechanisms that identify the target parameters and quantify the effects in terms of the body burden of toxicant. The body burden of toxicant depends on the organism's abilities to metabolize toxicants and on uptake and elimination characteristics. These processes depend, in turn, on attributes of an organism, such as the size and lipid content, that are described by the model (Lassiter & Hallam 1988; Kooijman & Haren 1990). Toxic effect models based on those tightly related principles that satisfactorily describe experimental data covering a wide range of toxicants, species and DEB-defined processes (Kooijman & Bedaux 1996b; Kooijman & Bedaux 1996c; Muller & Nisbet, unpublished).

One advantage of an approach using DEB models is that the parameters describing toxicological effects represent the organism's sensitivity to a compound, and are independent of experimental protocol (e.g. exposure time). This does not hold for classic measures, such as the LC50 and EC50. The no-effect concentration, which defines the highest concentration that will never cause an effect, may be used as a model parameter. This quantity is more relevant than the no-observed-effect concentration, a measure that is often used in risk assessment studies, but which has serious methodological and statistical problems (Kooijman & Bedaux 1996d). Another benefit from using a DEB model is that the toxicity of a compound can be related to its physico-chemical properties, such as degree of ionization and fat solubility. In addition to physico-chemical data, a description of a class of similarly acting compounds only requires a proportionality factor and toxicological data on a single member (Kooijman & Bedaux 1996a).

In biotechnology, DEB models aid the design and operation of production and treatment plants. DEB models have been used to describe the formation rates of biomass, fermentation products, such as ethanol, and secondary products, such as penicillin (Hanegraaf 1997). They are therefore useful in deriving the economically optimal conditions for biotechnological production. Likewise, DEB models are involved in the design and operation of sewage treatment plants, which produce much bacterial biomass (sludge), a product that needs to be processed at considerable costs. Since waste water contains food for bacteria, sludge production is minimized by increasing the sludge content of the treatment plant (Muller *et al.* 1995). Sludge production is also minimized by increasing the abundance of bacterial grazers (Ratsak *et al.* 1993; Ratsak *et al.* 1994; Ratsak *et al.* 1996).

Future challenges: DEB models in evolutionary time

Throughout this article we have identified areas of DEB theory that are ripe for future research. However, probably the most pressing challenge is to relate DEB models to the mainstream of evolutionary theory. To date, the most powerful contribution of DEB models has been to identify body-size scaling relationships that may be understood without appeal to optimization, or to other evolutionary concepts. There remain many questions requiring consideration of changes over evolutionary time. Here we highlight two.

First, we do not have a good understanding of the patterns of interspecific variation in those DEB parameters that describe adaptive traits, for example κ, which quantifies partitioning of energy between growth and reproduction, or the critical parameters

Journal of Animal Ecology, **69**, 913–926

that determine the timing of transitions between life stages. The natural (and traditional) starting point for such a study is to investigate how a change in a parameter value affects the expected lifetime reproductive output of an individual in a population at equilibrium (R_0) (e.g. Sibly & Calow 1986 and references therein; Stearns & Hoekstra 2000 and references therein). By using a DEB-based formula for R_0 (see equation 1), we ensure that energetic-based trade-offs are incorporated. When an individual with a modified parameter value appears in a population at equilibrium, it will be favoured by selection if it is able to replace itself at a lower food density than the current equilibrium density. In other words, a change in parameter values is advantageous when R_0 is larger than one at the current food conditions. Very few such calculations have been attempted (e.g. chapter 4 in Gurney & Nisbet 1998; Lika & Nisbet 2000).

However, a much more fundamental challenge is to predict a priori the appropriate strategy for allocation of energy in organisms that exhibit simultaneous commitment to growth and reproduction. Simple models of energy allocation suggest that in a constant environment, the optimal strategy for an individual is the 'bang-bang' option of committing 100% of net production (assimilation less maintenance) to growth until a certain age, and thereafter 100% to reproduction (e.g. Bulmer 1994). While consistent with the life histories of some organisms, the bang-bang strategy is not followed by the many organisms that simultaneously grow and reproduce, and which motivated the development of the κ-rule model. An analysis of allocation strategies in the latter model showed that there are circumstances where bang-bang allocation is inferior to a constant-fraction allocation to reproduction (L. Lika & S.A.L.M. Kooijman, unpublished). This is because the κ-rule model recognizes costs and trade-offs in juvenile development that are absent in the simpler models. The most commonly invoked explanation for the existence of mixed allocation strategies is bet-hedging in a spatially or temporally variable environment (Cohen 1966; King & Roughgarden 1982a; King & Roughgarden 1982b; Bulmer 1994). Thus, DEB modelling reopens the debate on whether or not mixed strategies are an evolutionary response to uncertain environments.

Acknowledgements

We thank W.S.C. Gurney, E. McCauley, W.W. Murdoch, A.M. de Roos, and W.G. Wilson for many discussions of dynamic energy budget models, and J.H. Brown, J.J. Childress, and B. Enquist for discussions of scaling relations. We thank A. Brooks, L. Goldwasser, P. Hosseini, E. Noonburg, and W.G. Wilson for comments on earlier drafts of the MS. The research was supported by the National Center for Ecological Analysis and Synthesis (NCEAS), the US Office of Naval Research, and by the US Minerals Management Service, US Department of the Interior, under MMS Agreement no. 14-35-0001-30761. The views and conclusions contained in this document should not be interpreted as necessarily expressing the official policies, either express or implied, of the US Government. It was also supported by grant 013/1204.10 to SALMK from the Dutch Goverment, National Research Programme on global air pollution and climate change.

References

Andersen, T. (1997). *Pelagic Nutrient Cycles: Herbivores as Sources and Sinks*. Springer-Verlag, Berlin.

Arditi, R. & Ginzburg, L.R. (1989) Coupling in predator–prey dynamics: ratio-dependence. *Journal of Theoretical Biology*, **139**, 311–326.

Arditi, R., Ginzburg, L.R. & Akcakaya, H.R. (1991) Variation in plankton densities among lakes: a case for ratio-dependent predation *Models American Naturalist, Bf*, **138**, 1287–1296.

Bazin, M.J., Rapa, V. & Saunders, P.T. (1974) The integration of theory and experiment in the study of predator–prey dynamics. *Ecological Stability* (eds M. Usher & M. Williamson). Chapman & Hall, London.

Bazin, M.J. & Saunders, P.T. (1979) An application of catastrophe theory to study a switch in *dictyostelium discoideum*. *Kinetic Logic: A Boolean Approach to the Analysis of Complex Regulatory Systems* (ed. R. Thomas) pp. 481–501. Springer-Verlag, Berlin.

von Bertalanffy, L. (1957) Quantitative laws in metabolism and growth. *Quarterly Review of Biology*, **32**, 217–231.

Bremer, H. & Dennis, P.P. (1987) Modulation of chemical composition and other parameters of the cell by growth rate. *Escherichia Coli and Salmonella Typhimurium* (ed. F. Neidhardt), pp. 1527–1542. American Society of Microbiology, Washington.

Bulmer, M. (1994) *Theoretical Evolutionary Ecology*. Sinauer.

Calder,W.A.C. III (1984) *Size, Function and Life History*. Harvard University Press, Cambridge, Mass.

Childress, J.J. & Somero, G.N. (1990) Metabolic scaling: a new perspective based on scaling of glycolytic enzyme activities. *American Zoologist*, **30**, 161–173.

Cohen, D. (1966) Optimizing reproduction in a randomly varying environment. *Journal of Theoretical Biology*, **12**, 110–129.

Donachie, W.D. & Robinson, A.C. (1987) Cell division: parameter values and the process. *Escherichia coli and Salmonella typhimurium* (ed. F. Neidhardt), pp. 1578–1593, American Society of Microbiology, Washington.

Droop, M.R. (1973) Some thoughts in nutrient limitations in algae. *Journal of Phycology*, **9**, 264–272.

Gurney, W.S.C., McCauley, E., Nisbet, R.M. & Murdoch, W.W. (1990) The physiological ecology of *Daphnia*: formulation and tests of a dynamic model of growth and reproduction. *Ecology*, **71**, 716–732.

Gurney, W.S.C., Middleton, D.A.J., Nisbet, R.M., McCauley, E., Murdoch, W.W. & de Roos, A.M. (1996) Individual energetics and the equilibrium demography of structured populations. *Theoretical Population Biology*, **49**, 344–368.

Gurney, W.S.C. & Nisbet, R.M. (1998). *Ecological Dynamics*. Oxford University Press, Oxford.

Journal of Animal Ecology, **69**, 913–926

Hallam, T.G., Lassiter, R.R. & Kooijman, S.A.L.M. (1989) Effects of toxicants on aquatic populations. *Applied Mathematical Ecology, Vol 18* (eds S. Levin, T. Hallam & L. Gross), pp. 352–382. Springer-Verlag, Berlin.

Hanegraaf, P.P.F. (1997) *Mass and energy fluxes in microorganisms according to the Dynamic Energy Budget theory for filaments.* PhD Thesis, Vrije Universiteit, Amsterdam.

King, D. & Roughgarden, J. (1982a) Graded allocation between vegetative and reproductive growth for annual plants in growing seasons of random length. *Theoretical Population Biology*, **22**, 1–16.

King, D. & Roughgarden, J. (1982b) Multiple switches between vegetative and reproductive growth in annual plants. *Theoretical Population Biology*, **21**, 194–204.

Koch, A.L. (1970) Overall controls on the biosynthesis of ribosomesin growing bacteria. *Journal of Theoretical Biology*, **28**, 203–231.

Kooi, B.W., Boer, M.P. & Kooijman, S.A.L.M. (1999) Resistance of a food chain to invasion by a top predator. *Mathematical Biosciences*, **157**, 217–236.

Kooi, B.W. & Kooijman, S.A.L.M. (1994a) Existence and stability of microbial prey–predator systems. *Journal of Theoretical Biology*, **170**, 75–85.

Kooi, B.W. & Kooijman, S.A.L.M. (1994b) The transient behaviour of food chains in chemostats. *Journal of Theoretical Biology*, **170**, 87–94.

Kooi, B.W. & Kooijman, S.A.L.M. (1997) Population dynamics of rotifers in chemostats. *Nonlinear Analysis-Theory Methods and Applications*, **30**, 1687–1698.

Kooijman, S.A.L.M. (1986) Population dynamics on basis of budgets. *The Dynamics of Physiologically Structured Populations* (eds J. Metz & O. Diekmann), pp. 266–297. **Vol. 68** of *Lecture Notes in Biomathematics*. Springer-Verlag, Berlin.

Kooijman, S.A.L.M. (1988) The von Bertalanffy growth rate as a function of physiological parameters: a comparative analysis. *Mathematical Ecology* (eds T. Hallam, L. Gross & S. Levin), pp. 3–45. World Scientfic, Singapore.

Kooijman, S.A.L.M. (1993) *Dynamic Energy Budgets in Biological Systems: Theory and Applications in Ecotoxicology*. Cambridge University Press, New York.

Kooijman, S.A.L.M. (1995) The stoichiometry of animal energetics. *Journal of Theoretical Biology*, **177**, 139–149.

Kooijman, S.A.L.M. (2000) *Dynamic Energy Mass Budgets in Biological Systems*. Cambridge University Press, Cambridge.

Kooijman, S.A.L.M. & Bedaux, J.J.M. (1996a) *The Analysis of Aquatic Toxicity Data*. VU University Press, Amsterdam.

Kooijman, S.A.L.M. & Bedaux, J.J.M. (1996b) Analysis of toxicity tests on *Daphnia* survival and reproduction. *Water Research*, **30**, 1711–1723.

Kooijman, S.A.L.M. & Bedaux, J.J.M. (1996c) Analysis of toxicity tests on fish growth. *Water Research*, **30**, 1633–1644.

Kooijman, S.A.L.M. & Bedaux, J.J.M. (1996d) Some statistical properties of estimates of no-effect concentrations. *Water Research*, **30**, 1724–1728.

Kooijman, S.A.L.M. & Haren, R.J.F. (1990) Animal energy budgets affect the kinetics of xenobiotics. *Chemosphere*, **21**, 681–693.

Kooijman, S.A.L.M. & Metz, J.A.J. (1984) On the dynamics of chemically stressed populations: the deduction of population consequences from effects on individuals. *Ecotoxicology and Environmental Safety*, **8**, 254–274.

Kooijman, S.A.L.M., Muller, E.B. & Stouthamer, A.H. (1991) Microbial dynamics on the basis of individual budgets. *Antonie Van Leeuwenhoek*, **60**, 159–174.

Kooijman, S.A.L.M. & Nisbet, R.M. (2000) How light and nutrients affect life in a closed bottle. *Thermodynamics and Ecological Modelling* (ed. S.E. Joirgensen) pp. 19–60. Lewis Publishers, New York (in press).

Lassiter, R.R. & Hallam, T.G. (1988) Survival of the fattest: a theory for assessing acute effects of hydrophobic, reversibly acting chemicals on populations. *Ecology*, **109**, 411–429.

Lika, L. & Nisbet, R.M. (in press) A dynamic energy budget model based on partitioning of net production. *Journal of Mathematical Biology*.

Mangel, M. (1996) Computing expected reproductive success of female Atlantic salmon as a function of smolt size. *Journal of Fish Biology*, **49**, 877–882.

Marr, A.G., Nilson, E.H. & Clark, D.J. (1962) The maintenance requirement of *Escherichia coli*. *Annals of the New York Academy of Sciences*, **102**, 536–548.

McCauley, E., Murdoch, W.W., Nisbet, R.M. & Gurney, W.S.C. (1990) The physiological ecology of *Daphnia*: development of a model of growth and reproduction. *Ecology*, **71**, 703–715.

McCauley, E., Nisbet, R.M., de Roos, A.M., Murdoch, W.W. & Gurney, W.S.C. (1996) Structured population models of herbivorous zooplankton. *Ecological Monographs*, **66**, 479–501.

Monod, J. (1942) *Recherches Sur la Croissance Des Cultures Bacteriennes*, 2nd edn. Herman, Paris.

Muller, E.B. (1994) *Bacteria energetics in aerobic wastewater treatment.* PhD Thesis, Vrije Universiteit, Amsterdam.

Muller, E.B., Stouthamer, A.H., van Verseveld, H.W. & Eikelboom, D. (1995) Aerobic domestic waste water treatment in a pilot plant with complete sludge retention by cross-flow filtration. *Water Research*, **29**, 1179–1189.

Murdoch, W.W., Nisbet, R.M., McCauley, E., de Roos, A. & Gurney, W. (1998) Plankton abundance and dynamics across nutrient levels: tests of hypotheses. *Ecology*, **79**, 1339–1356.

Nisbet, R.M., McCauley, E., Gurney, W.S.C., Murdoch, W.W. & de Roos, A.M. (1997) Simple representations of biomass dynamics in structured populations. *Case Studies in Mathematical Modeling: Ecology, Physiology and Cell Biology* (eds H. Othmer, F. Adler, M. Lewis & J. Dillon), pp. 61–79. Prentice Hall.

Nisbet, R.M., Ross, A.H. & Brook, A.J. (1996) Empirically-based dynamic energy budget models: theory and an application to ecotoxicology. *Nonlinear World*, **3**, 85–106.

Noonburg, E., Nisbet, R., McCauley, E., Gurney, W., Murdoch, W. & de Roos, A. (1998) Experimental testing of dynamic energy budget models. *Functional Ecology*, **12**, 211–222.

Paloheimo, J.E., Crabtree, S.J. & Taylor, W.D. (1982) Growth model of *Daphnia*. *Canadian Journal of Fisheries Aquatic Sciences*, **39**, 598–606.

Pirt, S.J. (1965) The maintenance energy of bacteria in growing cultures. *Proceedings of the Royal Society of London Series B: Biological Sciences*, **163**, 224–231.

Ratsak, C.H., Kooi, B.W. & van Verseveld, H.W. (1994) Biomass reduction and mineralization increase due to the ciliate *tetrahymena pyriformis* grazing on the bacterium *pseudomonas fluorescens*. *Water Science and Technology*, **29**, 119–128.

Ratsak, C.H., Kooijman, S.A.L.M. & Kooi, B.W. (1993) Modelling of growth of an oligochaete on activated sludge. *Water Research*, **27**, 739–747.

Journal of Animal Ecology, **69**, 913–926

Ratsak, C.H., Maarsen, K.A. & Kooijman, S.A.L.M. (1996) Effects of protozoa on carbon mineralization in activated sludge. *Water Research*, **30**, 1–12.

de Roos, A.M. (1997) A gentle introduction to physiologically structured population models. *Structured Population Models in Marine, Freshwater, and Terrestrial Systems* (eds S. Tuljapurkar & H. Caswell), pp. 119–204. Chapman & Hall.

de Roos, A.M., McCauley, E., Nisbet, R.M., Gurney, W.S.C. & Murdoch, W.W. (1997) What individual life histories can (and cannot) tell about population dynamics. *Aquatic Ecology*, **31**, 37–45.

Ross, A.H., Gurney, W.S.C. & Heath, M.R. (1993a) Ecosystem models of Scottish sea lochs for assessing the impact of nutrient enrichment. *ICES Journal of Marine Science*, **50**, 359–367.

Ross, A.H., Gurney, W.S.C. & Heath, M.R. (1994) A comparative study of the ecosystem dynamics of four fjords. *Limnology and Oceanography*, **39**, 318–343.

Ross, A.H., Gurney, W.S.C., Heath, M.R., Hay, S.J. & Henderson, E.W. (1993b) A strategic simulation model of a fjord ecosystem. *Limnology and Oceanography*, **38**, 128–153.

Ross, A.H. & Nisbet, R.M. (1990) Dynamic models of growth and reproduction of the mussel *mytilus edulis* L. *Functional Ecology*, **4**, 777–787.

Sibly, R.M. & Calow, P. (1986) *Physiological Ecology of Animals: An Evolutionary Approach*. Blackwell Scientific Publications, Oxford, UK.

Stearns, S.C. & Hoekstra, R.F. (2000) *Evolution: an Introduction*. Oxford University Press, Oxford.

Stouthamer, A.H. & Kooijman, S.A.L.M. (1993) Why it pays for bacteria to delete disused DNA and to maintain megaplasmids. *Antonie Van Leeuwenhoek*, **63**, 39–43.

Tsuchiya, H.M., Drake, J.F., Jost, J.L. & Fredrickson, A.G. (1972) Predator–prey interactions of *Dictyostelium discoideum* and *Escherichia coli* in continuous culture. *Journal of Bacteriology*, **110**, 1147–1153.

West, G.B., Brown, J.H. & Enquist, B.J. (1997) A general model for the origin of allometric scaling laws in biology. *Science*, **276**, 122–126.

Widdows, J. & Donkin, P. (1991) Role of physiological energetics in ecotoxicology. *Comparative Biochemistry and Physiology C-Comparative Pharmacology and Toxicology*, **100**, 69–75.

Zonneveld, C. (1996) Modelling the kinetics of non-limiting nutrients in microalgae. *Journal of Marine Systems*, **9**, 121–136.

Zonneveld, C. (1992) *Animal energy budget: a dynamic approach*. PhD Thesis, Vrije Universiteit, Amsterdam.

Zonneveld, C. (1998a) Light-limited microalgal growth: a comparison of modelling approaches. *Ecological Modelling*, **113**, 41–54.

Zonneveld, C. (1998b) A cell-based model for the chlorophyll a to carbon ratio in phytoplankton. *Ecological Modelling*, **113**, 55–70.

Received 27 October 1999; revision received 27 April 2000

Journal of Animal Ecology, **69**, 913–926

J. Math. Biol. 41, 361–386 (2000)
Digital Object Identifier (DOI):
10.1007/s002850000049

Mathematical Biology

Konstadia Lika · Roger M. Nisbet

A Dynamic Energy Budget model based on partitioning of net production

Received: 11 May 1998 / Revised version: 18 February 2000 /
Published online: 4 October 2000 – © Springer-Verlag 2000

Abstract. We formulate a Dynamic Energy Budget (DEB) model for the growth and reproduction of individual organisms based on partitioning of net production (i.e. energy acquisition rate minus maintenance rate) between growth and energy reserves. Reproduction uses energy from reserves. The model describes both feeding and non-feeding stages, and hence is applicable to embryos (which neither feed nor reproduce), juveniles (which feed but do not reproduce), and adults (which commonly both feed and reproduce). Embryonic growth can have two forms depending on the assumptions for acquisition of energy from yolk. By default, when the energy acquisition rate exceeds the maintenance rate, a fixed proportion of the resulting *net production* is spent on growth (increase in structural biomass), and the remaining portion is channelled to the reserves. Feeding organisms, however, modulate their allocation of net production energy in response to their total energy content (energy in the reserves plus energy bounded to structural biomass). In variable food environment an organism alternates between periods of growth, no-growth, and balanced-growth. In the latter case the organism adopts an allocation strategy that keeps its total energy constant. Under constant environmental conditions, the growth of a juvenile is always of von Bertalanffy type. Depending on the values of model parameters there are two long-time possibilities for adults: (a) von Bertalanffy growth accompanied by reproduction at a rate that approaches zero as the organism approaches asymptotic size, or (b) abrupt cessation of growth at some finite time, following which, the rate of reproduction is constant. We illustrate the model's applicability in life history theory by studying the optimum values of the energy allocation parameters for constant environment and for each of the dynamic regimes described above.

1. Introduction

Dynamic Energy Budget (DEB) models describe the rates at which an individual organism acquires energy and utilizes it for physiological processes related to maintenance, growth and reproduction. DEB models are based on simple assumptions about the rates at which the organism acquires energy from its environment, and

K. Lika: Department of Biology, University of Crete, GR-71409, Iraklion, Crete, Greece. e-mail:lika@biology.uch.gr

R.M. Nisbet: Department of Ecology, Evolution and Marine Biology, University of California, Santa Barbara CA 93106-9610, USA. e-mail: nisbet@lifesci.lscf.ucsb.edu

Key words: Dynamic energy budget model – Net production – Growth – Reproduction – Life history theory

rules that describe how acquired energy is partitioned among maintenance, growth and reproduction. The fundamental hypothesis underlying a DEB model is that a set of physiological state variables (age, size, energy reserves, etc.) together with environmental variables (food density, temperature, etc.) fully determine the life history of individuals.

DEB models constitute a basis for developing physiological structured models [16,30] which aim to relate phenomena at the population level to the physiology of individuals. They are also used for applications in toxicology [7, 12–14, 17] and biotechnology [24–26]. DEB models are appropriate for life history studies since individual organisms are widely recognized as the units on which natural selection operates [2].

A wide variety of DEB model formulations have been developed, ranging from general, parameter-sparse models [11] to models which include more biological detail and may be taxon-specific and parameter-rich [4, 8–10]. How much detail is relevant depends on the objective of any particular study, for example, a parameter sparse model is desirable for interspecies comparisons.

Most DEB models in the literature fall into one of two families, which we call *net assimilation* and *net production* models [6, 20, 21]. The two groups of models differ mainly in their assumptions concerning allocation of energy to reproduction. Nisbet et al. [20] show that the assumptions concerning energy allocation may strongly influence predictions on toxicant response, and Gurney et al. [5] found that different energy allocation strategies result in different behavior at the population level.

The most complete body of theory to date for DEB models exists for a net assimilation model developed by Kooijman [11]. He formulated a single, parameter-sparse, mechanistic model to describe the energetics of embryos, juveniles and adults. Species differ only in their parameter values. Net production models, although they have been more widely used [1, 8–10, 22, 28], have been formulated only for juveniles and adults (feeding stages). The theory in this paper was motivated by the need to formulate a net production model in a way that covers feeding and non feeding stages of an organism, so that further testing of the two energy allocation strategies can be made.

Our objective is to formulate and analyze a mathematically consistent, representation of the energetics of embryos, juveniles and adults, based on a net production model. The model is formulated and its well-posedness is analyzed in section 2. We are particularly interested in the possibility of abrupt changes in qualitative dynamics arising from changes in model parameters; this is studied in section 3. In section 4, we illustrate the use of the model in life history theory.

2. Mathematical model

Our DEB model is based on simple, mechanistic rules for the processes of the energy uptake and use by individual organisms. The model uses differential equations to describe the rates at which the organism acquires energy from its environment and utilizes it for maintenance growth and reproduction. These rates depend on the state of the organism and its environment. The model distinguishes three life stages: embryos, juveniles, and adults. Embryos differ from juveniles and adults in

the way they acquire energy; juveniles and adults acquire energy from the ambient food, whereas an embryo absorbs energy from the yolk of the egg, which is taken to be its 'environment'. Moreover, embryos and juveniles do not reproduce, whereas adults can reproduce. We develop the model for organisms that are isomorphic (i.e. they do not change shape during growth), heterotrophic (i.e. they use organic material as their source of energy), and ectothermic (i.e. they do not regulate their body temperature).

The state of the organism is described by two variables; volume of structural biomass V, mainly in the form of proteins (hereafter refer to as biovolume), and total reserves of stored energy E, commonly a combination of carbohydrates, lipids and proteins. The use of biovolume as a state variable allows description of size related measurements of the organism. For instance, for isomorphic organisms length is proportional to $V^{1/3}$, surface area is proportional to $V^{2/3}$, weight is proportional to V, etc. Details on the relationships between size measures may be found in Kooijman [11].

The energy flows within the organism are schematically depicted in Fig. 1. All model variables and parameters are listed in Table 1. All the parameters assume positive values. The key assumption of the model is that maintenance, i.e. the energy required by processes necessary to keep the organism alive (e.g. turnover of structural body proteins, production of scales etc.), is debited directly from the energy acquired by the organism. By default, when the energy acquisition rate A exceeds the maintenance rate M, a fixed proportion α of the resulting *net production* $A - M$ is spent on growth (increase in biovolume), the remaining portion, $1 - \alpha$, is channelled to the reserves. Feeding organisms, however, modulate their allocation of net production energy in response to their total energy content (energy in the reserves plus energy bounded to structural biomass). Cessation of growth occurs when there is a decrease in organism's energetic value. Initiation of growth occurs when the current energetic state exceeds its maximum value ever attained in the past. This assumption is implemented to take into account alternating periods of starvation and re-feeding.

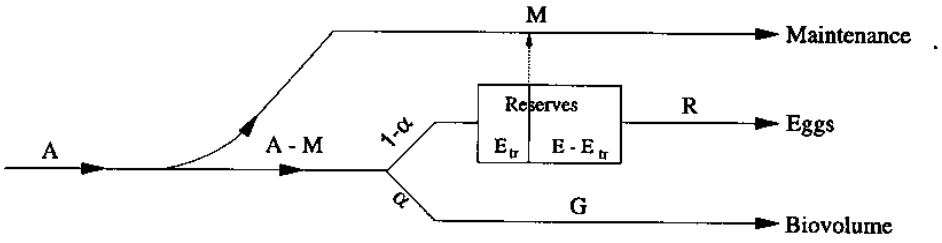

Fig. 1. Assumed energy fluxes through an organism. The organism acquires energy at a rate (A) dependent on its size and its environment. Maintenance costs (M) are debited directly from acquired energy (A). A fixed fraction α of the net production energy ($A - M$) is allocated to growth and the remaining $1 - \alpha$ to the reserves. When maintenance costs cannot be met from current acquired energy, reserves are used to cover the deficit. Allocation to reproduction (R) proceeds when reserves exceed a threshold level (E_{tr}).

Table 1. The variables and parameters of the energy budget model. e, t, and L in the second column denote the dimensions of energy, time and length.

Symbol[a]	Dimension	Interpretation
state variables		
V	L^3	Biovolume
E	e	Energy reserves
environment		
Y	e	Yolk energy
$[Y]$	$e\ L^{-3}$	Size-specific yolk energy
f	–	Scaled functional response
parameters		
$\{A_m\}$	$e\ L^{-2}\ t^{-1}$	Maximum surface area specific assimilation rate
$\{A_{me}\}$	$e\ L^{-2}\ t^{-1}$	Maximum surface area specific acquisition rate for embryos
$[M]$	$e\ L^{-3}\ t^{-1}$	Maintenance cost per unit biovolume per time
$[G]$	$e\ L^{-3}$	Energy costs for a unit increase in biovolume
α	–	Fractional allocation to growth
σ	t^{-1}	Allocation of excess storage to reproduction
V_b	L^3	Biovolume at birth
V_p	L^3	Biovolume at puberty
v	$L\ t^{-1}$	Parameter related to embryonic growth
compound parameters		
$\gamma = \frac{[M]}{3[G]}$	t^{-1}	Growth rate constant
$[E_m] = \frac{[G](1-\alpha)}{\alpha}$	$e\ L^{-3}$	Maximum energy density
$V_m = \left(\frac{\{A_m\}}{[M]}\right)^3$	L^3	Maximum biovolume
$E_{tr} = [E_m]V_p$	e	Threshold energy level for reproduction

[a] The following conventions are used: quantities which are expressed per unit of biovolume have square brackets [ ] and quantities which are expressed per unit of surface area have braces { }

Maintenance. The model assumes zero maintenance cost for reserves. The maintenance rate M is taken to be proportional to biovolume, i.e.

$$M = [M]V, \tag{1}$$

where $[M]$ is the amount of energy needed to maintain a unit of biovolume per unit of time. Following Kooijman's [11] notational conventions, we are using square brackets [ ] to denote quantities expressed per unit of biovolume, and braces { } to denote quantities expressed per unit of surface area.

Growth. The conversion efficiency $[G]$ of energy to biovolume is assumed to be constant. Thus

$$\frac{dV}{dt} = \frac{G}{[G]}, \tag{2}$$

where G is the energy flux to growth (Fig. 1).

The individual dynamics for the three life stages are described below. Because of the difference in the mode of energy acquisition, embryos are discussed separately from juveniles and adults.

2.1. Embryonic stage

Embryos do not feed but they absorb energy from the yolk of the egg and use it first for maintenance. A fraction α of the remaining energy is used for growth and the rest is deposited ('internalized') as storage material in embryonic tissue. Differential equations describing the embryo's dynamics can only be derived once we have rules that specify the energy acquisition rate, i.e. the flux A in Fig. 1. We consider two approaches to modeling this acquisition flux which lead to two alternative formulations of embryonic development. The two approaches make identical assumptions on the partitioning of the energy between growth and storage but they differ in their assumptions concerning the rules that define the energy flux from yolk to embryo and in the rules that determine the transition from embryonic to juvenile stage, i.e. the end of embryonic development and the commencement of feeding. For the first formulation we assume that the transition occurs when the embryo reaches a fixed size V_b at which the yolk energy drops to zero. For the second formulation we assume that the transition occurs when the rate of acquisition of energy cannot cover maintenance of an embryo of a size V_b.

Formulation 1. The first and simplest approach to modeling the energy flux from yolk to embryo assumes that energy is transfered at a rate proportional to the embryo's surface area. This implies that the energy acquisition rate is $A = \{A_{me}\}V^{2/3}$, where $\{A_{me}\}$ is a proportionality constant which can be interpreted as the maximum acquisition rate per unit of surface area. The rate at which the yolk energy Y is depleted is then described by

$$\frac{dY}{dt} = -\{A_{me}\}V^{2/3}. \tag{3}$$

According to the net production energy allocation scheme, a fixed proportion α of the net production $A - M$ is channelled to growth and the remaining portion is deposited as storage material in embryonic tissue. Using equations (1) and (2), the rates of change of biovolume and energy reserves in the embryo are then given by

$$\frac{dV}{dt} = \frac{\alpha}{[G]}\left(\{A_{me}\}V^{2/3} - [M]V\right), \tag{4}$$

$$\frac{dE}{dt} = (1-\alpha)\left(\{A_{me}\}V^{2/3} - [M]V\right). \tag{5}$$

Initially the biovolume and the energy reserves of the embryo are infinitesimally small. If biovolume at birth V_b is specified, then the initial yolk energy Y_0 is not a free parameter, its value being determined from equation (3) and the condition

$Y = 0$ at the end of embryonic development. We assume that $V_b^{1/3} < \frac{\{A_{me}\}}{[M]}$, to ensure that the energy acquisition rate exceeds the maintenance rate so that the size V_b can be reached. The initial energy yolk energy as well as the incubation period are needed for life history studies and for developing physiologically structured population models. The formulae that give the initial yolk energy Y_0 and the incubation time a_b, as well as details on the dynamics of the embryo may be found in Appendix A.

Formulation 2. The second approach adopts Kooijman's [11] representation of depletion of yolk energy. We define the *size-specific* yolk energy $[Y]$ to be the (absolute) amount of energy in the yolk relative to the biovolume of the embryo ($[Y] \equiv \frac{Y}{V}$). Kooijman assumes that the decrease of the *size-specific* yolk energy is a first order process, i.e. $\frac{d[Y]}{dt} = -a[Y]$. He assumes the parameter a to be inversely proportional to the length of the embryo, and the rate of decrease of the size-specific yolk energy is then given by

$$\frac{d[Y]}{dt} = -vV^{-1/3}[Y], \tag{6}$$

where the dimension of the parameter v is length per time.

The embryo's energy acquisition rate A is the rate at which the absolute amount of energy stored in yolk is utilized. Thus,

$$A = -\frac{dY}{dt} = -\left(V\frac{d[Y]}{dt} + [Y]\frac{dV}{dt}\right). \tag{7}$$

Following the net production scheme described above and using equations (1), (2), (6) and (7), the rates of increase of biovolume and energy reserves in embryos are given by the following equations

$$\frac{dV}{dt} = \frac{\alpha}{[G]V + \alpha Y}\left(vV^{2/3}Y - [M]V^2\right), \tag{8}$$

$$\frac{dE}{dt} = \frac{(1-\alpha)[G]}{[G]V + \alpha Y}\left(vV^{2/3}Y - [M]V^2\right). \tag{9}$$

The dynamics of the absolute yolk energy are then described by

$$\frac{dY}{dt} = -\frac{Y}{[G]V + \alpha Y}\left(v[G]V^{2/3} + \alpha[M]V\right). \tag{10}$$

The initial biovolume of an embryo is negligibly small. Although the initial size-specific yolk energy is therefore infinitely large, the initial (absolute) yolk energy Y_0 is finite. As with formulation 1, Y_0 is not a free parameter, its value can be determined from equations (6) and (8) and the conditions at the end of embryonic development, which occurs when the acquired energy cannot cover maintenance demands of the embryo of fixed size V_b. In Appendix A we give the details of the

calculations for determining Y_0. These details also permit the calculation of the incubation time a_b.

The systems of equations (4–5) and (8–9) both imply that $\frac{dE}{dV} = \frac{[G](1-\alpha)}{\alpha} \equiv [E_m]$, i.e., the rate at which energy reserves change per unit change of biovolume is constant. The initial biovolume and internal energy reserves are negligibly small compared with those at the end of embryonic development. Hence, using the assumption that $V(0) = E(0) = 0$, we obtain that $E(t) = [E_m]V(t)$. For both formulations it follows that energy reserves are proportional to embryo biovolume throughout embryonic development, and that $E(a_b) = [E_m]V_b$, a result we use as the initial condition for the energy reserves of a juvenile.

Figure 2 illustrates the predictions of the two formulations of embryonic development (see Appendix A for analytic proof). The biovolume and yolk energy reserves are, respectively, increasing and decreasing functions of time. Figure 2a and b illustrate the possible type of graphs representing the solutions of equations (3) and (4) (i.e. formulation 1). The curve representing the yolk energy Y is concave during development. The curve of the biovolume V, depending on the parameters, might be convex (Fig. 2a) implying that the rate of increase of V increases during embryonic development, or it might have a point of inflection (Fig. 2b), implying that the development is fast during the first part of the incubation period following a retardation of development. Figure 2c illustrates the graphs representing the solutions of equations (10) and (8) (i.e. formulation 2). The curves of the yolk energy

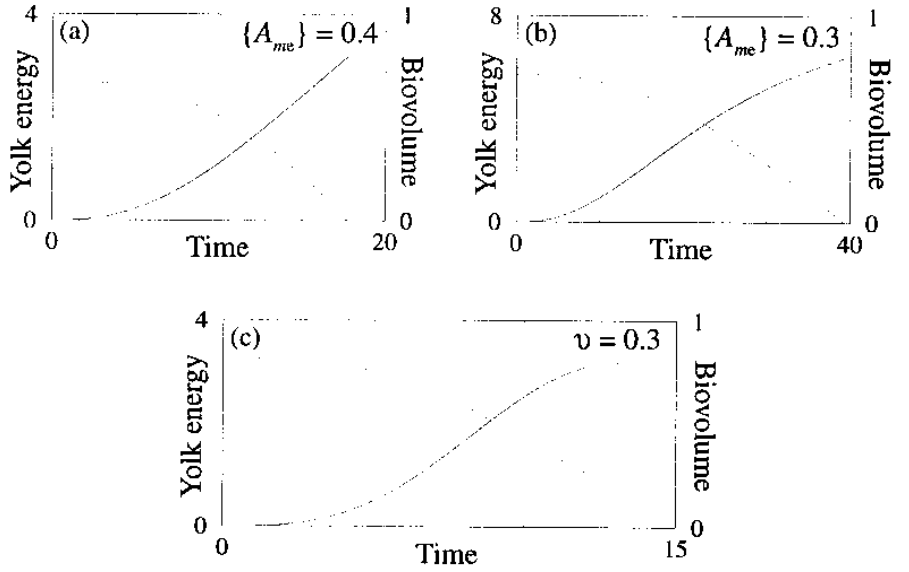

Fig. 2. Dynamics of embryo biovolume (V) (solid curve) and yolk energy (Y) (dotted curve) during embryonic development. (a) and (b) Solutions of equations (4) and (3). (c) Solutions of equations (10) and (8). (See text for details.) The parameter values, common to both formulations, determining the resulting trajectories are: $\alpha = 0.6$, $[G] = 0.9$, $[M] = 0.3$, $V_b = 0.8$, and $V(0) = 10^{-6}$.

and biovolume now both have a point of inflection. Both formulations of embryonic development capture the qualitative dynamics observed during embryonic growth as illustrated in [11, pages 86–87].

2.2. *Juvenile and adult stage*

Assimilation. We assume that feeding organisms ingest food at a rate proportional to the surface area of their food catching apparatus. In addition, we assume that the ingestion rate of the organism of any given size is proportional to a measure $f \in [0, 1)$ of the food environment. The quantity f (called the scaled functional response) represents the ratio of the organism's feeding rate to the maximum feeding rate for an organism of that size. We assume that f is an increasing function of the ambient food density, which in general is a function of time. The conversion efficiency of ingested food to assimilated energy is assumed to be constant. Hence, the assimilation or acquisition rate A for an isomorph of biovolume V is

$$A = \{A_m\} f V^{2/3}, \tag{11}$$

where $\{A_m\}$ is the maximum assimilation rate per unit surface area.

Reproduction. Although reproduction involves a series of discrete events (e.g. births, oviposition), the energy flow to reproduction can be regarded as a continuous process. We assume that stored energy reserves are used for reproduction by mature individuals at a rate proportional to the amount of reserves in excess of a threshold energy level E_{tr}. This threshold energy is related to maturation and is taken to be equal to energy reserves of the organism at puberty. The exact expression for E_{tr} is given later in this section. Thus, the reproduction rate R is

$$R = \sigma (E - E_{tr})_+, \tag{12}$$

where σ is the allocation rate of excess storage to reproduction. The subscript '+' means that the reproduction rate is zero when the term within parentheses is negative. The threshold energy cannot be used for reproduction but it can be used for maintenance under starvation conditions. A similar approach in modeling reproduction is used by Ross and Nisbet [28], but they assume that the threshold energy level is proportional to biovolume.

Energy allocation rules. Using the net production energy allocation scheme described above and illustrated in Fig. 1, assimilated energy is first used for maintenance. When the rate of assimilated energy A in (11) exceeds the maintenance rate M in (1), the net production $A - M$ is allocated to growth and reserves, depending on the total energy of the organism. When current assimilated energy cannot meet maintenance costs, energy in reserves is used to cover the deficit. Energy in the reserves is also used by mature individuals for reproduction at a rate given by (12). The individual is assumed to die instantaneously when energy in the reserves drops to zero.

The primary determinant of the dynamics of the state variables is the allocation of net production to growth (i.e. increase in V) and reserves. When the net production $A - M$ is negative, the organism does not grow, and energy from reserves is used to meet the deficit and meet maintenance requirements. When net production is positive, the default allocation rule is (as already noted) to assign a fixed fraction α of net production to growth. Under some circumstances (discussed later in this section), this rule leads to a *decrease* in the total energy content Φ, $\Phi := E + [G]V$, of the organism. Our key concept is that the organism adopts an allocation strategy that attempts to avoid such a decrease in total energy. The rate of change of the total energy content is equal to the difference between the energy gained from food and the energy lost for maintenance and reproduction, i.e. $\Phi' = A - M - R$. Thus we assume that an organism at time t makes the default allocation to growth only if

$$\Phi(t) \geq \Phi_{max}(t) := \max_{0 \leq \tau \leq t} \Phi(\tau) \quad \text{and} \quad \Phi'(t) > 0. \tag{13}$$

We call this "the growth condition"; when it holds, the changes in biovolume and reserves are described by the "growth equation"

$$\frac{dV}{dt} = \frac{\alpha}{[G]} \left(\{A_m\} f V^{2/3} - [M]V \right), \tag{14a}$$

$$\frac{dE}{dt} = (1 - \alpha) \left(\{A_m\} f V^{2/3} - [M]V \right) - \sigma \, (E - E_{tr})_+ . \tag{14b}$$

If the growth condition is not met, the organism alters allocation to growth as follows: First, if the total energy content at time t is less than Φ_{max}, then all net production is assigned to reserves. The system then follows the "no-growth" equations

$$\frac{dV}{dt} = 0, \tag{15a}$$

$$\frac{dE}{dt} = \{A_m\} f V^{2/3} - [M]V - \sigma \, (E - E_{tr})_+ . \tag{15b}$$

Second, if the total energy content at time t is equal to Φ_{max} and $\Phi'(t^-) = 0$[1], then there are two possibilities. If $\Phi''(t^+)$ is non-positive when evaluated with *both* the growth and no-growth equations, then the system follows the no-growth equations (15). However, if $\Phi''(t^+)$ is negative when evaluated with the growth equations and positive when evaluated with the no-growth equations, then the system follows a trajectory which we call "balanced-growth" that keeps Φ constant. Thus the equations for balanced-growth are

$$\{A_m\} V^{2/3} f - [M]V - \sigma (E - E_{tr})_+ = 0, \tag{16a}$$

$$E + [G]V = \Phi_{max}. \tag{16b}$$

[1] $\Phi^{(n)}(t^-)$ and $\Phi^{(n)}(t^+)$ denote respectively the left and right $n - th$ order derivative of Φ

The time t is measured from birth where $V(0) = V_b$ and $E(0) = [E_m]V_b$. A juvenile individual becomes an adult, and therefore it is able to reproduce, on reaching a fixed size V_p. We assume that the threshold energy E_{tr} is equal to $[E_m]V_p$, which is the maximum value energy reserves reach during the juvenile period. The latter follows from equations (14)–(16). This assumption ensures that juveniles do not reproduce, as the reproduction terms in (14b), (15b), and (16a) are zero, since $E \leq E_{tr}$.

The theory developed in this section generalizes to variable environments, which cause one or more of the model parameters to vary with time. Of particular biological interest is variation in the food supply which leads to time dependence of the parameter f representing the scaled functional response. The trajectories for the balanced-growth can be found by differentiating equation (16a) after substitution of E from (16b). We obtain V from the equation

$$\frac{dV}{dt} = \begin{cases} f' \dfrac{3\{A_m\}V}{3([M] - \sigma[G])V^{1/3} - 2\{A_m\}f}, & \text{if } \Phi_{max} - [G]V - E_{tr} > 0, \\ f' \dfrac{3\{A_m\}V}{3[M]V^{1/3} - 2\{A_m\}f}, & \text{if } \Phi_{max} - [G]V - E_{tr} \leq 0. \end{cases} \tag{17}$$

E is then calculated using equation (16b). In Appendix B we analyze the dynamics within the different growth regimes and the transitions between regimes for the situation where $f \in [0, 1)$ is continuous and differentiable function of time.

For simplicity we nondimensionalize equations (14) – (16) by introducing the scaled variables

$$\ell = \left(\frac{V}{V_m}\right)^{1/3} \quad \text{and} \quad \mathscr{E} = \frac{E}{V_m[G]},$$

where $V_m \equiv \left(\frac{\{A_m\}}{[M]}\right)^3$ is the maximum biovolume an organism attained when food is abundant and the organism never ceases growth. With this change of variables the growth condition takes the form

$$\Psi(t) \geq \Psi_{max} := \max_{0 \leq \tau \leq t} \Psi(\tau) \quad \text{and} \quad \Psi'(t) > 0, \quad \text{with} \quad \Psi(t) = \mathscr{E}(t) + \ell^3(t). \tag{18}$$

The dynamics of the scaled variables ℓ and $\mathscr{E}$ are given by

$$\frac{d\ell}{dt} = \gamma\alpha(f - \ell), \tag{19a}$$

$$\frac{d\mathscr{E}}{dt} = 3\gamma(1-\alpha)\ell^2(f-\ell) - \sigma\left(\mathscr{E} - \frac{1-\alpha}{\alpha}\ell_p^3\right)_+, \tag{19b}$$

for all t for which inequality (18) holds. The parameter $\gamma \equiv \frac{[M]}{3[G]}$ represents the rate at which the organism would approach maximum size if all net production energy were allocated to growth, and ℓ_p is the scaled length at puberty.

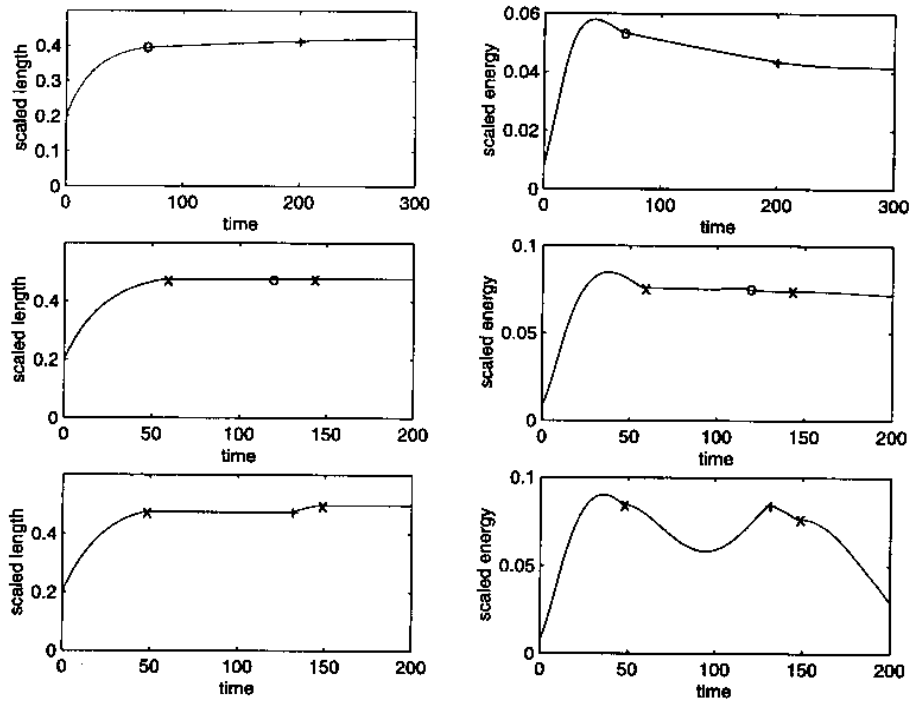

Fig. 3. Trajectories of the scaled length and scaled energy reserves as functions of time for an individual growing in variable food conditions (top: $f(t) = 0.4 + 0.1t/(t + 10^3)$, middle: $f(t) = 0.5 + 0.001\sin(2\pi(t + 10)/120)$, bottom: $f(t) = 0.5 + 0.02\sin(2\pi(t + 10)/120)$). The marks indicate the transitions between the different regimes. The beginning of the growth, no-growth, and balanced-growth regimes is marked by "+", "×", and "○", respectively. The parameter values determining the resulting trajectories are: $\gamma = 0.11$, $\alpha = 0.4$, $\ell_b = 0.2$, $\ell_p = 0.3$, and $\sigma = 0.05$.

When the growth condition (18) is not met, then the scaled variables ℓ and $\mathscr{E}$ are given by the scaled "no-growth" equations

$$\frac{d\ell}{dt} = 0\,, \tag{20a}$$

$$\frac{d\mathscr{E}}{dt} = 3\gamma\ell^2(f - \ell) - \sigma\left(\mathscr{E} - \frac{1-\alpha}{\alpha}\ell_p^3\right)_+\,, \tag{20b}$$

or the scaled "balanced-growth" equations

$$3\gamma\ell^2(f - \ell) - \sigma\left(\mathscr{E} - \frac{1-\alpha}{\alpha}\ell_p^3\right)_+ = 0 \tag{21a}$$

$$\mathscr{E} + \ell^3 = \Psi_{max}. \tag{21b}$$

Numerical simulations indicate that an organism enters a balanced-growth regime when f increases with a relatively small slope. Figure 3 shows the

trajectories of the scaled length and scaled energy reserves for some choices of the function f. The top figures show a transition from growth to balanced-growth for a functional response which increases slowly with time. The middle and bottom figures correspond to periodic functions with the same period but different amplitudes. We observe that balanced-growth is induced when f increases slowly.

3. Dynamics in constant environment

We consider the special case where the scaled functional response f is constant. In this case, it follows from the analysis in Appendix B, that the organism can be only in a growth or no-growth regime depending on parameters values.

We assume that a newborn is in the growth stage, i.e. at $t = 0$ system (19) governs the individual dynamics. This is true only if f is larger than ℓ_b, the scaled length at birth. If $f \leq \ell_b$ the individual will survive without growing for a finite time utilizing its reserves. If, in addition, equations (19) hold for all positive t, then it follows that the scaled length ℓ as a function of time is given by the von Bertalanffy equation

$$\ell(t) = f - (f - \ell_b)e^{-\gamma\alpha t}. \tag{22}$$

The duration of the juvenile period at constant food density with the functional response $f > \ell_p$ is

$$a_p = \frac{1}{\gamma\alpha} \ln \frac{f - \ell_b}{f - \ell_p}. \tag{23}$$

At lower food densities with $f < \ell_p$, the length ℓ_p will not be reached.

The scaled energy is then given by

$$\mathscr{E}(t) = \begin{cases} \dfrac{1-\alpha}{\alpha}\ell^3(t), & 0 \leq t \leq a_p, \\ \dfrac{1-\alpha}{\alpha}\ell_p^3 + 3\gamma(1-\alpha)(f-\ell(t))\displaystyle\int_{a_p}^{t} \ell(\tau)^2 e^{(\sigma-\gamma\alpha)(\tau-t)}\,d\tau, & t > a_p. \end{cases} \tag{24}$$

In Appendix C, we prove that $\sigma \geq \gamma$ is a necessary and sufficient condition for the growth condition to hold for all positive time. Thus, for $\sigma \geq \gamma$ the dynamics of the scaled variables ℓ and $\mathscr{E}$ are defined by system (19) for all $t \geq 0$, which can be solved explicitly resulting to equations (22) and (24). Furthermore, it follows from (24) that if $\sigma \geq \gamma$, then $\mathscr{E}(t) > \dfrac{1-\alpha}{\alpha}\ell_p^3$ (in the original variables $E(t) > [E_m]V_p$) for $t > a_p$, i.e. the energy reserves do not drop below the threshold energy for reproduction. For $\sigma < \gamma$, growth ceases at some finite time t_s during the adult stage (see Appendix C) such that

$$\Psi'(t_s) \equiv 3\gamma\ell^2(t_s)(f - \ell(t_s)) - \sigma\left(\mathscr{E}(t_s) - \frac{1-\alpha}{\alpha}\ell_p^3\right) = 0.$$

In this case the dynamics of the scaled variables are defined by the system (19) for $0 \leq t < t_s$, and for $t \geq t_s$ by $\dfrac{d\ell}{dt} = 0$ and $\dfrac{d\mathscr{E}}{dt} = 0$. Thus, for constant f and for

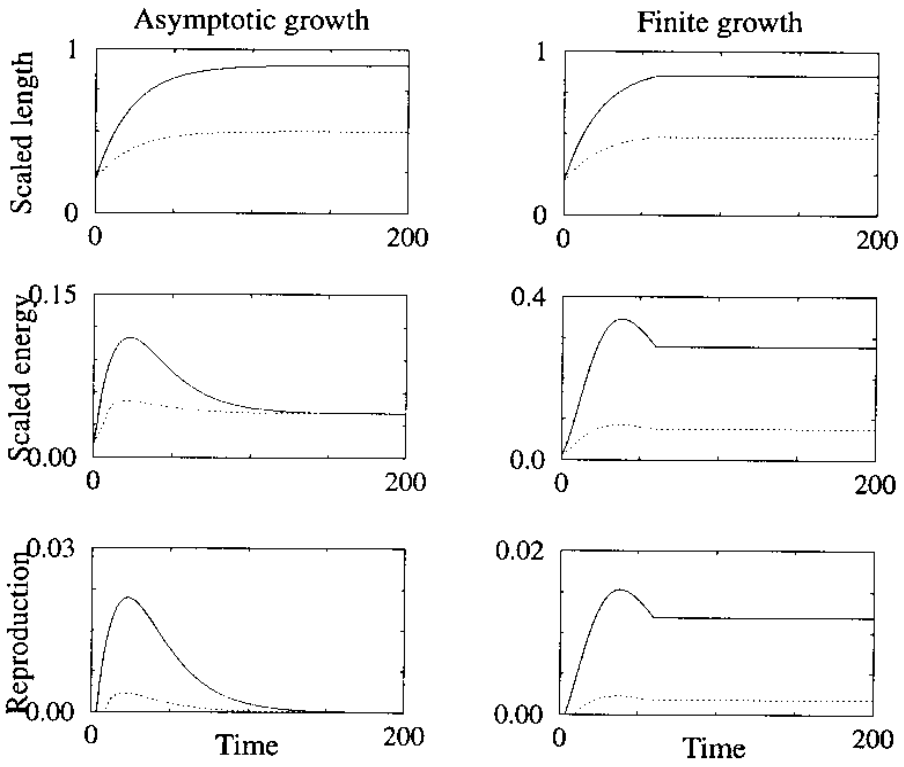

Fig. 4. Typical trajectories of the scaled length, scaled energy reserves, and reproduction rate as functions of time for an individual growing in constant food conditions (solid curve: high food, dotted curve: low food). Left column: asymptotic growth ($\sigma \geq \gamma$). Right column: finite growth ($\sigma < \gamma$). The parameter values determining the resulting trajectories are: $\gamma = 0.11$, $\alpha = 0.4$, $\ell_b = 0.2$, $\ell_p = 0.3$, $\sigma = 0.3$ (asymptotic growth) and $\sigma = 0.05$ (finite growth).

$t \geq t_s$, all net production energy is allocated to reproduction implying that ℓ and $\mathscr{E}$ remain constant.

Typical trajectories for the asymptotic growth ($\sigma \geq \gamma$) and finite growth ($\sigma < \gamma$) cases are shown in Fig. 4. In the case $\sigma \geq \gamma$, the length approaches an asymptotic size which depends on f and the energy reserves approach the threshold value. Note that the peak of reproduction is at an intermediate age and as the animal gets older and approaches asymptotic size, the rate of energy allocation to reproduction decreases and approaches zero asymptotically. In the case $\sigma < \gamma$ the growth curve is of the von Bertallanffy type until the organism reaches a size at which energy acquired cannot meet maintenance and reproduction demands. At that point growth stops and reproduction continues at a constant rate.

4. Implications for life history theory

One classic problem in life history theory is to determine the strategies for allocating energy between growth, storage and reproduction that will be favored by natural selection. A DEB model that is fully specified for all life stages allows us

to address a restricted version of that question, namely *assuming that the organism is constrained to follow the rules of our DEB model*, what are the "optimal" values of the model parameters?

The optimization approach rests on the assumption that there exists some quantity related to fitness that is maximized by natural selection [18,27,29]. Once a measure of fitness is identified, the next step is to choose adaptive life history traits, defined by a set of rules for the life history patterns of the organism, that maximize fitness. The issue of what is being maximized has been the subject of many discussions, partly because the appropriate measure of fitness changes with circumstances. In an unlimited, homogeneous, and constant environment the appropriate measure of fitness is the intrinsic growth rate r [2,27,29], which can be obtained by solving the characteristic equation,

$$\int_0^\infty e^{-rt}\beta(t)S(t)\,dt = 1,$$

where $\beta(t)$ is the average rate of offspring production by an individual at age t and $S(t)$ is the probability that a newborn will survive to age t. The functions β and S, in general, might depend on the environment and the state of the organism. In a stationary environment the most commonly used measure of fitness is the lifetime reproductive success or net reproduction (R_0) [2,27] defined as

$$R_0 = \int_0^\infty \beta(t)S(t)\,dt.$$

R_0 is the average number of offspring that an individual is expected to produce during its lifetime. If the individual is a member of a population at equilibrium then it provides on the average one offspring, i.e. $R_0 = 1$. In this situation, providing R_0 is an increasing function of the resource density, evolution minimizes the level of resource per individual at which an individual produces on average one viable offspring during its entire lifetime [19]. In other words, an individual, which is a member of a population at equilibrium, will be favored by selection if it is able to replace itself at a lower resource level than the current equilibrium density.

We assume that juveniles and adults have the same constant, age independent, per capita death rate δ, so that the survival function has the form

$$S(t) = e^{-\delta t}.$$

We further assume that energy allocated to reproduction is converted *immediately* to eggs. For an organism whose energy allocation scheme for growth and reproduction follows the rules described in section 2 the fecundity function then has the form

$$\beta(t) = \begin{cases} 0 & t < a_p, \\ \dfrac{\sigma\left(\mathscr{E} - \frac{1-\alpha}{\alpha}\ell_p^3\right)_+}{y_0} & t \geq a_p, \end{cases}$$

where the numerator represents the rate of commitment of reserves to reproduction and y_0 is the cost to make one egg with initial energy Y_0 (given by (27) or (31)),

scaled to the maximum size V_m and the energy cost for growth $[G]$. The cost for the conversion of the reserve energy of the mother to the initial energy of an egg is small in most cases since these type of energy reserves are chemically related, so we ignore it. For constant environmental conditions the scaled length, ℓ, and the scaled energy, $\mathscr{E}$, are given by equations (22) and (24), respectively. Substituting the particular formulae for β and S into R_0 equation, we find that

$$R_0 = \frac{3\gamma(1-\alpha)\sigma}{y_0}\left(\int_{a_p}^{t_s}(f-\ell(t))e^{-\delta t}\int_{a_p}^{t}\ell^2(\tau)e^{(\sigma-\gamma\alpha)(\tau-t)}\,d\tau\,dt + \frac{e^{-\delta t_s}}{\sigma\delta(1-\alpha)}(f-\ell(t_s))\ell^2(t_s)\right), \tag{25}$$

where t_s is the time growth ceases which is a finite positive number given by equation (35) when $\sigma < \gamma$, and infinity when $\sigma \geq \gamma$ (see Appendix C). In the latter case ($\sigma \geq \gamma$) the equation for R_0 takes the form

$$R_0 = \frac{3\gamma(1-\alpha)\sigma(f-\ell_p)e^{-\delta a_p}}{y_0(\sigma+\delta)}\left(\frac{f^2}{\delta+\alpha\gamma} - \frac{2f(f-\ell_p)}{\delta+2\alpha\gamma} + \frac{(f-\ell_p)^2}{\delta+3\alpha\gamma}\right). \tag{26}$$

It can be shown that for $\sigma \geq \gamma$, R_0 is a monotone increasing function of f for all $f \in (\ell_p, 1)$. The restriction that f must be larger than ℓ_p is required in order for the individual to become adult. For $\sigma < \gamma$ numerical simulations suggest that R_0 increases with f. Thus, we measure fitness by the lowest value of the functional response f for which $R_0 = 1$.

Our next step is to choose adaptive life history traits that 'maximize' fitness. A classical physiological trade-off in life history theory is the allocation of resources between growth and reproduction. In our DEB model the parameter α quantifies the allocation of energy to growth and storage, and σ the consequent allocation of excess storage to reproduction. Thus we aim to determine the optimal pair of α and σ that will minimize f subject to $R_0 = 1$.

Setting $R_0 = 1$ in equation (25), we obtain a relationship between the values of the functional response f at which the organism can replace itself and the parameters α and σ. We assume that the cost of an offspring, Y_0, is given by equation (27). The results do not change if Y_0, is given by equation (31) in Appendix A. Figure 5 shows a contour plot on the (σ, α)-plane; along each contour level f has the same value. We find that for small δ the functional response takes the minimum value at some point $(\sigma^\star, \alpha^\star)$ with $\sigma^\star \in (0, \gamma)$ (Figure 5a). This implies that for long lived animals selection favors the individuals that cease growth and continue to reproduce at a constant rate, thereby avoiding the decline in reproduction that would occur as asymptotic size is approached. Figure 5b illustrates that for large δ the functional response is minimized at the maximum σ ($\sigma > \gamma$) the organism can adopt. This implies that for short lived animals selection favors those individuals that allocate stored energy to reproduction at the maximum rate. The model predicts that individuals that adopt this strategy have high reproduction rate at early age and as they get older the reproduction rate decreases to zero (Fig. 4).

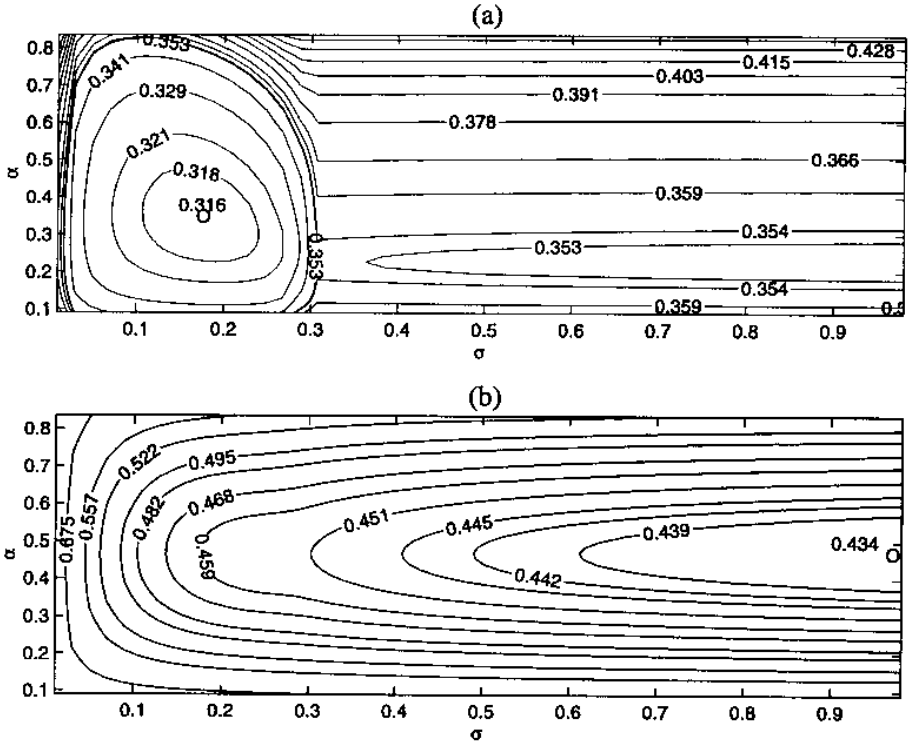

Fig. 5. Contour plots on the (σ, α)-plane; along each contour level f has the same value. The numbers indicate the value of f along each line. The circle (○) indicates the optimal pair of values (σ^*, α^*) at which f takes its minimum value. The parameter values determining the resulting plots are: $\gamma = 0.3$, $\ell_b = 0.2$, $\ell_p = 0.3$, $\delta = 0.01$ (a), and $\delta = 0.1$ (b).

5. Discussion

We have developed a general model of the life history of an individual organism, based on partitioning of net production. The model has a pair of ordinary differential equations together with a history-dependent non-linearity (equation (13)) that stops growth whenever there is a decline in the total energy stored in the organism (structure + reserves). Similar conditions have been invoked by previous authors (for example the "weight-for-length" rule in [4], and variant of Kooijman's net assimilation model that "switches off" reproduction when food is scarce (chapter 4 of [11]). However, to the best of our knowledge, the analysis in this paper is the first mathematical study of the effects of such a condition.

We focused on the dynamics of individual organisms under constant environmental conditions. Even in this simple situation, the qualitative dynamics depend in unexpected ways on model parameter values. Embryonic growth can have two forms depending on the assumptions for acquisition of energy from yolk. The growth of a juvenile is always of von Bertalanffy type, but there are two long-time possibilities for adults: (a) von Bertalanffy growth accompanied by reproduction at a rate that approaches zero as the organism approaches asymptotic size, or (b) abrupt cessation of growth at some finite time, following which, the rate of repro-

duction is constant. We are currently engaged in research (with W.S.C. Gurney, E. McCauley, W.W. Murdoch, A.M. de Roos, and others) that will test these predictions on aquatic organisms. There are many problems in interpreting individual growth curves, so this investigation is beyond the scope of the present paper.

Much of the motivation for careful formulation of DEB models comes from the need to have a formulation that is valid in temporally varying environments. Of particular interest is temporal variation in the scaled functional response (f) within the range [0,1), corresponding to fluctuations in food availability for the organism. Numerical and analytical studies suggest that our DEB model is well-defined, when f varies continuously with time, but more rigorous study of the dynamics of both our model and Kooijman's model would be most valuable.

Extension of our analysis to cover variable environments is also of importance for the application of DEB models to life history theory. The calculations in this paper are very restrictive, yielding only the optimum values of certain model parameters for an organism that experiences a constant environment and prioritizes energy allocation in accordance with our model rules. In an unchanging environment, simple models (lacking reserves and an embryonic stage) suggest that the optimal strategy for an individual is the "bang-bang" option of committing 100% of net production to growth until a certain age, and thereafter 100% to reproduction [2]. Thus even our "optimal" organisms might be displaced by otherwise identical animals following the bang-bang strategy. While consistent with some life histories, the bang-bang strategy is not followed by the many organisms that simultaneously grow and reproduce, and which motivated the development of Kooijman's [11] model and our own. The most commonly invoked 'explanation' for the existence of the latter type of organism is bet-hedging in a spatially or temporally variable environment [2, 15]. Thus future DEB-based studies of life histories in variable environments must tackle two very distinct questions. First there is the obvious question of how our conclusions on optimal strategies change for a variable environment. But more fundamentally, we have to ask whether our model, or any other DEB model makes evolutionary sense, by asking whether our equations represent a good description of the optimum strategy for an individual making unconstrained choices in a fluctuating environment.

Appendix A

In this appendix we calculate the initial yolk energy (Y_0) of an egg, the duration of embryonic development (a_b), and examine the behavior of the functions Y and V representing, respectively, the yolk energy and the embryo biovolume for the two formulations described in section 2.

Formulation 1. For the first formulation (equations (3)–(5)), birth occurs when the embryo reaches a fixed size V_b at which the yolk energy drops to zero. To derive Y_0 we first solve equation (4) with initial condition $V(0) = 0$ to find that the growth curve is given by

$$V(t) = V_{me}\left(1 - e^{-\gamma\alpha t}\right)^3$$

and the incubation time is

$$a_b = \frac{1}{\gamma\alpha} \ln \frac{V_{me}^{1/3}}{V_{me}^{1/3} - V_b^{1/3}},$$

where $V_{me} = \left(\frac{\{A_{me}\}}{[M]}\right)^3$ and $\gamma = \frac{[M]}{3[G]}$. It is clear from these equations that $V_b^{1/3}$ must be less than $\frac{\{A_{me}\}}{[M]}$, in order to ensure that the embryonic development last for a finite period of time.

Using the above two equations and the conditions at birth, integrating equation (3) from 0 to a_b yields the initial yolk energy

$$Y_0 = \frac{\{A_{me}\}}{2\gamma\alpha}\left(2V_{me}^{2/3}\ln\frac{V_{me}^{1/3}}{V_{me}^{1/3} - V_b^{1/3}} - V_b^{1/3}\left(2V_{me}^{1/3} + V_b^{1/3}\right)\right). \quad (27)$$

We now examine the behavior of Y and V during embryonic development. ¿From equations (3) and (4) it follows that Y and V are, respectively, decreasing and increasing functions of time. The second derivative of Y with respect to t is

$$\frac{d^2Y}{dt^2} = -\frac{2\alpha\{A_{me}\}V^{1/3}}{3[G]}\left(\{A_{me}\} - [M]V^{1/3}\right),$$

which is negative in $(0, a_b)$ provided that $V_b^{1/3} < \frac{\{A_{me}\}}{[M]}$. Therefore, the function $Y(t)$ is concave.

The second derivatives of V with respect to t is

$$\frac{d^2V}{dt^2} = \frac{\alpha^2V^{1/3}}{[G]^2}\left(\frac{2}{3}\{A_{me}\} - [M]V^{1/3}\right)\left(\{A_{me}\} - [M]V^{1/3}\right).$$

It follows that if $0 < V_b^{1/3} \leq \frac{2}{3}\frac{\{A_{me}\}}{[M]}$, then $\frac{d^2V}{dt^2} > 0$ for all $t \in (0, a_b)$. If $\frac{2}{3}\frac{\{A_{me}\}}{[M]} < V_b^{1/3} < \frac{\{A_{me}\}}{[M]}$, then $\frac{d^2V}{dt^2}$ is positive in $(0, t_1)$ and negative in (t_1, a_b), where $t_1 = \frac{\ln 3}{\gamma\alpha}$ is the time the embryo reaches a size at which maintenance rate is 2/3 of the energy acquisition rate. In this case, the function $V(t)$ has a point of inflection at t_1, and it is convex in $(0, t_1)$ and concave in (t_1, a_b).

Formulation 2. For the second formulation (equations (6)–(10)), birth occurs when the energy acquired from the egg cannot meet maintenance costs of the embryo of fixed size V_b, i.e., when $Y \leq \frac{[M]}{v}V_b^{4/3}$. To derive Y_0 we nondimensionalize equations (6) and (8) by setting

$$y = \frac{[Y]}{[E_m]},\ x = \left(\frac{V}{V_{me}}\right)^{1/3},$$

$$[E_m] = \frac{[G](1-\alpha)}{\alpha},\ V_{me} = \left(\frac{v[E_m]}{[M]}\right)^3,\ \gamma = \frac{[M]}{3[G]}.$$

Equations (6) and (8) then become

$$\frac{dy}{dt} = -\frac{3\gamma\alpha}{1-\alpha}\frac{y}{x} \quad \text{and} \quad \frac{dx}{dt} = \gamma\alpha\frac{y-x}{(1-\alpha)y+1}. \tag{28}$$

Consequently,

$$\frac{dx}{dy} = -\frac{1-\alpha}{3}\frac{x(y-x)}{y((1-\alpha)y+1)}, \tag{29}$$

The substitution $z = x^{-1}$ converts equation (29) into the linear equation

$$\frac{dz}{dy} = \frac{1-\alpha}{3((1-\alpha)y+1)}\left(z - \frac{1}{y}\right),$$

which gives x in terms of y by

$$x = \frac{1}{((1-\alpha)y+1)^{1/3}}\left(\frac{1}{x_b((1-\alpha)y_b+1)^{1/3}} - \frac{1-\alpha}{3}\int_{\frac{1}{(1-\alpha)y+1}}^{\frac{1}{(1-\alpha)y_b+1}} s^{1/3}(1-s)^{-1}\,ds\right)^{-1}, \tag{30}$$

where x_b and y_b are, respectively, the values of the scaled variables x and y at the end of embryonic stage, which by assumption $x_b = y_b$. Letting $x \to 0$ and $y \to \infty$ such that $x^3 y = \dfrac{Y}{V_{me}[E_m]} \to \dfrac{Y_0}{V_{me}[E_m]}$, from (30) we obtain

$$Y_0 = \frac{V_{me}[E_m]}{1-\alpha}\left(\frac{1}{x_b((1-\alpha)x_b+1)^{1/3}} - \frac{1-\alpha}{3}\int_0^{\frac{1}{(1-\alpha)x_b+1}} s^{1/3}(1-s)^{-1}\,ds\right)^{-3}$$

with $x_b = (\frac{V_b}{V_{me}})^{\frac{1}{3}}$. In terms of the unscaled variables, the initial yolk energy is given by

$$Y_0 = \frac{[G]}{\alpha}\left(\frac{v^{1/3}}{V_b^{1/3}(3\gamma\alpha V_b^{1/3}+v)^{1/3}} - \frac{\gamma\alpha}{v}\int_0^{\frac{v}{3\gamma\alpha V_b^{1/3}+v}} s^{1/3}(1-s)^{-1}\,ds\right)^{-3}. \tag{31}$$

Thus, to determine the initial energy of an egg we need to know only the size of the individual at birth.

Using (30) and the first of (28) we can also find the incubation time. After some algebra the result is

$$a_b = \frac{1}{\gamma\alpha}\int_0^{z_b} \frac{dz}{(1-z)z^{2/3}\left(\frac{vz^{1/3}}{\gamma\alpha V_b^{1/3}} - B_{z_b}(\frac{4}{3},0) + B_z(\frac{4}{3},0)\right)}, \tag{32}$$

with $B_z(\frac{4}{3},0) = \displaystyle\int_0^z s^{1/3}(1-s)^{-1}\,ds$ and $z_b = \dfrac{v}{3\gamma\alpha V_b^{1/3}+v}$.

We now examine the behavior of V and Y during embryonic development. Equations (8) and (10) imply that V and Y are, respectively, increasing and decreasing functions of time. The second derivatives of V with respect to t is

$$\frac{d^2V}{dt^2} = \frac{aV^{1/3}}{([G]V + \alpha Y)^2} h_1(V, Y),$$

where

$$\begin{aligned} h_1(V, Y) &= \alpha \left(\frac{2}{3} vY - [M]V^{4/3}\right)\left(vY - [M]V^{4/3}\right) \\ &\quad - v\left(v[G]V + [M]V^{4/3}\right). \end{aligned}$$

Now, $h_1(V(t), Y(t))$ approaches a positive number as $t \to 0$ (i.e. $V \to 0$ and $Y \to Y_0$) and a negative as $t \to a_b$ (i.e. $V \to V_b$ and $Y \to \frac{[M]}{v} V_b^{4/3}$). This implies that h_1 changes at least once sign in $(0, a_b)$. We will show that h_1 changes sign only once in $(0, a_b)$, and therefore $\frac{d^2V}{dt^2}$ has only one zero, by showing that h_1 is a monotone decreasing function of time. After some algebra, we can show that h_1 increases in Y and decreases in V during embryonic development. Since V increases and Y decreases with time, we then obtain that

$$\frac{dh_1}{dt} = \frac{\partial h_1}{\partial V}\frac{dV}{dt} + \frac{\partial h_1}{\partial Y}\frac{dY}{dt} < 0.$$

Therefore, there is only one point $t_2 \in (0, a_b)$ such that $h_1(V(t_2), Y(t_2)) = 0$. Consequently, the function V has only one point of inflection at t_2, and it is convex in $(0, t_2)$ and concave in (t_2, a_b).

Similarly, the second derivatives of Y with respect to t is

$$\frac{d^2Y}{dt^2} = -\frac{V^{1/3}Y}{([G]V + \alpha Y)^2} h_2(V, Y),$$

where

$$\begin{aligned} h_2(V, Y) &= \alpha \left(vY - [M]V^{4/3}\right)\left(\frac{2}{3} v[G] + \alpha[M]V^{1/3}\right) \\ &\quad - v[G]V\left(v[G] + \alpha[M]V^{1/3}\right). \end{aligned}$$

Now, $h_2(V, Y)$ approaches a positive number as $t \to 0$ (i.e. $V \to 0$ and $Y \to Y_0$) and a negative as $t \to a_b$ (i.e. $V \to V_b$ and $Y \to \frac{[M]}{v} V_b^{4/3}$). This again implies that h_2 changes sign in $(0, a_b)$. It can be shown that h_2 changes sign only once in $(0, a_b)$. Indeed, taking the derivatives of h_2 with respect to Y and V, we find that

$$\frac{\partial h_2}{\partial Y} = \alpha v(\frac{2}{3} v[G] + \alpha[M]V^{1/3})$$

and

$$\frac{\partial h_2}{\partial V} = -v[G](v[G] + \frac{16}{9}\alpha[M]v^{1/3}) + \frac{1}{3}\alpha^2[M]V^{-2/3}(vY - 5[M]V^{4/3}).$$

It is clear that $\frac{\partial h_2}{\partial Y} > 0$. If $V^{4/3} \geq \frac{vY}{5[M]}$, then $\frac{\partial h_2}{\partial Y} < 0$, while if $V^{4/3} < \frac{vY}{5[M]}$, then $\frac{\partial h_2}{\partial Y}$ can also be positive. In the latter case, it can be shown that $h_2 > 0$. Therefore, for all t such that $V^{4/3}(t) \geq \frac{vY(t)}{5[M]}$

$$\frac{dh_2}{dt} = \frac{\partial h_2}{\partial V}\frac{dV}{dt} + \frac{\partial h_2}{\partial Y}\frac{dY}{dt} < 0$$

Consequently, the function Y has only one point of inflection, say, at t_3, and it is concave in $(0, t_3)$ and convex in (t_3, a_b).

Appendix B

In this appendix we study the behavior of the model within the different growth regimes and the transitions between them. We assume that $f \in [0, 1)$ is a continuous and differentiable function of time. All other parameters are positive constants.

First we consider the initial value problem (14) for $t > t_0$, with $V(t_0) = V_0$ and $E(t_0) = E_0$. The change of variable $L = V^{1/3}$ reduces (14a) into a linear equation in L. From the basic theory of linear differential equations it then follows that there exists a unique function V that satisfies (14a) for all $t > t_0$ and also $V(t_0) = V_0$. Substituting the solution V into equation (14b) we obtain a differential equation $E' = F(t, E)$ with F locally Lipschitz in the second variable. Using standard theory of differential equations [3], there exists a unique function E that satisfies (14b) and $E(t_0) = E_0$.

Similarly, if we assume that the system is described by the no-growth equations (15), then there exist continuously differentiable functions V and E that satisfy (15) for $t > t_0$, and also $V(t_0) = V_0$ and $E(t_0) = E_0$.

Within a balanced-growth regime the total energy content Φ of the organism is constant and Φ'' is negative when evaluated with the growth equation and positive when evaluated with the no-growth equation. We find that

$$\Phi''_{ng} = \{A_m\}V^{2/3}f',$$

$$\Phi''_{g} = \begin{cases} \frac{1}{3}V^{-1/3}\left(3\{A_m\}Vf' - \frac{dV}{dt}(3([M] - \sigma[G])V^{1/3} - 2\{A_m\}f)\right), & \text{if } E > E_{tr}, \\ \frac{1}{3}V^{-1/3}\left(3\{A_m\}Vf' - \frac{dV}{dt}(3[M]V^{1/3} - 2\{A_m\}f)\right), & \text{if } E \leq E_{tr}, \end{cases}$$

where the subscripts "ng" and "g" mean that the function is evaluated at V and E from the no-growth and growth equations, respectively. Necessary conditions for the individual to be in a balanced-growth regime are $f' > 0$ and $3([M] - \sigma[G])V^{1/3} - 2\{A_m\}f > 0$ or $3[M]V^{1/3} - 2\{A_m\}f > 0$. These conditions ensure that the denominators in equation (17) do not change sign and $\frac{dV}{dt} > 0$. Thus the organism does not shrink in size and there exists a continuously differentiable function V that satisfies equation (17).

In a variable food environment an organism may alternate between growth, no-growth, or balanced-growth regimes. The initial values of V and E in a regime will be their final values from the preceeding regime. Consequently, by construction,

the functions V and E are continuous and piecewise differentiable for all $t \geq 0$. Furthermore, the function $\Phi(t) = E(t) + [G]V(t)$ is continuously differentiable for $t > 0$. Indeed, if t_k, $k = 0, 1, \ldots$ denote the transition times, then on each of the subintervals (t_k, t_{k+1}) the function Φ is continuously differentiable since it is the sum of continuously differentiable functions and

$$\Phi'(t) = \{A_m\} f(t) V^{2/3}(t) - [M]V(t) - \sigma(E(t) - E_{tr})_+ \equiv A - M - R.$$

In addition, since the functions V and E are continuous at t_k, $\lim_{t \to t_k^-} \Phi'(t) = \lim_{t \to t_k^+} \Phi'(t) = c$, where $c = \{A_m\} f(t_k) V^{2/3}(t_k) - [M]V(t_k) - \sigma(E(t_k) - E_{tr})_+$. Consequently, the derivative $\Phi'(t)$ exists at the points t_k and $\Phi'(t_k) = c$.

Next we show the transitions between different growth regimes. Let us first assume that at some time t_0 the organism enters the growth regime with $V(t_0) = V_0$ and $E(t_0) = E_0$; i.e. the dynamics of V and E are described by (14a) and (14b) for $t > t_0$. If there exists a time $t_1 > t_0$ such that $\Phi'(t_1) = 0$ and $\Phi' \leq 0$ on an interval $(t_1, t_1 + a)$ with $a > 0$, the organism stops growth and enters a no-growth or balanced-growth regime. If $\Phi''_{ng}(t_1^+) \leq 0$ implying $\Phi'_{ng}(t_1^+) \leq 0$, the organism enters a no-growth regime. If $\Phi''_{ng}(t_1^+) > 0$ implying $\Phi'_{ng}(t_1^+) > 0$, the organism enters a balanced-growth regime.

Now suppose that the organism enters the no-growth regime at some time t_0 and also that there exists a time $t_1 > t_0$ and $a > 0$ such that for $t \in (t_1, t_1 + a)$ $\Phi(t) \geq \Phi_{max}(t)$ and $\Phi' \geq 0$, where Φ_{max} is the maximum total energy the individual attained in the past. If $\Phi'(t_1) > 0$ then, by continuity of Φ', $\Phi'_g(t_1^+) > 0$ and the organism enters the growth regime. If $\Phi'(t_1) = 0$ then the organism enters a growth regime if $\Phi''_g(t_1^+) \geq 0$ and a balanced-growth regime if $\Phi''_g(t_1^+) < 0$.

Thus, the organism enters a balanced-growth regime at some time t_0 for which $\Phi'(t_0^-) = 0$, $\Phi(t_0) = \Phi_{max}(t_0)$, when $\Phi''_g < 0$ and $\Phi''_{ng} > 0$ on a small interval to the right of t_0. The organism exits the balanced-growth regime when either both Φ''_g and Φ''_{ng} are positive or $\Phi''_g > 0$ and $\Phi''_{ng} < 0$ (organism enters the growth regime) or both Φ''_g and Φ''_{ng} are negative (organism enters the no-growth regime).

Appendix C

The following proposition gives a necessary and sufficient condition on the model parameters for which an individual growing in a constant environment reaches asymptotic size; that is, growth does not stop in finite time.

Proposition 1. *Let* $(\ell(t), \mathscr{E}(t))$ *be the solution of system (19) with initial conditions* $(\ell(0), \mathscr{E}(0)) = (\ell_b, \frac{1-\alpha}{\alpha}\ell_b^3)$. *Then* $\Psi'(t) > 0$ *and* $\Psi(t) \geq \max_{0 \leq \tau \leq t} \Psi(\tau)$ *for all* $t \geq 0$, *where* $\Psi(t) = \mathscr{E}(t) + \ell^3(t)$, *if and only if* $\sigma \geq \gamma$.

Proof. For constant $f > \ell_p$ and initial conditions $(\ell_b, \frac{1-\alpha}{\alpha}\ell_b^3)$, the solution of system (19) is given by equations (22) and (24). The inequality $\Psi(t) \geq \max_{0 \leq \tau \leq t} \Psi(\tau)$

for all $t \geq 0$ is equivalent to $\Psi'(t) \geq 0$ for all $t \geq 0$. Therefore, we must show that $\Psi'(t) > 0$ for all $t \geq 0$ if and only if $\sigma \geq \gamma$.

Using (24), we find that

$$\Psi'(t) = \begin{cases} 3\gamma\,(f - \ell(t))\,\ell^2(t) & 0 \leq t \leq a_p \\ 3\gamma(f - \ell(t))\left(\ell^2(t) - \sigma(1-\alpha)e^{-(\sigma-\gamma\alpha)t}\displaystyle\int_{a_p}^{t} \ell^2(\tau)e^{(\sigma-\gamma\alpha)\tau}\,d\tau\right) & t > a_p \end{cases} \tag{33}$$

Note that $\Psi'(t) > 0$ for all $t \in [0, a_p]$.

From the Mean Value Theorem for integrals, we have that for any $t > a_p$ there exists $\xi \in [a_p, t]$ such that

$$\int_{a_p}^{t} \ell^2(\tau)e^{(\sigma-\gamma\alpha)\tau}\,d\tau = \ell^2(\xi)\int_{a_p}^{t} e^{(\sigma-\gamma\alpha)\tau}\,d\tau = \frac{\ell^2(\xi)(e^{(\sigma-\gamma\alpha)t} - e^{(\sigma-\gamma\alpha)a_p})}{\sigma - \gamma\alpha}$$

Therefore, for any $t > a_p$

$$\Psi'(t) = 3\gamma(f - \ell(t))\left(\ell^2(t) - \theta\ell^2(\xi)\left(1 - e^{(\sigma-\gamma\alpha)(a_p - t)}\right)\right) \tag{34}$$

for some $\xi \in [a_p, t]$, where $\theta = \dfrac{\sigma(1-\alpha)}{\sigma - \gamma\alpha}$. We will prove the proposition by contradiction.

Let $\sigma \geq \gamma$ (equivalently $0 < \theta \leq 1$) and suppose that $\Psi'(t_s) \leq 0$ at some finite time $t_s > a_p$. Then from (34), for any $t > a_p$ and $\xi \in [a_p, t]$

$$\begin{aligned} \Psi'(t) &= 3\gamma(f - \ell(t))\left(\ell^2(t) - \theta\ell^2(\xi) + \theta\ell^2(\xi)e^{(\sigma-\gamma\alpha)(a_p - t)}\right) \\ &> 3\gamma(f - \ell(t))\left(\ell^2(t) - \theta\ell^2(\xi)\right) \\ &> 3\gamma(f - \ell(t))\ell^2(t)(1 - \theta) \geq 0. \end{aligned}$$

This is a contradiction. This proves that if $\sigma \geq \gamma$ then $\Psi'(t) > 0$ for all $t > a_p$.

Now suppose that $\Psi'(t) > 0$ for all $t > a_p$ and $\sigma < \gamma$. Then from (33) we must also have that

$$\psi(t) > 0 \quad \forall\, t > a_p \qquad \text{and} \qquad \lim_{t\to\infty} \psi(t) \geq 0,$$

where

$$\psi(t) \equiv \ell^2(t) - \sigma(1-\alpha)e^{-(\sigma-\gamma\alpha)t}\int_{a_p}^{t} \ell^2(\tau)e^{(\sigma-\gamma\alpha)\tau}\,d\tau.$$

If $\gamma\alpha < \sigma < \gamma$, then $\theta \geq 1$ and

$$\lim_{t\to\infty}\int_{a_p}^{t} \ell^2(\tau)e^{(\sigma-\gamma\alpha)\tau}d\tau = +\infty.$$

Using L' Hospital's rule, we find that

$$\lim_{t\to\infty} \frac{\displaystyle\int_{a_p}^{t} \ell^2(\tau)e^{(\sigma-\gamma\alpha)\tau}d\tau}{e^{(\sigma-\gamma\alpha)t}} = \frac{f^2}{\sigma - \gamma\alpha}.$$

Thus,

$$\lim_{t\to\infty} \psi(t) = f^2(1-\theta) < 0.$$

Similarly, if $\sigma < \gamma\alpha$, then $\theta < 0$ and

$$\lim_{t\to\infty} \int_{a_p}^{t} \ell^2(\tau) e^{(\sigma-\gamma\alpha)\tau} d\tau = -\frac{f^2}{\sigma-\gamma\alpha} > 0.$$

Thus,

$$\lim_{t\to\infty} \psi(t) = -\infty.$$

Finally, if $\sigma = \gamma\alpha$, then $\psi(t) = \ell^2(t) - \sigma(1-\alpha)\int_{a_p}^{t} \ell^2(\tau)\, d\tau$ and $\lim_{t\to\infty} \psi(t) = -\infty$.

Consequently, the assumption $\sigma < \gamma$ leads to contradiction. Hence, if $\Psi'(t) > 0$ for all $t > a_p$ then $\sigma \geq \gamma$. Q.E.D.

Proposition 1 implies that if $0 < \sigma < \gamma$ growth stops at some finite time. It can be shown that there is a finite $t_s = \inf\{t > 0 : \Psi'(t) = 0\}$ for $\sigma \in (0, \gamma)$ and that as $\sigma \to 0^+$ or $\sigma \to \gamma^-$, $t_s \to \infty$. We can find t_s from equation

$$\ell^2(t_s) - \sigma(1-\alpha)e^{-(\sigma-\gamma\alpha)t_s} \int_{a_p}^{t_s} \ell^2(\tau) e^{(\sigma-\gamma\alpha)\tau}\, d\tau = 0, \tag{35}$$

where $\ell(t) = f - (f-\ell_b)e^{-\gamma\alpha t}$. Substituting the expression for ℓ the integral can be evaluated exactly resulting in a nonlinear equation for t_s. We calculate t_s using the bisection method [23].

Acknowledgements. We thank Steve Ellner, Bill Gurney, Tom Hallam, Bas Kooijman, Ed McCauley, Erik Muller, Bill Murdoch, Erik Noonburg, Andre de Roos and Will Wilson for many discussions of DEB models. We gratefully acknowledge the constructive criticisms of Odo Diekmann and an anonymous referee. The research was supported by grant DEB -9319301 from the National Science Foundation, by grants N00014-93-1-0952 and N00014-99-10024 from the Office of Naval Research, and by the Minerals Management Service, U.S. Department of the Interior, under MMS Agreement No. 14-35-0001-30761. The views and conclusions contained in this document are those of the authors and should not be interpreted as necessarily representing the official policies, either express or implied, of the U.S. Government.

References

1. Brockhuizen, N., Gurney, W.S.C., Jones, A., Bryant, A.D.: Modelling compensatory growth. *Functional Ecology*, **8**(6), 770–782 (1994)
2. Bulmer, M.: *Theoretical Evolutionary Ecology*. Sinauer, (1994)
3. Coddington, E.A., Levinson, N.: Theory of Ordinary Differential Equations. McGrow Hill, New York, (1955)
4. Gurney, W.S.C., McCauley, E., Nisbet, R.M., Murdoch, W.W.: The physiological ecology of Daphnia: Formulation and tests of a dynamic model of growth and reproduction. Ecology, **71**, 716–732 (1990)
5. Gurney, W.S.C., Middleton, D.A.J., Nisbet, R.M., McCauley, E., Murdoch, W.W., de Roos, A.M.: Individual energetics and the equilibrium demography of structured populations. Theoretical Population Biology, **49**, 344–368 (1996)

6. Gurney, W.S.C., Nisbet, R.M.: Ecological Dynamics. Oxford University Press, (1998)
7. Hallam, T.G., Lassiter, R.R., Kooijman, S.A. L.M.: Effects of toxicants on aquatic populations. In S. Levin, T. Hallam, and L. Gross, editors, Applied Mathematical Ecology, volume 18, pages 352–382, Berlin Heidelberg, (1989) Springer-Verlag.
8. Hallam, T.G., Lassiter, R.R., Li, J., Suarez, L.A.: Modelling individuals employing an integrated energy response: Application to Daphnia. Ecology, **71**(3), 938–954 (1990)
9. Kitchell, J.F., Koonce, J.F., O'Neill, R.V., Shugart, J.H.H., Magnuson, J.J., Booth, R.S.: Model of fish biomass dynamics. Trans. Amer. Fish Soc., **(4)**, 786–798 (1974)
10. Kitchell, J.F., Stewart, D.J., Weininger, D.: Applications of a bioenergetics model to yellow perch (*perca flavescens*) and walleye (*stizostedion vitreum vitreum*). J. Fish Res. Board Can., **34**, 1922–1935 (1977)
11. Kooijman, S.A.L.M.: Dynamic Energy Budgets in Biological Systems. Theory and Applications in Ecotoxicology. Cambridge University Press, (1993)
12. Kooijman, S.A.L.M., Bedaux, J.J.M.: The Analysis of Aquatic Toxicity Data. VU University Press, Amsterdam, (1996)
13. Kooijman, S.A.L.M., Haren, R.J.F.: Animal energy budgets affect the kinetics of xenobiotics. Chemosphere, **21**, 681–693 (1990)
14. Lassiter, R.R., Hallam, T.G.: Survival of the fattest: A theory for assessing acute effects of hydrophobic, reversibly acting chemicals on populations. Ecology, **109**, 411–429 (1988)
15. McNamara, J.M.: Optimal life histories for structured populations in variable environments. Theor. Pop. Biol., **51**, 94–108 (1997)
16. Metz, J.A.J., Dikmann, O.: The Dynamics of Physiologically Structured Populations, volume 68 of Lecture Notes in Biomathematics. Springer-Verlag, Berlin, West Germany, (1986)
17. Muller, E.B., Nisbet, R.M.: Sublethal effects of toxic compounds on dynamic energy budgets: theory and applications. submitted, (1997)
18. Mylius, S.D., Diekmann, O.: On evolutionary stable life histories, optimization and the need to be specific about density dependence. Oikos, **74**, 218–224 (1995)
19. Nisbet, R.M., Gurney, W.S.C., Metz, J.A.J.: Stage structure models applied in evolutionary ecology. In S. Levin, T. Hallam, and L. Gross, editors, Applied Mathematical Ecology, 18, 428–449, Berlin Heidelberg, (1989) Springer-Verlag.
20. Nisbet, R.M., Ross, A.H., Brooks, A.J.: Empirically–based dynamic energy budget models: theory and an application to ecotoxicology. Nonlinear World, **3**, 85–106 (1996)
21. Noonburg, E.G., Nisbet, R.M., McCauley, E., Gurney, W.S.C., Murdoch, W.W., de Roos, W.W.: Experimental testing of dynamic energy budget models. Functional Ecology, 1998. in press.
22. Paloheimo, J.E., Crabtree, S.J., Taylor, W.D.: Growth model of Daphnia. Can. J. Fish. Aquat. Sci., **39**, 598–606 (1982)
23. Press, W.H., Flanney, B.P., Tenkolsky, S.A., Vetterling, W.T.: Numerical Recipes in Fortran. Cambridge University Press, (1988)
24. Ratsak, C.H., Kooi, B.W., van Verseveld, H.W.: Biomass reduction and mineralization increase due to the ciliate tetrahymena pyriformis grazing on the bacterium pseudomonas fluorescens. Water Sci. Tech., **29**, 119–128 (1994)
25. Ratsak, C.H., Kooijman, S.A. L.M., Kooi, B.W.: Modelling of growth of an oligochaete on activated sludge. Water Res., **27**, 739–747 (1993)
26. Ratsak, C.H., Maarsen, K.A., Kooijman, S.A. L.M.: Effects of protozoa on carbon mineralization in activated sludge. Water Res., **30**, 1–12 (1996)
27. Roff, D.A.: The Evolution of Life Histories: Theory and Analysis. Chapman & Hall, (1992)

28. Ross, A.H., Nisbet, R.M.: Dynamic models of growth and reproduction of the mussel mytilus edulis L. Functional Ecology, **4**, 777–787 (1990)
29. Stearns, S.C.: The Evolution of Life Histories. Oxford University Press, (1992)
30. Tuljapurkar, S., Caswell, H.: Structured Population Models in Marine, Freshwater, and Terrestrial Systems. Chapman & Hall, (1997)

Bulletin of Mathematical Biology (2000) **62**, 1163–1189
doi:10.1006/bulm.2000.0203
Available online at http://www.idealibrary.com on IDEAL

Survival and Production in Variable Resource Environments

ERIK B. MULLER* AND ROGER M. NISBET
Department of Ecology,
Evolution and Marine Biology,
University of California,
Santa Barbara,
CA 93106-9610, U.S.A.
E-mail: muller@lifesci.ucsb.edu

A dynamic energy budget (DEB) model describes the rates at which organisms assimilate and utilize energy from food for maintenance, growth, reproduction and development. We study the dynamic behavior of one particular DEB model, Kooijman's κ-rule model, whose key assumption is that somatic and reproductive tissues are competing for energy. We assume an environment in which the food density fluctuates either periodically or stochastically (pink noise). Both types of fluctuations stimulate growth; the magnitude of the (average) increase in size depends on both the strength and duration of the fluctuations. In a stochastic environment, the risk of mortality due to starvation increases with increasing fluctuation intensity. The mean lifespan is also a function of the model parameter κ characterizing the partitioning of energy between somatic and reproductive tissues. Organisms committing a large fraction of resources to reproduction endure periods of food shortage relatively well. The effects of food fluctuations on reproduction are complex. With stochastic food, reproduction in survivors increases with increasing fluctuation intensities, but lifetime reproduction decreases. Periodic fluctuations may enhance reproduction, depending on the value of κ. Thus, a variable food supply stimulates growth, increases mortality and may enhance reproduction, depending on life history.

INTRODUCTION

Organisms acquire energy from their environment and use it for growth and propagation. These and other expenditures are commonly modeled in terms of budgets. The simplest models assume a few fluxes that do not change over time, and use a mass or energy balance equation to analyse experimental results. More complex models use dynamic equations to describe the change of a potentially large number of many different budgets and fluxes. Models of both types abound in biology, and some date back more than a century (Duclaux, 1898). Our interest here is in simple

*Author to whom correspondence should be addressed

0092-8240/00/061163 + 27 $35.00/0

dynamic models with a limited number of budgets, which we call dynamic energy budget (DEB) models. A DEB model describes the rates at which organisms assimilate and utilize energy from food for maintenance, growth, reproduction and development. These rates depend on the state of the organism (age, size, sex, nutritional status, etc.) and the state of its environment (food density, temperature, etc.). In this paper we study the behavior of one particular DEB model in a variable food environment.

Most DEB models are specific to one life stage of an organism or a (group of) species, the goal being to get a close match between data and model descriptions [see e.g., Kitchell *et al.* (1977), McCauley *et al.* (1990) and Mangel (1996)]. Another approach, followed here, is to use a single model that is sparse in parameters and mechanistically justifiable, but that nevertheless describes a broad spectrum of biological phenomena and life forms. Species are similar because they follow the same principles for budgeting, but they are different because they have different parameter values. A well-known example of this approach is von Bertalanffy's (1957) theory of growth, which uses only two parameters to fit the growth of many species with remarkable success. We study the most comprehensive model based on this approach, the κ-rule model developed by Kooijman (1986, 2000) (see Fig. 1). This model uses mechanistic reasoning to describe the growth and propagation of a wide range of species, ranging from bacteria to mammals, and with further mechanistic assumptions, the model can be used to derive inter-specific scaling relationships for physiological processes and body size. The model has been used in the study of the dynamics of (structured) populations (De Roos, 1997; Kooijman *et al.*, 1999), simple food chains (Kooi and Kooijman, 1994) and ecosystems (Kooijman and Nisbet, in press), and it provides a basis for many concepts used in ecotoxicology (Kooijman and Bedaux, 1996a,b).

Although DEB models, including the κ-rule model, were developed specifically for variable food environments (McCauley *et al.*, 1990; Ross and Nisbet, 1990; Kooijman, 2000; Lika and Nisbet, in press), to date most applications make an assumption of constant food. However, a model that fits organisms in a constant environment may not be appropriate when ambient conditions change with time. With constant food, different models can make similar predictions, whereas transient dynamics reveal the more distinctive implications of the assumptions of a model (Nisbet *et al.*, 1996). It is therefore important to analyse model behavior in a dynamic food environment.

We study the behavior of the κ-rule model in a fluctuating food environment. We consider two types of food fluctations. One is a periodically variable food environment, which may represent diurnal or seasonal changes; the other is an environment in which food fluctuates stochastically but with some memory for previous food levels (pink noise). We study survival and performance as a function of the strength and the time scale of the food fluctuations, and also as a function of a potentially adaptive model parameter, the parameter specifying the division of resources between somatic and reproductive tissues. We first examine the dy-

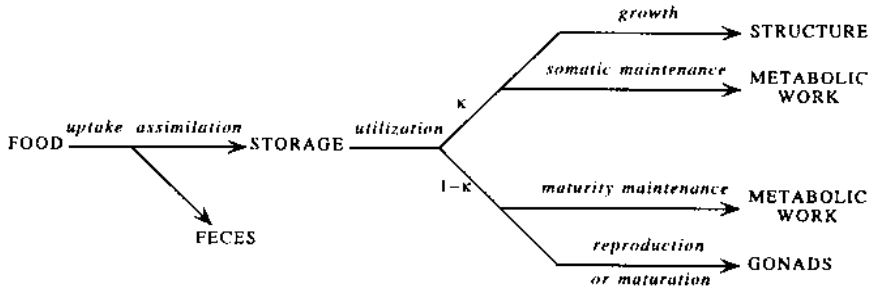

Figure 1. Kooijman's κ-rule model assumes that an organism ingests food at a rate dependent on its size and the food density (Kooijman, 2000). Energy is extracted from food and added to the reserves. The rate at which energy becomes available to the organism depends on its size and stored energy density. Provided somatic maintenance requirements are met, a fixed proportion κ of the available energy is allocated to somatic maintenance and growth combined, and the remaining $1 - \kappa$ to either maturation (for embryos and juveniles) or to reproduction and maturity maintenance (for adults). Growth ceases when this fixed fraction κ just meets somatic maintenance demands. Then, the organism may still reproduce, provided that energy made available exceeds the requirements for somatic and maturity maintenance.

namics of model equations analytically, which examination gives access to the long-term dynamics in a periodically fluctuating food environment. Because of the nonlinearities of the model, however, we need to rely on numerical studies for an understanding of the transient dynamics. Numerical analysis is also the primary means by which we study model behavior in a stochastically variable food environment. We illustrate model behavior with the marine mussel *Mytilus edulis*, for which realistic parameter values are available.

The Model

The DEB model used in this study, the κ-rule model, is outlined in Fig. 1, and its assumptions are listed in Table 2. Kooijman (2000) has documented an elaborate justification of the assumptions, and a derivation of model equations can be found in Kooijman (1986, 2000), Zonneveld and Kooijman (1989), Van Haren and Kooijman (1993) and Nisbet *et al.* (1996). Here, for brevity, we restrict our presention of the model to ectothermic, heterotrophic organisms that do not change shape during growth [for a model extension that includes autotrophs see Kooijman and Nisbet (in press) and Kooijman (2000, pp. 159–185); for species that do change shape during growth, see, Kooijman (2000, pp. 26–29); and for endothermic organisms see, Kooijman (2000, pp. 92–96)].

The assumptions in Table 2 imply that the dynamics of an organism's growth and reproduction are described by two differential equations. One specifies the dynamics of structural body volume V, the other specifies the dynamics of the density of

Table 1. Symbols. A bar over a symbol refers to asymptotic values.

Symbol	Dimension	Interpretation
a	—	amplitude of scaled food density
a_c	—	critical amplitude of scaled food density
e	—	scaled stored energy density
$\bar{e}_c$	—	critical highest scaled stored energy density in limit cycle
$\bar{e}_{\max}$	—	highest scaled stored energy density in limit cycle
e_{rm}	—	scaled cumulative energy density committed to reproduction
f	—	scaled food density or scaled functional response
f_a	—	average scaled food density
g	—	energy investment ratio, $\propto \frac{1}{\kappa}$
L	length	shell length
m	time^{-1}	maintenance rate coefficient
r	time^{-1}	von Bertalanffy growth rate, $\frac{mg}{3(f+g)}$
S	time^{-1}	squared food fluctuation intensity
V	volume	structural biovolume
V_b	volume	structural biovolume at birth
V_m	volume	maximum structural biovolume, $\frac{\upsilon}{mg}$
V_p	volume	structural biovolume at maturation
V_∞	volume	ultimate structural biovolume at constant food, $f^3 V_m$
z	—	random variable
γ	time$^{-1/2}$	Gaussian white noise
κ	—	energy partitioning coefficient
τ	time	memory retention time
υ	volume$^{1/3}$ time^{-1}	energy conductance rate
ω	rad time^{-1}	angular frequency
ω_c	rad time^{-1}	critical angular frequency

the energy reserves, $[E]$, defined as the amount of stored energy per unit of structural volume. Reserve density has a maximum value $[E_m]$, which is independent of the size of the organism and the feeding conditions. The rate of change of stored energy density depends on the rate A at which energy is assimilated from food, and the rate at which energy is utilized. The assimilation rate is written in the form $A = A_m f V^{2/3}$, where the proportionality constant A_m represents the maximum surface area specific assimilation rate and f is the scaled functional response (type II). The rate at which energy reserves are released for utilization is a first order process inversely proportional to $V^{1/3}$. When maintenance requirements can be met this way, a fraction κ of the energy released from the reserves is used for the somatic processes of maintenance and growth, with maintenance having priority; the remainder is used for reproduction (adults), development (juveniles) and for maintenance of the state of maturity. This is the κ-rule. The κ-rule cancels when maintenance demands cannot be met this way. Then, maintenance requirements are being paid first, and the remainder is used for reproduction and development. When even this is insufficient, that is, the rate at which energy is released from

Table 2. Assumptions of the κ-rule model for ectothermic heterotrophs.

- There are two state variables: structural body volume, and stored energy density scaled to its maximum.
- There are six energy fluxes: assimilation; somatic maintenance; somatic growth; development; maintenance of the state of maturity; and reproduction. These energy fluxes are irreversible.
- There are maximally three life stages: embryos, which neither feed nor reproduce; juveniles, which may feed but do not reproduce; and adults, which may feed and reproduce.
- The rate of food uptake is proportional to the surface area of an organism, and is a hyperbolic function of the food density (type II functional response).
- Energy assimilated from food becomes part of the reserves. The dynamics of the energy reserve density are first order, with a rate that is inversely proportional to the volumetric length of an organism.
- A fixed fraction of the energy released from the reserves is commited to somatic maintenance and growth; the remainder is used for maturity maintenance, and development or reproduction. Maintenance demands have priority, and the partitioning of energy is modified to meet somatic maintenance.
- Death due to starvation occurs when somatic maintenance requirements cannot be met.
- The chemical compositions of structure and reserves are constant (homeostasis), and thus the following are constant:
  - the conversion efficiency of food into energy;
  - the cost to form a unit of structure;
  - the cost to maintain a unit of structure for a period;
  - the cost to maintain the state of maturity for a period;
  - the cost to form a unit of reproductive matter.
- Life stage transitions occur when the cummulative amount of energy spent on maturation exceeds a threshhold. An embryo initially has a negligibly amount of structure, and, when propagation is via eggs, its energy reserve density at hatching equals that of its mother during egg formation.

reserves is less than the rate at which energy is needed to maintain viability, the organism dies. It takes a constant amount of energy $[M]$ to maintain a unit of structure for a period of time, and a constant amount of energy $[G]$ to form a unit of structure.

Although the model describes flows of energy, our primary interest is in the dynamics of quantities (e.g., size, rate of reproduction) whose dimensions do not involve energy. It is convenient to scale variables and parameters to take account of this, and, following Kooijman (2000), we define the following quantities: the scaled density of energy reserves, $e \equiv \frac{[E]}{[E_m]}$; the energy conductance rate, $v \equiv \frac{A_m}{[E_m]}$; the maintenance rate coefficient, $m \equiv \frac{[M]}{[G]}$; and the investment ratio, $g \equiv \frac{[G]}{\kappa[E_m]}$. Note that g depends on κ, a primary parameter we use explicitly at several points in this study. This scaling with g is a bit unfortunate, but is a price worth paying to retain notation consistent with the large body of literature on the κ-rule model.

With e replacing $[E]$ as the state variable for energy reserves, the state equations now become

$$\frac{de}{dt} = vV^{-\frac{1}{3}}(t)(f(t) - e(t)), \tag{1}$$

$$\frac{dV}{dt} = \frac{(\upsilon e(t) V^{\frac{2}{3}}(t) - mgV(t))_+}{e(t) + g}, \tag{2}$$

The subscript '+' in equation (2) means that an organism cannot shrink, i.e., $\frac{dV}{dt} = 0$ whenever $\upsilon e(t) V^{\frac{2}{3}}(t) - mgV(t) < 0$, i.e., when the default energy committed to somatic tissues is insufficient to meet maintenance demands. The maximum structural body volume, V_m, an organism can attain is $V_m = \left(\frac{\upsilon}{mg}\right)^3$; V_m is proportional to κ^3, because of its dependency on g.

We also seek to quantify reproduction. The assumptions specify the rate at which energy is committed to reproduction. We divide the amount of energy committed to reproduction by the maximum structural volume an organism would attain with abundant food if it were to devote all its energy to somatic tissues, and scale the resulting density by the maximum possible density of the energy reserves. This measure is the scaled cumulative reproductive output, e_{rm}. Provided that the organism has reached the size of an adult, that is $V \geq V_p$, the dynamics of e_{rm} follow (Kooijman, 2000, pp. 100–101)

$$\frac{de_{rm}}{dt} = \begin{cases} \frac{\kappa^3(1-\kappa)}{V_m}\left(\frac{ge(\upsilon V^{2/3} + mV)}{g+e} - mgV_p\right) & \text{if } e \geq \frac{V^{1/3}}{V_m^{1/3}} \\ \frac{\kappa^3}{V_m}(\upsilon e V^{2/3} - mg(\kappa V + (1-\kappa)V_p))_+ & \text{if } \frac{\kappa V^{1/3}}{V_m^{1/3}} > e > \frac{V^{1/3}}{V_m^{1/3}}. \end{cases} \tag{3}$$

The first condition is true for growing organisms, whereas the second applies to non-growing individuals. Note that this equation does not necessarily define the actual reproduction rate. The model assumes a continuous and irreversible allocation of energy reserves for reproductive purposes, but the release of reproductive matter may be a discrete event.

The model simplifies considerably when the food level is constant. The scaled density of stored energy will approach an equilibrium, that is, $\bar{e} = f$, so that equation (2) can be solved analytically. The solution of equation (2) is the well-known von Bertalanffy growth equation,

$$V^{1/3}(t) = V_\infty^{1/3} - (V_\infty^{1/3} - V_0^{1/3})e^{-rt}, \tag{4}$$

where $V_\infty^{1/3} = fV_m^{1/3}$ is the ultimate volumetric length of the organism at a given food level, and $r \equiv \frac{mg}{3(f+g)}$, is the von Bertalanffy growth rate parameter which defines how fast an organism approaches its ultimate size. For practical purposes, the volumetric lengths in equation (4) can be substituted for an experimentally convenient length measure, such as shell length in mussels, since we confined this presentation to isomorphic organisms.

Food Availability

We now want to understand how model organisms perform in a variable food environment. Food levels may fluctuate in many different ways. We consider two

idealized forms of variation, one in which food levels vary deterministically, and one in which food levels are in part driven by a stochastic process. For both types, we assume that the variations operate directly on the scaled functional response rather than on the food density, an assumption that makes it relatively easy to compare model behavior under different fluctuation regimes. The form of the scaled functional response in the model is type II, but we note that our analysis holds for any dimensionless form that takes values between 0 and 1.

For deterministic food variations we assume a periodically changing food environment resembling, for instance, the alternation of high and low food due to diurnal or seasonal changes. For simplicity, we only consider single frequency variations. Assuming a scaled functional response that fluctuates sinusoidically with an amplitude a, angular frequency ω, and a mean value f_a between 0 and 1, we have

$$f(t) = f_a + a\sin(\omega t), \qquad a \leq \min\{f_a, 1 - f_a\}. \tag{5}$$

Over a full period, the mean scaled functional response is f_a, and the mean square deviation from f_a is $0.5a^2$. In contrast to the symmetrical fluctuations in the scaled functional response, the unscaled food density shows narrow seasonal peaks and changes little in the off-season, a pattern that gets more pronounced with increasing f_a and a. This pattern is consistent with food variations in environments in which a season with excess food alternates with a longer, less productive season, a pattern common in temperate and polar regions.

In order to simulate a stochastic environment, we assume pink noise $z(t)$ is added to the mean value for the scaled functional response [see, Nisbet and Gurney (1982, pp. 240–246)]. However, because $0 \leq f \leq 1$, we require to bound possible outcomes to ensure f stays within this range. So,

$$f(t) = \begin{cases} 0 & \text{if } f_a + z(t) < 0 \\ f_a + z(t) & \text{if } 0 \leq f_a + z(t) \leq 1 \\ 1 & \text{if } f_a + z(t) > 1, \end{cases} \tag{6}$$

where $z(t)$ is a random variable whose dynamics are given by

$$\frac{dz}{dt} = \frac{-z}{\tau} + S^{1/2}\gamma(t), \tag{7}$$

in which τ is the memory retention time, which quantifies the exponentially fading memory for previous values of $z(t)$, and γ is Gaussian white noise with intensity $S^{1/2}$. The pink noise assumption ensures that food is likely to be abundant at some time if it was abundant just prior to that moment, and scarce when it was scarce just before. Gaussian white noise generates a random walk, but f is bounded here. Unless $f_a = 0.5$, the distribution of $f(t)$ is skewed, and this skewedness increases with the intensity of the fluctuations. When $f_a = 0.5$ the distribution is symmetrical. Then, like the deterministic case, the expected value for the scaled functional response is f_a and, while depending on the cut off of f, the mean square displacement from f_a is maximally $S^2\tau$.

DYNAMICS IN VARIABLE FOOD ENVIRONMENTS

We wish to solve two questions with regard to variable food environments. First: 'Can an organism survive in a variable food environment?', and second: 'Given that an organism survives in a variable food environment, what is the form of the long-term dynamics?' The latter question is relevant since older organisms that have (apparently) ceased growth will have dynamics that are arbitrarily close to those long-term dynamics. Because of the nonlinearities in the model, neither the transient dynamics with deterministically fluctuating food, nor the behavior of the model when food varies stochastically can be determined analytically. In a later section, we address these issues via numerical studies. We show here that, under certain circumstances, an organism may survive a periodically varying food environment for an indefinite time, and that the long-term dynamics of the state variables determine the environmental conditions for survival at any time. We also compare long-term reproduction in periodically variable food environments with that in a constant environment.

We show in the Appendix that, provided the organism survives, its scaled energy reserve density approaches the limit cycle

$$\bar{e}(t) = f_a + \frac{a}{\sqrt{1 + \left(\frac{\omega \bar{V}^{1/3}}{\upsilon}\right)^2}} \sin(\omega t + \phi), \tag{8}$$

where $\phi = \tan^{-1} \frac{\omega \bar{V}^{1/3}}{\upsilon}$, is a measure (in radians) of the extent to which fluctuations in e ultimately lag behind f. The organism continues to grow until it attains a size $\bar{V}$ given by

$$\bar{V} = \left(\frac{\bar{e}_{\max} \upsilon}{mg}\right)^3, \tag{9}$$

with $\bar{e}_{\max}$ being the highest scaled energy density in the limit cycle, which occurs when $\sin(\omega t + \phi) = 1$. Figure 2 illustrates the transient approach to the long-term dynamics discussed above.

Equations (8) and (9) reveal three important model features. First, the long-term dynamics of e and V are independent of initial conditions. Provided an organism can survive periods of low food availability, it will ultimately grow to a certain size and exhibit certain reserve dynamics independent of the season it was born. Second, the highest scaled energy density in the limit cycle and the ultimate size increase with the amplitude of the food fluctuations. Thus, surviving organisms grow bigger the more intense the fluctuations in the food environment. Third, the capacity of the energy reserves to buffer changes in the food environment depends on the rate at which the food environment changes relative to the dynamics of energy reserves. When food levels are changing relatively slowly, that is ω is small, $\bar{e}_{\max}$ will be close to $f_a + a$, and reserves are fluctuating with an amplitude similar

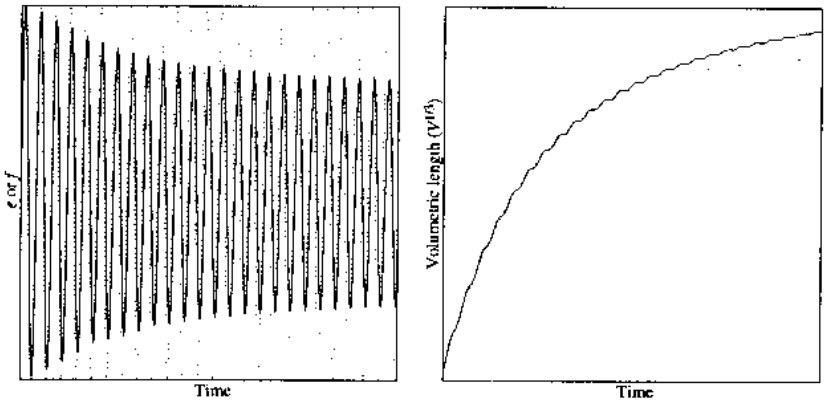

Figure 2. The scaled stored energy density (solid curve; left curve) tracks (with a lag) the scaled food density (dotted curve; left panel) in a variable food environment. As the organism grows, the time that the scaled stored energy density lags behind the scaled food density increases, while the amplitude of the energy density decreases. Its length as a function of time is shown in the right panel (solid curve); the dotted curve in the right panel represents growth at constant food.

to that of food availability. However, in a rapidly changing food environment $\bar{e}_{\max}$ will be close to f_a and, from the organism's point of view, the environment will be virtually constant.

Now assume that an organism is born into an environment similar to that of its mother, implying that $e(0)$ is in the range of values for the scaled functional response it will experience (see Table 2). Then, if an organism is able to survive through a limit cycle, it is also able to survive through the transient (see the Appendix). Thus we can simply study long-term dynamics in order to answer questions about the environmental conditions that ensure viability. The organism grows to a size proportional to the highest scaled energy density in the limit cycle, but its long-term survival depends on the lowest scaled density of energy reserves in the limit cycle $\bar{e}_{\min}$. Equation (8) implies $\bar{e}_{\min} = \bar{e}_{\max} - 2a\left(1 + \left(\frac{\omega \bar{e}_{\max}}{mg}\right)^2\right)^{1/2}$. Because survival requires that $V(t) \leq \left(\frac{e(t)v}{\kappa mg}\right)^3$ for all t (see the Appendix), we get the following condition for long-term survival:

$$\frac{2a}{\sqrt{1 + \frac{\omega^2 \bar{e}_{\max}^2}{m^2 g^2}}} - \bar{e}_{\max}(1 - \kappa) \leq 0. \tag{10}$$

Using equations (8)–(10), we can now determine the highest scaled density $\bar{e}_c$ of energy reserves in an organism that is just able to survive,

$$\bar{e}_c = \frac{2f_a}{1 + \kappa}. \tag{11}$$

The highest amplitude a_c at which an organism is able to survive periods of low

food is

$$a_c = (\bar{e}_c - f_a)\sqrt{1 + \frac{\omega^2 \bar{e}_c^2}{m^2 g^2}}, \tag{12}$$

which reduces to

$$a_c = f_a \frac{1 - \kappa}{1 + \kappa} \tag{13}$$

in a very slowly changing food environment. Finally, the slowest angular frequency ensuring survival from starvation is ω_c, with

$$\omega_c = \frac{mg(1 + \kappa)}{2f_a}\sqrt{\left(\frac{a(1 + \kappa)}{f_a(1 - \kappa)}\right)^2 - 1}. \tag{14}$$

A prominent role in these expressions for critical values is played by κ, the parameter that defines the partitioning of resources over somatic and reproductive tissues (note that the compound parameter g is inversely proportional to κ). Indirectly, it also determines the organism's abilities for surviving poor food conditions; the potential for survival declines with decreasing κ.

Having determined the long term behavior of the state variables, we can now calculate long-term reproduction. From equation (3) the long-term reproduction rate is

$$\frac{d\bar{e}_{rm}}{dt} = \kappa^3 mg\left(\bar{e}_{\max}^2 \bar{e}(t) - \kappa \bar{e}_{\max}^3 - (1 - \kappa)\frac{V_p}{V_m}\right), \tag{15}$$

with $\bar{e}(t)$ given by equation (8). Integration over a full period then yields the ultimate reproductive output in one cycle ρ, as

$$\rho = \frac{2\pi}{\omega}\kappa^3 mg\left(\bar{e}_{\max}^2 f_a - \bar{e}_{\max}^3 \kappa - (1 - \kappa)\frac{V_p}{V_m}\right). \tag{16}$$

Unlike long-term growth, ultimate reproduction may be reduced in a variable food environment. In a constant environment the ultimate reproduction during a time interval $2\pi/\omega$ equals

$$\frac{2\pi}{\omega}\kappa^3 mg(1 - \kappa)(f_a^3 - V_p/V_m). \tag{17}$$

Thus, ultimate reproduction in a constant environment exceeds that in a variable food environment when $\kappa \geq \frac{\bar{e}_{\max}^2 f_a - f_a^3}{\bar{e}_{\max}^3 - f_a^3}$. Organisms with $\kappa \in \left(0, \frac{\bar{e}_{\max}^2 f_a - f_a^3}{\bar{e}_{\max}^3 - f_a^3}\right)$ perform better in a variable food environment.

Table 3. Parameter values of the mussel *Mytilus edulis* with $\kappa = 0.8$.

Symbol	Value	Correction factor[a]	Reference
d_m[b]	0.333	—	(Van Haren and Kooijman, 1993)
g	1.286	$\frac{0.8}{\kappa}$	(Van Haren and Kooijman, 1993)
L_b	0.001 m	—	(Seed, 1976)
L_m	0.100 m	$\frac{\kappa}{0.8}$	(Van Haren and Kooijman, 1993)
L_p[c]	0.003 m	$\frac{\kappa}{4(1-\kappa)}$	(Seed, 1976)
m[d]	0.583 y^{-1}	—	(Kooijman, 2000, p. 275)
v[d]	0.075 m y^{-1}	—	(Kooijman, 2000, p. 275)

[a] The values of parameters that depend on κ are calculated by multiplying the correction factor with the value listed. [b] Converts volumetric length into shell length, $L = d_m V^{1/3}$. [c] The assumptions imply $L_p \propto \kappa/(1-\kappa)$ (Zonneveld and Kooijman, 1989). [d] Normalized to 20 °C (Kooijman, 2000).

Numerical Studies

In the previous sections, we analysed the behavior of the κ-rule model in a dynamic food environment. We were able to specify long-term dynamics and survival conditions in the situation where food varied deterministically. However, transient dynamics with deterministic food remained largely undetermined, as did the behavior of an organism in a stochastic environment. In the next two subsections, we study our system numerically. We explore model behavior as a function of environmental parameters in the forcing functions, and as a function of the life history parameter κ, since this parameter tends to be highly variable within a species. We illustrate model behavior with parameters appropriate for the marine mussel *Mytilus edulis* (see Table 3); initial values not mentioned in the table are $f(0) = 0.5$ and $e(0) = 0.5$, and the phase of the period with deterministic food fluctuations is 0 rad.

We assume an environment in which food levels vary either deterministically or stochastically around $f_a = 0.5$, which allows us to explore a maximum range of fluctuation intensities. We wish to be able to compare in some systematic way the results of the deterministic and stochastic simulations, and therefore calibrate the stochastic intensity of food fluctuations, $S^{1/2}$, to the deterministic amplitude a. We set $S = a^2/\tau$, so that, neglecting the effects of cut off of f in the stochastic case, the mean squared displacement of f from f_a is similar with both types of food variation. With periodically variable food, we consider fluctuations with a period of a day, year and decade, which, relative to a mussel's physiology, represent a food density that is changing rapidly, moderately slowly or very slowly. For stochastic food, we take the memory retention time τ in stochastic simulations equal to the period of the deterministic cycles, since this yields sets of deterministic and stochastic runs in which the memory for previous food values operate on a similar time scale. In addition, we study the effects of a really long retention time, corresponding to a period of a century in our transformation, which may serve

as a caricature of climatologically induced changes in food availability beyond an organism's life span.

1. Periodic Food

We now analyse dynamics in a periodically variable food environment, and study how the performance of mussels changes with the amplitude, and period of the fluctuations, as well as with κ, the partitioning coefficient of growth and reproduction. Only two of the three periods studied, a year and a decade, have a significant effect on the performance of mussels. Daily fluctuations are so fast that from the mussel's point of view the environment is essentially stable. Regardless of the intensity of the fluctuations, the scaled stored energy density e fluctuates minimally, and consequently, growth and reproductive output with daily food fluctuations are indistinguishable from production at the average, constant food level (results not shown). Furthermore, daily fluctuations do not impair the mussel's ability to survive. Equation (14) gives the period of fluctuation critical for long term survival. With $f_a = 0.5$, a mussel with $\kappa = 0.9$ can withstand any fluctuation with a fluctuation less than 12 days; a mussel with $\kappa = 0.1$ can survive fluctuations with a period less than 2 months.

Fluctuations with periods of a year or a decade do have a significant impact. We demonstrated above that the ultimate length is proportional to the maximum stored energy density in the limit cycle [see equation (9)]. In line with this, Fig. 3 shows that mussels with variable food are almost always bigger than their conspecifics at constant food. With an annual fluctuation [see Fig. 3(a)], the exceptions are found in the bad periods during the early years (this trend is most pronounced when the phase is a half period—simulations not shown). Also, the time to reach a size arbirarily close to the ultimate size increases with amplitude. The fraction of a period in which e is sufficiently high for growth declines in time, causing the growth trajectory to flatten off slowly, this trend being more pronounced at higher amplitudes. Qualitatively similar results are obtained with a period of a decade. Figure 3(b) and (c) show trends that are more pronounced than with annual fluctuations.

Organisms not only grow bigger when there are large fluctuations in the food environment, they also consume more food. A question of economic interest, e.g., in mariculture, is how the efficiency of biomass formation depends on fluctuations in food supply. We express this efficiency in terms of a cumulative yield, defined as the ratio of the amount of structure formed to the cumulative amount of food consumed, and scale this yield to the yield at constant food. There is a subtle problem involved in this measure: it ignores the reserves, which may, in part, become structure. Therefore, in comparisons with this cumulative yield measure, only individuals with an equal amount of stored energy should be considered. Scaled cumulative yields show two trends (results not shown). First, yields oscillate in

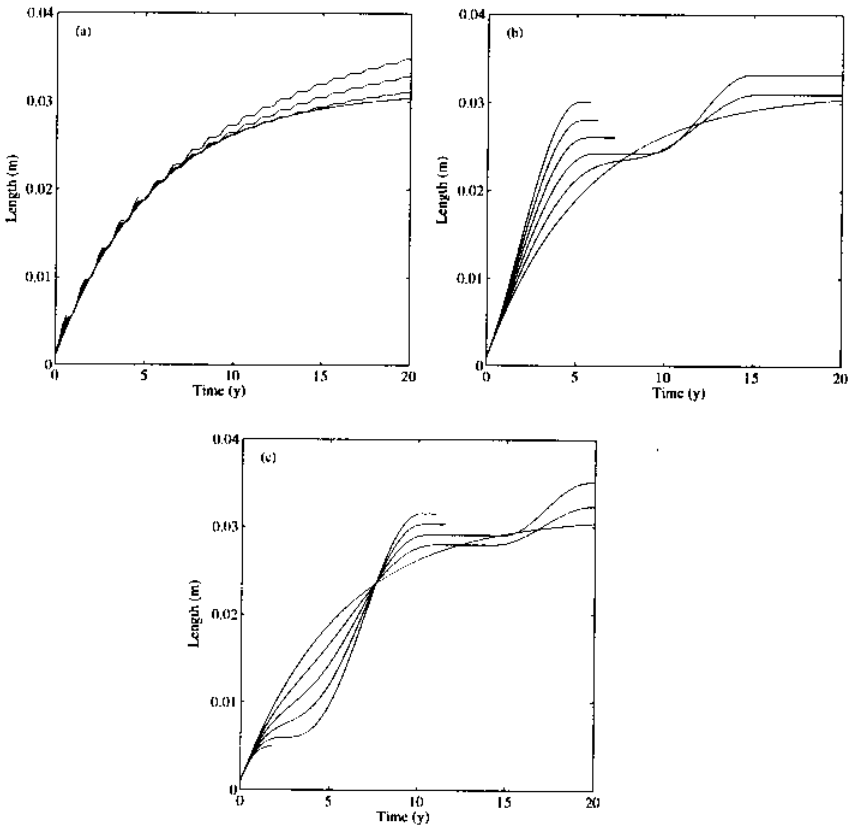

Figure 3. Periodic food fluctuations stimulate growth. The period of the fluctuations is (a) a year; (b) a decade with the simulations starting at the onset of the growth season; and (c) a decade with the simulations starting at the onset of the bad season. The smooth curve refers to growth at constant food ($f = 0.5$), and subsequent curves mark growth at increasing amplitudes [(a) ranges from 0.1 to 0.5 with 0.1 intervals]; growth curves end when the organism starved to death. Parameters values are for the mussel *Mytilus edulis* (see Table 3) with $\kappa = 0.5$.

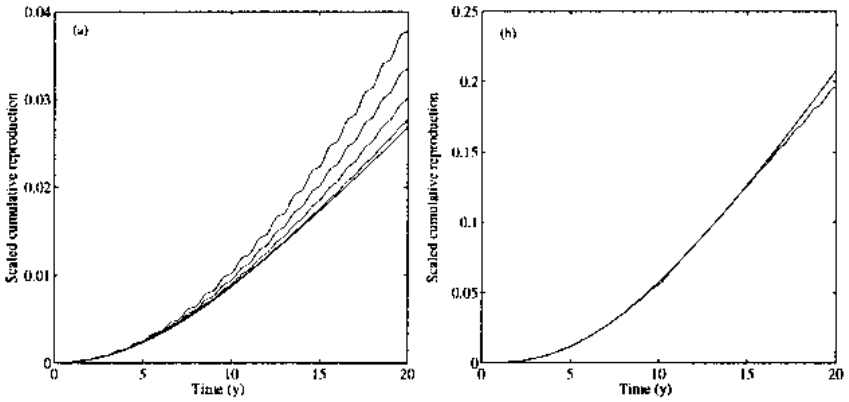

Figure 4. Periodic food fluctuations enhance the reproductive output of organisms that already commit relatively a large fraction of their resources to reproduction [(a), $\kappa = 0.1$], but reduce reproduction in organisms favoring growth over reproduction; [(b), $\kappa = 0.9$]. The smooth curve refers to reproduction at constant food ($f = 0.5$), and subsequent curves mark growth at increasing amplitudes [(a) ranges from 0.1 to 0.5 with 0.1 intervals] in an annually fluctuating food environment; interrupted curves, some of them hardly distinguishable in the right panel, indicate that the organism starved to death. Parameters values are appropriate to the mussel *Mytilus edulis* (see Table 3).

response to fluctations in food availability. Second, scaled cumulative yields are, initially, higher with increasing amplitude. Later this trend is reversed, but not until the organism has approached its ultimate size fairly closely. This implies that food fluctuations enhance the efficiency of biomass formation as long as there is substantial growth.

Perhaps more important from an ecological perspective is how food fluctuations affect reproductive output. As discussed in a previous section, food fluctations enhance the long-term reproduction of surviving mussels that have a relatively low value for κ, whereas fluctuations decrease the reproductive output of mussels with a high value for κ. These trends emerge early, as Fig. 4(a) illustrates for a mussel with a low κ living in an environment with annually varying food. With a high κ, the trend is less conspicous since animals soon starve to death under those conditions [see Fig. 4(b)]. The figures also show that κ has a great effect on reproduction. Mussels with a high κ reproduce more than those of the same age with a low κ.

The life span of mussels may decrease dramatically when the availability of food fluctuates, especially when κ is high (see Fig. 5). κ specifies the partitioning of energy between somatic and reproductive tissues, and therefore determines the size to which a mussel will grow. Since larger animals require more energy for maintenance purposes, a higher value for κ may imply a reduction in life span. The amplitude of the food fluctuations determines the level to which the energy reserves will decline during the off season, and thus directly affects the survival potential of a mussel, but it also indirectly affects the life span of a mussel through its stimulating effects on growth. The period of the fluctuations is also important because the

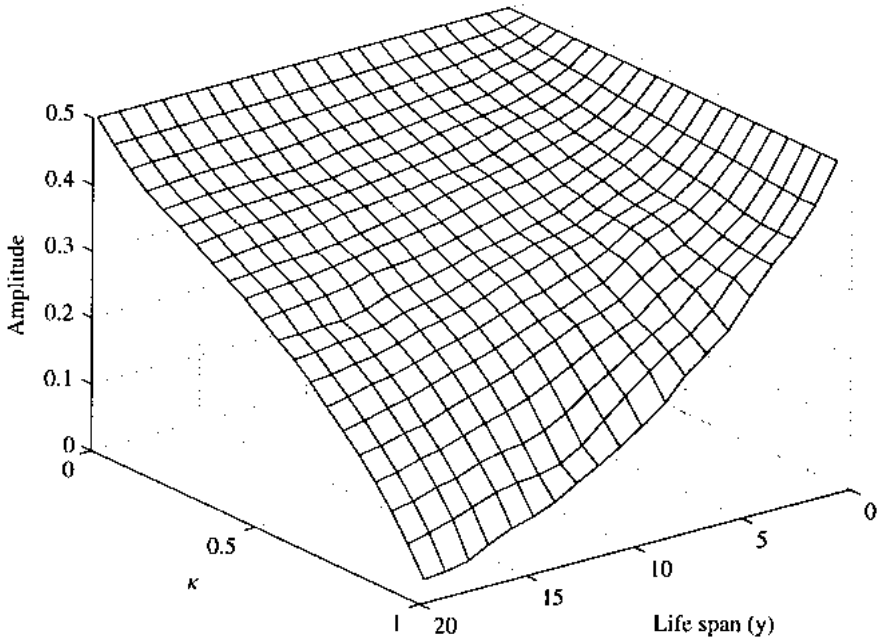

Figure 5. The life span of organisms is reduced by the amplitude of food fluctuations and by κ; a low value for κ implies an individual that commits a relatively large fraction of resources to reproduction and a small fraction to growth. Parameters values are appropriate to the mussel *Mytilus edulis* in an annually variable food environment (see Table 3).

buffering capacity of the storage compartment declines when the period increases. Finally, the timing of birth may be crucially important, as is illustrated by Fig. 3(b) and (c). These figures show simulations when the period of the fluctuations is ten years, which is such a long period that the dynamics of stored energy closely follow the dynamics of food. Mussels that started their settled life at the onset of the good period will survive for at least 5 years. They are born into an environment that initially becomes increasingly hospitable, and then grow to a large size, especially at high values for κ. They therefore quickly die when food becomes scarce. On the other hand, mussels that settle at the onset of the bad spell remain small, which, except at the highest amplitudes, enables them to survive until the next bad period. They thus become older than their conspecifics that start life with a feast.

2. Stochastic Food

We again study the behavior of the model as a function of the partitioning coefficient κ and as a function of environmental variation, which in the case of stochastically fluctuating food is characterized by two parameters: the intensity of the food fluctuations and the memory retention time of previous food levels. We first illustrate model behavior with sample realizations of food and storage dynamics, and

then examine expected production and survival patterns (a 1000 realizations are used to calculate expected values).

Figure 6(a) and (c) show samples of environments in which food fluctuates with a moderate intensity and with a memory retention time of a day or a year. Figure 6(b) and (d) show corresponding dynamics of the scaled density of energy reserves in a mussel. Dynamics of energy reserves are smoother than those of food. Reserves buffer changes in the food environment, and changes with the highest frequency are the ones that are most effectively buffered. As a result, the mussel experiences an environment in which food fluctuates with a memory retention time of a day as it were relatively stable. With higher memory retention times, however, the scaled density of energy reserves follows relatively closely the scaled food density; with a memory retention time of a century, the trends of both densities are essentially the same (results not shown). Figure 6(a) and (b) also indicate that the buffering capacity is a function of size. The buffering capacity increases in time, since the mussel has grown over time (results not shown), resulting in slower storage dynamics [cf. equation (1)].

On average, the size and cumulative reproductive effort of mussels increase with the intensity of food fluctuations (see Fig. 7). Organisms in variable food environments tend to be bigger and to reproduce more than their conspecifics in a constant food environment. This increase is also a function of the memory retention time of the fluctuations in food supply. The increase in production with variable food is negligibly small when the memory retention time is a day (results not shown), but with a retention time of a year (results not shown) or a decade (see Fig. 7) the increase is substantial. With a memory retention time of a decade, at the highest fluctuation intensity examined, the average length after 20 years is about 40% percent higher and reproductive output is more than twice as high as production at constant food. However, with even higher memory retention times, this increase of production with fluctuation intensity becomes less pronounced. In an environment in which food fluctuates with a memory retention time of a century, the percentage of increase is 10% and 25% for length and cumulative reproduction, respectively (results not shown).

Thus, growth and reproduction are predicted to be highest in environments where food levels vary strongly but slowly. One reason for this is that high levels of food densities become more common at higher fluctuation intensities. This causes mussels to be fat for occasional periods, during which they commit extra energy to growth. Because organisms cannot shrink, they become bigger in a variable food environment, and larger organisms reproduce more. This mechanism for enhanced production is increasingly important with increasing memory retention times. With a low memory retention time, extremes in food densities do not last long and are thus effectively buffered by the energy reserves. With a high memory retention time, reserve levels track the availability of food, and extreme food levels translate into high reserve levels. When the memory retention time is substantially higher than the lifespan, however, the mussel experiences relatively little variation in food

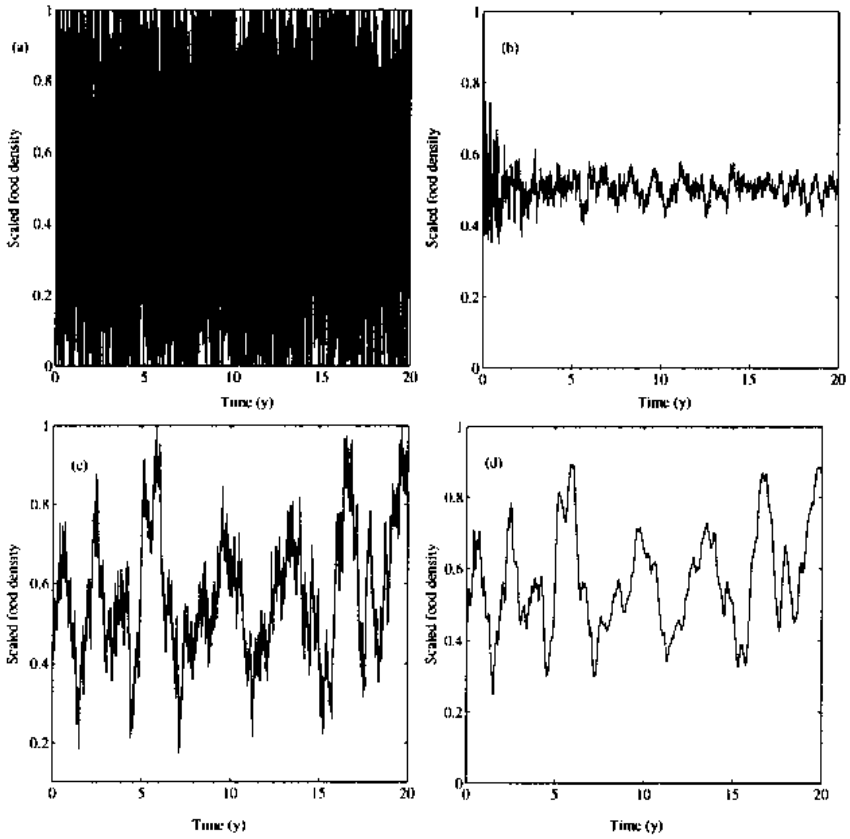

Figure 6. An organism experiences changes in its food environment through changes in its reserves. In a stochastic environment with a memory retention time of 1 day, the scaled food density (a) is much more volatile than the scaled stored energy density (b); with a memory retention time of 1 year, the scaled food density (c) is more closely followed by the scaled stored energy density (d). Parameters values are appropriate to the mussel *Mytilus edulis* (see Table 3) with $\kappa = 0.5$ and $S = 0.09\tau^{-1}$.

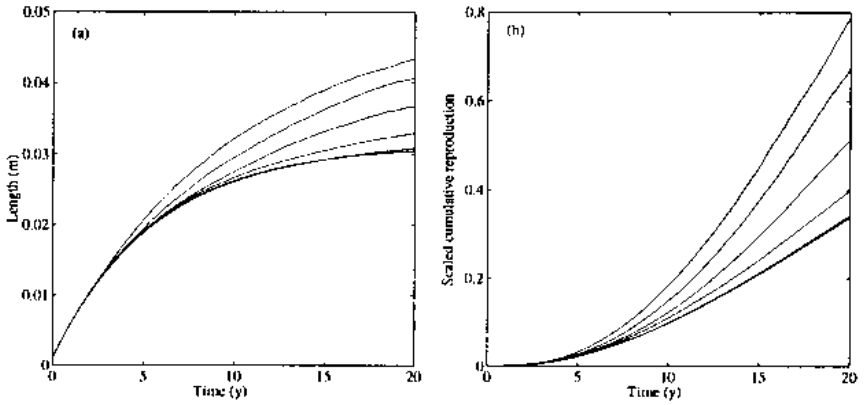

Figure 7. The average size (a) and reproduction (b) of surviving organisms increases with the intensity of stochastic food fluctuations. From top to bottom and in sequential order, the curves represent average production with $S = 0.025y^{-1}, 0.016y^{-1}, 0.009y^{-1}, 0.004y^{-1}, 0.001y^{-1}$ and $0y^{-1}$, respectively. Parameters values are appropriate to the mussel *Mytilus edulis* (see Table 3) with $\kappa = 0.5$ and $\tau = 10y$.

availability during its life time; production patterns are then relatively close to those observed at constant food conditions.

There is another mechanism explaining why average size and reproduction increase with the intensity and memory retention time of food fluctuations. When the value of these two parameters increase, the likelihood of persistently low levels of food and energy reserves, and thus starvation, increase as well. Survivors are likely to have experienced the relatively better food environments. Therefore, the scaled density of energy reserves in surviving mussels tends to increase with time. At the highest fluctuation intensity, the upward drift in reserve levels after 20 years ranges from zero with a retention time of a day to 40% with a memory retention time of a decade. Those elevated levels of energy availability evidently support higher levels of average growth and reproduction.

The probability of survival to any given age depends on the intensity and memory retention time of the food fluctuations (see Fig. 8). Survival probabilities decline when food fluctuations become more intense. The effect of the memory retention time on survival is more complex. The survival probability to any given age shows a minimum at some intermediate memory retention time. With a memory retention time of a day, death through starvation is a sporadic event, even at the highest fluctuation intensity (results not shown). At the highest intensity with a memory retention time of a year, however, none of the 1000 realizations included an organism that survived for 20 years [see Fig. 8(a)]. With higher memory retention times, the odds for survival improve [see Fig. 8(b)], and mortality is not an important issue when the memory retention stretches well beyond the life span of the organism [see Fig. 8(c)]. The reason for this is that the organism is then unlikely to experience large environmental change during its life time. We note that the

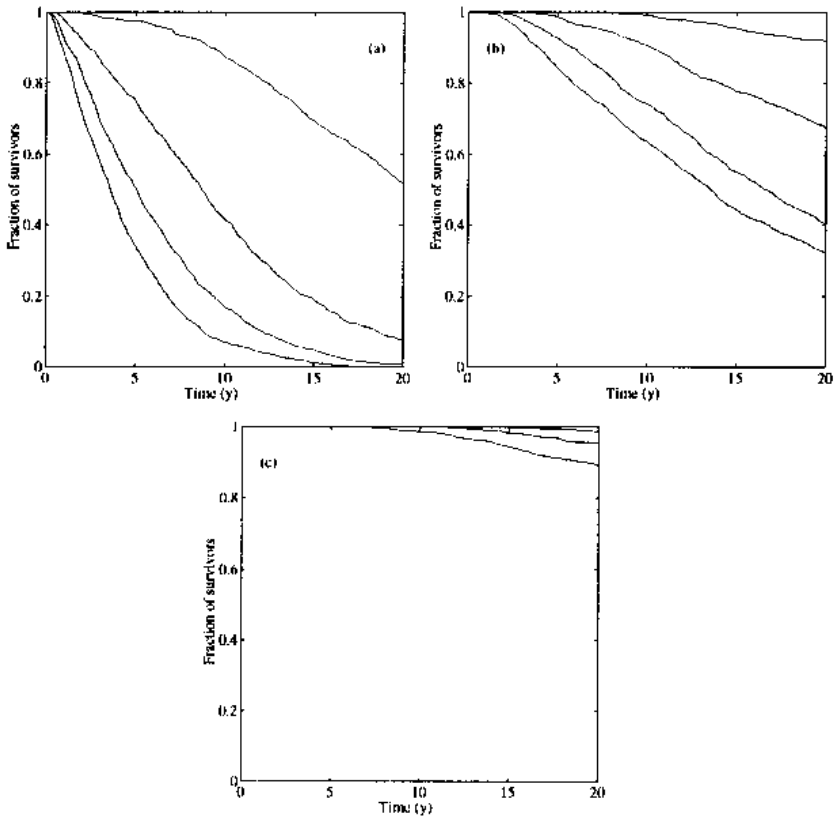

Figure 8. The probability of survival to a given age in a stochastically variable food environment declines with the intensity of the food fluctuations and depends on the memory retention time of the environment for previous food levels. The memory retention time τ is (a) $1y$, (b) $10y$ or (c) $100y$ (with $\tau = 1d$, survival was 100%). In all panels, the curves represent survival probabilities with, from bottom to top and in sequential order, $S = 0.25\tau^{-1}$, $0.16\tau^{-1}$, $0.09\tau^{-1}$, $0.04\tau^{-1}$, respectively. With $S = 0.01\tau^{-1}$, mortality is nil. Parameters values are appropriate to the mussel *Mytilus edulis* (see Table 3) with $\kappa = 0.5$.

survival probability depends on κ, because organisms with a low value of κ remain relatively small and are better able to survive periods of starvation.

So far, we have discussed average cumulative production of organisms that managed to survive in a stochastically variable food environment, that is, the average cumulative production of survivors. The question remains how fluctuations in food availability affect the expected future cumulative production of a newborn. Calculations of those measures include the final size and cumulative reproduction output of dead mussels. At the lower fluctuation intensities, mortality remains of minor importance during the time spanned by the simulation, and thus the average production of survivors of a given age is close to the expected future cumulative production of a newborn once it has reached the same age (see Fig. 9). At the

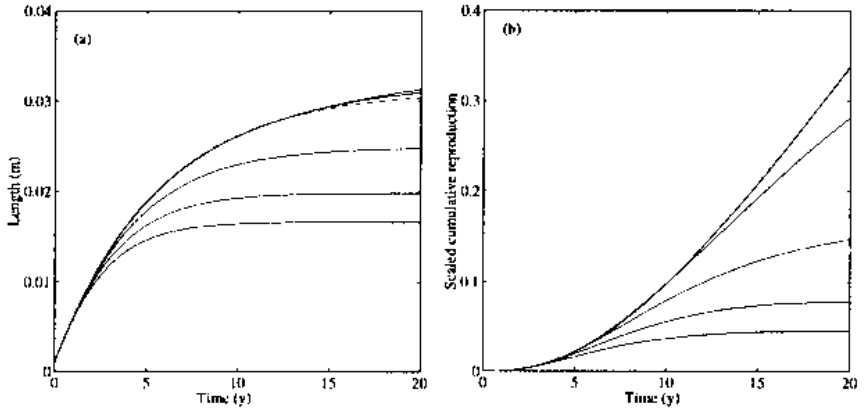

Figure 9. The expected growth (a) and reproduction (b) to a given age are stongly reduced by intense stochastic food fluctuations because of mortality due to starvation, but mild food fluctuations may stimulate production. The dotted curve in both panels represent production at constant food, and the solid curves represent production with, in sequential order and from bottom to top, $S = 0.25y^{-1}$, $0.16y^{-1}$, $0.09y^{-1}$, $0.04y^{-1}$ and $0.01y^{-1}$, respectively. Parameters values are appropriate to the mussel *Mytilus edulis* (see Table 3) with $\kappa = 0.5$ and $\tau = 1y$.

higher fluctuation intensities, however, the expected future cumulative production of a newborn tends to stabilize as time progresses, since the number of survivors declines (see Figs 8 and 9). Then, the expected future size of a newborn remains substantially smaller than with constant food, although the average size of surviving mussels increases with fluctuation intensities. Even more dramatic is the decline in the expected future cumulative reproduction of a newborn with increasing fluctuation intensities. Whereas individuals in a stable food environment keep producing off-spring at a steady rate, the expected future reproduction rate of a newborn declines in time in an intensely variable food environment (see Fig. 9) as mortality takes it toll. Then, the expected future cumulative reproductive output converges to lifetime production as the probability of survival to a given age approaches zero. Those trends of expected future reproduction and growth of newborns no longer hold with very long memory retention times. Mortality then has relatively little impact, even at the higher fluctuation densities.

Discussion

The model makes the following predictions about (average) growth and mortality in a variable environment. Organisms grow bigger in a variable food environment than in a constant environment with similar average food availability. Ultimate size increases with the amplitude and period of deterministic food cycles, and with the intensity and memory retention time of stochastic food fluctuations. In variable food environments, organisms grow to a size related to the peaks in food availability, rather than to the mean. Food fluctuations may lead to death from starvation,

the likelihood of which increases with the strength and duration of the fluctuations. Two processes are involved here: starvation requires a sustained period of low food, but in addition the larger individuals that are present in a fluctuating environment have greater maintenance costs than their smaller counterparts living at constant food and are hence particularly vulnerable to food stress. These mechanisms of starvation are also in effect at the population level when organisms are able to deplete their food source (Kooijman *et al.*, 1989).

Model predictions on growth in periodic food environments are in line with observations backing Bergmann's rule. Bergmann's rule states that the size of homeothermic organisms increases with latitude; this trend is also common for ectotherms [see e.g., Brown and Lomolino (1998, pp. 488–493)]. Usually, this trend is related to some temperature measure, such as summer maxima or seasonal fluctuations. Food availability increasing with latitude has also been suggested as possible explanation (Kooijman, 2000, pp. 233–234). The model predicts that there is a phenotypical trend showing increasing body size with stronger seasonal food fluctuations. Because food availability often covaries with temperature, our results suggest that organisms become bigger with increasing latitude due to an increasing seasonal variability in food.

The predicted effects of food fluctuations on reproduction are more complex. In a periodically variable food environment, reproduction may increase or decrease with the amplitude of the fluctuations, depending on κ, the parameter characterizing the partitioning of energy between somatic and reproductive tissues. Individuals with a high value for κ commit a relative large fraction of their resources to growth, whereas individuals with a low value for κ give a higher priority to reproduction. High-κ individuals reproduce less with increasing amplitude, but low-κ individuals reproduce more. Although any organism becomes bigger in a periodically variable food environment, and thus feeds at a higher rate, only low-κ individuals translate this extra food intake (partly) into off-spring. High-κ individuals need this extra food intake for maintenance requirements, which also increase with size. Because of the strong size dependence of reproductive output, stochastic variation in the food environment normally leads to enhanced reproduction by individuals that survive the fluctuations. However, in most cases, this increase is accompanied by a still stronger decrease in survival probabilities, causing the expected life time reproduction to decline [see Fig. 9(b)].

The dependency of reproduction patterns on κ in periodic food environments is of particular interest as κ is an adaptive parameter whose value for any particular organism may reflect the intensity of the food fluctuations in a particular environment. The model suggests that a low value for κ would represent a food environment that fluctuates relatively strongly. Also, survival decreases with increasing κ. Thus, individuals in a highly variable food environment are likely to evolve towards a lower κ, a higher reproductive rate and a lower physiological potential for growth than their conspecifics in a less variable food environment. This is in agreement with many data showing increasing clutch sizes in birds and litter sizes in mammals

with increasing lattitude (Brown and Lomolino, 1998). However, the genotypical decrease of growth potential that accompanies a lower value of κ would diminish the above described increase in size due to higher food maxima, causing this trend to be less pronounced.

There are unresolved issues with the rules for partitioning of energy in the model. In general, the parameter κ may be a function of size; for example, the proportion of assimilate assigned to reproduction by the water flea *Daphnia pulex* increases with size (Paloheimo *et al.*, 1982). Recently, it has shown that size dependence in κ is consistent with the other assumptions of his DEB model (Kooijman, 2000), but the effects on dynamics even in a constant environment have not been worked out. Without restrictions on the mathematical form for the size dependence, there is scope for a very wide repertoire of dynamic behavior; further progress would be greatly helped by the development of a mechanistic representation of how an organism's size affects competition for resources between somatic and reproductive tissue.

An equally serious issue is that organisms may change the energy partitioning rules in response to environmental cues that covary with current or anticipated food availability. For example, photoperiod affects reproduction during starvation in the snail *Lymnea stagnalis*; in summer starving animals continue to commit energy to reproduction, but they cut down on this commitment in spring when food tends to be relatively scarce (Zonneveld and Kooijman, 1989). While the precise changes in the expression of the κ-rule are likely to be species specific, an organism that reduces reproduction when there are insufficient resources for growth in a variable environment might be expected to live longer than one that continues to reproduce, since the former organism depletes energy reserves more slowly during periods of starvation.

This observation has led to a variant (here called variant 1) of the κ-rule model, applicable to organisms that cease reproduction when they do not grow (Zonneveld and Kooijman, 1989). We briefly investigated the implications of this modified κ-rule model, though we made a few technical changes to make the model mathematically fully consistent. We also investigated a second variant that allows organisms, which grow and reproduce as in the classic formulation, to utilize all of their reserves before dying of starvation, in contrast to the classic formulation and variant 1, both of which assume that an organism dies when the utilization flux in Fig. 1 is insufficient to meet maintenance costs. With our default parameter set and deterministic food fluctuating with a period of one year, the classic version and variant 1 yield almost indistinguishable growth and reproduction patterns in a periodic food environment. Survival patterns with variant 1 are also similar to the patterns with the classic formulation, which rebuts the intuition articulated above, but is consistent with a previous study of starvation times (Nisbet *et al.*, 1996). In sharp contrast, however, if the organism is able to access all reserves in order to meet maintenance (variant 2), its resistance to starvation is greatly increased, and only in extremely fluctuating food environments does the organism starve to death.

The results from the second variant in the preceding paragraph must be interpreted with considerable caution. The assumptions of the κ-rule model have a strong mechanistic basis and cannot be changed in an *ad hoc* manner without taking care to consider the implications. In particular, the energy utilization flux is derived from assumptions on reserve homeostasis, and an assumption modifying the utilization of energy during starvation must take account of the costs of such a change and should have strong empirical support. Currently, we lack an assumption with these qualities.

We have shown how a variable food environment affects the survival and production of individual organisms that grow in accordance with the κ rule model. A variable food supply stimulates growth, increases mortality and may enhance reproduction, depending on the life history of an organism. More work is needed to investigate the impact of food fluctuations on the evolution of life history parameters and on population dynamics. The work reported in the present paper gives strong guidance on the likely effects on growth and reproduction, and highlights the need for better mechanistic models of mortality.

APPENDIX

In this appendix, we derive the long-term dynamics of the state variables assuming deterministic variation in the environment, in which the scaled functional response fluctuates in a simple periodic fashion. We also show that, in most cases, if an organism is ultimately viable, it can survive the transient periods of starvation that it experienced earlier in life.

The dynamics of the scaled density of energy reserves e and structural biovolume V are given by

$$\frac{de}{dt} = \upsilon V^{-\frac{1}{3}}(t)(f(t) - e(t)), \tag{A1}$$

$$\frac{dV}{dt} = \frac{(\upsilon e(t)V^{\frac{2}{3}}(t) - mgV(t))_+}{e(t) + g}, \tag{A2}$$

where f is the scaled functional response, υ is the energy conductance rate, m is the maintenance rate coefficient, and g is the energy investment ratio.

The dynamics of e are first order and linear in e, and can thus be solved with standard methods, provided that the organism survives to time t. With $e(0)$ being the initial value for $e(t)$, the integral solution reads as

$$e(t) = \exp\left[-\upsilon \int_0^t V^{-1/3}(s)ds\right] \left(e(0) + \int_0^t f(t)\upsilon V^{-1/3}(s)\exp\left[\upsilon \int_0^s V^{-1/3}(r)dr\right]ds\right). \tag{A3}$$

Since

$$\upsilon V^{-1/3}(s)\exp\left[\upsilon\int_0^s V^{-1/3}(r)dr\right]=\frac{d(\exp[\upsilon\int_0^s V^{-1/3}(r)dr])}{ds}, \tag{A4}$$

equation (A3) is equivalent to

$$e(t)=\exp\left[-\upsilon\int_0^t V^{-1/3}(s)ds\right]\left(e(0)+\int_0^t f(t)d\left(\exp\left[\upsilon\int_0^s V^{-1/3}(r)dr\right]\right)\right). \tag{A5}$$

Integration by parts yields

$$e(t)=f(t)+\exp\left[-\upsilon\int_0^t V^{-1/3}(s)ds\right]\left(e(0)-f(0)-\int_0^t f'(s)\exp\left[\upsilon\int_0^s V^{-1/3}(r)dr\right]ds\right). \tag{A6}$$

Further analysis requires a specification of $f(t)$. In particular, we are interested in the consequences of a sinusoidically fluctuating scaled food density with angular frequency ω, amplitude a and mean value f_a. The second integral in equation (A6), $A\equiv\int_0^t f'(s)\exp\left[\upsilon\int_0^s V^{-1/3}(r)dr\right]ds$, can now be evaluated:

$$\begin{aligned}A&=a\omega\int_0^t\cos(\omega s)\exp\left[\upsilon\int_0^s V^{-1/3}(r)dr\right]ds\\&=\frac{a\omega}{2}\int_0^t(\exp[\iota\omega t]+\exp[-\iota\omega t])\exp\left[\upsilon\int_0^s V^{-1/3}(r)dr\right]\\&=\frac{a\omega}{2}\left(\int_0^t\exp\left[\int_0^s(\iota\omega+\upsilon V^{-1/3}(r))dr\right]ds\right.\\&\quad\left.+\int_0^t\exp\left[\int_0^s(-\iota\omega+\upsilon V^{-1/3}(r))dr\right]ds\right)\\&=\frac{a\omega}{2}\left(\left[\frac{\exp[\int_0^s(\iota\omega+\upsilon V^{-1/3}(r))dr]}{\iota\omega+\upsilon V^{-1/3}(s)}\right]_0^t+\left[\frac{\exp[\int_0^s(\iota\omega+\upsilon V^{-1/3}(r))dr]}{-\iota\omega+\upsilon V^{-1/3}(s)}\right]_0^t\right).\end{aligned}$$

After some tedious algebra we get

$$A=a\omega\left(\frac{-\upsilon V_b^{-1/3}}{\omega^2+(\upsilon V_b^{-1/3})^2}+\exp\left[\upsilon\int_0^t V^{-1/3}(s)ds\right]\left(\frac{\omega\sin\omega t+\upsilon V^{-1/3}(t)\cos\omega t}{\omega^2+(\upsilon V^{-1/3}(t))^2}\right)\right), \tag{A7}$$

in which $V_b \equiv V(0)$ is the structural body volume at birth. Substituting this result back into equation (A6) yields

$$e(t) = f_a + \left(e(0) - f_a + \frac{a\omega\upsilon V_b^{-1/3}}{\omega^2 + \upsilon^2 V_b^{-2/3}}\right)\exp\left[-\upsilon\int_0^t V^{-1/3}(s)ds\right] + \frac{a}{1+\left(\frac{\omega V^{1/3}(t)}{\upsilon}\right)^2}\left(\sin\omega t - \frac{\omega V^{1/3}(t)}{\upsilon}\cos\omega t\right). \quad \text{(A8)}$$

We are now able to determine the long-term dynamics of e and V. Because υ and V are positive and bounded above, the middle term in equation (A8) fades with time, and since $V^{1/3}$ is a non-decreasing function of time, the other two terms represent a sinusoid with a non-increasing amplitude (and non-decreasing period). The highest scaled energy density in a cycle of this sinusoid, $e_{\max}$, decreases as the organism grows. This implies that growth eventually ceases, since V is bounded through e [see equation (A2)]. An organism will continue to grow provided $V^{1/3} \leq e_{\max}\upsilon/mg$, and has a maximum volumetric length given by $\bar{V}^{1/3} = e^*_{\max}\upsilon/mg$ for some $e^*_{\max}$. Now assume some cycle n in which the organism reaches its maximum volumetric length supported by that cycle, $V_n^{1/3}$; then $V_n^{1/3} = e_{\max}(n)\upsilon/mg$. If the organism continues to grow in some later cycle o, then we must have $e_{\max}(o) > e_{\max}(n)$. But we already know that $e_{\max}(o) \leq e_{\max}(n)$. Hence, growth is bounded, implying that the dynamics of e will approach the limit cycle

$$\bar{e}(t) = f_a + \frac{a}{\sqrt{1+\left(\frac{\omega\bar{V}^{1/3}}{\upsilon}\right)^2}}\sin(\omega t + \phi), \quad \text{(A9)}$$

where $\phi = \tan^{-1}\frac{\omega\bar{V}^{1/3}}{\upsilon}$ is a measure (in radians) of the extent to which fluctuations in e ultimately lag behind f. Then, $e^*_{\max} = \bar{e}_{\max}$ the highest scaled energy density in the limit cycle, and $\bar{V}^{1/3} = \bar{e}_{\max}\upsilon/mg$.

It is highly likely that if an organism is able to survive the limit cycle, it is also able to survive the transient. It is sufficient to assume that $e(0)$ lies within the range of possible values for $f(t)$, which is true in the κ-rule model, for instance, when off-spring experiences a food environment similar to that of the mother (the model assumes that hatchlings have the same energy density as the mother at the time of egg laying). The model assumes that an organism is viable when the energy mobilized from the reserves is sufficient to meet somatic maintenance demands, that is, when

$$V^{1/3}(t) \leq \frac{e(t)\upsilon}{\kappa mg}, \quad \text{(A10)}$$

in which κ is the parameter partitioning reserves between somatic and reproductive tissues. With $V_m^{1/3} = \upsilon/mg$, the maximum volumetric length an organism can

attain, equation (A10) implies that death is inevitable when $e(t) = \frac{\kappa V^{1/3}(t)}{V_m^{1/3}}$ while $\frac{de}{dt} \leq 0$, that is, while $V^{1/3}(t) > \frac{f(t)V_m^{1/3}}{\kappa}$ [see equation (A1)]. Because $\kappa \in (0, 1]$ and $f(t) \leq f_a + a \equiv f_{\max}$, an organism is nonviable when $V^{1/3}(t) > f_{\max} V_m^{1/3}$. But with a periodically variable scaled food density $V^{1/3}(t) \leq \bar{V}^{1/3} = \bar{e}_{\max} V_m^{1/3} < f_{\max} V_m^{1/3}$. Hence, organisms that are viable in the limit cycle, are also viable during transient dynamics.

ACKNOWLEDGEMENTS

We are greatly indebted to Bas Kooijman, Dina Lika and Erik Noonburg for inspiring discussions and improvements of the manuscript. This research was supported by the Office of Naval Research (grant no. 00014-99-1-0024), by the Minerals Management Service (MMS agreement #14-35-0001-30761 and #14-35-0001-30758, Task #15117), and by the National Center for Ecological Analysis and Synthesis. The views and conclusions contained in this document are those of the authors and should not be interpreted as necessarily representing the official policies, either express or implied, of the U.S. Government.

REFERENCES

Brown, J. H. and M. V. Lomolino (1998). *Biogeography*, 2nd edn, Sunderland, MD: Sinauer Associates, Inc.

De Roos, A. M. (1997). A gentle introduction to physiologically structured population models, in *Structured-Population Models in Marine, Terrestrial, and Freshwater Systems*, Vol. 18, S. Tuljapurkar and H. Caswell (Eds), New York: Chapman & Hall, pp. 119–204.

Duclaux, E. (1898). *Traité de Microbiologie*, Paris: Masson et Compagnie.

Kitchell, J. F., D. J. Stewart and D. Weininger (1977). Applications of a bioenergetics model to perch (*Perca flavescens*) and walleye (*Stizostedion vitreum*). *J. Fish. Res. Board of Canada* **34**, 1922–1935.

Kooi, B. W. and S. A. L. M. Kooijman (1994). Existence and stability of microbial prey-predator systems. *J. Theor. Biol.* **170**, 75–85.

Kooijman, S. A. L. M. (1986). Population dynamics on basis of budgets, in *The dynamics of Physiologically Structured Populations*, Lecture Notes in Biomathematics, J. A. J Metz and O. Diekmann (Eds), Berlin: Springer Verlag.

Kooijman, S. A. L. M. (2000). *Dynamic Energy and Mass Budgets In Biological Systems*, Cambridge: Cambridge University Press.

Kooijman, S. A. L. M. and J. J. M. Bedaux (1996a). Analysis of toxicity tests on *Daphnia* survival and reproduction. *Water Res.* **30**, 1711–1723.

Kooijman, S. A. L. M. and J. J. M. Bedaux (1996b). Some statistical properties of estimates of no-effect concentrations. *Water Res.* **30**, 1724–1728.

Kooijman, S. A. L. M., B. W. Kooi and T. G. Hallam (1999). The application of mass and energy conservation laws in physiologically structured population models of heterotrophic organisms. *J. Theor. Biol.* **197**, 371–392.

Kooijman, S. A. L. M. and R. M. Nisbet How light and nutrients affect life in a closed bottle. Lewis Publishers, Thermodynamics and Ecology, in press.

Kooijman, S. A. L. M., N. van der Hoeven and D. C. van der Werf (1989). Population consequences of a physiological model for individuals. *Funct. Ecol.* **3**, 325–336.

Lika, K. and R. M. Nisbet A dynamic energy budget model based on partitioning of net production. *J. Math. Biol.*, in press.

Mangel, M. (1996). Computing expected reproductive success of female atlantic salmon as a function of smolt size. *J. Fish Biol.* **49**, 877–882.

McCauley, E., W. W. Murdoch, R. M. Nisbet and W. S. C. Gurney (1990). The physiological ecology of *Daphnia*—development of a model of growth and reproduction. *Ecology* **71**, 703–715.

Nisbet, R. M. and W. S. C. Gurney (1982). *Modelling Fluctuating Populations*, New York: John Wiley & Sons.

Nisbet, R. M., A. H. Ross and A. J. Brooks (1996). Empirically-based dynamic energy budget models: theory and an application to ecotoxicology. *Nonlinear World* **3**, 85–106.

Paloheimo, J. E., S. J. Crabtree and W. D. Taylor (1982). Growth model of *Daphnia*. *Can. J. Fish. Aquat. Sci.* **39**, 598–606.

Ross, A. H. and R. M. Nisbet (1990). Dynamic models of growth and reproduction of the mussel *Mytilus edulis* I. *Funct. Ecol.* **4**, 777–787.

Seed, R. (1976). Ecology, in *Marine Mussels, their Ecology and Physiology*, B. L. Bayne (Ed.), Cambridge, UK: Cambridge University Press, pp. 13–65.

Van Haren, R. J. F. and S. A. L. M. Kooijman (1993). Application of a dynamic energy budget model to *Mytilus edulis* (l). *Neth. J. Sea Res.* **31**, 119–133.

von Bertalanffy, L. (1957). Quantitative laws in metabolism and growth. *Q. Rev. Biol.* **32**, 217–231.

Zonneveld, C. and S. A. L. M. Kooijman (1989). Application of a dynamic energy budget model to *Lymnaea stagnalis* (l). *Funct. Ecol.* **3**, 269–278.

Received 2 February 2000 and accepted 8 August 2000

Stoichiometric Food Quality and Herbivore Dynamics

Erik B. Muller[1] *, Roger M. Nisbet[1], Sebastiaan A. L. M. Kooijman[2],
James J. Elser[3] and Edward McCauley[4]

[1]Department of Ecology, Evolution and Marine Biology,
University of California, Santa Barbara CA 93106-9610, USA.

[2]Department of Theoretical Biology, Institute of Ecological Science,
Vrije Universiteit, de Boelelaan 1087, 1081 HV Amsterdam, the Netherlands.

[3]Department of Biology, Arizona State University, Tempe AZ 85287, USA.

[4]Ecology Division, Department of Biological Sciences,
University of Calgary, Calgary, Alberta, T2N 1N4 Canada.

February 12, 2001

running title: growth limitations in herbivores.

keywords: synthesizing unit; Droop model; Monod model; stoichiometric requirements; multiple limitation; growth model; food quality

Submitted to Ecology Letters; filename: herbilimitrev.tex

*corresponding author, muller@lifesci.ucsb.edu; fax (805) 893 3777

Abstract

Herbivores may grow with nutrient or energy limitation, depending on food abundance and the chemical composition of their food. We present a model that describes herbivore growth as a continuous function of two limiting factors. This function uses the synthesizing unit concept, has the hyperbolic Monod model as a limiting case, and has the same number of parameters as the Monod model coupled to Liebig's discontinuous minimum rule. We use the model to explore nutrient-limited herbivore growth in a closed system with algae, *Daphnia* and phosphorus as the limiting nutrient. Phosphorus in algae may influence *Daphnia* growth, but this influence changes in time and is most pronounced when algae and *Daphnia* populations show large amplitude cycles. Relative to classic models that only consider food quantity as a determinant of *Daphnia* growth, our model shows richer dynamical behavior. In addition to the standard positive equilibrium, which may be stable or unstable depending on nutrient availability, a new positive equilibrium may arise in our model when mortality rates are relatively high. This equilibrium is unstable and reduces the likelihood of long term persistence of *Daphnia* in the system.

1 Introduction

Plants and algae have highly variable nutrient contents. Because new herbivore biomass is produced with a tightly controlled elemental composition, a herbivore may experience energy or nutrient limitation, depending on the abundance and composition of its food. Recently, this problem has attracted considerable attention from aquatic and terrestrial ecologists, as it is believed that the elemental composition of primary producers relative to the stoichiometric requirements of herbivores underlies major aspects of community organization and dynamics [1, 11, 8, 7]. We develop a new model describing herbivore growth with two potentially limiting compounds, and illustrate model behavior for a system with *Daphnia* and phosphorus limited algae. Recent evidence shows that phosphorus limited *Daphnia* growth can be induced in laboratory cultures [28, 27, 3] and observed *in situ* [4, 7].

Traditionally, models describing the dynamics of plant and herbivore populations use a single currency, usually carbon, to describe the growth of herbivores (see *e.g.* [21] and references therein). An implicit assumption is that food quantity rather than its composition influences herbivore growth. When food composition becomes an issue, Liebig's minimum rule is usually invoked [26, 10, 1, 16]. The minimum rule asserts that only one compound can be truly limiting at any particular time, with the consequence that an organism may live in a borderline environment in which the limiting compound switches continually. Having a switch in a model is mathematically inconvenient and also implies that physiological regulation systems are unduly taxed in borderline environments. Near the switch, the minimum rule cannot describe growth realistically, and thus it would be advantageous to have an equation describing growth as a continuous function of multiple limiting factors.

Drawing on recent advances in biochemistry [13, 14], we present a model of synthesizing units with which the effects of multiple limiting compounds can be described. Synthesizing units are 'servers' that handle a potentially wide range of limiting compounds and form one or more products. We first discuss and illustrate the qualities of a synthesizing unit by implementing the concept in the simple Monod model [19], which is also the routine choice in previous models implementing the minimum rule (see *e.g.* [10]). We then incorporate the synthesizing unit concept in a model for aquatic producers (algae) and consumers (*Daphnia*) with producers growing according to Droop [5] and consumers feeding with a type II functional response. We explore the dynamics of this system using a range of natural parameter values, and identify conditions under which phosphorus in food

may strongly influence *Daphnia* growth.

2 Synthesizing Units

A synthesizing unit converts substrates into products while meeting the stoichiometric requirements for product formation. An enzyme is an obvious example of a synthesizing unit, but we have also in mind an abstract representation of the biomass producing machinery in an organism, in which 'substrates' are components in food and the 'product' is biomass. It is this latter picture that we will use later in modeling the biomass synthesis rate of *Daphnia*. In this section we outline the theory of a synthesizing unit and compare its dynamics to the Monod model with a minimum rule.

A synthesizing unit can handle an arbitrarily large number of substrates and products, but here we restrict ourselves to two different substrates and one product - see [13, 14] for a more exhaustive presentation. We consider a synthesizing unit with n_1 binding sites for substrate x_1 and n_2 binding sites for substrate x_2. The synthesizing unit is said to be in its binding stage if one or more of its binding sites are empty; the production stage starts with the occupation of all sites and ends with the release of products. We assume that substrate particles arrive at the binding sites of the synthesizing unit according to a Poisson process, and that the binding sites operate independently. The probability that an arriving substrate particle attaches to a binding site suitable for that substrate is constant, provided the site is empty (otherwise, the binding probability is zero). If binding and production are irreversible events, and the production period is exponentially distributed with mean $\dot{J}_m^{-1}$, it can be shown that the average rate at which the synthesizing units deliver product, $\dot{J}$, is approximately [13, 14]

$$\dot{J} = \frac{1}{\frac{1}{\dot{J}_m} + \frac{n_1}{\dot{J}_1} + \frac{n_2}{\dot{J}_2} - \left(\frac{\dot{J}_1}{n_1} + \frac{\dot{J}_2}{n_2}\right)^{-1}}, \tag{1}$$

in which $\dot{J}_1$ and $\dot{J}_2$ are the average rate at which the synthesizing unit binds x_1 and x_2, respectively. $\dot{J}_m$ is the maximum rate at which a synthesizing unit can deliver product.

When one of the substrate fluxes is very high, the reciprocal of this flux and the term in parentheses in the denominator is very small and, consequently, equation 1 reduces to a simple hyperbolic expression. Thus, Monod's model [19], which has the same functional form as the type II functional response, is a special case of the synthesizing unit concept. However, rates in the Monod model are usually expressed in terms of the substrate concentration rather than its flux. If concentrations are

proportional to fluxes, the synthesizing unit concept provides a modeling framework that is more general than the Monod model. Later in this paper we use flux measures in describing assimilation rates.

Monod's model frequently serves as a framework for Liebig's minimum rule, which with two potentially limiting compounds can be written as [10]:

$$\dot{J} = \min\left(\frac{1}{\frac{1}{\dot{J}_m} + \frac{n_1}{\dot{J}_1}}, \frac{1}{\frac{1}{\dot{J}_m} + \frac{n_2}{\dot{J}_2}}\right), \tag{2}$$

where 'min' specifies that the production rate is the lower value of the two ratios. In homogeneous environments, concentrations may be substituted for the flux measures in 2; then, the conventional half saturation constants are proportional to $n_1\dot{J}_m$ and $n_2\dot{J}_m$.

Figure 1 illustrates that production with synthesizing units changes smoothly and continuously as the dominant limiting factor changes. The lines almost parallel to the axes in Figure 1a show convergence to classic Monod dynamics as the flux of one compound increases; this convergence is especially rapid when the flux of the most limiting factor is relatively low. Thus, the range of concentrations over which two compounds simultaneously and substantially limit the production rate may be narrow. Figure 1b shows that the synthesizing unit model nicely fits data generated by the Monod model with minimum rule. Thus, the credit that the minimum rule often gets due to its excellent fits of experimental data (see *e.g.* [5]) carries over to the synthesizing unit concept (however parameter *values* do not carry over and require re-estimation).

In the context of synthesizing units, the previously unambiguous term 'the limiting factor' requires redefinition, since any substrate, irrespective of its abundance, makes some contribution to the production rate. However, one substrate is likely to have a stronger limiting effect than the other, and it is convenient to define a dominant limiting substrate or most limiting compound. We say that substrate x_1 is the dominant limiting substrate when $n_1/\dot{J}_1 > n_2/\dot{J}_2$. Then, it takes more time for the synthesizing unit to bind the required number of copies of substrate x_1 than to bind the required number of copies substrate x_2.

3 Producer and Consumer Dynamics

We now consider a system containing a producer and a consumer and assume that the system is closed for nutrients and biomass. We assume that one nutrient always limits producer growth, and

call this simply 'the nutrient'; other nutrients and light energy are assumed to be abundant. We also assume that nutrient in dead biomass and feces is instantaneously remineralized, and that any free nutrient is immediately taken up by the producer.

For producers, we follow the distinction that Kooijman makes between 'structure' and 'reserves' [14], and assume that the mass of producer consists of nutrient reserves and structural biomass, each having a constant but different chemical composition (the biomass composition of producers may change as the amount of reserves relative to structure changes). This assumption specifies the chemical composition of producer biomass, and we cannot further assign particular classes of molecules to either reserves or structure. Of course, our classification should overlap substantially with what is usually understood as reserves and structure, but subtleties beyond the scope of this paper do exist - see [22]. Furthermore, we assume a constant carbon to nutrient ratio in consumers, which may vary mildly in practice [3]. Thus, the system has three state variables representing the structure of the producer, the nutrient reserves of the producer and the biomass of the consumer. Figure 2 illustrates this system with *Daphnia* as the consumer, alga as the producer, and phosphorus as the limiting nutrient.

We assume that the producer grows according to Droop [5, 14], and that the specific feeding rate of the consumer, j_p follows a type II functional response. The dynamics of the density of producer structure X_p (in C moles of biomass) are

$$\frac{dX_p}{dt} = \dot{r}_{pm} X_p \left(1 - \frac{n_p}{n_p + m}\right) - j_p X_c; \qquad j_p \equiv \frac{j_{pm} X_p}{(X_p + K)}, \tag{3}$$

where j_{pm} is the maximum specific feeding rate, K the half saturation constant of the consumer, $\dot{r}_{pm}$ the maximum specific growth rate of producers, n_p the nutrient to carbon ratio in producer structure, and m the producer nutrient reserve density, defined as the total amount of nutrient in the reserves per unit of producer structure. The quantity $n_p + m$ is commonly referred to as the cell quota of the producer, and n_p as the minimum cell quota. We assume that all rates scale directly with biomass, and that consumers have a per capita mortality rate, $\dot{h}$, that is independent of their age. Then, $\dot{h}$ equals the specific rate at which biomass is lost due to mortality [21]. If the specific consumer biomass synthesis rate $\dot{r}_c$ is some function of j_p and m to be specified later, then the dynamics of the consumer density is

$$\frac{dX_c}{dt} = \left(\dot{r}_c(j_p, m) - \dot{h}\right) X_c. \tag{4}$$

Because the system is closed for nutrients and free nutrients are instantaneously taken up by producers, the nutrient reserve density follows from the balance equation:

$$m = \frac{(N_{tot} - n_c X_c)}{X_p} - n_p, \tag{5}$$

in which n_c the nutrient to carbon ratio in consumer structure, and N_{tot} is the density of total nutrient in the system.

Consumers assimilate nutrients and carbon from producer structure and reserves, and we now assume that synthesizing units describe the rate at which consumers synthesize biomass. Nutrient reserves may be devoid of carbon, for instance, when polyphosphates are a major component of nutrient reserves. However, nutrient reserves may contain carbon when, for instance, the limiting nutrient is nitrogen and the producer stores this element in part in storage protein. Producer structure contains both nutrients and carbon. We assume that the synthesizing unit does not discriminate between producer structure and reserves with regard to the origin of carbon and nutrients. We ignore subtle differences in energetic overheads involved in assimilating carbon or nutrients from producer structure and reserves, and assume that the consumer assimilates the two elements with a constant efficiency.

We have two choices for implementing maintenance. We can either debit this expenditure from the assimilation fluxes before biomass is formed, or add a loss term accounting for the respiration of biomass for maintenance purposes. Both options have conceptual problems, essentially due to the fact we do not consider energy reserves in consumers (if considered, energy reserves would allow for a variable carbon to nutrient ratio in consumers). We will address these issues in a future paper; for this paper, we choose the second option, which is the simpler and commoner of the two. Then, the maintenance and mortality rates add to a single loss term.

Using equation 1, we can now write down the expression for the specific biomass synthesis rate of the consumers. The arrival flux of producer structure to the synthesizing unit is proportional to the feeding rate, and the arrival flux of nutrient reserves is proportional to the product of feeding rate and nutrient reserve density. Because producer structure and nutrient reserves may both contain nutrients and carbon, the arrival fluxes of nutrients and carbon are weighted sums of j_p and mj_p, in which the weights consist of parameters representing stoichiometric requirements, assimilation efficiencies and growth overheads. To avoid the introduction of a large number of symbols, we combine those parameters in weighting factors and call them yield coefficients. A yield coefficient

defines how much biomass (in moles of carbon) a consumer can make from a mole of carbon or nutrient in producer structure or nutrient reserves. The specific consumer biomass synthesis rate is

$$\dot{r}_c = \left(\dot{r}_{cm}^{-1} + ((y_{p2} + y_{n2}m)j_p)^{-1} + ((y_{n1}m + y_{p1})j_p)^{-1} - ((y_{p1} + y_{p2} + m(y_{n2} + y_{n1}))j_p)^{-1}\right)^{-1} - \dot{k}, \tag{6}$$

in which $\dot{k}$ is the maintenance rate, $\dot{r}_{cm}$ is the maximum specific consumer biomass synthesis rate, y_{p1} and y_{p2} are the yield coefficients for assimilating nutrients and carbon from producer structure, and y_{n1} and y_{n2} are the yield coefficients for assimilating nutrients and carbon from the nutrient reserves. All yields are nonnegative and mass balance constraints dictate that $y_{p1} \leq n_p/n_c$ (when $y_{p1} = n_p/n_c$, all nutrients from producer structure can potentially be assimilated); $y_{p2} \leq 1$ (when $y_{p2} = 1$, all carbon from producer structure can be potentially assimilated and there is no growth overhead); $y_{n1} \leq 1/n_c$ (when $y_{n1} = 1/n_c$, all nutrients from producer nutrient reserves can potentially be assimilated); $y_{n2} \leq 1$ (when $y_{n2} = 1$, all carbon from producer nutrient reserves can be potentially assimilated and there is no growth overhead).

In order to visualize the limiting contribution of nutrients to the rate at which consumers synthesize biomass, we use the concept of the dominant limiting factor defined in the previous section. Nutrients are the dominant limiting factor for consumer biomass synthesis when $(y_{p2} + y_{n2}m)j_p > (y_{p1} + y_{n1}m)j_p$. We define the ratio of these two expressions as the limitation coefficient, L,

$$L = \frac{y_{p2} + y_{n2}m}{y_{p1} + y_{n1}m}. \tag{7}$$

When $L > 1$, nutrients are the dominant limiting factor for consumer biomass synthesis.

4 Daphnids and Algae with low Phosphorus

We illustrate the behavior of the system with parameter values that are reasonable for a phosphorus limited system with algae as producers and with daphnids as consumers (see Table 1). Some parameters show a large natural variability, notably the total phosphorus content of the system, the P to C ratio in algal structure, and the mortality rate in *Daphnia* populations, and we therefore examine the dynamics for a range of values. We keep the algal carrying capacity, which equals the total phosphorus density divided by the P to C ratio in algal structure, below 200 μM carbon (roughly equaling 2.5 mg C. l^{-1}), and thus explore a range that covers oligotrophic and eutrophic environments. For simplicity, we assume that algal phosphorus reserves lack carbon, and that daphnids can,

if needed, assimilate all the phosphorus in their food with a 100% efficiency, implying that the yield coefficients for assimilating phosphorus are determined by the P to C ratios in algal structure and *Daphnia* biomass. We also assume that the maximum specific biomass synthesis rate in *Daphnia* is very large and set $1/\dot{r}_{cm}$ equal to zero. Thus, the growth potential of *Daphnia* is bounded through the feeding rather than the assimilation process.

A natural starting point for our analysis is to ignore the potential contribution of phosphorus to the *Daphnia* biomass synthesis rate. Then, equation 6 reduces to $\dot{r}_c = y_{p2}j_p$, and the system is similar to the classic Rosenzweig-MacArthur model ([24]), except that it replaces the constant carrying capacity ((N_{tot}/n_p) in the logistic equation for algal growth with a variable factor that depends on consumer density (namely, $(N_{tot} - n_c X_c)/n_p$). Despite this difference, our model ignoring the contribution of food phosphorus content on *Daphnia* growth has the same qualitative behavior as the Rosenzweig-MacArthur model. The phase plane plot in Figure 3a shows a hump shaped isocline for algae, and a straight vertical isocline for *Daphnia* (the isocline for algae shows the combinations of algal and *Daphnia* densities at which the algal density does not change; similarly, the isocline for *Daphnia* shows the non-growth combinations for *Daphnia*). The intercept of the two isoclines marks the viable or positive equilibrium, at which both populations coexist at constant densities (other equilibria are at (0,0) - no algae, no daphnids; and ($(N_{tot}/n_p$,0) - algae at carrying capacity, no daphnids). This viable equilibrium is stable at relatively low total phosphorus densities, and unstable at high total phosphorus densities. At these high total phosphorus densities, the densities of algae and *Daphnia* fluctuate in limit cycles with amplitudes that become progressively larger with increasing total phosphorus densities, a phenomenon called the 'paradox of enrichment'.

If we now add the possibility of phosphorus limited *Daphnia* growth, hump shaped isoclines for both algae and *Daphnia* arise. These isoclines may fail to cross, or may cross once or twice (see Figure 3). With a single crossing, the model dynamics are qualitatively similar to the simplified model version discussed above (see Figure 3b). The viable equilibrium may be stable or unstable, depending on the total phosphorus density, and the model shows the paradox of enrichment. Furthermore, as in the simplified model, *Daphnia* can always persist in this system, provided a viable equilibrium exists.

With a single viable equilibrium, the dynamics of algae and *Daphnia* may show population cycles like those in simple producer-consumer models (see Figure 4). With similar parameter values to

those in Figure 3b, population cycles are relatively large (see 4c). Relative to the simplified model ignoring the contribution of phosphorus to *Daphnia* growth, the limit cycles show somewhat smaller amplitudes for the *Daphnia* density and somewhat higher peaks in the algal density (results not shown). Since *Daphnia* growth is restricted by algal phosphorus content, the control that *Daphnia* can exert on algal growth is less than in the simplified model and the so called 'prey escape cycles' are more pronounced.

A reduction in the total phosphorus density reduces the cycle amplitudes(see Figure 4a and c). With a relatively high total phosphorus density of 0.45μM P, the limitation coefficient is periodically greater than 1 (see Figure 4d), implying that for part of the time phosphorus is the dominant limiting compound for *Daphnia* biomass synthesis. Figure 4c and d show that phosphorus limitation is especially prevalent during periods of very low algal densities. With a relatively low total phosphorus density of 0.30μM P, however, the contribution from phosphorus in determining the biomass synthesis rate of *Daphnia* is insignificant at any time (see Figure 4b). Loss rates also affect the prevalence of phosphorus limitation for *Daphnia*, as low maintenance and mortality rates lead to large amplitude cycles and hence favor periodical bouts of relatively strong phosphorus limited *Daphnia* growth (results not shown). In general, factors that tend to destabilize the system also emphasize periods with strong phosphorus limited conditions for *Daphnia*.

The algae and *Daphnia* isoclines may also cross twice (see Figure 3c), or they may fail to cross (see Figure 3d). In the latter case, the *Daphnia* loss rates are too high for coexistence. *Daphnia* cannot persist and the algae grow to their carrying capacity. The former case is more interesting as it yields two viable equilibria (see Figure 3c), and it arises when the combined mortality and maintenance rates are relatively high but not so high that the *Daphnia* isocline remains completely below the algal isocline. The equilibrium to the left has the same local properties as the one in Figure 3b; the novel equilibrium to the right is a saddle, implying that it is unstable and that the dynamics of the system depend on initial conditions. Combinations of algal and *Daphnia* densities inside the area enveloped by the solid line in Figure 3c yield dynamics related to the equilibrium to the left, the algal and *Daphnia* densities are likely converge to limit cycles. In contrast, combinations of algal and *Daphnia* densities outside the area marked by the solid curve will always lead to the extinction of *Daphnia*, while algae will increase to the carrying capacity. Thus, this system with the algal density at carrying capacity can not be invaded by *Daphnia* (unless the inoculum is very high). The potential

dynamics with a second viable equilibrium are mathematically complex, and it suffices to state here that the shape of the enveloped area may change considerably when parameters are altered, and that at high total nutrient densities, *Daphnia* may go extinct, regardless initial conditions.

5 Discussion

The principal message of this paper is the value of the synthesizing unit as a tool for modeling biomass formation from assimilation fluxes. While producing results similar to those from the minimum rule (the standard choice for modeling growth with multiple limiting factors - see *e.g.* [1, 16]), the synthesizing unit approach provides a mechanistic basis for describing the inefficiencies that occur near a switch between limiting factors. Models based on synthesizing units are sparse in parameters; indeed, the simplest type of synthesizing unit used in this paper requires no parameters beyond those characterizing the assimilation fluxes.

We have used the synthesizing unit concept in models describing the growth of herbivores subsisting on a producer made up of 'reserves' and 'structure' that differ in elemental composition. We have parameterized our models for *Daphnia* subsisting on phosphorus-limited phytoplankton. But the formalism is general and could be equally well applied to any consumer feeding on a food source with variable nutrient content, for instance, to herbivorous insects in terrestrial food webs where carbon to nutrient ratios in primary producers are much higher than in aquatic systems [6].

Our results confirm and generalize previous findings by Andersen [1] and Loladze *et. al* [16] that *Daphnia* may go extinct in circumstances where food composition strongly influences *Daphnia* growth. Long term persistence of *Daphnia* depends on several parameters, notably the P to C ratio in algal structure, total phosphorus density, and the combined loss rates of *Daphnia*. Those parameters affect the shape of the isoclines and determine the number and nature of equilibria in our model. Fortunately, there is extensive empirical information for both the value of those parameters and their range in natural lakes (see Table 1), and we can therefore explore the effects of this variation in parameter values in natural systems. For example, an increase in the total phosphorus density increases the peaks of both isoclines and their intercepts with the x axis. An increase in combined *Daphnia* loss rates does not affect the shape of the algal isocline, but reduces the peak of the *Daphnia* isocline and its intercept with the x axis. Going from low to high *Daphnia* loss rates, the system has first one, then two and finally no viable equilibria (see Figure 3b, c and d). The range in loss rates

over which two equilibria exist is very narrow for most parameter combinations.

An increase in the P to C ratio in algal structure does not directly affect the shape of the *Daphnia* isocline, but reduces the peak of the algal isocline and lowers the carrying capacity. Thus, the likelihood for *Daphnia* persistence increases and the odds for having two viable equilibria decreases. With a moderate P to C ratio in algal structure of 0.004 and a total phosphorus density of 0.4 μM (carrying capacity is 100 μM C), the combined loss rates have to be as high as 0.23 d^{-1} in order to have two viable equilibria, while with a marginal increase to 0.25 d^{-1}, the system does not support a viable *Daphnia* population. Those loss rates are high for *Daphnia*. With a very low P to C ratio in algal structure of 0.0005 and a total phosphorus density of 0.05 μM (carrying capacity is again 100 μM C), the combined loss rates must be smaller than 0.04 d^{-1} in order to have a a viable *Daphnia* population; this loss rate is unrealistically low. Those examples show that, under constant growth conditions, most systems with *Daphnia* and algae will tend to have only one viable equilibrium.

Our results are consistent with experimental results and field observations that the phosphorus content of food can have an effect on the growth of *Daphnia* [28, 27, 3, 4, 7]. However, the magnitude of this effect changes in time and depends strongly on the size of the population cycles of algae and, to a lesser extent, *Daphnia* (see Figure 4). A high mortality rate tends to reduce the prevalence of phosphorus limited growth conditions for *Daphnia*. Consequently, we conjecture that the introduction of a predator will reduce the influence of algal phosphorus on *Daphnia* growth; confirmation of this will require study of tritrophic chains in models with explicit stoichiometry.

Consumers may play an important role in the recycling of nutrients in producers. Empirical information on nutrient recycling can be analyzed with our model. Consumers necessarily excrete nutrients during maintenance processes at a rate $\dot{k} n_c X_c$ in order to maintain a constant body composition. Additionally, consumers release the nutrients that they did not assimilate from their food; this release rate is $(j_p(n_p + m) - \dot{r}_c n_c)X_c$. Another source of nutrient recycling is the decomposition of dead consumers at a rate of $\dot{h} n_c X_c$. Commonly, the remineralization potential of consumers is expressed as the nutrient release rate as a fraction of the feeding rate [8]. This remineralization potential equals $n_p + m + n_c(\dot{k} + \dot{h} - \dot{r}_c)/j_p$. Figure 5 shows a model fit of this remineralization potential to empirical data. These data, compiled by Elser and Urabe [8], are from widely different sources and contain measurements on zooplankton from marine and aquatic systems. Despite the heterogeneity in source material, we obtain a good fit, even assuming that parameter values are

similar in all systems. The C to P ratio in consumers is about 70, and the minimal C to P ratio in producers about 300, but the error bound on the latter is very high (see Figure 5). The ratio of the combined loss rates and the feeding rate is 0.21. Those parameter values are reasonable for systems with *Daphnia* (see Table 1).

Finally, we note that it is possible to use synthesizing units to describe herbivore growth in many subtly different ways, all consistent with stoichiometric constraints. In this paper we have used arrival fluxes based on assimilation rates of elemental matter. With this assumption, the effect of food quality is simply to change the consumers assimilation efficiency in response to the state of its food. Andersen [1] notes that this assumption may overstate the effects of food composition, as the energy in large quantities of food is assumed unavailable to meet maintenance demands. Some authors [1, 12] have proposed non-mechanistic, alternative representations of herbivore growth in response to this concern. We have work in progress on a family of models based on synthesizing units with different choices for the arrival fluxes, which will provide a mechanistic basis for these alternate models.

Acknowledgements

This work is the fruit of a coincidental meeting between two working groups at the National Center for Ecological Analysis and Synthesis, Santa Barbara. We are indebted to Tom Andersen, Sebastian Diehl and Jotaro Urabe for stimulating discussions, and John Polking for numerically robust software to construct phase plane plots. E.B.M. and R.M.N. received support from the Office of Naval Research (grant no. 00014-99-1-0024), and by the Minerals Management Service (MMS agreement #14-35-0001-30761 and #14-35-0001-30758, Task #15117).

References

[1] T. Andersen. *Pelagic Nutrient Cycles*, volume 129 of *Ecological Studies*. Springer- Verlag, Berlin, 1997.

[2] R.N. Bohrer and W. Lampert. Simultaneous measurement of the effect of food concentration on assimilation and respiration in Daphnia magna strauss. *Functional Ecology*, 2:463–471, 1988.

[3] W.R. DeMott, R. Gulati, and K. Siewertsen. Effects of phosphorus deficient diets on the carbon and phosphorus balance of Daphnia magna. *Limnology and Oceanography*, 43(6):1147–1161, 1998.

[4] W.R. DeMott and R.D. Gulati. Phosphorus limitation in Daphnia: evidence from a long term study of three hypereutrophic dutch lakes. *Limnology and Oceanography*, 44(6):1557–1564, 1999.

[5] M.R. Droop. The nutrient status of algal cells in continuous culture. *Journal of the Marine Biology Association of the United Kingdom*, 54:825–855, 1974.

[6] J.J. Elser, W.F. Fagan, R.F. Denno, D.R. Dobberfuhl, A. Folarin, A. Huberty, S. Interlandi, S.S. Kilham, E. McCauley, K.L. Schulz, E.H. Siemann, and R.W. Sterner. Nutritional constraints in terrestrial and freshwater food webs. *Nature*, 408:578–580, 2000.

[7] J.J. Elser, K. Hayakawa, and J. Urabe. Nutrient limitation reduces food quality for zooplankton: Daphnia response to seston phosphorus enrichment. *Ecology*, In Press.

[8] J.J. Elser and J. Urabe. The stoichiometry of consumer-driven nutrient recycling: theory, observations and consequences. *Ecology*, 80(3):735–751, 1999.

[9] D.S. Glazier. Separating the respiration rates of embryos and brooding females of daphnia magna: implications for the costs of brooding and the allometry of metabolic rate. *Limnology and Oceanography*, 36:354–362, 1991.

[10] J.P. Grover. *Resource Competition*. Chapman and Hall, London, 1997.

[11] D.O. Hessen. Stoichiometry in food webs - Lotka revisited. *Oikos*, 79(1):195–200, 1997.

[12] D.O. Hessen and B. Bjerkeng. A model approach to planktonic stoichiometry and consumer-resource stability. *Freshwater Biology*, 38:447–471, 1997.

[13] S.A.L.M. Kooijman. The synthesizing unit as model for the stoichiometric fusion and branching of metabolic fluxes. *Biophysical Chemistry*, 73:179–188, 1998. 360.

[14] S.A.L.M. Kooijman. *Dynamic Energy Budgets and Mass Budgets in Biological Systems*. Cambridge University Press, Cambridge, second edition, 2000.

[15] W. Lampert. Studies on the carbon balance of Daphnia pulex de Geer as related to environmental conditions. ii. the dependence of carbon assimilation on animal size, temperature, food concentration and diet species. *Archiv fur Hydrobiologie*, Suppl. 48:310–335, 1977.

[16] I. Loladze, Y. Kuang, and J.J. Elser. Stoichiometry in producer-grazer systems: a Lotka-Volterra type model. *Bulletin of Mathematical Biology*, 62:1137–1162, 2000.

[17] E. McCauley, W.W. Murdoch, R.M. Nisbet, and W.S.C. Gurney. The physiological ecology of Daphnia - development of a model of growth and reproduction. *Ecology*, 71(2):703–715, 1990. 93.

[18] E. McCauley, W.W. Murdoch, and S. Watson. Simple models and variation in plankton densities among lakes. *American Naturalist*, 132:383–403, 1988.

[19] J. Monod. La technique de culture continue; theory et applications. *Annales de L'Institute Pasteur*, 79:390–410, 1950. box.

[20] R.M. Nisbet, E. McCauley, A.M. De Roos, W.W. Murdoch, and W.S.C. Gurney. Population dynamics and element cycling in an aquatic plant-herbivore system. *Journal of Theoretical Population Biology*, 40:125–147, 1991.

[21] R.M. Nisbet, E. McCauley, W.S.C. Gurney, W.W. Murdoch, and A.M. De Roos. Simple representations of biomass dynamics in structured populations. In H.G. Othmer, F.R. Adler, M.A. Lewis, and J.C. Daloon, editors, *Case Studies in Mathematical Modeling -Ecology, Physiology, and Cell Biology*, pages 61–79. Prentice Hall, Upper Saddle River, N.J., 1997. 109.

[22] R.M. Nisbet, E.B. Muller, K. Lika, and S.A.L.M. Kooijman. From molecules to ecosystems through dynamics energy budget models. *Journal of Animal Ecology*, 69:913–926, 2000. 448.

[23] J.C. Polking. Ode software for matlab, url http://math.rice.edu/ dfield/, 1999.

[24] M.L. Rosenzweig and R.H. MacArthur. Graphical representation and stability conditions for predator-prey interactions. *The American Naturalist*, 97:209–223, 1963.

[25] R.E.H. Smith and J. Kalff. Size-dependent phosphorus uptake kinetics and cell quota in phytoplankton. *Journal of Phycology*, 18:275–284, 1982.

[26] D. Tilman. Resource competition and community structure. volume 17 of *Monographs in Population Biology*. Princeton University Press, Princeton, 1982.

[27] J. Urabe, J. Clasen, and R.W. Sterner. Phosphorus limitation of Daphnia growth: is it real? *Limnology and Oceanography*, 42(6):1436–1443, 1997.

[28] J. Urabe and R.W. Sterner. Regulation of herbivore growth by the balance of light and nutrients. *Proceedings of the National Academy of Science, USA*, 93:8465–8469, 1996.

[29] S. Watson, E. McCauley, and J.A. Downing. Variation in algal community structure with enrichment. *Canadian Journal of Fisheries and Aquatic Sciences*, 49:2605–2610, 1992.

symbol	interpretation	default value	range	dimension	source
$\dot{h}$	specific mortality rate	0.15†	0 - 0.3†	d^{-1}	[18]
$\dot{J}$	production flux	-	-	$\#\,t^{-1}$	
$\dot{J}_m$	maximum production flux	-	-	$\#\,t^{-1}$	
$\dot{J}_1$	binding rate of substrate x_1	-	-	$\#\,t^{-1}$	
$\dot{J}_2$	binding rate of substrate x_2	-	-	$\#\,t^{-1}$	
$\dot{j}_p$	specific feeding rate of consumer	-	-	d^{-1}	
$\dot{j}_{pm}$	maximum specific feeding rate of consumer	1.0	-	d^{-1}	[20, 21]
K	saturation constant of consumer feeding	12	-	μMC	[15, 17]
$\dot{k}$	specific maintenance rate	0†	0-0.3†	d^{-1}	[2, 17, 9]
L	limitation coefficient	-	-	-	
m	nutrient reserve density	-	-	$\mu MP\,\mu MC^{-1}$	
n_1	number of binding sites for substrate x_1	-	-	$\#$	
n_2	number of binding sites for substrate x_2	-	-	$\#$	
n_c	nutrient to carbon ratio in consumer structure	0.0125	0.010-0.015	$\mu MP\,\mu MC^{-1}$	[6]
n_p	nutrient to carbon ratio in producer structure	0.0033	0.0005-0.0050‡	$\mu MP\,\mu MC^{-1}$	[6]
N_{tot}	density of total nutrient	0.45	0.1 - 0.5‡	μM	[29]
$\dot{r}_c$	specific consumer biomass synthesis rate	-	-	d^{-1}	
$\dot{r}_{cm}$	maximum specific consumer biomass synthesis rate	∞	-	d^{-1}	
$\dot{r}_{pm}$	maximum specific growth rate of producers	1.0	-	d^{-1}	[25]
X_p	producer density	-	-	μMC	
X_c	consumer density	-	-	μMC	

y_{n1}	yield coefficient for assimilating nutrients from producer nutrient reserves	80	70-100	$\mu MC\,\mu MP^{-1}$	[6]
y_{n2}	yield coefficient for assimilating carbon from producer nutrient reserves	0.0	-	$\mu MC\,\mu MP^{-1}$	
y_{p1}	yield coefficient for assimilating nutrients from producer structure	0.327	0.05 -0.50	-	[6]
y_{p2}	yield coefficient for assimilating carbon from producer structure	0.5	-	-	[20, 21]

Table 1: List of symbols and values; a # represents a number, and quantities representing rates contain a dot.

† the default value of the combined mortality and maintenance rates is 0.15 d^{-1}, and the range examined is 0 - 0.30 d^{-1}.

‡ values varied such that the algal carrying capacity, N_{tot}/n_p, is between 0 and 200 μM C.

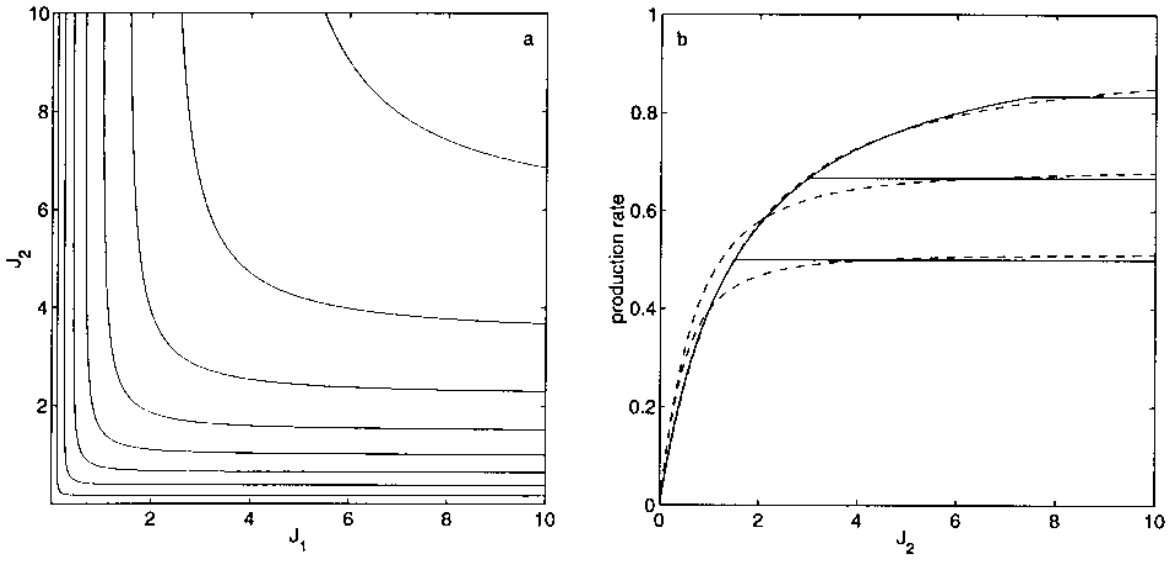

Figure 1: Synthesizing units describe the dynamics of growth at multiple limitations with smooth transitions between limiting compounds, while generally keeping a close match with Liebig's minimum rule. The left panel shows how the contour of the per capita rate of biomass synthesis changes as function of the assimilation flux of two growth limiting compounds; $n_1 = 1$, $n_2 = 1.5$, $\dot{J}_m = 1$ and the contour interval is 0.1. The right panel shows least squares fits of the synthesizing unit model (broken line) to artificial data generated by Liebig's minimum rule (solid line). Parameters used for the minimum rule are $n_2 = 1.5$ and $\dot{J}_m = 1$, and in sequential order from bottom to top, $n_1 = 1$, $n_1 = 2$ and $n_1 = 5$.

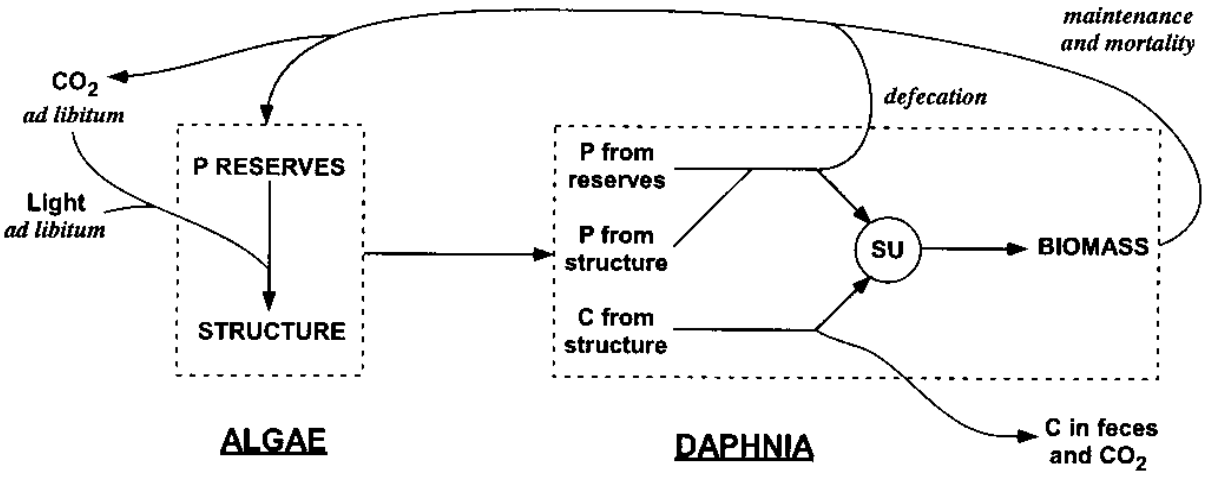

Figure 2: Diagram of system with algae and *Daphnia* in which algae experience a phosphorus limitation. Algae consist of structural biomass and phosphorus reserves, each having a constant elemental composition (the phosphorus content of algae changes as the amount of reserves relative to structure changes). *Daphnia* assimilates phosphorus and carbon from ingested algae to form biomass with constant elemental composition. Both elements influence the biomass synthesis rate of *Daphnia* through synthesizing units (SU). *Daphnia* excretes the phosphorus that is not assimilated and that is released during the respiration of biomass for maintenance purposes. This phosphorus, plus the phosphorus recycled instantaneously from *Daphnia* corpses, is immediately taken up by algae.

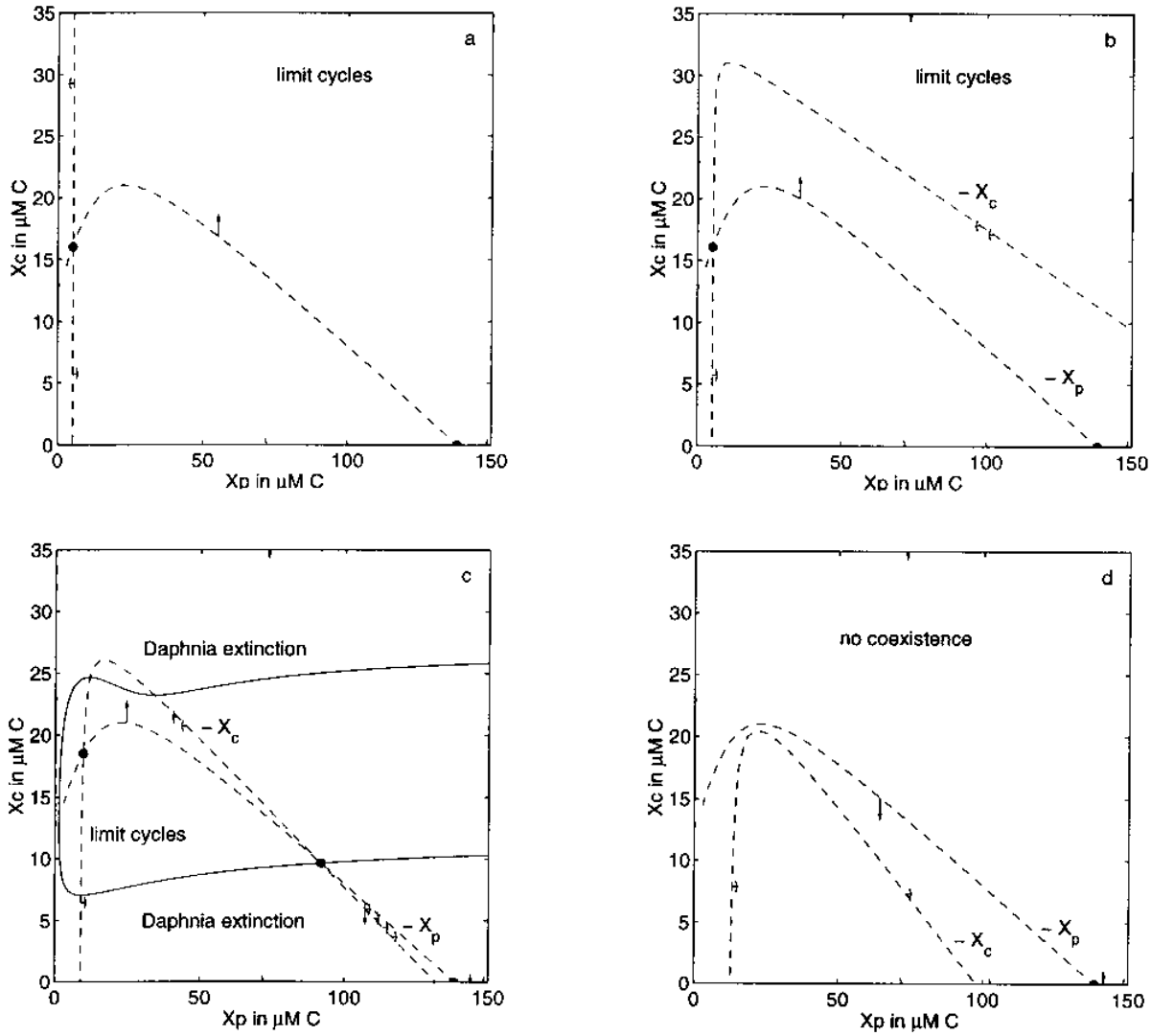

Figure 3: When phosphorus does not affect *Daphnia* growth (a), one positive equilibrium may exist (marked with the dot at (5,16)); the stability of this equilibrium gives way to limit cycles with increasing total phosphorus densities. Inclusion of phosphorus as a determinant of the biomass synthesis rate of *Daphnia* causes the *Daphnia* isocline to bend. With a relatively low combined loss rate, the algal and *Daphnia* isoclines may cross once and both populations converge either to a stable equilibrium or limit cycles, depending on the total phosphorus density (b). With higher combined loss rates, two positive equilibria arise and the long-term dynamics of the system depend on initial conditions (c). Inside the area enveloped by the solid line, the dynamics converge to limit cycles; outside this area, *Daphnia* will go extinct and algae grow to their carrying capacity. With yet higher mortality rates, the isoclines fail to cross (d), and *Daphnia* can not persist. Parameter values are in Table 1, and the combined loss rates are 0.15 d^{-1}, (a and b), 0.21 d^{-1} (c), and 0.25 d^{-1} (d) Phase plane plots are constructed with pplane5 [23].

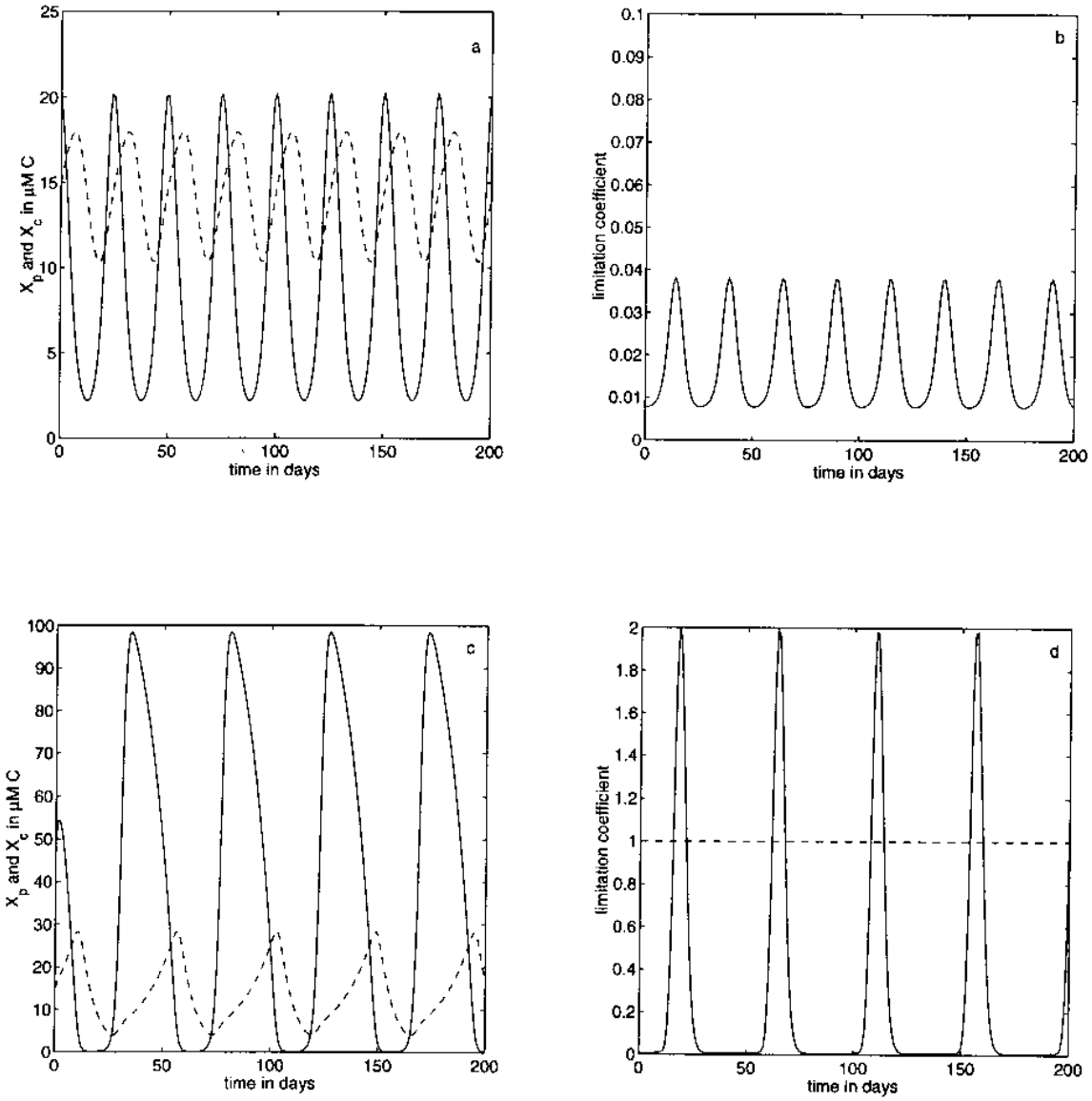

Figure 4: The impact algal phosphorus can have on *Daphnia* growth depends on the stability of the system. With a low total phosphorus density of 0.3 μM, the densities of algae (solid line) and *Daphnia* (broken line) fluctuate with a relatively low amplitude (a), and algal phosphorus contributes little to the biomass synthesis rate of *Daphnia* (b). With a high total phosphorus density of 0.45 μM, algae (solid line) and *Daphnia* (broken line) show large amplitude cycles (c), and the limitation coefficient is periodically above 1 (d), implying that algal phosphorus is at times the dominant limiting factor for *Daphnia* growth. Parameter values are in Table 1.

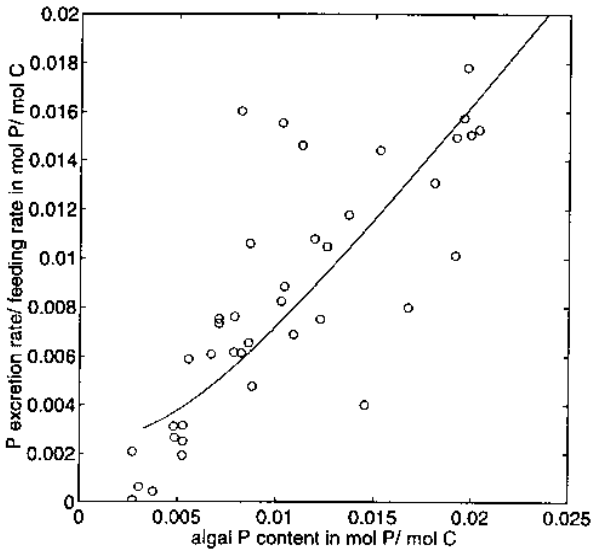

Figure 5: The model predicts the rate at which consumers excrete phosphorus relative to their feeding rate. This rate is a nonlinear function of algal phosphorus content, and also depends relatively strongly on the feeding rate. The line represents a model fit to empirical data compiled by [8]. Nonlinear least squares parameter estimates are (with standard error): $(\dot{k} + \dot{h})/jp = 0.2093$ ($\pm$ 0.038), $n_c = 0.0147$ ($\pm$ 0.0048), $n_p = 0.0032$ ($\pm$ 1.9 10^5). The parameter y_{p2} can not be estimated and its value has been held at 0.5; it is assumed that, if needed, *Daphnia* can assimilate all phosphorus from algae, and therefore $_{yp1} = n_p/n_c$ and $y_{n1} = 1/n_c$.

SUBLETHAL EFFECTS OF TOXIC COMPOUNDS ON DYNAMIC ENERGY BUDGETS; THEORY AND APPLICATIONS

Erik B. Muller[1] and Roger M. Nisbet.
Department of Ecology, Evolution and Marine Biology
University of California, Santa Barbara
Santa Barbara
CA 93106-9610

[1]corresponding author
e_muller@lifesci.lscf.ucsb.edu
Phone (805) 893 2962
Fax (805) 893 4777

I

ABSTRACT

Many toxic compounds in the environment affect the performance of organisms by reducing food consumption, growth and reproduction. These sublethal effects are modeled using a dynamic energy budget (DEB) model, which specifies how rapidly an organism takes up food and utilizes the energy therein to maintain itself, to grow and to reproduce. It is assumed that all organismal energy fluxes except those supporting maintenance processes decline hyperbolically with the internal toxicant concentration in excess of a critical value, the no-effect concentration. Fluxes supporting maintenance processes are assumed to increase linearly with this toxicant measure. It is also assumed that toxicants have a similar impact on each energy flux, an assumption leading to model that is maximally sparse in parameters and structure. Thus toxicants directly affect the rates of feeding, assimilation and maintenance, and indirectly reduce growth and reproduction rates. The model succesfully describes experimental data on feeding, respiration and growth by oysters, mussels, fish and earthworms in the presence of various metals and lipophilic compounds, added singly or in the form of a mixture. The model is also used to analyze data from a field experiment, where it succesfully describes how the growth of mussels is impaired when they are exposed to produced water released by an oil production platform.

KEYWORDS

toxicity model; dynamic energy budget model; one compartment model; bioaccumulation; no-effect concentration; toxic effect; sublethal effect; growth.

INTRODUCTION

Many compounds accumulate in organisms and then cause a reduction in growth. A large body of literature models the accumulation of toxic compounds in terms of exchange between organism and environment. These models range in sophistication from simple one-compartment models to more detailed descriptions where a growth model plays a role in determining toxicant uptake (Eby et al. 1997; Jackson 1997; Landrum et al. 1992). However, most bioaccumulation models have no feedback term through which toxicants affect organismal performance. One important mechanism for this feedback is that toxicants may cause a reduction in feeding and an increase in respiration. Such effects have been described in terms of scope for growth, defined as the excess of energy assimilation rate over respiration rate (Donkin et al. 1989; Widdows and Donkin 1991). Scope for growth is a particularly appealing concept for ecological applications, as it sidesteps the issue of chemical cause, and focuses directly on physiological effect. However, predicting the consequences of changes in scope for growth requires coupling a growth model with a dynamic model for toxicant exchange and physiological effects.

Organisms require energy from food to remain viable, to grow and to reproduce. Dynamic energy budget models use differential or difference equations to describe how an individual organism distributes its energy expenditures (which may be expressed in units of energy or food). DEB modeling is a tradition that dates back at least a century, when Duclaux (1898) assumed budgets for maintenance and growth in order to model sugar consumption by baker's yeast. Since then, DEB models have been developed independently in other biological disciplines, leading to the wide variety of DEB models that are in use today. Examples include the bioenergetic models widely used in fishery biology (Kitchell et al. 1974; Kitchell et al. 1977), and the models of Pirt (Pirt 1965) and Marr (Marr et al. 1962) that are paradigmatic in microbiology.

The form taken by DEB models varies both within and among disciplines. This diversity derives in part from different modeling objectives. In particular, some models aim to answer specific questions, with the importance of any particular mechanism being decided in terms of its relevance to modeling goals. Consequently, one mechanism may get emphasis, while others are lumped or even ignored, all depending on aims. An important consideration for a fish biologist may be swimming costs, whereas a microbiologist may need to model specifically the formation of antibiotics. As a result, many DEB models are designed to describe in detail the performance of a particular species (e.g., McCauley et al. 1990; Ross and Nisbet 1990), or of a group of related species (Hewett and Kraft 1993; Kitchell et al. 1977). Those models aim at, and frequently achieve, a close match between data and model descriptions. However, taxon specific models have one obvious, yet serious limitation: they cannot be used to compare taxa. In ecotoxicology, this implies, for instance, that the large body of knowledge from routine toxicity

tests with waterfleas cannot be used in a model specifically targeting at fish, even if the toxic compound involved has precisely the same mode of action in both taxa.

This example points to the need for general DEB models based on mechanisms that are common to a broad range of organisms. Species are generally assumed to differ only in their parameter values; however, particular attributes of a taxon may be added, provided that additions do not alter the general core of the model. One such model, developed by Kooijman (1993, p224-232), successfully describes growth and reproduction in organisms ranging from bacteria and to whales. It has been succesfully used to describe processes influenced by energy availability at different levels of biological organization, such as ribosomal translation rates in Escherichia coli (Kooijman et al. 1991), and predator-prey dynamics in chemostats (Kooi and Kooijman 1994). Our goal in this paper is to extend Kooijman's model to describe sublethal effects of toxicants.

Some previous studies of the accumulation and effects of toxic compounds have used general DEB models. Changes in the body burden of a toxicant have been related to the state variables describing size and fatness, characteristics that determine the rates of toxicant exchange and the potential for toxicant accumulation (Kooijman and Vanharen 1990; Lassiter and Hallam 1990; Van Haren et al. 1994). Toxic effects have been modeled through changes in the values of DEB model parameters. Using this approach, Kooijman and co-workers (1996a; 1996b; 1996c; 1996) have developed a method to assess no-effect concentrations in routine toxicity tests, and Klok and De Roos (1996) have studied consequences of copper contamination for earthworm populations. These authors have considered several possibilities for toxic effects by formulating a set of alternative assumptions about target parameters (specific combinations of toxic effect and species are thus possible), and left open which assumption represents experimental data best. Moreover, some assumptions make predictions that are absurd at a relatively high toxicant concentration. In this paper we aim for greater consistency and greater generality.

We develop a model that describes the changes in vital rates induced by toxicants at sublethal concentrations. The section on theory describes a DEB model, a toxicokinetic model, and a toxic effect model, which describes the feedback of accumulated toxicants on energy budgets. In the following section, we test model predictions against diverse experimental data, including feeding, respiration and growth by oysters, mussels, fish and earthworms. The effects studied are induced by metallic or lipophilic toxicants, added singly or in the form of a mixture. Our motivation in testing the model against several data sets is to establish its broad credibility, before applying it in field situations where data limitations preclude direct testing. The data we consider offer rigorous challenges to many of the model assumptions, but the fit of model to data is good. Having established the broad credibility of the model, we illustrate its application to a field situation: the interpretation of growth data from a field experiment in which mussels are

exposed to produced water released by an oil production platform. The model extends our understanding of the toxic effects of produced water by adding predictive power, not available from routine statistical analyses.

MODELS

We formulate in this section three simple and general submodels, simple to compare theory to experimental data and general to embrace various species and toxicants. First, vital rates are described with a DEB model developed by Kooijman and Metz (1984). Kooijman (1993) discusses extensively the credibility of the model assumptions, and exemplifies the model with data from a wide variety of heterotrophic organisms. We largely follow the notation in that publication, of which one peculiarity needs attention: the use of square brackets around a variable or parameter, a use that reflects that the variable or parameter depends on body volume. Second, toxicant dynamics are specified with a particular form of a one-compartment model. One-compartment models are widely used in ecotoxicology (see Landrum et al. 1992, for a review) . Finally, a model for the sublethal effects of toxicants is developed in the last subsection.

1. Dynamic Energy Budget Model

DEB models describe how animals assimilate and utilize energy from food. In the Kooijman-Metz model (see Figure 1), a heterotrophic organism can use the energy assimilated from ingested food for three purposes: maintenance, growth and reproduction. Energy is commited irreversibly and continuously, but the maturation and release of reproductive material may be a discontinuous process, implying a temporary buffer of energy for reproduction. The energy balance equation thus reads as

$$A = M + G + R \qquad (1)$$

where A is the rate at which energy is assimilated from ingested food, M the rate at which energy is spent on maintenance, and G and R are the rates at which energy is invested in growth and reproduction, respectively. For the purposes of this paper, A, M and G need to be specified; a derivation of reproductive output (and investment in juvenile maturation) is not needed - see Kooijman and Metz (1984).

The assimilation rate depends on the rate of food uptake, I. It is assumed that I is proportional to the surface area of the food catching apparatus. The Kooijman-Metz model assumes isomorphic organisms, *i.e.*, ones that do not change shape during growth. The volume of the organism, V, is then proportional to the cube of a length measure, and any of its surface areas is proportional to $V^{2/3}$. It is also assumed that the organism responds hyperbolically to food density (type II functional response), yielding a scaled functional response, f, which takes values between 0 and 1. Consequently,

$$I = I_m f V^{2/3} \tag{2}$$

with I_m being the maximum surface area specific uptake rate (units of food per unit of surface area per unit of time). The energy contained in ingested food is assimilated, a process for which a constant efficiency is assumed. This constant assimilation efficiency equals I_m/A_m, where A_m is the maximum surface area specific assimilation rate (units of energy per unit of surface area per unit of time). The assimilation rate is thus simply proportional to the ingestion rate given in equation (2).

Maintenance and growth are assumed to consume a fixed fraction, κ, of the assimilated energy, with maintenance taking priority over growth; the remaining fraction, $1-\kappa$, is commited to reproduction. The maintenance rate is assumed to be proportional to the size of an animal, or $M = [M]V$, with $[M]$ being the volume specific maintenance rate (energy unit per volume unit per time unit). The rate at which an organism increases in size is assumed to be proportional to the rate of commitment of energy to growth, so that $G = [G]dV/dt$, with $[G]$ being the volume specific investment in growth (energy unit per volume unit). With these assumptions, the growth dynamics are

$$\frac{dV}{dt} = \left(\frac{\kappa A_m}{[G]} f V^{2/3} - \frac{[M]}{[G]} V \right)_+ \tag{3}$$

where the subscripted 'plus' means that growth is zero when the term within brackets is negative, which happens when assimilate dedicated to growth and maintenance is insufficient to meet the demand for maintenance (then, energy fluxes must be prioritized differently; but this case is not encountered in this study). When the food density is constant, equation (3) implies that the asymptotic size is $V_\infty^{1/3} = \kappa A_m f / [M]$.

In practice, growth is often expressed in terms of an increase in length, L, which is proportional to $V^{1/3}$ in isomorphs. The growth dynamics expressed in this way are:

$$\frac{dL}{dt} = \gamma\left(L_\infty - L\right)_+ \tag{4}$$

where L_∞ is the asymptotic length at constant food conditions, and $\gamma \equiv [M]/3[G]$ is the growth rate parameter, which has the dimension per time. This equation can be solved for constant food densities and for a constant body burden of toxicant (see below), and yields the von Bertalanffy growth curve,

$$L(t) = L_\infty - (L_\infty - L_0)e^{-\gamma t}. \tag{5}$$

The link between model variables and many measurable quantities requires additional assumptions. Size is often expressed as dry or wet weight, which are assumed to be proportional to biovolume. Extra assumptions are also required to analyze data on respiration. Respiration reflects the loss of usable energy, to which each energy flux may contribute. The contribution of a flux is assumed to be proportional to its magnitude (Kooijman 1995). Then, the respiration rate is a linear combination of the assimilation, maintenance, growth and reproduction rate. Made explicit in biovolume and the parameters associated with assimilation and maintenance, the respiration rate, r, is

$$r = \alpha A_m V^{2/3} + \beta\,[M]V \tag{6}$$

where α and β are compound parameters that include $[G]$, κ and the proportionality factors converting the energy loss associated with assimilation, maintenance, growth and reproduction into moles of oxygen.

2. Toxicokinetics

A one-compartment model describes the change in the body burden of toxicant as the difference between the rates for toxicant uptake and removal. Most models take uptake proportional to body mass, but here the uptake rate is assumed proportional to the surface area of an organism, so proportional to $V^{2/3}$. This recognizes that compounds must cross a surface to enter an organism, whether it is via the gut, gills, skin or lungs. Surface dependent uptake agrees with data on, for instance, mussels taking up PCB congeners (Gilek et al. 1996). In addition, it is

assumed that the the uptake rate is proportional to the toxicant concentration in food, C_x, and the ambient concentration of 'dissolved' toxicant, C_d. The removal rate is analogously modeled as a function of size and a toxicant concentration. Toxicants can leave an animal via molts, gills, kidneys or gut but, again, must cross a surface to get removed (removal via egg deposition is not considered here). Consistently, the removal rate is assumed to be proportional to the surface area of an animal. The removal rate is additionally assumed proportional to the density of toxicant in the organism, the body burden of toxicant, $[Q]$.

Consequently, the total amount of toxicant in an animal, Q, changes according to

$$\frac{dQ}{dt} = (k_{da}C_d + k_{xa}fC_x - k_{ad}[Q])V^{2/3} \qquad (7)$$

in which k_{da} and k_{xa} are the surface area specific uptake rates for dissolved and food-associated toxicants, respectively; they have the interpretation of ambient volume cleared of toxicant per unit of animal surface and per time. The toxicant conductance rate, k_{ad}, specifies the rate of toxicant removal (length unit per time unit).

The dynamics of the body burden of toxicant are now obtained by applying the chain rule for differentation (recall that $Q=[Q]V$). So,

$$\frac{d[Q]}{dt} = V^{-1/3}(k_{da}C_d + k_{xa}fC_x) - [Q]\left(k_{ad}V^{-1/3} + \frac{1}{V}\frac{dV}{dt}\right). \qquad (8)$$

The expression for growth in this equation accounts for the dilution of $[Q]$ due to growth. In a constant environment, the body burden of toxicant eventually reaches an equilibrium value, $[Q]^*$. Then, the animal will have ceased to grow (see equation (3)) and $[Q]^*=(k_{da}C_d+k_{xa}fC_x)/k_{ad}$. If the toxicant is taken up only directly from the environment, $[Q]^*=C_dk_{da}/k_{ad}$, the ratio of the exchange parameters being known as the bioconcentration factor. Similarly, if the toxicant is taken up only via food, $[Q]^*=fC_xk_{xa}/k_{ad}$.

Studies reporting on effects of toxicants unfortunately seldom use the body burden as a toxicant measure. Instead, the available toxicant measure is often the nominal concentration, the initial concentration in the environment. Then, the body burden of toxicant needs to be reconstructed, which requires a scaling of the body burden with model parameters. In general, a scaling reduces the number of parameters in a model, while all mechanisms are retained.

A reconstruction of the body burden of toxicant is feasible if ambient toxicant levels are constant, which is approximately true when the system volume is sufficiently large or when toxicants and food are regularly replenished. Accordingly, in the presentation below, the ambient

toxicant concentration is assumed to be constant. With a toxicant taken up only directly from the environment, a reconstruction of the body burden of toxicant can be obtained after scaling the body burden with the bioconcentration factor, yielding a body concentration, C_a, with dimensions equivalent to the ambient concentration. After substitution of $C_a \equiv k_{ad}\,[Q]/k_{da}$ and changing the size measure to length, equation (8) becomes

$$\frac{dC_a}{dt} = \frac{k_{ad}}{L}\left(C_d - C_a\right) - 3C_a\frac{1}{L}\frac{dL}{dt} \tag{9}$$

where k_{ad} has a new value because of the change in size measure. The parameter for toxicant uptake has disappeared as an explicit constant, leaving the toxicant conductance rate as the single parameter to determine toxicant exchange. For toxicants (also) taken up with food, a similar scaling of the body burden of toxicant also leads to equation (9).

Experimental data on growth may contain insufficient information to estimate the toxicant conductance rate from equation (9). Such data can be analyzed by assuming extreme values for the toxicant conductance rate: either very high or zero (Kooijman and Bedaux 1996b). Given initial conditions, this method yields two reconstructions for the body burden of toxicant, and these reconstructions span the range of all possible outcomes. If the toxicant conductance rate is very high, the toxicant concentration in the ambient can be directly used as a measure for the body burden. For this purpose, the toxicant conductance rate must be high with respect to the von Bertalanffy growth rate and the inverse of the experimental duration. As a consequence, dilution of the body burden due to growth is a negligibly slow process, and the body burden will rapidly approach its equilibrium value. In effect, then, the body burden of toxicant is always approximately proportional to the ambient concentration.

If, on the other hand, the toxicant conductance rate is negligibly slow, the bioconcentration factor and, consequently, C_a are not defined. The body burden of toxicant thus needs to be scaled in another way. With $S_a \equiv [Q]/k_{da}$, an expression is obtained that lacks an explicit reference to the exchange parameters, but contains all the mechanisms of the toxicokinetic model. Substitution of S_a in equation (8) gives

$$\frac{dS_a}{dt} = \frac{C_d}{L} - \frac{3S_a}{L}\frac{dL}{dt}. \tag{10}$$

in which S_a is the body concentration expressed in an ambient concentration measure times time per length.

3. Toxic Effects

Toxicants, at sublethal levels, are assumed to affect energy budgets by changing the parameter values in the DEB model. These parameters specify efficiencies, rates and the partitioning of energy between somatic and reproductive tissue. We consider toxicants that alter the flow rates of energy. The assumptions are:

(i) Toxicants have no effect on energy budgets up to a fixed tissue level, the no-effect concentration (NEC).

(ii) Energy fluxes decline hyperbolically with the effective toxicant concentration (the body burden of toxicant minus the NEC), except those supporting maintenance processes which increase linearly with the effective toxicant concentration.

(iii) Toxic effects have a similar impact on each energy flux, implying that the toxicological parameters, the NEC and the scaling parameter K_i, have the same value in each expression.

Consequently, three primary parameters of the DEB model are affected by toxicants: the maximum surface area specific rate of feeding, I_m; the maximum surface area specific rate of energy assimilation, A_m; and the volume specific maintenenance rate, $[M]$. Efficiency parameters are not affected, since they represent ratio's of rates, so that effects cancel. Effects on the partitioning parameter are not considered. Substitutions to be made in previous equations are:

$$I_m = \frac{I_{m,0}}{1+\frac{([Q]-[Q_{nec}])_+}{K_i}}; A_m = \frac{A_{m,0}}{1+\frac{([Q]-[Q_{nec}])_+}{K_i}}; [M] = [M]_0\left(1+\frac{([Q]-[Q_{nec}])_+}{K_i}\right) \quad (11)$$

where the indexed zero's refer to parameter values in absence of toxicants, and $[Q]$ and $[Q_{nec}]$ are body burden of toxicant and NEC, respectively. The subscripted plus implies that toxic effects are not experienced when $[Q] \leq [Q_{nec}]$. Scaling of $[Q]$, $[Q_{nec}]$ and K_i with the bioconcentration factor (see previous subsection), yields C_a, C_{nec} and K_i', which subtitute their unscaled counterparts in the toxic effect functions.

Compound parameters that are derived from the rate parameters, the ultimate length, L_∞, and the von Bertalanffy growth rate, γ, become

$$L_\infty = \frac{L_{\infty,0}}{\left(1+\frac{([Q]-[Q_{nec}])_+}{K_i}\right)^2}; \qquad \gamma = \gamma_0\left(1+\frac{([Q]-[Q_{nec}])_+}{K_i}\right) \quad (12)$$

It may seem odd that the von Bertalanffy growth rate increases with the toxicant concentration. However, this growth rate by itself does not determine how fast an organism grows; rather it specifies how fast the organism approaches its ultimate size (see equation (5)), which is reduced in the presence of toxicants. Indeed, equation (4) shows that the initial rate of increase in length equals γL_∞, which decreases hyperbolically with the toxicant concentration.

The rationale for these assumptions is as follows. Assumption (i) reflects the possibility that energy fluxes may be unaffected by toxicant levels up to some critical value. For example, some toxicants are detoxified through degradation, trace elements are functionally incorporated in enzymes and divalent metals are compartmentalized or bound by metallothionins, proteins for metal homeostasis. Furthermore, an organism may physiologically adapt to low toxicant levels, *e.g.*, by increasing the concentration of just a few enzymes. These and other neutralization mechanisms have a marginal effect on energy budgets, since they demand only small changes in body composition (while still allowing that some organs or specialized cells to accumulate a large amount of toxicants). The simplest way to take neutralization mechanisms into account is to assume a concentration below which toxic effects are not observed, *i.e.*, a constant NEC.

Assumption (ii) aims to represent toxicants that reduce the rate of energy transduction through biological systems. As the principal, sublethal mode of action, this representation is plausible for many metals and lipophilic compounds. Metallic toxicants readily bind to ligands, most notably the sulphydryl groups of proteins, and thereby inhibit enzyme activity (Byczkowski and Sorenson 1984). Lipophilic toxicants dissolve in the lipid bilayers (membranes) encapsulating cells and organelles, and thereby hamper the functioning of these membranes (see Sikkema et al. 1995, for reviews; Van Wezel and Opperhuizen 1995). The effects, albeit not well understood, often depend on the hydrophobicity of the toxicant (Verhaar et al. 1992), and may include inhibition of membrane embedded enzymes (Franks and Lieb 1994), and a reduction of membrane resistance (Sikkema et al. 1995).

In the model context, such toxicants thus reduce the rate at which energy is acquired by and delivered at DEB model processes, except maintenance, which represents a demand rather than a supply. Maintenance demands are assumed to increase in the presence of toxicants, since an organism aims at stability, including stable intracellular ion concentrations. It takes more energy to maintain stable ion concentrations at a lower resistance of cell membranes, a reduction that can caused by toxicants (Sikkema et al. 1995).

The reason for choosing a hyperbolic response to the toxicant concentration for feeding and assimilation, and the inverse of that for maintenance, is that it matches concepts in enzyme kinetics, which has analogies at all levels of biological organization. Analogies are routinely used at the level of organelles (see Figure 2), organisms (type II functional response) and populations

(population growth rate of microorganisms (Monod 1950)). Enzyme performance is reduced when inhibitory compounds are present. Enzymatic conversion rates decline as a hyperbolic function of the inhibitor concentration, the shape of the function depending on the working mechanism of the inhibitor (Segel 1993). We have choosen non-competitive inhibition kinetics as a paradigm, since it is mathematically the most tractable form, and the mechanism of this type of inhibition may be because of a common enzymatic attribute, such as having a sulphur ligand. Moreover, many heavy metals are known as non-competitive inhibitors (Byczkowski and Sorenson 1984).

Assumption (iii) is somewhat arbitrary, although there are mathematical and biological arguments supporting it. The assumption keeps the model maximally sparse in parameters, which is important in model testing. The credibility of a model with many parameters can be evaluated only when a large body of quantitative information is avaliable, and such elaborate data sets are very rare in ecotoxicology. Furthermore, the assumption keeps the model structure maximally simple. It implies that parameters describing efficiencies cannot be affected, since an efficiency is the ratio of two rates, so that effects cancel. The assimilation efficiency, for instance, is the ratio between the rate parameters specifying feeding and assimilation. A similar argument holds for two other efficiency parameters, the growth cost parameter, $[G]$, and the scaling parameter in the scaled functional response (not explicitely introduced).

A rival, equally arbitrary assumption states that at any sublethal concentration, only one process is noticably affected by a toxicant (Kooijman and Bedaux 1996a; Kooijman and Bedaux 1996b; Kooijman et al. 1996). This assumption leads to more complexity than our assumption, since in this case a suite of models results. Each submodel assumes toxic effects on a different parameter, which may be a rate or efficiency parameter. However, experimental results demonstrate that at least some toxicants cause effects on multiple processes. For instance, mussels feed slower and respire faster in the presence of pentachlorophenol or tributyltin (Widdows and Donkin 1991; Widdows and Page 1993).

It is important to extend the toxicity model to include effects of multiple toxicants, since in most environments organisms are exposed to a variety of toxicants. The simplest way to include multiple toxicants is to assume that a contaminated environment can be diluted to a critical level below which the organism is unaffected by the contaminants, and that above that level the contaminants work additively (Walker et al. 1996, p165-167). This implies that the effects of a toxicant can be substituted by another through appropriate dosing. If the ratio of toxic compounds in the environment is constant, and if the various compounds are exchanged at approximately equal rates by the organism, then the sum of scaled body burdens of toxicant is proportional to any single scaled body burden, and toxic effects can be described as in equations

(11) and (12), with $[Q]$ being the body burden of toxicant of any of the compounds present, and with $[Q_{nec}]$ and K_i being compound parameters for the NEC and toxicity scaling, respectively.

METHODS

Model parameters were estimated from data with (predominantly) non-linear regression techniques. For this purpose, it was assumed that differences between observations and model predictions were the result of normally distributed sampling error. It was assumed that noise had only occured in biological variables (rates of feeding and respiration, length, etc.), not in physical and (bio)chemical variables (time, concentration, body burden of toxicant). The residuals squared were weighted with the number of measurements, except, mostly, residuals squared of sizes, which were weighted with length squared because the variation in growth data tend to increase with a constant coefficient of variation (Kooijman 1993, p121). When multiple data sets were involved, parameters were estimated from all data sets simultaneously.

Regression problems were solved numerically (see, e.g., Burden and Faires 1988, for a description of numerical methods). Sums of squares were differentiated with respect to the parameters using the forward difference method. The roots of the normal equations were solved with the Gauss-Newton method. Inverse problems were solved using the fourth order Adams Predictor-Corrector method.

TESTS WITH EXPERIMENTAL DATA

Ideally, an evaluation of our model would involve separate experimental tests of each of the model assumptions, followed by tests of their predictions when combined in the model. This ideal is unattainable, as experimental information on several of the key state variables (*e.g.*, changes over time of body burden of toxicant) is seldom available (see for tests of the DEB model Kooijman 1993; Kooijman and Metz 1984). Our model tests are therefore indirect. The model assumptions are combined in different ways to obtain a variety of model predictions, which are then compared to experimental results. Such an evaluation is increasingly convincing, the greater the diversity of the comparisons made, and the smaller the number of fitting parameters. Thus in this section we discuss the model's predictions on mitochondrial activity, feeding, respiration and growth. The toxicants considered include various metals and lipophilic compounds, the affected organisms being mussels, oysters, earthworms and zebrafish. Parameters are estimated by fitting data on specific organisms exposed to different levels of toxicant, the

credibility of the model being determined by its ability to fit a wide combination of toxicants and organisms with a small number of free parameters.

1. Effects on Mitochondrial Activity

We first consider a very simple system, a suspension of mitochondria with several toxicants. Although our model describes individual organisms, this simple system is relevant, since energy flows at suborganismal levels are supposed to be the basis of DEB assumptions, and mitochondria, being generators of ATP, are a key component in the transduction of energy. However, the data we discuss here have been collected *in vitro*, with substrates available in excess. *In vitro* fluxes are not regulated to meet metabolic demands. The results, therefore, do not indicate how the output of mitochondria *in vivo* changes as a result of toxicant action. Yet, the results are informative, because they illustrate how toxicants affect the capacity of a complex assemblage of membrane-embedded enzymes to conduct energy.

Mitochondrial activity is studied with cadmium (Kesseler and Brand 1994), 2,4,6-trichlorophenol (TCP) or 2,4-dinitrophenol (DNP) (Shannon et al. 1991) as toxicants. The examples thus include one metallic and two lipophilic compounds. Mitochondrial activities are fitted with an expression analogous to that for I_m in equation (11) with $[Q_{ncc}] = 0$. Toxicants are thus assumed to act as non-competitive inhibitors of mitochondrial activity (Segel 1993, p125-132). Figure 2 shows that this expression describes quite well the inhibition of mitochondrial ATP production by cadmium, TCP and DNP. Parameter estimates are given in the legend to the figure. The data with cadmium are particularly informative, since the authors corrected the nominal concentration for toxicologically inactive cadmium bound to chelating agents, thereby obtaining the free cadmium concentration. Comparing the lipophilic toxicants, TCP inhibits more strongly than DNP; the concentrations at which the mitochondrial activity is halved, K_i, being 37.5 and 69.9 μM, respectively. This is to be expected, because TCP is more lipophilic than DNP (Mackay et al. 1992), and lipophilicity is generally an indicator of toxicity (Van Wezel and Opperhuizen 1995; Verhaar et al. 1992).

2. Effects on Feeding and Respiration

Toxic effects on feeding and respiration are examined with data on similarly sized blue mussels, *Mytilus edulis*, which were briefly exposed to toluene (Donkin et al. 1989) or penta-chlorophenol (PCP) (Widdows and Donkin 1991). Figure 3 shows that PCP and toluene have

similar effects on feeding, and that PCP also affects respiration. The reported rates for feeding and respiration are scaled to the rates in absence of PCP and toluene. The available measure for toluene is the ambient concentration, and it is not immediately clear whether this is a legitimate measure to use in the toxicity model. It can be used, though, because the exposure time was very short (less than one hour). In clean organisms, the toxicant concentration initially increases linearly with time (see equation (8) for $[Q]=0$). Hence, in short experiments the body burden is about proportional to the exposure time and to the ambient concentration, a dependency that is in agreement with measurements with PCP as a toxicant (Widdows and Donkin 1991). A consequence of using the ambient toluene concentration is that parameter estimates will depend on exposure time, which is unfortunate but does not hamper a test of the model.

Also the measurements with PCP need a remark. We disregard the response at the highest PCP concentration, which deviates considerably from other measurements. The mussels ceased to feed, possibly because they closed their shells, which is their usual response to adverse environmental factors. Organisms that fail to feed will ultimately die, while this study focusses on sublethal responses to toxicants. Cessation of feeding also bears consequences for aerobic metabolism. Mussels that do not feed have little opportunity to acquire oxygen and, therefore, change partially to anaerobic metabolism (Wang and Widdows 1993). Then, respiration is not a proper measure for total metabolism and equation (6) is invalid.

Model fits are in good agreement with the experimental results (see Figure 3). Parameters estimated from both data sets with equations (2), (6) and (11) are the no-effect concentration (set at zero for PCP, its apparent value), the saturation constant and a compound parameter, $p \equiv \alpha A_{m,0}/\beta [M]_0$, which results from scaling the respiration rate in equation (6) (see figure legend for estimated values). The initial scaled rates and the size of the mussel are set on their measured values. The feeding rate is well fitted by a hyperbolic function of the ambient toluene concentration or body burden of PCP (see figure legend for parameter estimates). The predicted respiration rate increases almost linearly as a function of the body burden of PCP, a prediction that is supported by the data. Thus, the fits of feeding and respiration are both satisfactory, despite the fact that only two parameters are estimated from these two data stes. This result especially supports assumption (iii), which states that toxicants have a similar impact on each energy flux.

3. Effects on Growth

Toxicants affect growth indirectly, by reducing the uptake of food and assimilation of energy, and by increasing maintenance demands. The result of these toxicant induced changes on

growth are examined with data on bivalves, an earthworm and a fish. Neither of the data sets, however, contain information about the body burden of toxicant. This measure needs to be reconstructed from the ambient concentration (see Toxicokinetics Section). In principle, a reconstruction can be obtained by combining equations (3), (9) and (12), implying that it must be possible to estimate the toxicant conductance from data on growth. In practice, however, the quality of the data is too poor for this purpose. As discussed above, an alternative is to assume the toxicant conductance rate to be either very high or negligibly small, resulting in two accumulation curves, which mark the range of possible curves. For moderately lipophilic toxicants, which are generally rapidly exchanged (Hawker and Connel 1986), only the first extreme is considered, and because in all cases the experimental duration was relatively long, the nominal concentration is used as a measure for the body burden of toxicant. For metallic compounds, both extremes for the toxicant conductance rate are considered.

The first examples are on larval growth of the oyster *Crassostrea gigas* (Beiras and His 1994) and the mussel *M. galloprovencialis* (Beiras and His 1995) reared at different mercury concentrations. The experimental design was similar for both species. The larvae had been exposed to mercury since the fertilized egg stage and were regularly transfered to new vessels containing filtered sea water, mercury and algae. It is therefore assumed that the ambient mercury concentration and food density were sufficiently constant to apply equation (12) with equation (4), or with equations (4) and (10). So, in the absence of toxicants, larvae should exhibit von Bertalanffy growth. However, growth initially accelerated (see Figure 4), as is usual for larvae (Bayne 1976), which might be the result of food catching capacities increasing with size or time. Such a mechanism can be modeled, but for simplicity we assume that larvae need a fixed period to gain full feeding capabilities. Thus, it takes a fixed time delay until growth in the absence of toxicants becomes of the von Bertalanffy type. This time delay has to be given a pre-determined value for the mussel but could be estimated from the data on oyster larvae. Also the utimate size in absence of toxicants, $L_{\infty,0}$, needs to be chosen independently of the data, which contain little information about this parameter (estimation of this parameter requires a longer experimental duration). On the basis of published growth curves, we take $L_{\infty,0} = 350$ µM (see Bayne 1976), but selecting 10% higher or lower values scarcely affect fits and estimates of other parameters.

Figure 4 shows model fits to the growth data of oyster and mussel larvae, and Table 2 gives parameter estimates for one extreme case for toxicant exchange, that is, having a body burden that is always in equilibrium with the ambient concentration because of a high toxicant conductance rate (the other extreme, resulting from a negligibly small toxicant conductance rate, yields parameters that lack a clear biological interpretation). With the first extreme, the model properly predicts intitial and subsequent growth of both species at low mercury concentrations. Both species tolerate a little mercury in the ambient, the NEC is less than 8 nM, causing the

growth curves at the lowest (5 nM) and zero mercury concentration to be (almost) identical. Values for the toxicity scaling parameter, K_T, show that mercury is a little more toxic for oyster than for mussel larvae. With the other extreme assumption, *i.e.*, larvae fully retain mercury, the model correctly predicts that growth ceases at the highest mercury concentration, although the initial increase in size is too fast. The extremes thus complement each other in describing the data.

The second example is the effect of copper on growth of the earthworm *Lumbricus rubellus*. The earthworms were reared for more than 5 months and accumulated copper via ingestion of contaminated soil (Ma, cited in Klok and De Roos 1996). Parameters are estimated using the same methods as in the previous example, yielding a relatively high no-effect concentration (see Table 2), which is not surprising since copper is a trace element needed for growth. Figure 5 shows that high copper levels strongly reduce growth (the shape of the curves differs from the previous example as the size measure is weight rather than length). As before, assuming a high toxicant conductance rate gives better predictions at low copper levels, whereas the other extreme is more succesful in predicting that growth stops at the highest copper level. At lower levels, growth is reduced more than the model predicts. This may be the result of food becoming limited or coccoons being produced. Nonetheless, the fits are reasonable, which shows that the model is also applicable to non-aquatic organisms.

The third example concerns the zebrafish *Brachydanio rerio* growing with benzo(k)fluoranthene (Hooftman and Evers-De Ruiter 1992), or a with a mixture of benzo(k)fluoranthene and 5 other polycyclic aromatic hydrocarbons (PAH) (Hooftman et al. 1993). At the highest dose, the concentration of the constituents in the mixture, listed in the legend to Figure 5, equaled the no-observed-effect concentration (NOEC) of each PAH, which had been measured in previous experiments. Because the relative contribution of each component was constant, a suitable measure for the ambient toxicant concentration is the volume of PAH mixture added. The fish were kept in an intermittent flow-through system, so food and toxicant concentrations were relatively stable. The fish had been exposed to toxicants since the fertilized egg stage and were grown for 37 days after hatching. The final length reached was recorded as a function of the nominal toxicant concentration, but information about the growth trajectory is not available. Therefore, some parameters cannot be estimated. Values for the growth rate and the length at birth are taken from the literature (Kooijman and Bedaux 1996b). Free parameters are estimated with equation (4) and (12).

Figure 5 and Table 2 show how PAHs change the growth of zebrafish. With benzo(k)fluoranthene alone, mortality was significant at the higher concentrations, which indicates that the whole range of sublethal concentrations is covered. The first three data points represent the average length of 45-50 fish, the fourth and fifth 13 and 1 fish, respectively. Since

the data have been weighted accordingly (the standard deviation is consistently about 0.3 cm), the first three data points have the most influence on the fit. The NEC for benzo(k)fluoranthene is a little higher than the NOEC, 1.0 versus 0.7 nM, which is in line with the fact that the NOEC is an underestimation of the NEC. With the other example, the doses of the PAH mixture do not cover the whole range of sublethal concentrations. More fish survived, 75 at the lowest and 55 at the highest toxicant dose, than with the addition of benzo(k)fluoranthene alone, and, also, the difference in size at the highest and lowest dose is smaller. Yet, the reduction in growth is satisfactorily described by the model. This reduction cannot be explained by effects of benzo(k)fluoranthene alone, since the NEC for this compound is higher than its concentration in the highest dose of the mixture. The contribution of each of the PAH's to the growth retardation is well described by assuming that the PAH's work additively beyond a certain dilution of the mixture.

CASE STUDY: MUSSEL OUTPLANTS

Field conditions generally preclude testing of detailed, individual based models. However, model assumptions may then be tested in controlled experimental systems (see above), and a validated model can be applied to investigate the performance of organisms growing under field conditions. We apply our toxicity model to published data from a field experiment with two mussel species, *Mytilus edulis* and *M. californianus* (Osenberg et al. 1992). This experiment has been described in sufficient detail to enable application of the model. Bags with variously sized mussels were placed at six different locations near oil production platforms in the Santa Barbara Channel, off the California coast; the distance between bag and contamination source was between 1 and 1000 m. After four months size increments were determined. The mussels had been exposed to produced water, fossil water that is extracted during oil production and released into the environment. Produced water contains several heavy metals and is especially rich in barium. Although produced water was so strongly diluted that a change in ambient concentrations was not observed, even at the most contaminated site, mussels accumulated appreciable amounts of barium in their shells. Concommittantly, they grew and reproduced significantly less, either through effects of barium or other toxicants in produced water.

The application of the toxicity model to those data rests on the premises that the barium content in shells can be used as a cumulative measure of toxicant exposure, and that environmental conditions had been sufficiently smooth. Barium is potentially a substitute for calcium. Consequently, it is assumed that barium is incorporated irreversibly in the shell matrix, and that the relative contribution of barium during shell formation is proportional to the barium

concentration in soft tissue. Then, in equilibrium, the barium content of the shell is proportional to the ambient barium concentration, which holds for planktonic foraminifera incorporating barium in their skeleton (Lea and Spero 1992). Moreover, it is assumed that for all outplants the food density fluctuated around the same mean, and that these fluctuations were relatively small. This is reasonable as the experiment was carried out during the summer months, so phytoplankton densities and the temperature should have been relatively stable. Moreover, model simulations (not shown) establish that a growth curve at constant food provides a good approximation to one at variable food conditions, provided the fluctuations are not too large. With these simplifying assumptions, equations (4) and (12) can be used as before. The dependent variable is the size of the individual mussels after four months of exposure, and the independent variables are the initial length of individual mussels and the barium content in shell formed during exposure. There are only six measurements of barium content, because shell fragments from each location were pooled to enable analysis. Parameters to be estimated are the ultimate length, the growth rate and the toxicity scaling parameter. The no-effect concentration could not be determined, probably because all barium levels exceeded the no-effect concentration; we set this parameter at zero. Thus, three parameters are estimated from six data sets.

Figure 7 gives the final length as a function of the initial length at six different barium levels for *M. californianus*, and Figure 8 for *M. edulis*; the legends contain the parameter estimates. For presentation purposes, each data point represents the mean of four or five measurements and the results are spread out over two graphs. The bends in growth at the higher barium levels occur because animals (shells) cannot shrink; after a bend, the final length equals the initial lenght. The data exhibit a fair bit of scatter, *M. edulis* more than *M. californianus*, but the model is consistent with the observed reduction in growth performance. This reduction is small but, as determined previously, is statistically significant (Osenberg et al. 1992). Consequently, model fits are close to each other, and the highest barium content measured, 18.4 nmol. g^{-1}, is much lower than the values estimated for the toxicity scaling parameter, which are 82.7 (± 7.3) nmol. g^{-1} and 186.4 (± 54.5) nmol. g^{-1} in shells of *M. californianus* and *M. edulis*, respectively. The estimates also show that *M. californianus* is more sensitive to produced water than *M. edulis*.

The toxicity model thus satisfactorily describes the impact of produced water on the growth of mussels. It adds value to a previous analysis, which showed that the impact is significant (Osenberg et al. 1992). The model can explain why and how produced water reduces the growth (and reproduction) of marine organisms, and may therefore be used to make predictions. To illustrate this predictive power, we have calculated how a ten year old *M. edulis* would have performed in a polluted enviroment. For simplicity, we have considered a constant environment (temperature = 15°C; $f = 0.5$), and toxicants with rapid kinetics, implying that the

body burden of toxicant is always in equilibrium with the ambient concentration. These assumptions thus represent conditions not unlike those in the study with mussel outplants. Using parameter values for *M. edulis* from Van Haren *et al.* (1993) (which imply $L_{\infty,0}$ = 6.5 cm; γ_0= 0.45 yr^{-1}; κ = 0.8, and the length at settlement and maturation is 0.1 and 0.7 cm, respectively), we have determined growth and cumulative reproduction, defined as the lifetime reproductive output of an organism. An equation for reproduction is not given in the modeling section, but can be deduced from the assumptions given plus two extra assumptions that specify maturation (see Kooijman 1993). Growth and cumulative reproduction are expressed as a fraction of the respective values in a clean environment, that is, an environment in which toxicant levels do not exceed the NEC. Toxicant levels beyond the NEC are scaled to the toxicity scaling parameter, K_i; the scaled concentration is zero for toxicant levels at or below the NEC.

Figure 9 illustrates model predictions about how a ten year old blue mussel would have performed in a stable environment with toxicants. In a clean environment with food conditions specified above, mussels have grown to 6.4 cm, 0.1 short of the size maximally attainable in this environment. Growth declines rapidly as a function of the scaled toxicant concentration. At a scaled toxicant concentration equaling K_i, mussels become only 1.7 cm long. Also reproduction is severely reduced in the presence of toxicants. It seems that reproduction is more affected by toxicant action than growth, but this reflects for the main part a difference in scaling; differences largely disappear when size is expressed in a volumetric or mass measure. At a toxicant concentration equaling 0.2 K_i, cumulative reproductive output has dropped more than 80% as compared to reproduction in healthy mussels, and at concentrations beyond 1.8 K_i, mussels have not reproduced at all, because they did not reach adulthood, that is, they grew less than 0.6 cm in a decade.

It is informative to compare these simulation results with the experimental examples in this study. Estimates for K_i (see Table 2 and legends to the Figures) show that maximum toxicant levels in these experiments were usually less than K_i, and, in experiments with mussels, less than 0.5 K_i. The results suggests that the toxicant levels used in the experimental studies would have had a devastating effect on reproduction. In the case of the mussels outplanted near oil production platforms, where the highest level of barium in shells is between 0.1 and 0.2 K_i, reproductive output from an individual during a ten year period would have declined by more than 50% as compared to a healthy individual. This is despite the fact that barium levels in the ambient were too low for detection. Thus, even at very low ambient toxicant levels, a toxicant induced reduction in feeding and increase in maintenance demands may have a great impact on reproductive output and, thereby, the dynamics of a population.

DISCUSSION

In this paper, a simple DEB model is linked to a toxicokinetic model and extended with functions that describe the sublethal effects of toxicants. Toxicants are assumed to affect the energy transduction in organisms in a hyperbolic way. As a result, toxicants directly affect parameters that specify the rates of feeding, assimilation and maintenance, and indirectly reduce growth and reproduction rates. The model successfully describes how various lipophilic and metallic compounds, either added singly or in the form of a mixture, change the rates of feeding, respiration and growth in several animals.

Extending the scope of any model involves introducing new parameters and adding structure. Our extension of the DEB model introduces a minimum of additional parameters. For most practical purposes, one parameter, the toxicant conductance rate, arises from toxicokinetics. Two more are needed to specify toxic effects: a scaling parameter and the no-effect concentration, the latter being zero for really deleterious compounds. The increase in structural complexity of the model is minimal. Assuming that toxicant exchange between organism and environment is dynamic, a one-compartment model is the simplest way to model this exchange. Also, inclusion of toxic effects is achieved with a minimal number of rules, since toxicants are assumed to have a similar impact on each energy flux.

This simplicity is achieved at the cost of one subtle, conceptual inconsistency: in the model, the uptake rate of toxicants from food does not decline because of toxicant action, although the feeding rate does. An assumption of toxic effect on toxicant uptake via food would lead to dependence of the bioconcentration factor on the toxicant content of food, a property that would frustrate our scaling of the body burden of toxicant to its content in food (cf. equation (9)). This scaling is necessary when the available toxicant measure is the ambient toxicant concentration rather than the body burden of toxicant. In theses cases, the dynamics of toxicant exchange become quite cumbersome when feedback of toxicants on their uptake is taken into account. In the present study, we therefore accepted the inconsistency, which is unlikely to have major consequences in the only example where it plays a role: the growth of earthworms with copper. However, in other applications, it may be important to consider explicitly toxic effects on intake of toxicants with food.

Because our model is mechanistic, the new parameters are independent of the specifics of any experimental protocol (e.g. exposure time). This is not the case for classic measures, such as the EC_{50}, defined as the toxicant concentration causing a response half of the maximum effect on some process. Our toxicity parameters are related to the EC_{50} observed after a long exposure time, that is, when the body burden of toxicant is in equilibrium with the ambient concentration, but the nature of the relationship depends on the process(es) being studied. The ultimate EC_{50} for

feeding is simply the sum of the scaling parameter and the no-effect concentration. A similar results holds for respiration by non-growing organisms, that use energy mainly to meet maintenance demands. EC_{50}'s for growth and reproduction relate to the toxicity parameters in a more complex way, determined by the solution of the DEB model equations. These links are of considerable practical importance, as they open the possibility of relating our parameters to the large body of literature describing the observed dependence of EC_{50}s on simple physico-chemical properties of a toxicant, such as solubility in fat (Donkin et al. 1989) or degree of ionization in metals (McCloskey et al. 1996).

An alternative approach to modeling toxic effects has been used in previous studies by Kooijman and co-workers (Kooijman and Bedaux 1996a; Kooijman and Bedaux 1996b; Kooijman et al. 1996; Kooijman and Metz 1984). These authors use effect functions different from ours, and differentiate among effects on energy fluxes and conversion efficiencies. In order to avoid introducing too many parameters, they assume that the effects of toxiants on each flux differ in physiological cause, so that effects on one flux may be assumed to dominate. It then suffices to identify this dominant energy flux and to neglect effects on other fluxes. There are methodological challenges with this approach, as the alternative assumptions often make similar predictions. For example, equally good fits to data on growth and reproduction, may be obtained from a model that assumes the dominant toxic effect to be on either maintenance, assimilation or growth efficiency (Kooijman and Bedaux 1996a; Kooijman and Bedaux 1996b). Furthermore, at least in some cases, we know that both processes can simultaneously be affected, as is demonstrated by mussels that concommittantly reduce feeding and increase respiration in the presence of pentachlorophenol (see Figure 3) or tributyltin (Widdows and Page 1993). The distinction between the two approaches is thus the level of generality that is assumed. Our representation is less flexible and more general. Future experiments will tell which is the more useful approach.

Because our modeling framework is modular in structure, it can be amended or changed depending on specific demands. Toxic effects that are not instantaneous and sublethal can be included by formulating extra rules describing, for instance, mutagenic and teratogenic activity, and toxicant induced mortality (see Kooijman and Bedaux 1996a, for an example of the latter). (Note that the present rules for toxic effects include mortality due to toxicant induced starvation, that is, when assimilation falls short of maintenance.) The inclusion of such toxic effects thus do not necessarily require new models describing energy budgets or toxicant exchange. Similarly, the toxic effect functions can be singled out for use in other models. The functions are applicable to describe toxic effects in any model assuming a maintenance demand and a feeding rate dependent on food availability. In addition, the functions can be used in other models assuming

von Bertalanffy growth, since they imply effects on compound parameters, including the ultimate length and von Bertalanffy growth rate (see equation (12)).

In particular, our toxic effect model carries over seamlessly to the full version of Kooijman's DEB model (1993). The full version takes into account the dynamics of storage compounds and has priority rules for energy expenditure when food is scarce. This version thus allows an organism to survive in a variable food environment, whereas an organism growing according to the rules in the present study will immediately die when the instantaneous feeding rate is too low to meet maintenance demands. Because we have made assumptions on toxic effects without reference to food availability, our toxic effect functions are applicable in the full version, not only to describe toxic effects with constant food, but also with dynamic food. When food conditions are constant, a condition we have assumed to hold in all our analyses, the short and full versions describe the processes studied in this paper in a completely similar way. For presentational purposes, we have used the simpler, short version.

With dynamic food, however, the dynamics of the full version of the DEB model are complex. Increased complexity arises not only because the storage compounds provide a buffer against environmental fluctuations, leading to complex patterns in growth and reproduction, but also because they may lead to more complex toxicant dynamics. Lipophilic toxicants are likely to dissolve in storage materials better than in structure. Thus, a description of the dynamics of lipophilic toxicants requires a exchange model with multiple compartments when the fat content of the organism is subject to change, for instance, because of a variable food environment (Van Haren et al. 1994). Then, the fraction of the toxicants in the body that are toxicologically active must be identified. It seems unlikely that toxicants that are dissolved in reserve materials are directly harmful; they need to be mobilized first (Lassiter and Hallam 1990). Therefore, it is reasonable to take the toxicant concentration in structural biomass as the effective toxicant concentration; this assumption needs to be tested with experimental data.

Finally, we note that the sublethal effects modeled in this paper may lead to changes in the dynamics of a population. Such consequences of toxicant action can be understood and predicted with structured (or individual-based) population models (see Tuljapurkar and Caswell 1997, for structured population models), based on experimentally tested models of individual performance and toxic effects (Nisbet et al. 1997). The central assumption in these population models is that all members of the population grow, develop, reproduce and die in accordance with a dynamic model that describes individual energy aquisition and utilization in any environment. Structured population models are important practical tools, since they translate data obtained with relative ease from individuals into population level predictions, while experiments with populations are expensive, time-consuming, and commonly difficult to interpret because of the numerous possible responses of individuals to each other and to their environment. The DEB

model must be testable on individuals, because without rigorous testing of the individual model, the population model would rest on insecure foundations. Also, the DEB model must be general and simple, if the resulting structured model is to be mathematically tractable. The model in this paper meets all these requirements. However, further work is necessary before the model can be used to study population dynamics. Most important is the need to test predictions on reproductive output. Another important requirement is the need for better understanding of the relationship between mortality and energetics. We have work in progress on each of these themes.

ACKNOWLEDGMENTS

We thank Andy Brooks, Sally Holbrook, Ria Hooftman, Chris Klok, Bas Kooijman, Dina Lika, Erik Noonburg, Craig Osenberg and Russ Schmitt for their advice, data and numerical routines. This research was supported by the Office of Naval Research (Grant No N00014-93-1-0952), and by the Minerals Management Service, U.S. Department of the Interior, under MMS Agreement No. 14-35-0001-30761. The views and conclusions contained in this document are those of the authors and should not be interpreted as necessarily representing the official policies, either express or implied, of the U.S. Government.

REFERENCES

Bayne, B. L. 1976. The Biology Of Mussel Larvae. Pages 81-120. *in* B. L. Bayne editors. Marine Mussels: Their Ecology And Physiology. Cambridge University Press, Cambridge.

Beiras, R. and His, E. 1994. Effects Of Dissolved Mercury On Embryogenesis, Survival, Growth And Metamorphosis Of Crassostrea-Gigas Oyster Larvae. Marine Ecology-Progress Series **113**:95-103.

Beiras, R. and His, E. 1995. Effects Of Dissolved Mercury On Embryogenesis, Survival And Growth Of Mytilus Galloprovincialis Mussel Larvae. Marine Ecology-Progress Series **126**:185-189.

Burden, R. L. and Faires, J. D. 1988. Numerical Analysis. PWS-KENT Publishing Company, Boston.

Byczkowski, J. Z. and Sorenson, J. R. 1984. Effects of metal compounds on mitochondrial function: a review. Science of the Total Environment **37**:133-62.

Donkin, P., Widdows, J., Evans, S. V., Worall, C. M. and Carr, M. 1989. Quantitative structure-activity relationships for the effect of hydrophobic organic chemicals on rate of feeding by mussels (*Mytilus edulis*). Aquatic Toxicology **14**:277-294.

Duclaux, E. 1898. Traité de Microbiologie. Masson et Compagnie, Paris.

Eby, L. A., Stow, C. A., Hesselberg, R. J. and Kitchell, J. F. 1997. Modeling Changes in Growth and Diet on Polychlorinated Biphenyl Bioaccumulation in *Coregonus hoyi*. Ecological Applications **7**:981-990.

Franks, N. P. and Lieb, W. R. 1994. Molecular And Cellular Mechanisms Of General Anaesthesia. Nature **367**:607-614.

Gilek, M., Björk, N. and Näf, C. 1996. Influence Of Body Size On The Uptake, Depuration, And Bioaccumulation Of Polychlorinated Biphenyl Congeners By Baltic Sea Blue Mussels, Mytilus Edulis. Marine Biology **125**:499-510.

Hawker, D. W. and Connel, D. W. 1986. Bioconcentration of Lipophilic Compounds by Some Aquatic Organisms. Ecotoxicology and Environmental Safety **11**:184-197.

Hewett, S. W. and Kraft, C. E. 1993. The Relationship between Growth and Consumption: Comparisons across Fish Populations. Transaction of the American Fisheries Society **122**:814-821.

Hooftman, R. N. and Evers-De Ruiter, A. 1992. The Toxicity And Uptake Of Benzo(k)-fluoranthene Using *Brachydanio rerio* In An Early Life StageTest (Draft OECD Guideline). Report number IMW-R 92/218. TNO IMW, Delft, The Netherlands.

Hooftman, R. N., Henzen, L. and Roza, P. 1993. The Toxicity Of A Polycyclic Aromatic Hydrocarbon Mixture In An Early Life Stage Toxicity Test Carried Out In An Intermittent Flow-Through System. Report number IMW-R 93/253. TNO IMW, Delft, The Netherlands.

Jackson, L. J. 1997. Piscivores, Predation, and PCBs in Lake Ontario's Pelagic Foos Web. Ecological Applications **7**:991-1001.

Kesseler, A. and Brand, M. D. 1994. Localisation Of The Sites Of Action Of Cadmium On Oxidative Phosphorylation In Potato Tuber Mitochondria Using Top-Down Elasticity Analysis. European Journal Of Biochemistry **225**:897-906.

Kitchell, J. F., Koonce, J. F., O'Neill, R. V., Shugart, H. H., Magnuson, J. J. and Booth, R. S. 1974. Model of Fish Biomass Dynamics. Transaction of the American Fisheries Society **103**:786-798.

Kitchell, J. F., Stewart, D. J. and Weininger, D. 1977. Applications of a Bioenergetics Model to Perch (*Perca flavescens*) and Walleye (*Stizostedion vitreum*). Journal of the Fisheries Research Board of Canada **34**:1922-1935.

Klok, C. and De Roos, A. M. 1996. Population Level Consequences Of Toxicological Influences On Individual Growth And Reproduction In Lumbricus Rubellus (Lumbricidae, Oligochaeta). Ecotoxicology And Environmental Safety **33**:118-127.

Kooi, B. W. and Kooijman, S. A. L. M. 1994. The Transient Behaviour Of Food Chains In Chemostats. Journal Of Theoretical Biology **170**:87-94.

Kooijman, S. A. L. M. 1993. Dynamic Energy Budgets In Biological Systems. Cambridge University Press, Cambridge.

Kooijman, S. A. L. M. 1995. The Stoichiometry Of Animal Energetics. Journal Of Theoretical Biology **177**:139-149.

Kooijman, S. A. L. M. and Bedaux, J. J. M. 1996a. Analysis Of Toxicity Tests On Daphnia Survival And Reproduction. Water Research **30**:1711-1723.

Kooijman, S. A. L. M. and Bedaux, J. J. M. 1996b. Analysis Of Toxicity Tests On Fish Growth. Water Research **30**:1633-1644.

Kooijman, S. A. L. M. and Bedaux, J. J. M. 1996c. Some Statistical Properties Of Estimates Of No-Effect Concentrations. Water Research **30**:1724-1728.

Kooijman, S. A. L. M., Hanstveit, A. O. and Nyholm, N. 1996. No-Effect Concentrations In Algal Growth Inhibition Tests. Water Research **30**:1625-1632.

Kooijman, S. A. L. M. and Metz, J. A. J. 1984. On The Dynamics Of Chemically Stresses Populations: The Deduction Of Population Consequences From Effects On Individuals. Ecotoxicology And Environmental Safety **8**:254-274.

Kooijman, S. A. L. M., Muller, E. B. and Stouthamer, A. H. 1991. Microbial Growth Dynamics On The Basis Of Individual Budgets. Antonie Van Leeuwenhoek International Journal Of General And Molecular Microbiology **60**:159-174.

Kooijman, S. A. L. M. and Vanharen, R. J. F. 1990. Animal Energy Budgets Affect The Kinetics Of Xenobiotics. Chemosphere **21**:681-693.

Landrum, P. F., Lee, H. and Lydy, M. J. 1992. Toxicokinetics In Aquatic Systems - Model Comparisons And Use In Hazard Assessment. Environmental Toxicology And Chemistry **11**:1709-1725.

Lassiter, R. R. and Hallam, T. G. 1990. Survival Of The Fattest - Implications For Acute Effects Of Lipophilic Chemicals On Aquatic Population. Environmental Toxicology And Chemistry **9**:585-595.

Lea, D. W. and Spero, H. J. 1992. Experimental Determination Of Barium Uptake In Shells Of The Planktonic Foraminifera Orbulina-Universa At 22-Degrees-C. Geochimica Et Cosmochimica Acta **56**:2673-2680.

Mackay, D., Ph. D., Shiu, W. Y. and Ma, K. C. 1992. Illustrated handbook of physical-chemical properties and environmental fate for organic chemicals. Lewis Publishers, Boca Raton.

Marr, A. G., Nilson, E. H. and Clark, D. J. 1962. The Maintenance Requirement of *Escherichia coli*. Annals of the New York Academy of Sciences **102**:536-548.

McCauley, E., Murdoch, W. W., Nisbet, R. M. and Gurney, W. S. C. 1990. The Physiological Ecology Of Daphnia - Development Of A Model Of Growth And Reproduction. Ecology **71**:703-715.

McCloskey, J. T., Newman, M. C. and Clark, S. B. 1996. Predicting The Relative Toxicity Of Metal Ions Using Ion Characteristics - Microtox(R) Bioluminescence Assay. Environmental Toxicology And Chemistry **15**:1730-1737.

Monod, J. 1950. La Technique de Culture Continue; Théory et Applications. Annales de L'Institute Pasteur **79**:390-410.

Nisbet, R. M., Muller, E. B., Brooks, A. J. and Hosseini, P. 1997. Models Relating Individual and Population Response to Contaminants. Environmental Modeling and Assessment **2**:7-12.

Osenberg, C. W., Schmitt, R. J., Holbrook, S. J. and Canestro, D. 1992. Spatial scale of ecological effects associated with an open coast discharge of produced water. Pages 387-402. *in* J. P. Ray and F. R. Engelhardts, editors. Produced water: technological/environmental issues and solutions. Plenum Press, New York.

Pirt, S. J. 1965. The Maintenance Energy of Bacteria in Growing Cultures. Proceedings of the Royal Society London **B163**:224-231.

Ross, A. H. and Nisbet, R. M. 1990. Dynamic Models Of Growth And Reproduction Of The Mussel Mytilus-Edulis L. Functional Ecology **4**:777-787.

Segel, I. H. 1993. Enzyme Kinetics; Behavior and Analysis of Rapid Equilibrium and Steady-State Enzyme Systems. John Wiley & Sons, New York.

Shannon, R. D., Boardman, G. D., Dietrich, A. M. and Bevan, D. R. 1991. Mitochondrial Response To Chlorophenols As A Short-Term Toxicity Assay. Environmental Toxicology And Chemistry **10**:57-66.

Sikkema, J., Debont, J. A. M. and Poolman, B. 1995. Mechanisms Of Membrane Toxicity Of Hydrocarbons. Microbiological Reviews **59**:201-222.

Tuljapurkar, S. and Caswell, H. 1997. Structured-Population Models in Marine, Terrestrial, and Freshwater Systems. Population and Community Biology Series.

, vol. 18. Chapman & Hall, New York.

Van Haren, R. J. F. and Kooijman, S. A. L. M. 1993. Application Of A Dynamic Energy Budget Model To Mytilus-Edulis (L). Netherlands Journal Of Sea Research **31**:119-133.

Van Haren, R. J. F., Schepers, H. E. and Kooijman, S. A. L. M. 1994. Dynamic Energy Budgets Affect Kinetics Of Xenobiotics In The Marine Mussel Mytilus-Edulis. Chemosphere **29**:163-189.

Van Wezel, A. P. and Opperhuizen, A. 1995. Narcosis Due To Environmental Pollutants In Aquatic Organisms - Residue-Based Toxicity, Mechanisms, And Membrane Burdens. Critical Reviews In Toxicology **25**:255-279.

Verhaar, H. J. M., Vanleeuwen, C. J. and Hermens, J. L. M. 1992. Classifying Environmental Pollutants .1. Structure-Activity Relationships For Prediction Of Aquatic Toxicity. Chemosphere **25**:471-491.

Walker, C. H., Hopkin, S. P., Sibly, R. M. and Peakall, D. B. 1996. Principles of Ecotoxicology. Taylor and Francis, London.

Wang, W. X. and Widdows, J. 1993. Metabolic Responses Of The Common Mussel Mytilus-Edulis To Hypoxia And Anoxia. Marine Ecology-Progress Series **95**:205-214.

Widdows, J. and Donkin, P. 1991. Role Of Physiological Energetics In Ecotoxicology. Comparative Biochemistry And Physiology C-Comparative Pharmacology And Toxicology **100**:69-75.

Widdows, J. and Page, D. S. 1993. Effects Of Tributyltin And Dibutyltin On The Physiological Energetics Of The Mussel, Mytilus-Edulis. Marine Environmental Research **35**:233-249.

Table 1 Symbols and abbreviations.

TABLE 1 (2 pages)

Symbol	Interpretation	Dimension
A	assimilation rate	energy per time
A_m	maximum surface area specific assimilation rate	energy per unit surface area and per time
$A_{m,0}$	A_m in absence of toxicants	energy per unit surface area and per time
C_a	scaled tissue toxicant concentration, $k_{ad}[Q]/k_{ed}$	ambient concentration
C_d	dissolved toxicant concentration in ambient	ambient concentration
C_{nec}	scaled tissue no-effect concentration, $k_{de}[Q_{nec}]/k_{ed}$	ambient concentration
f	scaled food density, or functional response	-
G	rate of energy investment in growth	energy per time
$[G]$	volume specific cost for growth	energy per body volume
I_m	maximum surface area specific ingestion rate	ambient volume per unit surface area per time
$I_{m,0}$	I_m in absence of toxicants	ambient volume per unit surface area per time
k_{ad}	toxicant conductance rate	length per time
k_{de}	surface specific uptake rate of dissolved toxicants	ambient volume per unit surface area per time
k_{xa}	surface specific uptake rate of toxicants with food	ambient volume per unit surface area per time
K_i	saturation constant of toxicant action	tissue concentration
K_i'	saturation constant of toxicant action	ambient concentration
L	length	length

TABLE 1 (continued)

L_0	initial length	length
L_∞	ultimate length	length
$L_{\infty,0}$	idem, in absence of toxicants	length
M	maintenance rate	energy per time
$[M]$	volume specific maintenance rate	energy per body volume and per time
NEC	no-effect concentration	ambient or tissue concentration
NOEC	no-observed effect concentration	ambient or tissue concentration
p	compound parameter, $\alpha A_{m,0}/\beta[M_0]$	-
PAH	polycyclic aromatic hydrocarbons	-
$[Q]$	level of toxicant in tissue	tissue concentration
$[Q_{nec}]$	level of no-effective toxicant in tissue	tissue concentration
R	rate of energy investment in reproduction	energy per time
S_{ti}	scaled tissue toxicant concentration resistance, $[Q_a]/k_{du}$	ambient concentration times time per length.
V	body volume	body volume
V_∞	ultimate body volume, $(\kappa A_m f/[M])^3$	body volume
α	compound parameter, converts energy in moles of O_2	number per energy
β	compound parameter, converts energy in moles of O_2	number per energy
γ	von Bertalanffy growth rate	per time
γ_0	idem, in absence of toxicants, $[M]/3[G]$	per time
κ	partitioning constant for energy expenditure	-

Table 2 Parameter values with standard errors estimated from growth data.

TABLE 2

Species	*Crassostrea gigas*	*Mytilus gallo-provencialis*	*Lumbricus rubellus*	*Brachydanio rerio*	*Brachydanio rerio*
Toxicant	mercury	mercury	copper	benzo(k)fluor-anthene	PAH mixture
$L_{\infty,0}$ (µm, µm, $g^{1/3}$, cm, cm)	350	350	1.64 (± 0.01)	4.90 (± 0.04)	3.64 (± 0.01)
L_0 (µm, µm, $g^{1/3}$, cm, cm)	63.3 (± 3.9)	80.2 (± 1.5)	0.25 (± 0.02)	0.40	0.40
γ_0 (10^{-3} day^{-1})	55.7 (± 1.7)	57.1 (± 3.7)	7.2 (± 0.4)	10	10
K_i' (nM, nM, µmol g $soil^{-1}$, nM, -)	72.2 (± 6.5)	103.0 (± 14.0)	17.0 (± 0.8)	4.98 (± 0.21)	1.96 (± 0.04)
C_{nec} (nM, nM, µmol g $soil^{-1}$, nM, -)	7.4 (± 1.7)	4.8 (±3.8)	0.3 (± 0.2)	0.94 (± 0.05)	0.097 (± 0.007)
Time delay (day)	1.8 (± 0.3)	2	-	-	-

Figure 1 Energy flows in the dynamic energy budget model.

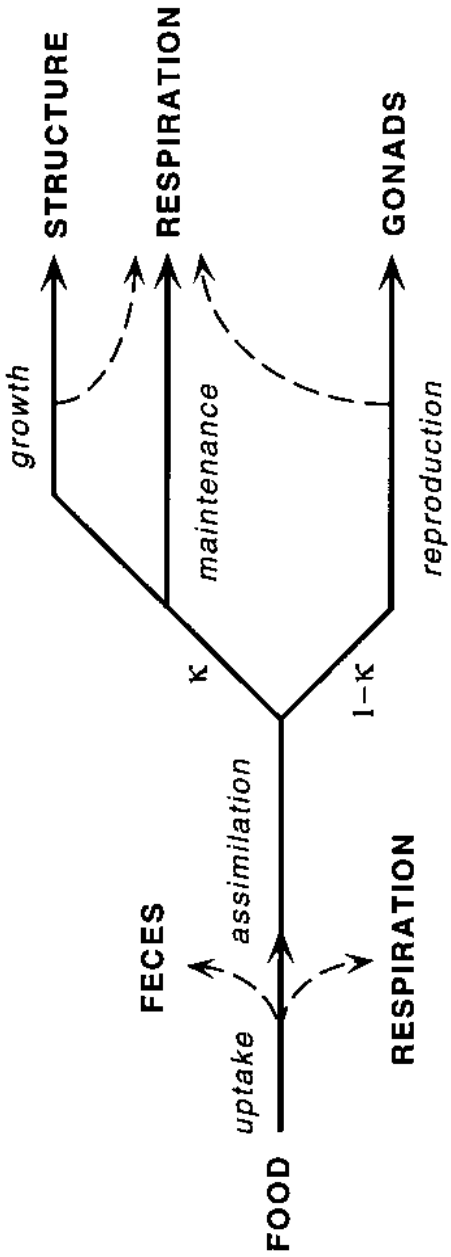

Figure 2 Mitochondrial activity is reduced in the presence of heavy metals or lipophilic toxicants. (a) The rate of oxygen reduction for ATP production is a hyperbolic function of the free cadmium concentration. Data are fitted assuming non-competitive inhibition kinetics (see text). Oxygen consumption for ATP formation in absence of cadmium is 135.5 (± 2.7) nmol O. mg protein^{-1}. min^{-1}, and K_i = 15.3 (± 1.1) µM (data from Kesseler and Brand 1994). (b) The oxygen reduction rate as hyperbolic functions of the 2,4,6-trichlorophenol (O—O) or 2,4-dinitrophenol (●- - -●) concentration. Oxygen consumption for ATP formation in absence of TCP and DNP are 216.1 (± 4.4) and 185.6 (± 0.8) nmol O. mg protein^{-1}. min^{-1}, respectively, and K_i = 37.5 (± 3.4) and 69.9 (± 2.2) µM, respectively (data from Shannon et al. 1991).

FIGURE 2a

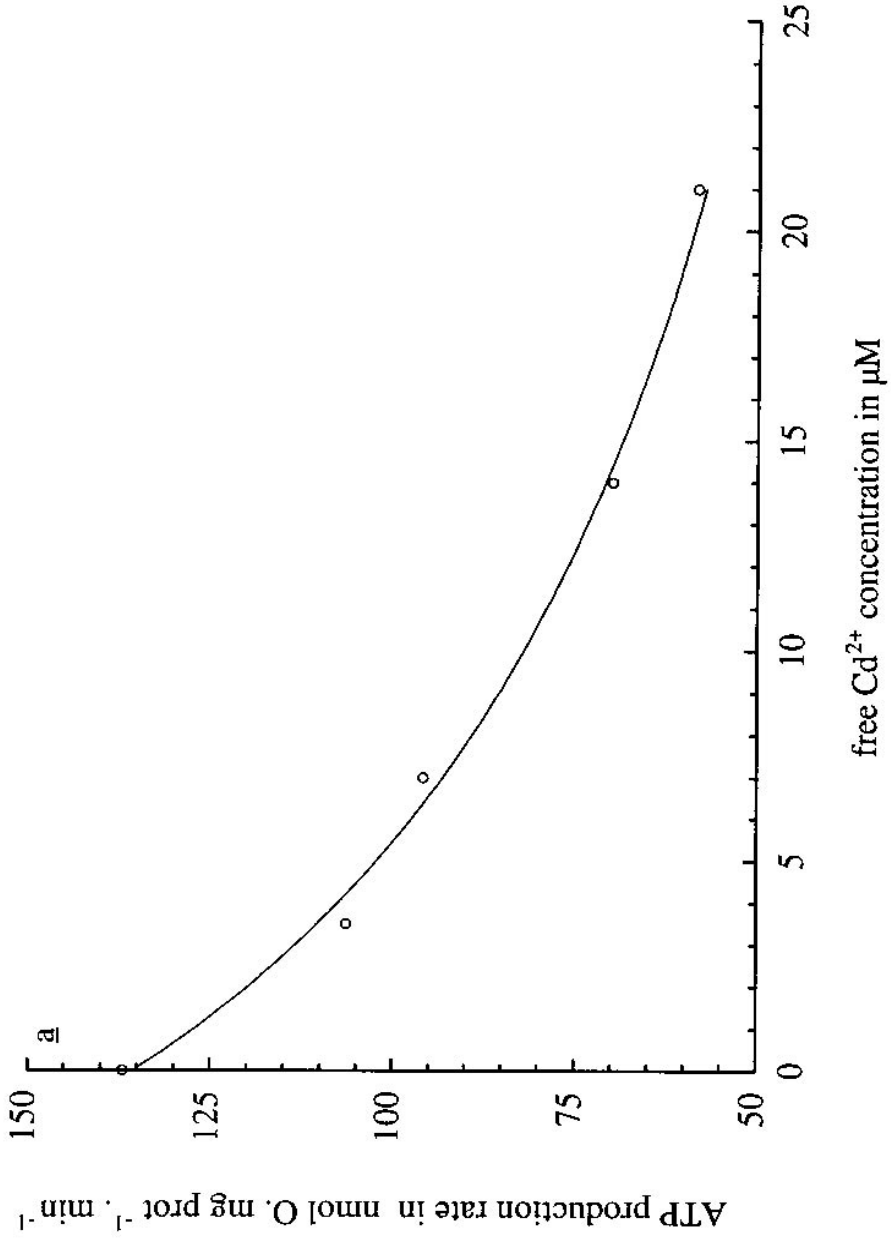

FIGURE 2b

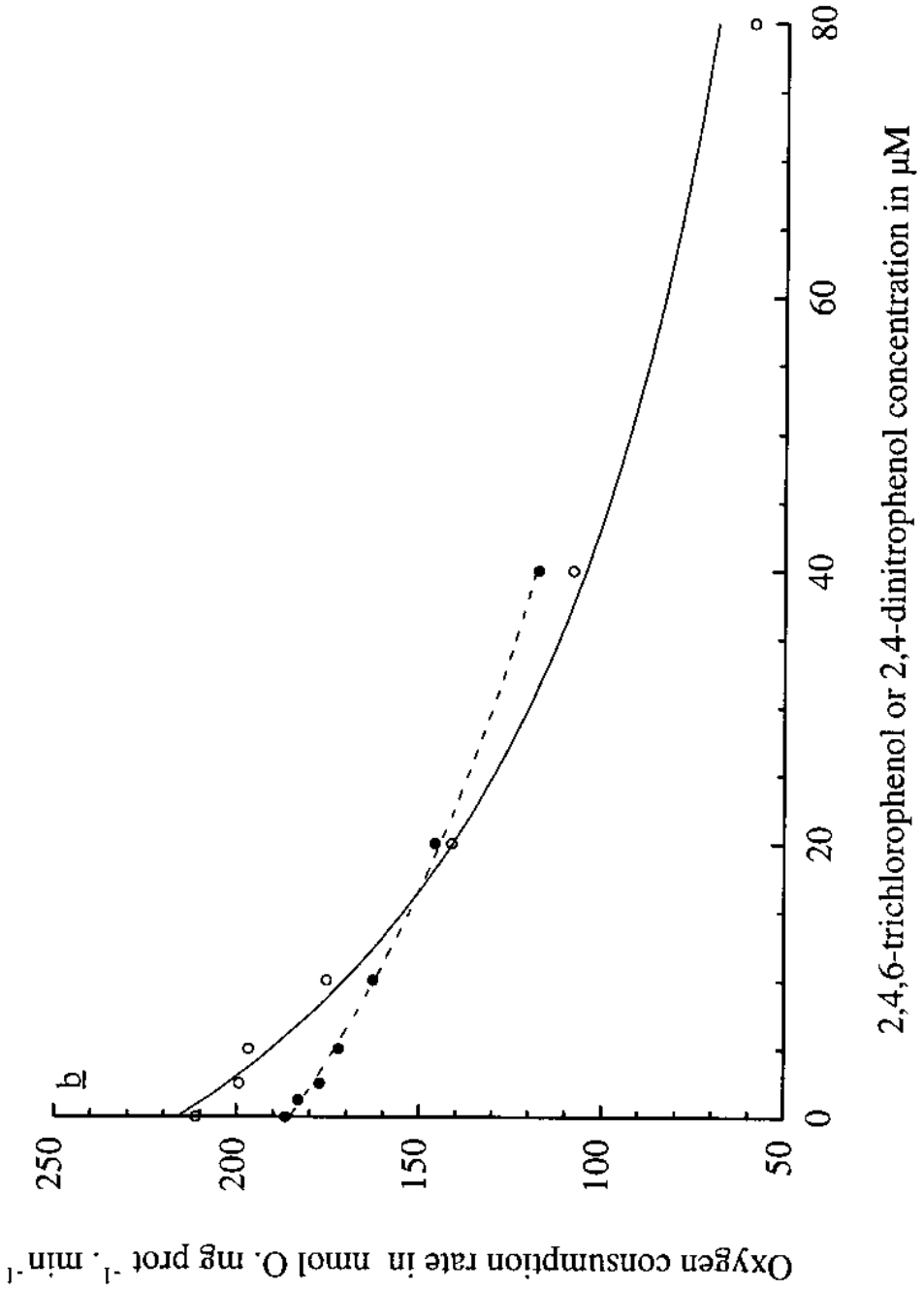
b
250
200
150
100
50
0
20
40
60
80
Oxygen consumption rate in nmol O. mg prot -1. min-1
2,4,6-trichlorophenol or 2,4-dinitrophenol concentration in µM

Figure 3 Feeding and respiration by *Mytilus edulis* is affected by toxicants. (a) Scaled clearance rate as a function of the ambient toluene concentration. Data are fitted with equation (11) giving C_{nec} = 10.78 (± 0.02) µM and K_i' = 10.431 (± 0.05) µM (data from Widdows and Donkin) (data from Donkin et al. 1989). (b) Scaled clearance rate (❍) and scaled oxygen consumption rate (●) as a function of the pentachlorophenol content in tissue. With exclusion of the data at the highest PCP concentration (see text) and $[Q_{nec}]$ fixed at zero, the parameters estimated with equation (11) and (6) are K_i = 55.4 (± 8.0) nmol. g^{-1} and the compound parameter p = 0.91 (± 0.48) (data from Widdows and Donkin 1991).

FIGURE 3a

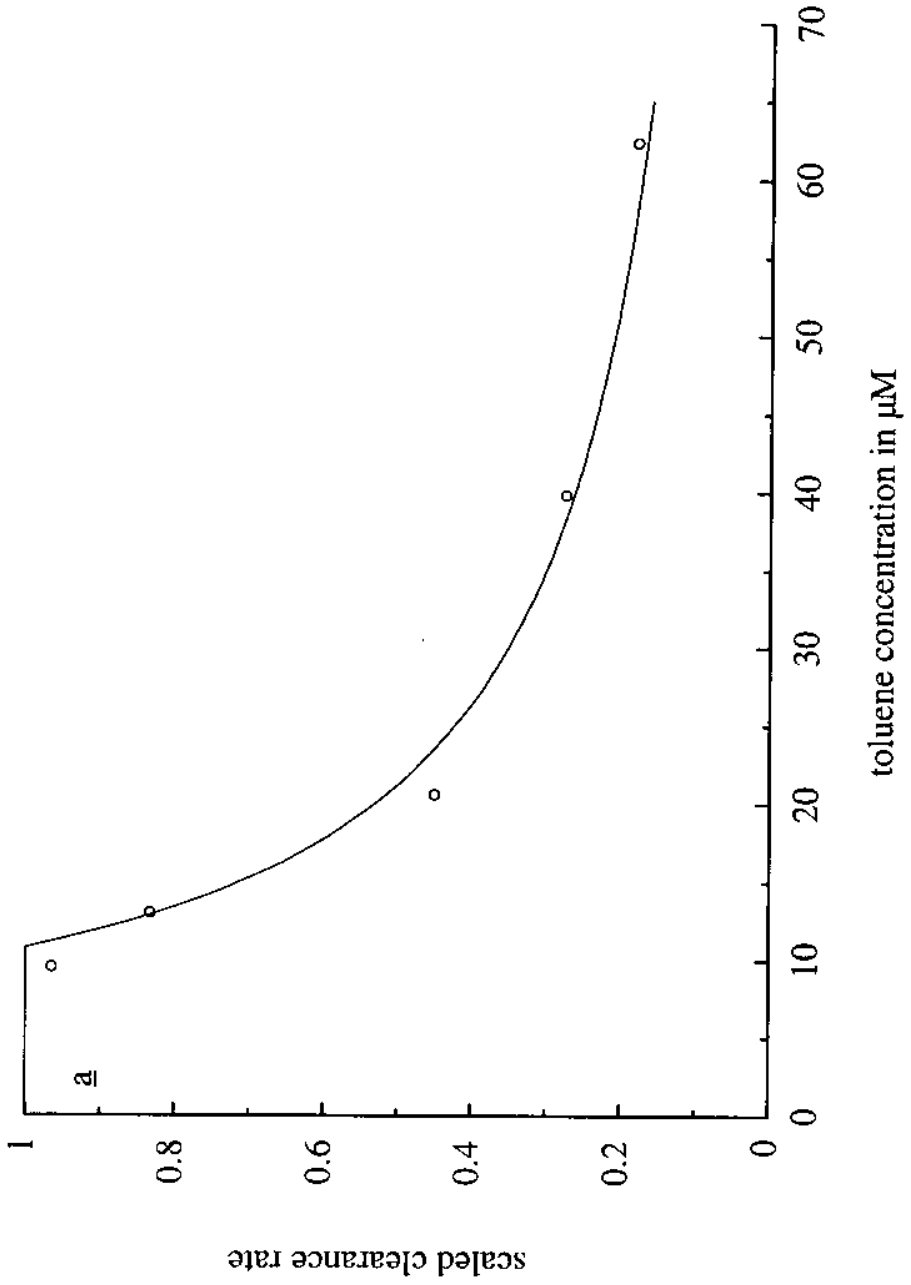

FIGURE 3b

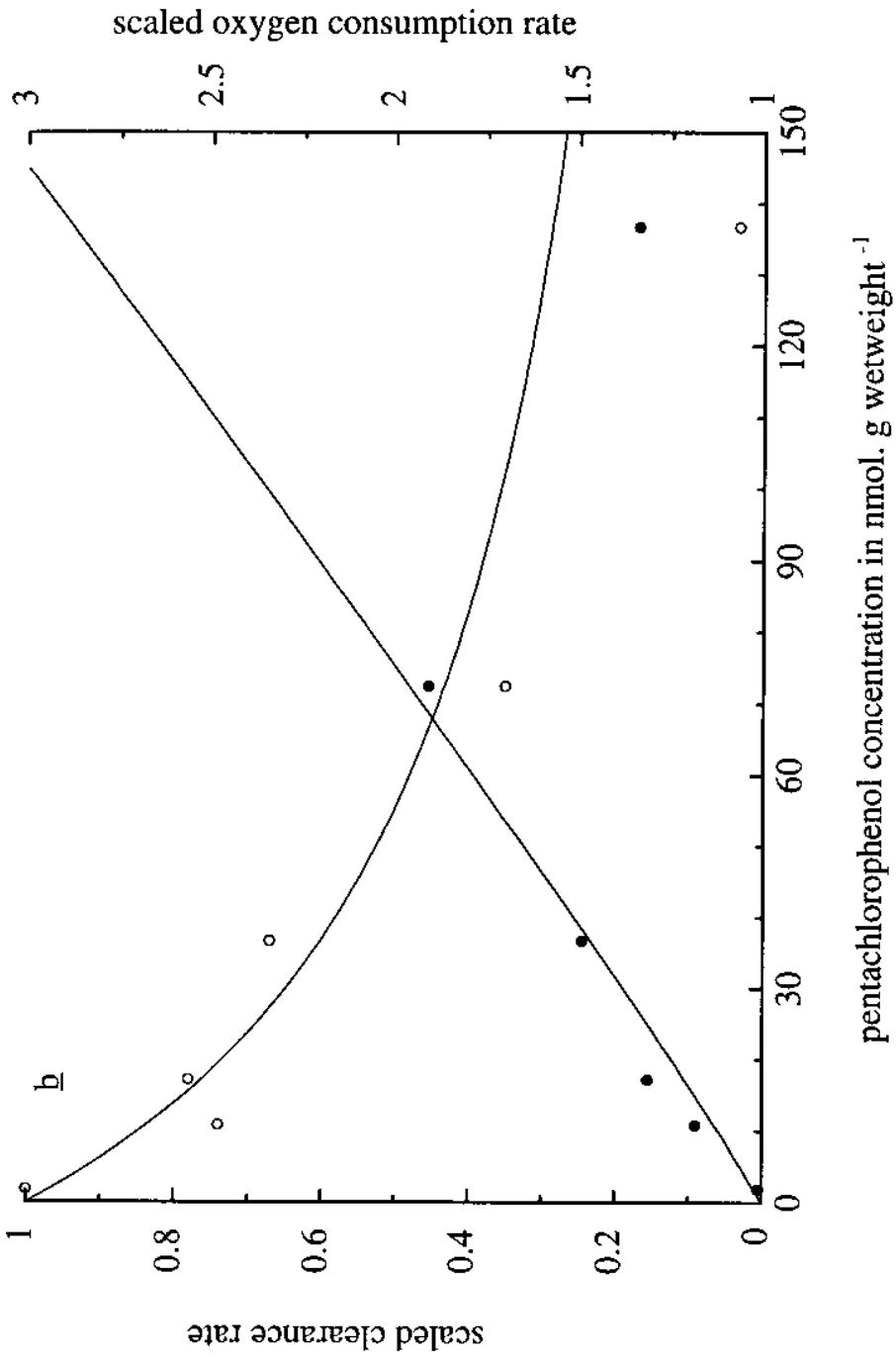
scaled oxygen consumption rate
3
2.5
2
1.5
1
150
120
90
60
30
0
pentachlorophenol concentration in nmol. g wetweight -1
b
1
0.8
0.6
0.4
0.2
0
scaled clearance rate

Figure 4 Growth of larvae of (a) *Crassostrea gigas* and (b) *Mytilus galloprovencialis* at nominal mercury concentrations of 0 (○), 5 (●), 10 (□), 20 (■), and 40 (✧) nM. Two model fits are shown. First, mercury is assumed to be fully retained in the larvae, and data are fitted with equation (4) and (12) while reconstructing the mercury levels in tissue with equation (10) (broken lines). Alternatively, mercury is assumed to be rapidly removed from the larvae, leading to tissue levels that are always in equilibrium with the ambient concentration, in which case data are fitted with equation (5) and (12) (solid lines). With the latter method, the growth curves at 0 and 5 nM mercury are (almost) identical and thus plotted on top of each other. Parameter estimates are listed in Table 2 (data from Beiras and His 1994; Beiras and His 1995).

FIGURE 4a

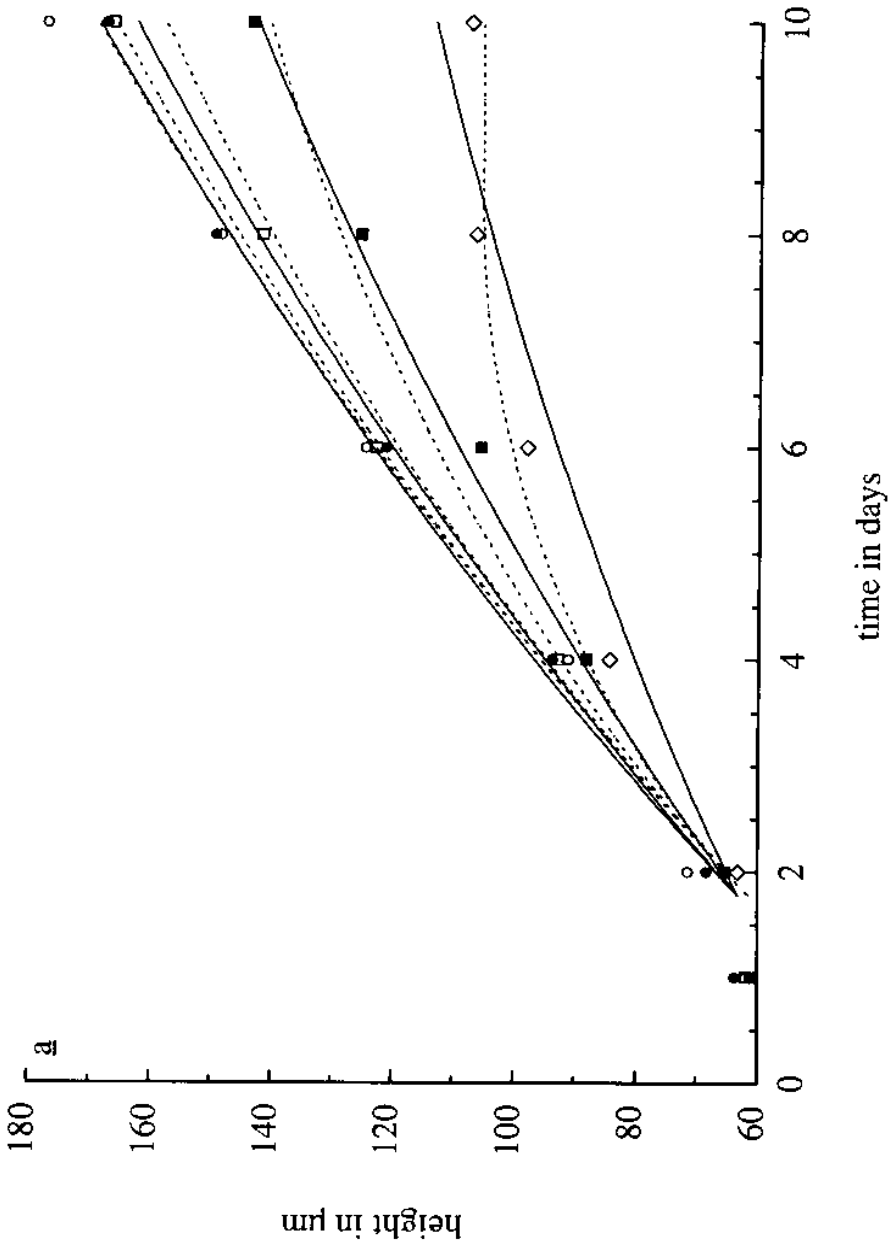

FIGURE 4b

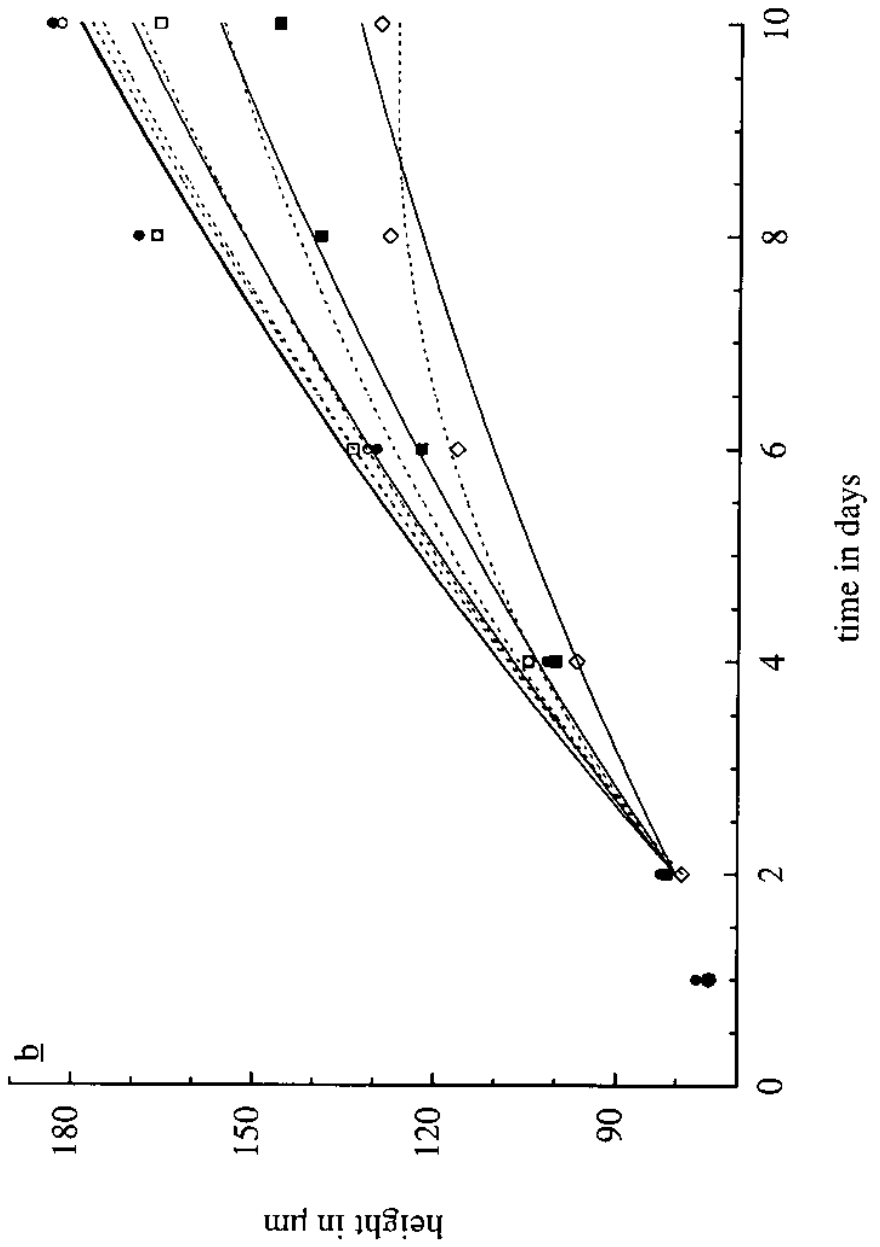

Figure 5 Growth of the earthworm *Lumbricus rubellus* in soils contaminated with copper. Note that size is expressed in wet weight rather than a length measure. The copper contents of soil are 0.2 (○), 0.9 (●), 2.3 (□) and 5.7 (■) µmol per gram dry weight. The fits represent two extreme cases for toxicant removal. Either copper is fully retained in the earthworms, in which case data are fitted with equation (4) and (12) while reconstructing the copper levels in tissue with equation (10) (broken lines). Or copper is rapidly removed from the earthworms, leading to tissue levels always being in equilibrium with the ambient concentration, in which case data are fitted with equation (5) and (12) (solid lines). Parameters are given in Table 2 (data from Ma, cited in Klok and De Roos 1996)

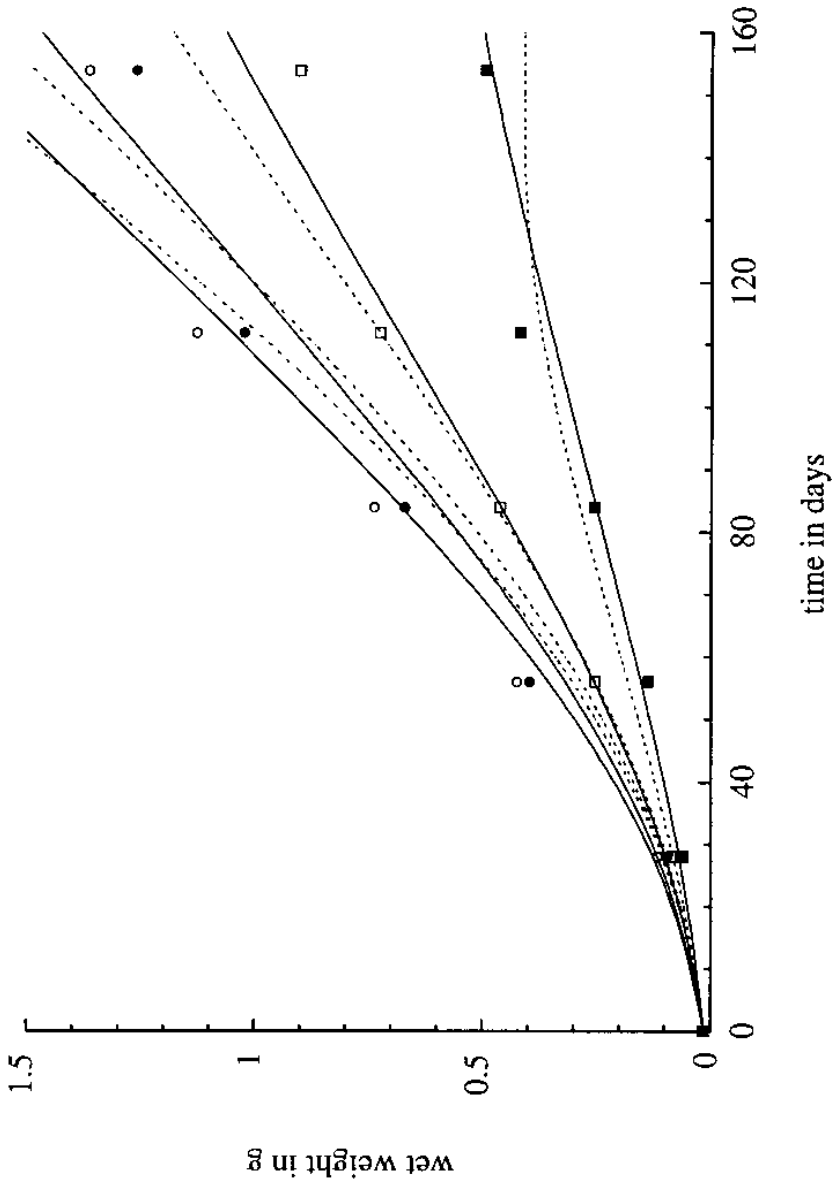

Figure 6 Length of the zebrafish *Brachydanio rerio* after 37 days of exposure to (a) benzo(k)-fluoranthene and (b) a mixture of polycyclic aromatic hydrocarbons, which contained at the highest dose the no observed effect concentration of 6 PAH's: 18 nM phenanthrene, 49 nM fluoranthene, 0.7 nM benzo(k)fluoranthene, 7.9 nM chrysene, 40 nM benzo(a)pyrene and 1.2 nM benzo(ghi)perylene. The data are fitted with equation (5); parameters are listed in Table 2 (data from Hooftman and Evers-De Ruiter 1992; Hooftman et al. 1993).

FIGURE 6a

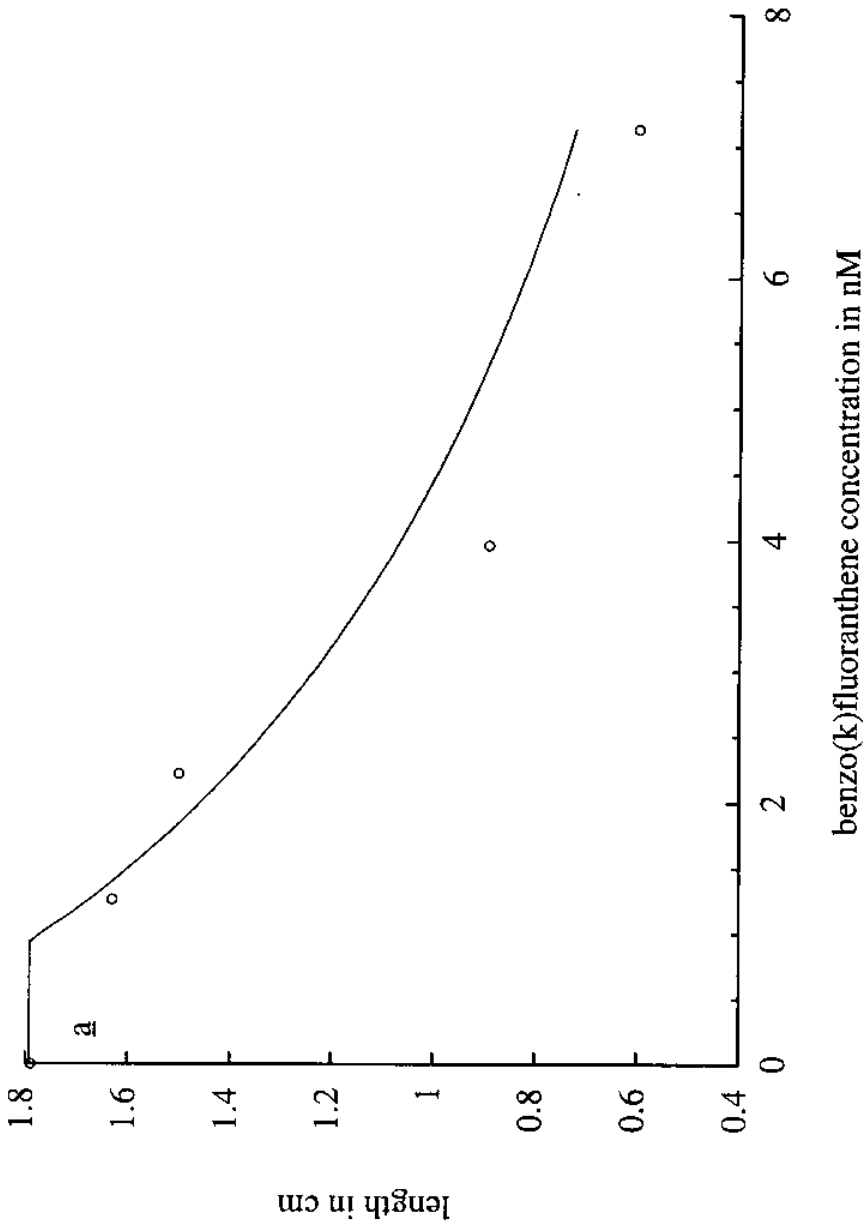

FIGURE 6b

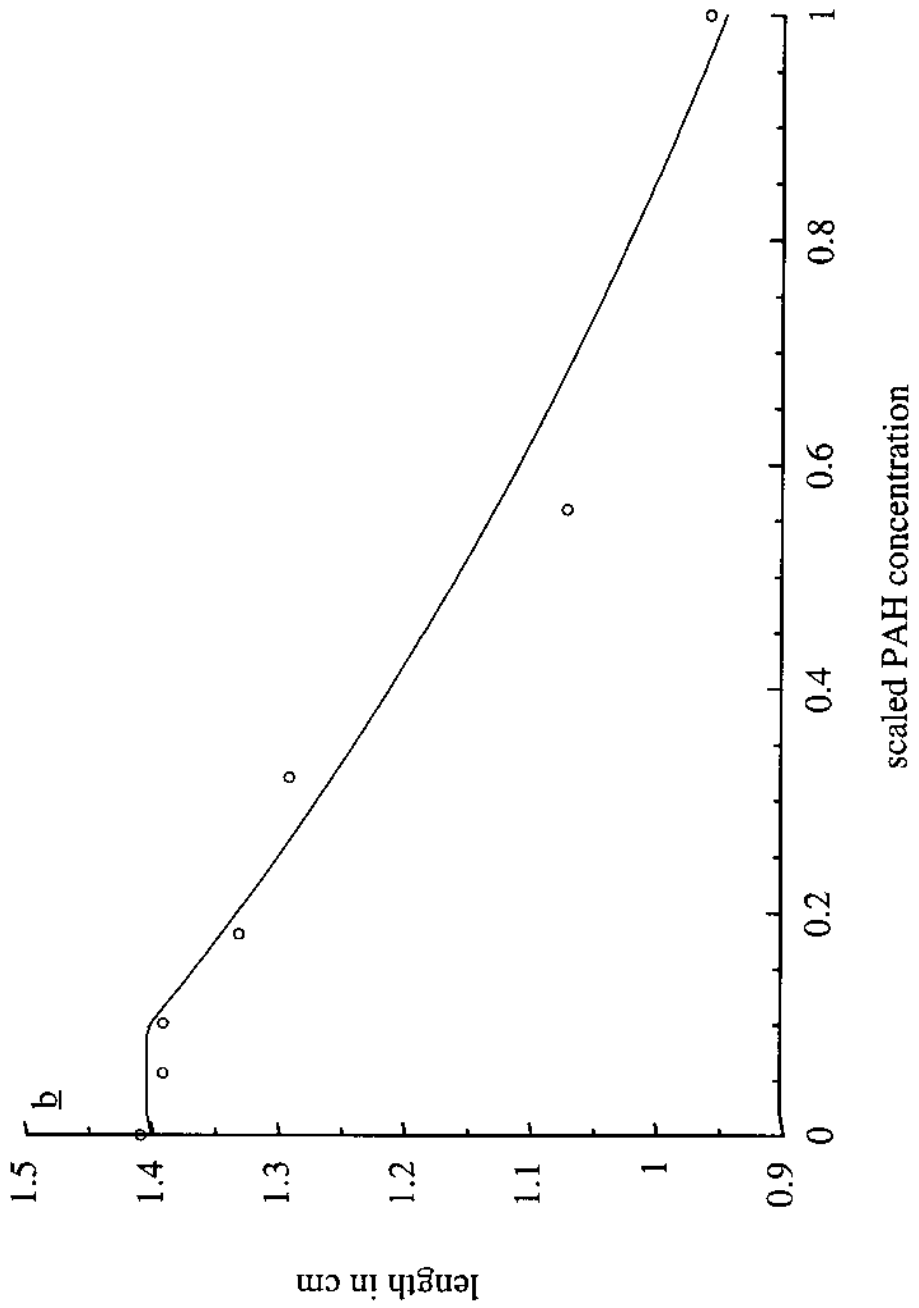
b
1.5
1.4
1.3
1.2
1.1
1
0.9
0
0.2
0.4
0.6
0.8
1
scaled PAH concentration
length in cm

Figure 7 Growth of *Mytilus californianus* at six locations near oil producing platforms in the Santa Barbara Channel, California. The points are averages of measurements on 4 or 5 animals, the error bars are standard deviations. The grey curves in the upper panel are the fits from the lower panel, and vice versa. The increase in size after 119 days of exposure is fitted with equation (5) as a function of the barium content in newly formed shell, which are 18.4 (○—○), 16.8 (●– – –●) and 14.2 (□----□) nmol. g^{-1} (a), and 5.6 (○—○), 4.7 (●– – –●) and 3.7 (□----□) nmol. g^{-1} (b). Parameter estimates are: K_i = 82.7 (± 7.3) nmol. g^{-1}; $L_{\infty,0}$ = 7.3 (± 0.2) cm; and γ_0 = 3.1 (± 0.2) 10^{-3} day^{-1} (data from Osenberg et al. 1992).

FIGURE 7a

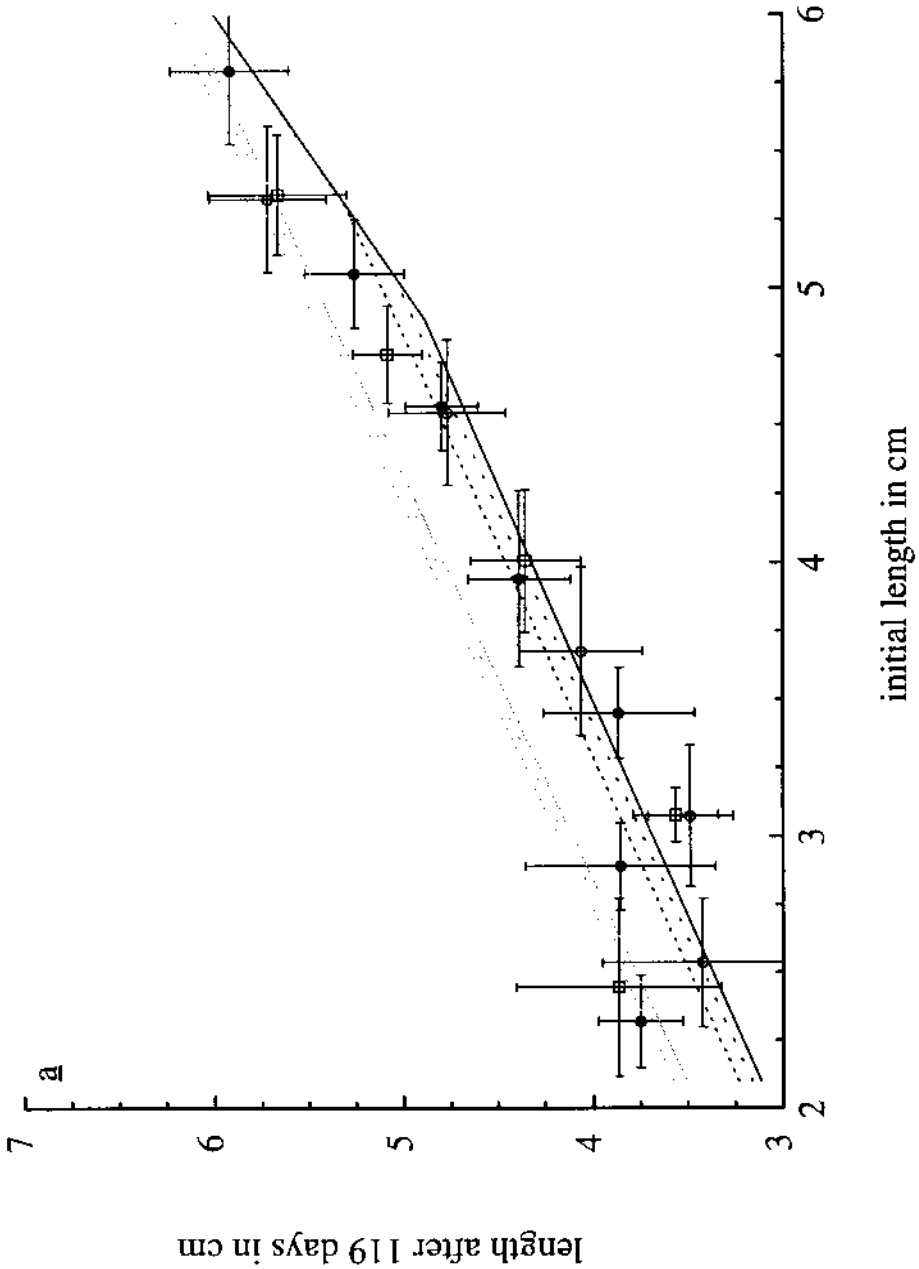

FIGURE 7b

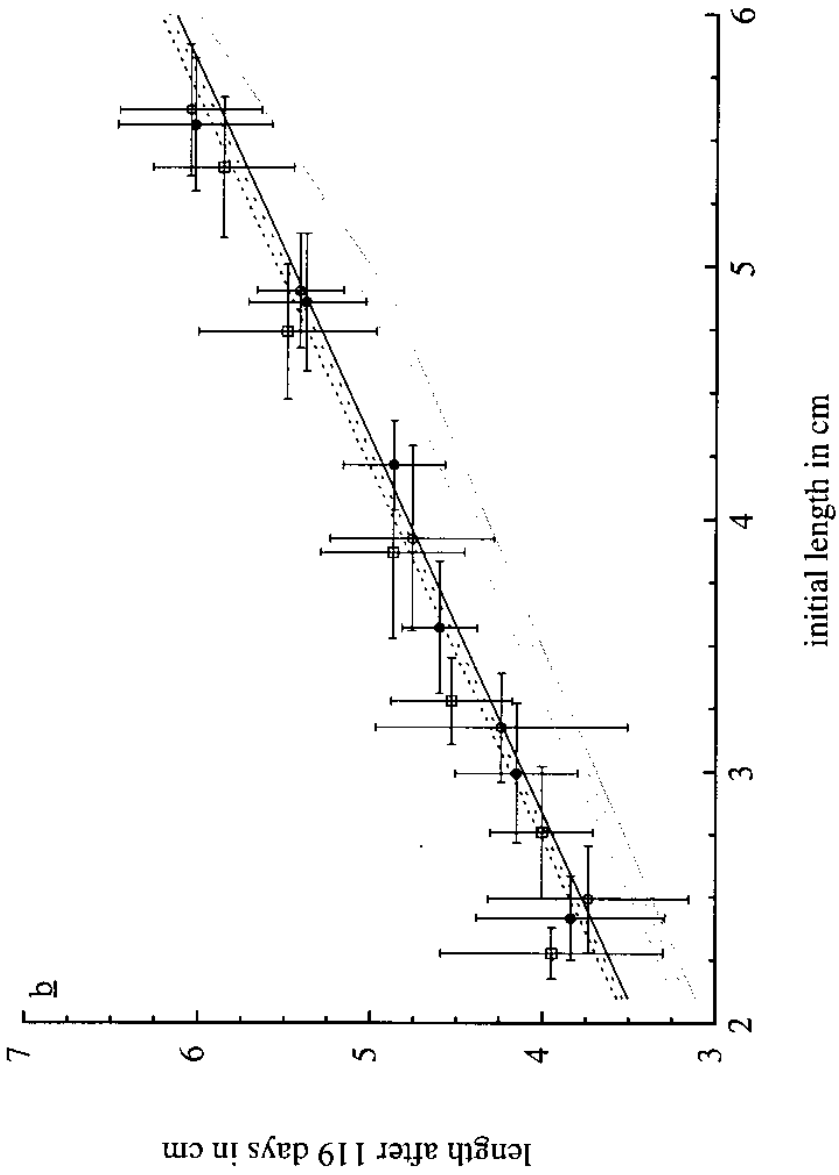
b
7
6
5
4
3
2
3
4
5
6
initial length in cm
length after 119 days in cm

Figure 8 Growth of *Mytilus edulis* at six locations near oil producing platforms in the Santa Barbara Channel, California. The points are averages of measurements on 4 or 5 animals, the error bars are standard deviations. The grey curves in the upper panel are the fits from the lower panel, and vice versa. The increase in size after 119 days of exposure is fitted with equation (5) as a function of the barium content in newly formed shell, which are 13.51 (○—○), 13.47 (●– – –●) and 13.11 (□----□) nmol. g^{-1} (a), and 7.21 (○—○), 4.88 (●– – –●) and 3.86 (□----□) nmol. g^{-1} (b). Parameter estimates are: K_i = 186.4 (± 54.5) nmol. g^{-1}; $L_{\infty,0}$ = 8.7 (± 0.5) cm; and γ_0 = 3.5 (± 0.3) 10^{-3} day^{-1} (data from Osenberg et al. 1992).

FIGURE 8a

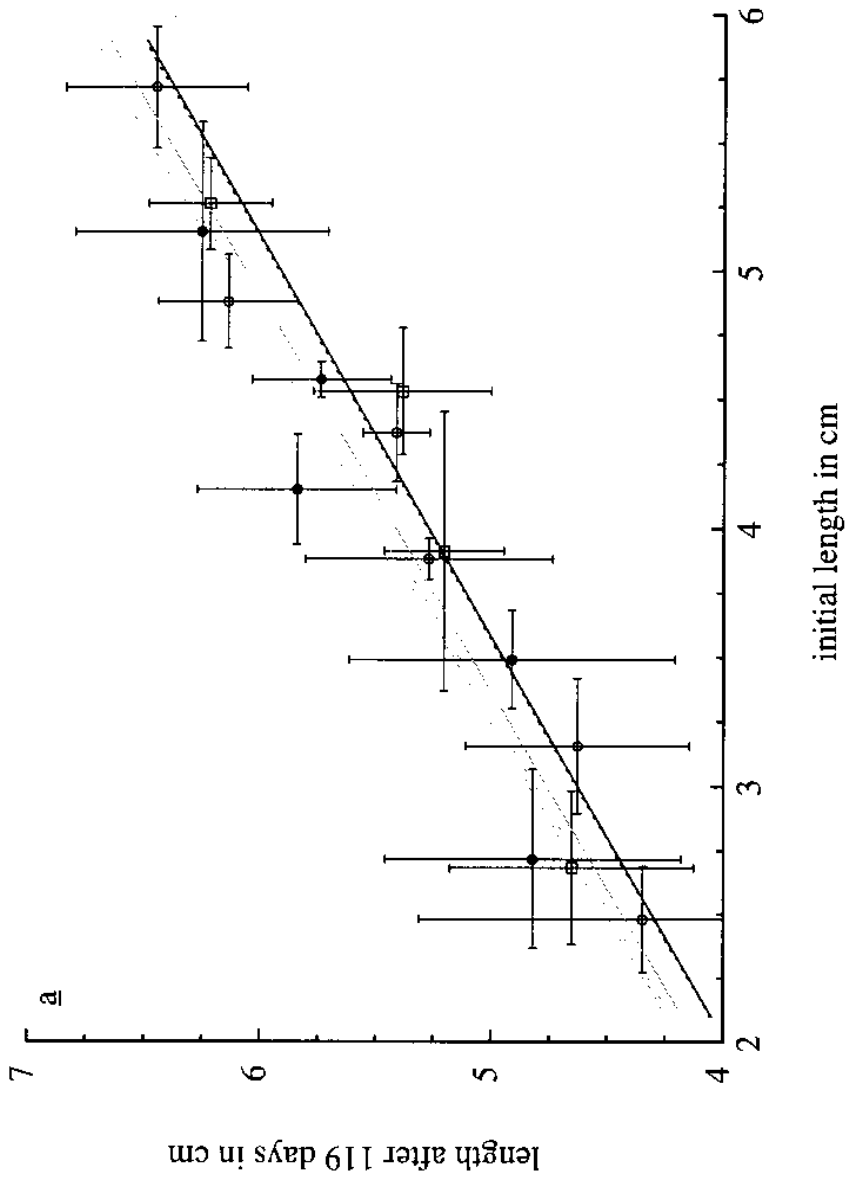

FIGURE 8b

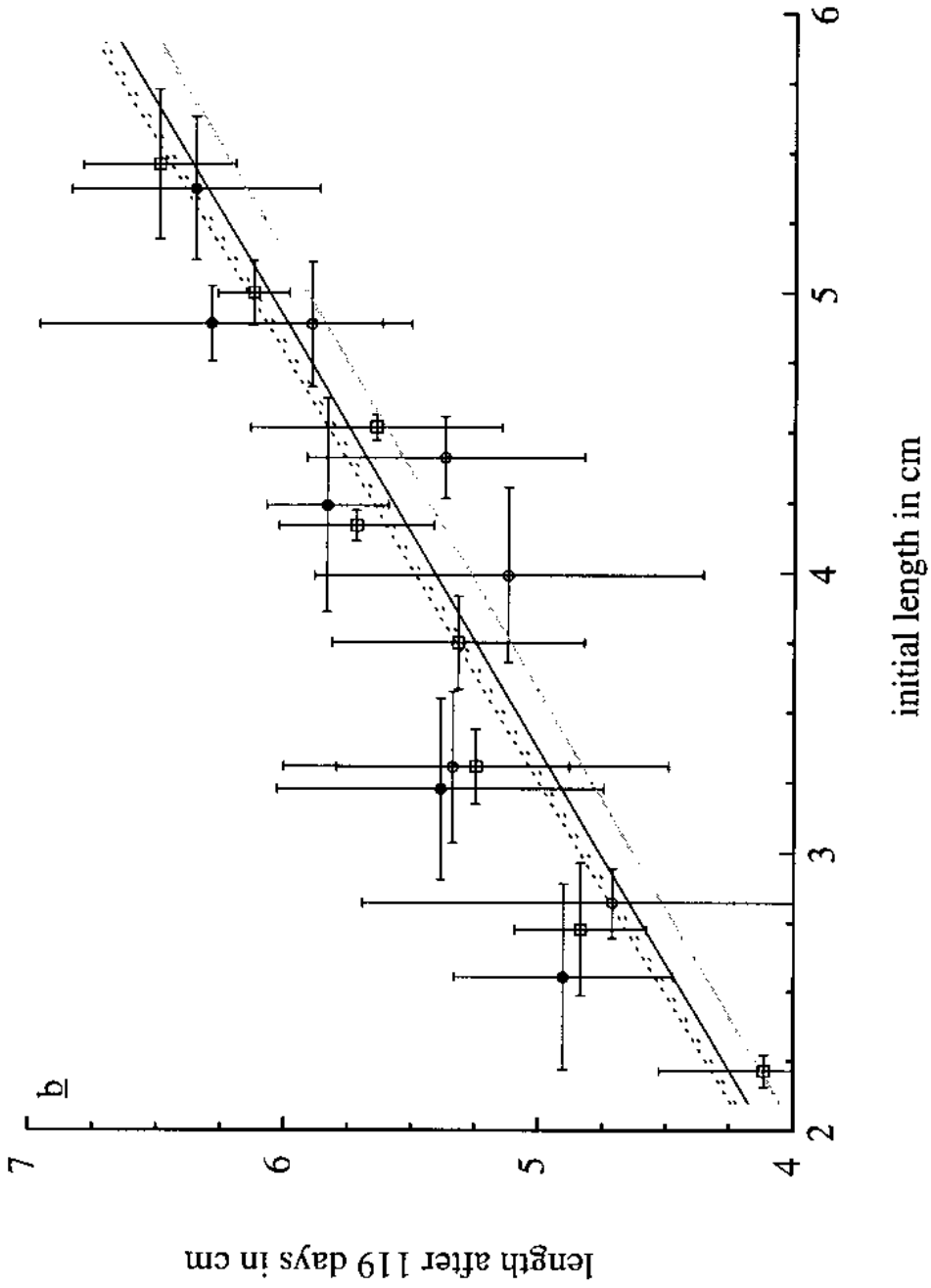

Figure 9 The lifetime performance of a ten year old mussel depends strongly on the presence of toxic compounds. Growth (—) and lifetime reproductive output (- - - -), scaled to the performance of an individual living in a clean environment, have been calculated using the concentration of a toxicant scaled to its toxicity parameter, K_i. It is assumed that the toxicant concentration in the body had been in equilibrium with the ambient concentration at all times, and that environmental conditions had been constant. Parameter values are taken from van Haren *et al.* (1993).

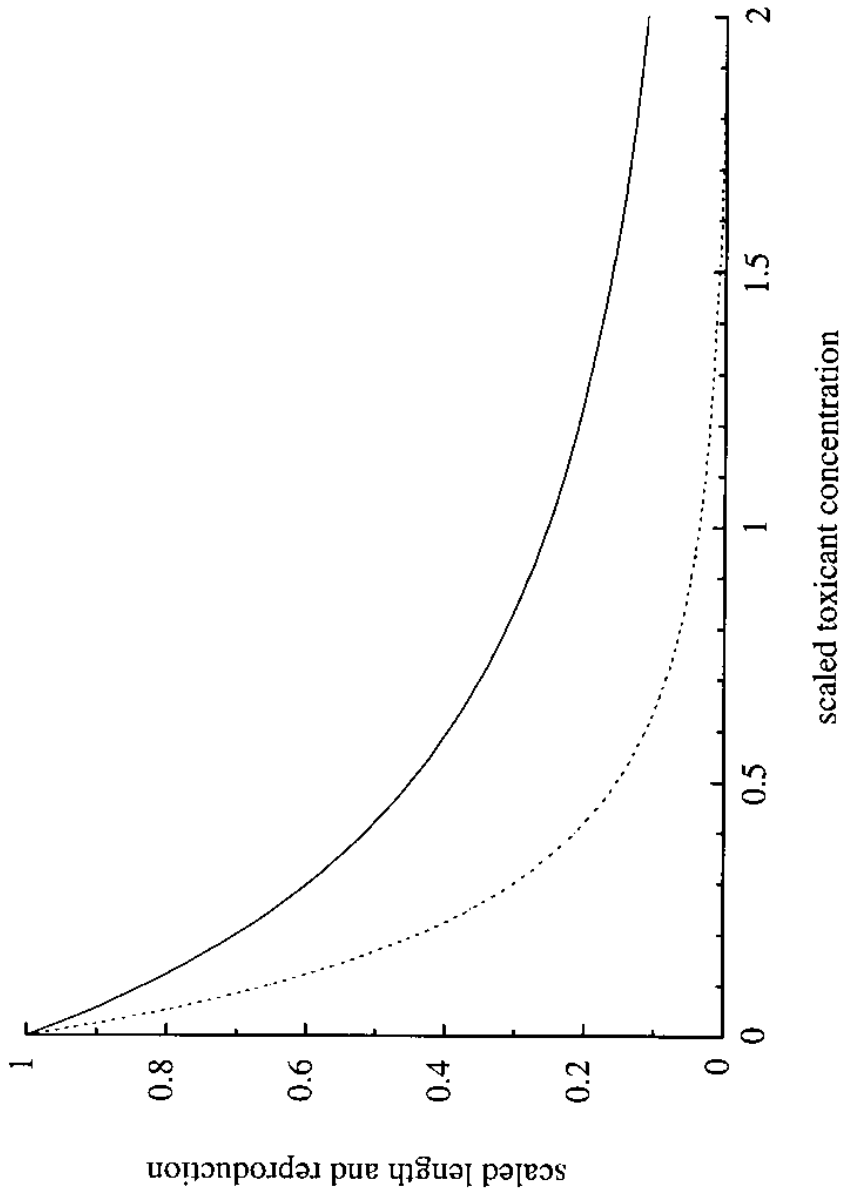

4th ESTMB meeting, SMB Annual meeting, Amsterdam, July 1999

Predictive Power of Simple Population Models Based on Dynamic Energy Budgets.

R.M. Nisbet, E. McCauley, W.S.C. Gurney, A.M. de Roos, W.W. Murdoch

Although individual-based population models may take account of species-specific details of the physiology and behavior of individual organisms, ecological theory aims at generality. Simple dynamic energy budget (DEB) models provide a basis for general theory relating individual physiology to population dynamics, but the theory is largely untested. We here report work where DEB models are tested against data on individual physiology, and then used to predict population dynamics. The predictions are compared with experimental results for the zooplankter \emph{Daphnia} by ourselves and others. We test a DEB model of growth and reproduction by fitting data describing individuals grown in isolation, and then comparing fitted values of parameters characterizing physiological rates to independently measured values. The DEB model assumptions, together with an assumption of age-and size-independent mortality, define a structured population model, which can be expressed in terms of a small number of ordinary differential equations. With no new adjustable parameters, the model correctly predicts equilibrium biomasses in laboratory populations. It correctly predicts the equilibrium density of "edible algae" in the field, and explains the outcome of laboratory studies of competition between two zooplankton species. The model makes incorrect predictions on population size-structure. The work provides some empirical justification for the use of simple models to predict the effects of environmental stress, and helps define their limitations.

4th ESTMB meeting, SMB Annual meeting, Amsterdam, July 1999

A Dynamic Energy Budget Model based on Partitioning of Net Production

Authors: Konstadia Lika* and Roger Nisbet

Dynamic energy Budget (DEB) models describe the rates at which an individual organism acquires energy from its environment and utilizes it for physiological processes related to maintenance, growth and reproduction. DEB models constitute a basis for developing physiological structured models. Most DEB models in the literature fall into one of two families: the {\it net assimilation} and {\it net production} models. The two groups of models differ mainly in their assumptions concerning allocation of energy. Gurney et al. [1] found that different energy allocation strategies result in different behavior at the population level. The most complete body of theory to date for DEB models exists for a net assimilation model developed by Kooijman [2]. Net production models, although they have been more widely used, have been formulated only for juveniles and adults (feeding stages).

We formulate a net production model in a way that covers feeding and non feeding stages of an organism, so that further testing of the two energy allocation strategies can be made. The model is based on partitioning of net production (i.e. energy acquisition rate minus maintenance rate) between growth and energy reserves. It is applicable to embryos (which neither feed nor reproduce), juveniles (which feed but do not reproduce), and adults (which commonly both feed and reproduce). Under constant environmental conditions, the growth of a juvenile is always of von Bertalanffy type. Depending on the values of model parameters there are two long-time possibilities for adults: (a) von Bertalanffy growth accompanied by reproduction at a rate that approaches zero as the organism approaches asymptotic size, or (b) abrupt cessation of growth at some finite time, following which, the rate of reproduction is constant. We illustrate the model's applicability in life history theory by studying the optimum values of the energy allocation parameters for each of the dynamic regimes described above.

[1] W.S.C. Gurney, D.A.J. Middleton, R.M. Nisbet, E. McCauley, W.W. Murdoch, and A.M. de Roos, Individual energetics and the equilibrium demography of structured
populations, {\it Theoretical Population Biology}, 49:344-368,1996.

[2] S.A.L.M Kooijman, Dynamic Energy Budgets in Biological Systems. Theory and Applicationsn in Ecotoxicology, Cambridge University Press, 1993.

4th ESTMB meeting, SMB Annual meeting, Amsterdam, July 1999

and

Annual meeting of The Ecological Society of America, Spokane, 1999

Living with variable food; survival and production in a dynamic energy budget (DEB) model for individuals.

E.B. Muller, R.M. Nisbet

A dynamic energy budget (DEB) model describes the rates at which organisms assimilate and utilize energy from food for maintenance, growth, reproduction and development. These rates depend on the state of the organism and of its environment. Despite being dynamic, DEB models are most often used in constant environments, either real or assumed. We study the dynamic behavior of a particularly extensive DEB model, Kooijman's KAPPA-rule model (1993, Dynamic Energy Budgets in Biological Systems, Cambridge University Press, New York), which has a key assumption that somatic and reproductive tissues are competing for energy. We assume an environment in which the scaled food density (type II) fluctuates either periodically or stochastically (pink noise). With both fluctations, and on the provision of survival, organisms grow more (on average) than their conspecifics growing in an average constant food environment, and this increase is a function of the intensity of the fluctuations. The intensity of the fluctations reduces the (average) lifespan. Reproduction shows a more complex picture. With periodic food, strong fluctations enhance reproduction in organisms that favor reproduction over growth, but reduce reproduction in organisms that give higher priority to growth. With stochastic food, reproduction in surviving individuals increases with the intensity of the food fluctuations, but the reproductive effort of a cohort may decline. These results illustrate the flexibility of the KAPPA-rule model.

American Society of Limnology and Oceonagraphy, Alburquerque, February 2001

Nisbet, R.M. EEMB, University of California, Santa Barbara, CA 93106.
Muller, E.B., EEMB, University of California, Santa Barbara, CA 93106.
McCauley, E. , Biological Sciences, Univ. of Calgary, Calgary, Canada.
Kooijman, S.A.L.M, Dept. Theoretical Biology, Vrije Universiteit, Amsterdam, The Netherlands.
Elser, J.J., Dept. Biology, Arizona State University, Tempe, AZ 85287.

MODELING THE EFFECTS OF HERBIVORE STOICHIOMETRY ON THE STABILITY OF PLANT-HERBIVORE SYSTEMS

There is a growing body of evidence suggesting that regulation of C:N:P ratios within herbivores affects recycling rates of N and P, growth of herbivores, population dynamics, and herbivore community structure. Previous work by T. Andersen on simple models of zooplankton and their algal food has shown that nutrient limitation of herbivore growth may lead to herbivore extinction, the precise conditions depending on (a) the ratio of the minimum nutrient quota of the algae to the (fixed) quota in the herbivore, and (b) the relationship between herbivore growth rate and algal quota. We generalize these findings by developing mechanistic representations of herbivore growth that use the concept of synthesizing unit, recently proposed by S.A.L.M. Kooijman. We find that the viability of the herbivore population depends strongly on the details of assumptions regarding feeding, assimilation and maintenance, and mortality.

SS19
TALK
Nisbet, R.M.

The Department of the Interior Mission

As the Nation's principal conservation agency, the Department of the Interior has responsibility for most of our nationally owned public lands and natural resources. This includes fostering sound use of our land and water resources; protecting our fish, wildlife, and biological diversity; preserving the environmental and cultural values of our national parks and historical places; and providing for the enjoyment of life through outdoor recreation. The Department assesses our energy and mineral resources and works to ensure that their development is in the best interests of all our people by encouraging stewardship and citizen participation in their care. The Department also has a major responsibility for American Indian reservation communities and for people who live in island territories under U.S. administration.

The Minerals Management Service Mission

As a bureau of the Department of the Interior, the Minerals Management Service's (MMS) primary responsibilities are to manage the mineral resources located on the Nation's Outer Continental Shelf (OCS), collect revenue from the Federal OCS and onshore Federal and Indian lands, and distribute those revenues.

Moreover, in working to meet its responsibilities, the **Offshore Minerals Management Program** administers the OCS competitive leasing program and oversees the safe and environmentally sound exploration and production of our Nation's offshore natural gas, oil and other mineral resources. The MMS **Royalty Management Program** meets its responsibilities by ensuring the efficient, timely and accurate collection and disbursement of revenue from mineral leasing and production due to Indian tribes and allottees, States and the U.S. Treasury.

The MMS strives to fulfill its responsibilities through the general guiding principles of: (1) being responsive to the public's concerns and interests by maintaining a dialogue with all potentially affected parties and (2) carrying out its programs with an emphasis on working to enhance the quality of life for all Americans by lending MMS assistance and expertise to economic development and environmental protection.